Bitumen fractions responsible for stabilizing water in oil emulsions

By

Fan Yang

A thesis submitted in partial fulfillment of the requirements for the degree of

Doctor of Philosophy

in

Chemical Engineering

Department of Chemical and Materials Engineering

University of Alberta

ABSTRACT

During the extraction of crude oil or bitumen, stable water-in-oil emulsions are inevitably formed. The emulsified water contains chloride ions and other organic acidic compounds that cause severe corrosion problems to the downstream plant equipment, creating operational and safety issues and hence additional operation costs. The breakup of water-in-oil emulsions can be facilitated by the coalescence/flocculation between water droplets in the oil phase. In this thesis, a new methodology was developed to isolate interfacial asphaltenes from water in asphaltene solution emulsions to study the drainage kinetics, thickness and stability of water-in-oil thin liquid films stabilized by this fraction of asphaltenes in comparison with other heavy oil components such as asphaltenes-, heavy oil- (bitumen) and deasphalted heavy oil- (maltenes) diluted in toluene. The asphaltenes were found to be responsible for the formation of thicker films and slowing down the drainage kinetics due to their specific ability to self-assemble and to form 3D network in the film. The film forming behavior of asphaltenes was found to be determined from a small sub-fraction of interfacially active asphaltenes. The emulsion stabilization capacity and interfacial behavior of this sub-fraction of asphaltenes were compared to that of whole asphaltenes and remaining asphaltenes using bottle tests, thin liquid film technique, and Langmuir trough experiments. The results from these different techniques revealed stabilizing mechanisms of emulsions and interfacial films by this sub-fraction of asphaltenes. Chemical characterization including ESI-MS, H-NMR, ^{13}C-NMR, FTIR and elemental analyses was used to construct chemical structures for this sub-fraction of asphaltenes and the remaining asphaltenes. These molecular structures of asphaltenes were used in Molecular Dynamics (MD) simulations in order to shed light on the functional groups and interactions that could be responsible for the aggregation and interfacial film formation of asphaltenes. Finally, the performance of an EO-PO block copolymer demulsifier on breaking up

the asphaltene in toluene solution—water interface was analyzed by a suite of techniques including bottle test, micropipette coalescence test, viscoelasticity analysis, and AFM, SEM and Brewster Angle Microscope (BAM) imaging.

Preface

Below is a statement of contributions to co-authored papers contained in this thesis:

1. **F. Yang**, P. Tchoukov, E. Pensini, T. Dabros, J. Czarnecki, Z. Xu, Asphaltene Subfractions Responsible for Stabilizing Water-in-Crude Oil Emulsions. Part 1: Interfacial Behaviors, Energy & Fuels 2014, 28(11), pp 6897-6904. I was responsible for designing and performing the experiments, data analysis and drafting/revising the paper. Tchoukov was deeply involved in experimental design, data interpretation and paper editing. Dabros and Czarnecki and Xu were involved in paper critics and editing.

2. **F. Yang**, P. Tchoukov, H. Dettman, R. Teklebrhan, L. Liu, T. Dabros, J. Czarnecki, J. Masliyah, Z. Xu, Asphaltene Subfractions Responsible for Stabilizing Water-in-Crude Oil Emulsions. Part 2: chemistry analysis and molecular simulation, *Energy & Fuels* 2015, 29 (8), pp 4783–4794. I was responsible for experimental design, data analysis and interpretation, and authoring of the paper. Tchoukov was deeply involved in experimental design and writing draft and revising the paper. Dettman was responsible for NMR sample preparation and analysis. She was also responsible for editing the NMR analysis part of the paper. Liu was responsible for molecular weight characterizations. Teklebrhan was responsible for both experiment and writing of the molecular simulation part in the paper. Dabros, Czarnecki, Masliyah and Xu were involved in paper critics and editing.

3. P. Tchoukov, **F. Yang**, Z. Xu, T. Dabros, J. Czarnecki, J. Sjoblom, Role of Asphaltenes in Stabilizing Thin Liquid Emulsion Films, *Langmuir* 2014, 30 (11), pp 3024–3033. I was responsible for designing and performing the experiments and writing roughly 40% of the paper. Tchoukov

was equally responsible in designing and performing the experiments and wrote the discussion part of the paper. Xu, Dabros, Czarnecki and Sjoblom were involved in paper critics and editing.

4. **F. Yang**, P. Tchoukov, E. Pensini, Y. Liang, T. Dabros, J. Czarnecki, Z. Xu, Demulsification Mechanisms of Water-in-Heavy Oil Emulsions Studied by Modified Thin Liquid Film Technique, submitted to *Journal of Colloid and Interface Science*. I was responsible for designing and performing the experiments and wrote the entire paper. Tchoukov was responsible in designing the experiments with me and was heavily involved in paper editing. Liang was responsible for the interfacial tension measurements. Pensini, Xu, Dabros, Czarnecki were involved in paper critics and editing.

5. E. Pensini, D. Harbottle, **F. Yang**, P. Tchoukov, Z. Li, J. Masliyah, Z. Xu, Performance of polymeric EO-PO demulsifiers to break water-in-oil emulsions, *Energy & Fuels* 2014 , 28(11), pp 6760-6771. I was heavily involved in the experimental design and data interpretation. I was also involved in performing Langmuir trough experiments. Pensini was responsible for the majority part of experiments and paper authoring.

Acknowledgements

I would like to take this opportunity to thank Professors Zhenghe Xu and Tadeusz Dabros for their support and guidance throughout the development of this project. Their instructions are instrumental in my desire and ability in thinking as a researcher and engineer.

I also owe much gratitude to Dr. Plamen Tchoukov with whom I had collaborated strongly in my research projects. During the course of these projects, he was always involved, informative and ready to help, his timely guidance and help were very critical in all the publications I was involved.

I also would like to thank Dr. Jan Czarnecki for his timely guidance and useful suggestions in the experimental design. I thank Dr. Heather Dettman for the NMR analysis on asphaltene samples and data interpretation, and Dr. Robel Teklebrhan for the molecular dynamic simulations. I also would like to mention that I had some awesome years in Dr. Zhenghe Xu's research group and special thanks to my office-mates/ friends, Dr. David Harbottle, Dr. Erica Pensini, Dr. Plamen Tchoukov, and Dr. Lan Liu.

I am also thankful for financial support from NSERC Oil Sands Research Chair Program.

Finally, I would like to express my deepest gratitude to my parents and my girlfriend for their ever lasting love, support and patience.

CONTENTS

CHAPTER 5 ASPHALTENE SUB-FRACTIONS RESPONSIBLE FOR STABILIZING WATER-IN-CRUDE OIL EMULSIONS - INTERFACIAL BEHAVIORS........................... 66

LIST OF FIGURES

LIST OF TABLES

CHAPTER 1 INTRODUCTION

1.1 OIL SANDS INDUSTRY

The mineable oil sands in Alberta contain about 7~14% bitumen, 85% mineral solids and 5% water by weight.[1] Bitumen is high molar mass viscous petroleum. After being extracted from the oil sands, bitumen can be upgraded into synthetic crude oil, SCO, having an API gravity of about 31, which can be further fractionated to gasoline, heating oil and diesel fuel in bitumen refining processes.

The extraction of bitumen from oil sands has been extensively studied. In 1920s, Karl Clark invented an extraction method based on the use of hot water, which is the well-known 'Clark Hot Water Extraction process' (CHWE).[1]A variation of this process has been widely used in the oil sands industry from its invention. Figure 1.1 shows a schematic flow process of bitumen extraction from oil sands.

In a warm-water bitumen extraction process, after oil sands are mined and the oil sand lumps are crushed, they are mixed with hot water under alkaline condition, which is achieved by sodium hydroxide addition.[2] The slurry generated as such is sent to a large primary separation vessel (PSV) through hydro-transport pipelines where bitumen is liberated from the sand grains and aerated. In the PSV, the aerated bitumen floats to the top of the vessel, whereas most of the solids settle to the bottom of the PSV, forming a waste stream known as tailings. Most water and fine solids containing some fugitive bitumen remains in the middle, forming so called middlings. The floated bitumen known as bitumen froth contains a substantial amount of fine solids and water, typically 60% bitumen, 30% water and 10% solids by weight.

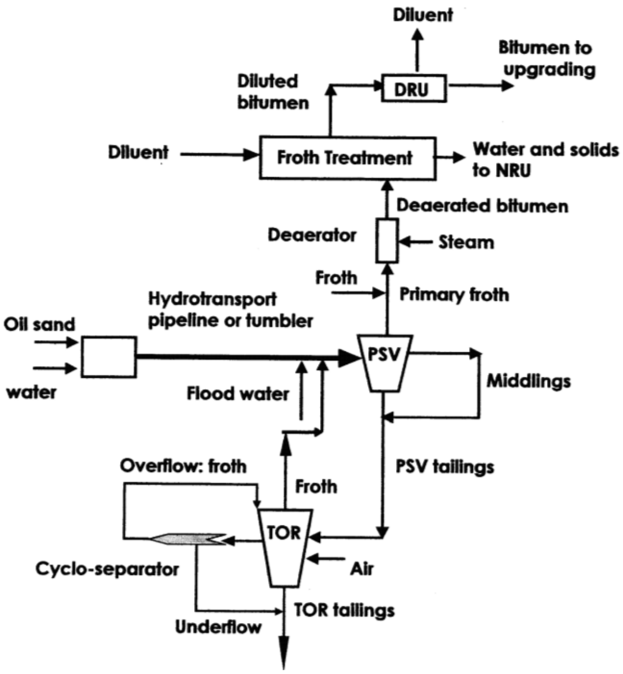

Figure 1.1 Schematic flow sheet of a hot-water bitumen extraction process [3]

After de-aeration, the bitumen froth is sent to the froth treatment unit in which the solids and water in the bitumen froth are removed by gravity separation. The cleaned bitumen is then sent to the upgraders after recovery of solvent to produce synthetic crude oil.

1.2 OILSANDS FROTH TREATMENT PROCESS

The bitumen froth-treatment process is essentially a cleaning process in which a solvent is used to dilute the bitumen in the froth. The solvent addition decreases the viscosity and enhances the density difference of the hydrocarbon and aqueous phases for effective gravity separation to remove most of the solids and water present in the froth.

Two kinds of froth treatment methods are being used in the oil sands industry. Currently, the naphtha-based froth-treatment is used by Syncrude and Suncor, and the paraffinic froth treatment is used by Shell Albian Sands and Imperial Oil Ltd.[4] In the paraffinic froth treatment, a high solvent to bitumen ratio is employed to trigger the controlled precipitation of asphaltenes from the bitumen. Since asphaltenes precipitate in the presence of solids and water droplets, acting as a flocculent, this method can achieve a nearly clean bitumen product with diminished amount of solids and water.[5]

In the naphtha-based froth treatment plant, the bitumen froth is first diluted with naphtha to decrease its viscosity and then centrifuged in a scroll type centrifuge at 1,100 g to remove the coarse solids and free water.[2] The preliminarily cleaned diluted froth is then sent to disc-nozzel type centrifuges (Alpha-Laval) operating at up to 5,500 g to be further cleaned. This process is used by Syncrude Canada. In other operations, after dilution of bitumen froth, inclined plater settlers and/or hydrocyclones are configured to achieve the similar separations. After the treatment, the final diluted bitumen product has roughly 2% water and 1% solids. The water remained in the diluted bitumen product is considerably hard to remove as it is in the form of emulsified water droplets of several microns in size.

Figure 1.2 shows micrographs of the naphtha-diluted froth and heptane-diluted froth. In naphtha-diluted froth, many small water droplets are found dispersed in it, whereas in heptane-diluted froth water droplets become larger and form large aggregates with precipitated asphaltenes and solids.

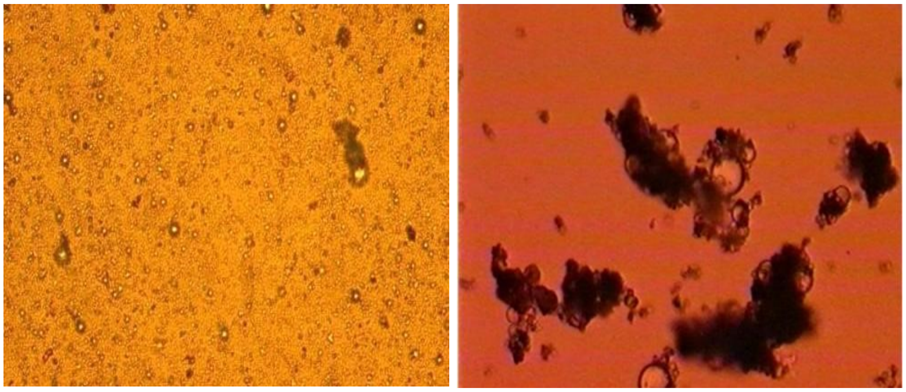

(a) Naphtha diluted froth ***(b) Heptane diluted froth***

Figure 1.2 Microscopic images of diluted froth.[4]

Both methods have advantages and drawbacks. The high bitumen quality achieved by the paraffinic method is at the cost of the loss of more expensive diluents trapped in asphaltene precipitates, which brings important economic and environmental issues. The naphtha-based froth treatment, on the other hand, does not trigger asphaltenes precipitation but suffers from the presence of residual water and fine solids in the final bitumen product. The remaining water contains dissolved substances such as naphthenic acids and chloride salts. These substances may later cause severe corrosion issues to the plant equipment, risk the production safety and raise operational costs.

1.3 OBJECTIVES AND ORGANIZATION OF THE THESIS

The main objective of this work is to gain new understanding of the stabilization mechanisms of different bitumen fractions which determine the stability of W/O emulsions that occur in oil sands industry through studying the interfacial properties of interfaces formed by these bitumen fractions and also through studying the property of the intervening thin liquid films formed between the two interfaces of water droplets being adjacent to each other.

The whole thesis is organized into 9 chapters and a brief description of each chapter is given below:

Chapter 1 gives a brief description of the oil sands industry and the froth treatment process. The importance and challenges of froth treatment process are also discussed. The objective of this thesis is introduced.

Chapter 2 is a literature review of current studies on the water in oil emulsion stabilized by different bitumen components. Studies on the stabilization of water emulsions by asphaltenes, resins, solids, and small surfactants are reviewed and discussed.

Chapter 3 discusses the major techniques used through out this study and the theoretical backgrounds of them.

Chapter 4 compares the interfacial and thin liquid film properties of asphaltenes and their counterpart in bitumen (maltenes). A distinctive stabilization mechanism by asphaltenes was discovered and related to their unique film forming behaviors.

Chapter 5 reveales that the uniques stabilization mechanism of asphaltene is due to a small fraction of asphaltenes which can be extracted using a method proposed. Interfacial and thin liquid film behaviors of these asphaltene fractions are compared and discussed.

Chapter 6 focused on chemistry interrogation of the extracted fraction of asphaltenes in Chapter 5 and model structures of different asphaltene fractions were proposed and compared based on structural data obtained through a suite of chemistry analyses. The interfacial and film forming behaviors of different asphaltene fractions were simulated using Molecular Dynamics Simulation and a stabilization model by asphaltenes was proposed based on these conclusions.

Chapter 7 studied the demulsification mechanism by an EO-PO demulsifier on water in asphaltene solution emulsions.

Chapter 8 introduced a modified Scheludko-Exerowa cell to be used on Thin Liquid Film (TLF) apparatus to allow for dosing of additional component to film forming oil phase in order to study the effect of a selected demulsifier on the film forming property of asphaltenes.

Chapter 9 organized the major conclusions in this thesis and recommended future work.

REFERENCES

---

1. Masliyah, J., Zhou, Z. J., Xu, Z., Czarnecki, J., & Hamza, H. (2004). Understanding water-based bitumen extraction from Athabasca oil sands. *The Canadian Journal of Chemical Engineering*, *82*(4), 628-654.

2. Sanford, E. C., & Seyer, F. A. (1979). Processibility of Athabasca tar sand using a Batch Extraction Unit-role of NaOH. *CIM bulletin*, *72*(803), 164-169.

3. Masliyah.J. Fundamentals of oil sands extraction. Course materials at University of Alberta

4. Romanova, U. G., Yarranton, H. W., Schramm, L. L., & Shelfantook, W. E. (2004). Investigation of oil sands froth treatment. *The Canadian Journal of Chemical Engineering*, *82*(4), 710-721.

5. Long, Y., Dabros, T., & Hamza, H. (2002). Stability and settling characteristics of solvent-diluted bitumen emulsions. *Fuel*, *81*(15), 1945-1952.

CHAPTER 2 LITERATURE REVIEW

2.1 WATER IN OIL EMULSION

The breakup of water-in-oil emulsions requires thorough understandings on the mechanism of their stability. Since the coalescence and coagulation of water-droplets depend on the properties of water/crude oil interfacial films, extensive research has been dedicated to this direction.

It has been reported that, at certain conditions, the interface between crude oil and water can sometimes appear as a 'skin' and prevent coalescence of emulsified water droplets in a crude oil environment. Due to the similar types of surface-active species in the system, the water in diluted bitumen emulsions were found to have very similar behaviors to that of emulsions found in conventional crude oils.

Better understanding of the interfacial properties of the interface was suggested to be the first step towards the solution to these problematic W/O emulsions. The studied emulsion interfacial properties include interfacial tension,[1] viscoelasticity,[2,3] and film compressibility.[4,5] It was widely reported that an interface with higher viscosity, elasticity and compressibility would result in emulsions with much higher stability.[1-5] The interfacial tension describes the energy needed to generate a unit area of new interface, thus a higher interfacial tension value would normally lead to lower emulsion stability.

Although the stability of the emulsion depends on the interfacial film properties, it is still an open question on what species are responsible for influencing the interfacial properties of water in a diluted bitumen system.

Yeung et al. first proposed a visual observation method, called the micropipette technique, to study the water/crude oil emulsion interface at microscopic scale that is close to the real system. It was observed that the aromaticity of the solvent and the dilution ratio can change the properties of the water/oil interface drastically as shown by the images in Figure 2.1.[6]

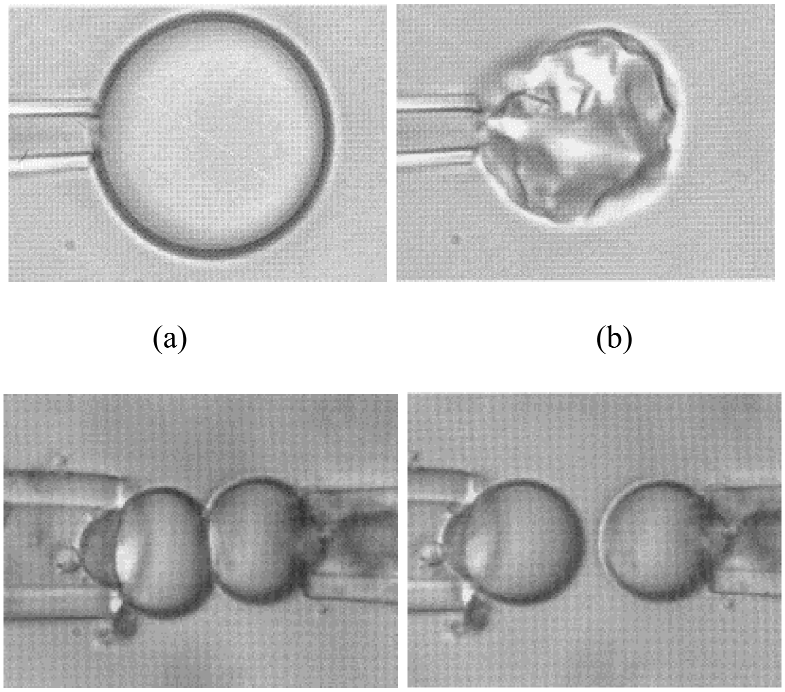

(a) (b)

(c) (d)

Figure 2.1 Steric nature of the oil/water interface (a) expelled water droplet (b) crumple interface when withdrawing water (c) head on head coalescence (d) non-sticky when separate.[7]

By immersing a water filled micropipette into the diluted bitumen in heptol (1:1 mixture of heptane and toluene by volume), a water droplet was expelled at the tip of the pipette. It was observed that below 1% bitumen concentration, the withdrawal of the water droplet back into the pipette would result in a crumpled interface, like a deflated balloon. These authors called this kind of film "rigid" and believed that this film is formed due to the irreversible adsorption of the surface-active species from bitumen. The rigid films were reported to be responsible for the emulsion stability.[8,9]

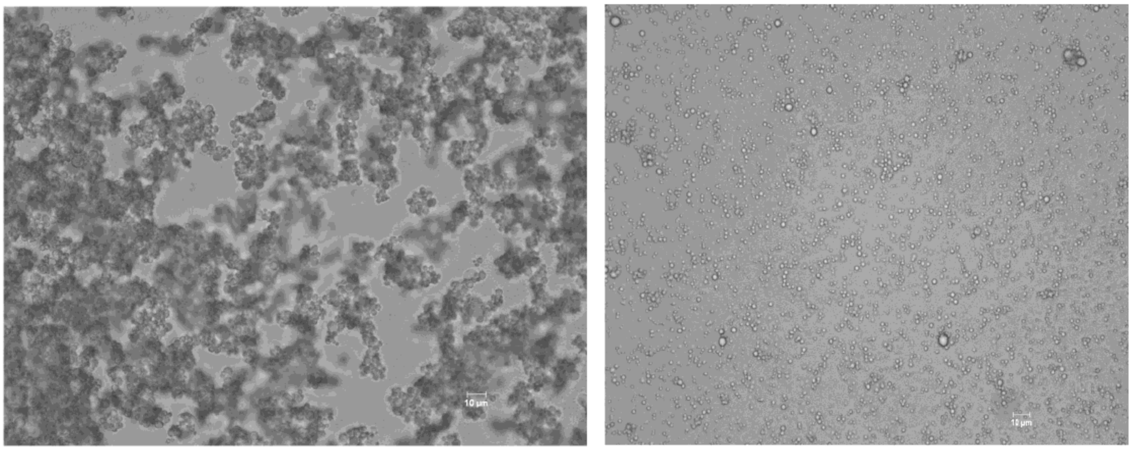

Figure 2.2 Dispersion of water droplets in diluted bitumen (left) clustering with rigid film, (right) dispersed well with non-rigid film. [10]

Using a novel extraction technique, Wu[10] successfully isolated the interfacial materials of the water in diluted bitumen emulsions. Wu reported that the rigidity of the interface is dependent on the types of adsorbed surface-active species, which could be controlled by the bitumen dilution ratios. The characterization of the collected interfacial materials revealed that, with a decrease of solvent to bitumen ratio in heptol, the interface of the emulsions changed from rigid to flexible. While the rigid film was found to be mainly composed of asphaltenes, carboxylic salts were found to be present in the flexible interfaces.

In Wu's study, however, water droplets associated with a rigid interfacial film were found to form clusters, lowering the emulsion stability by flocculation. These results suggest that the surface-active species of bitumen adsorbed at oil-water interface are responsible for changing the rigidity of the interface.

Table 2.1 Summary of IM compositions, interfacial rigidity and Emulsion stability in heptol diluted bitumen.[10]

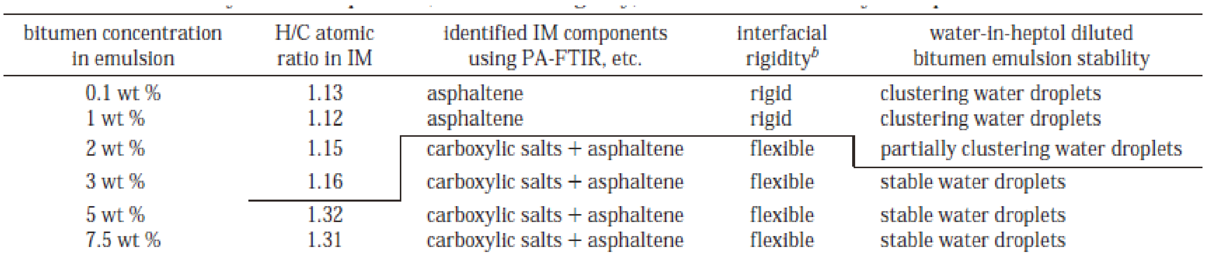

bitumen concentration in emulsion	H/C atomic ratio in IM	identified IM components using PA-FTIR, etc.	interfacial rigidity[b]	water-in-heptol diluted bitumen emulsion stability
0.1 wt %	1.13	asphaltene	rigid	clustering water droplets
1 wt %	1.12	asphaltene	rigid	clustering water droplets
2 wt %	1.15	carboxylic salts + asphaltene	flexible	partially clustering water droplets
3 wt %	1.16	carboxylic salts + asphaltene	flexible	stable water droplets
5 wt %	1.32	carboxylic salts + asphaltene	flexible	stable water droplets
7.5 wt %	1.31	carboxylic salts + asphaltene	flexible	stable water droplets

2.2 WATER-OIL INTERFACIAL FILM INFLUENCED BY DIFFERENT BITUMEN COMPONENTS

It is generally believed that the problematic water-oil interface is caused by the adsorption of surface-active species present in the bitumen. The composition of the adsorption layer depends on system conditions such as surfactant present, solvent aromaticities, dilution ratios, water chemistry, aging time, etc. Generally speaking, the interfacial components in a diluted bitumen system include asphaltenes, resins, and some small surfactant molecules such as naphthenic acids.

2.2.1 Asphaltenes

The role of asphaltenes in emulsion stabilization has been extensively studied and they are considered to be the major emulsion stabilizer among other bitumen fractions. The term ‘asphaltenes’ describes a solubility class in bitumen that is soluble in toluene, but insoluble in alkanes, such as pentane and heptane. Thus, the asphaltene fraction in bitumen contains thousands of different species with varying structures and molecular weights. Generally speaking, asphaltenes are large polyaromatic hydrocarbons composed of polyaromatic rings, aliphatic side chains and heterogeneous atoms such as S, N, O and sometimes, heavy metals such as nickel and vanadium. Figure 2.3 shows a proposed model of asphaltenes structure.

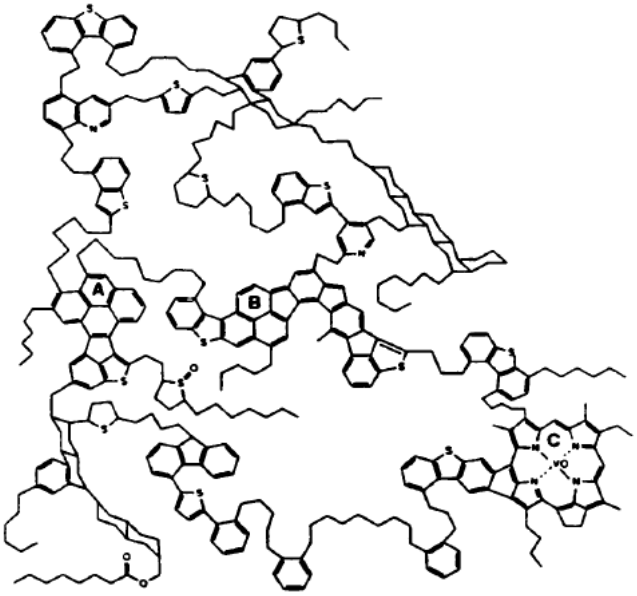

Figure 2.3. Proposed model of asphaltene structures[11]

Although asphaltenes were commonly found to enhance the stability of W/O emulsions, the mechanism of stabilization by asphaltene is still not fully understood. Ortiz et al. suggested that the rigidity of the interface is due to the crosslinking of asphaltene aggregates, which would form when asphaltene molecules stack together on their aromatic cores via lateral intermolecular forces.[12] The drastic change of interfacial property at a critical bitumen concentration coincides with the onset of asphaltenes precipitation concentration. This observation suggests that the property of the film should be related to the dispersion state of asphaltenes in the solvent.[11]

Yarranton et al.[13] found that, in a W/O emulsion stabilized with low concentration of asphaltene solution, the surface area of the emulsified water droplets is solely determined by the amount of soluble asphaltenes. Thus, Yarranton et al. reported that the emulsion stabilizing asphaltenes should be the fractions of asphaltenes that are more solvated but still surface-active. They considered the solvency state of asphaltene in two opposing ways. In a better solvent, the amount of solvated asphaltene is higher but their surface activity is lower, while in a poor solvent, there are less solvated asphaltene molecules but these molecules would have a higher surface activity. Thus, the most stable emulsion should form at a specific aromatic/paraffinic ratio of the solvent.

Dabros et al.[14] suggested that only a fraction of bitumen should be considered as a contributor in emulsion stability problems. These authors reported that with a fraction of bitumen being extracted with the removal of emulsified water from the toluene diluted bitumen, the remaining oil phase was not able to form stable emulsions. Only 2% of the bitumen enriched with polar groups and heterogeneous atoms was found to be responsible for emulsion stabilization.

While asphaltenes were widely acknowledged as the major emulsion stabilizer, other components in the bitumen are also found to influence the emulsion stability. These components include resins,[15] bi-wettable (bitumen-associated) fine solids,[16] and small surfactants such as naphthenic acids.[17]

2.2.2 Bitumen Associated Solids

Among these species, bitumen associated solids are generally considered to assist the stabilization of water-in-diluted bitumen emulsions.[16] These bitumen-associated solids are mostly clays contaminated by the organic materials adsorbed on their surfaces. The wettability of these solids can be drastically changed by the adsorbed species which make the solids to be asphaltene-like so that they tend to travel to the oil/water interface.

By studying model water in oil emulsions, Saukowski and Yarranton found that asphaltenes and solids could both adsorb at the oil/water interface.[18] They reported that the major types of solids adsorbed at the interface are pallet-like clays and the most stable interface was formed when the fractional area coverage ratio of asphaltenes to solids was 2:1. They proposed that the asphaltenes would immobilize the solids on the surface while the solids at the interface would make the asphaltene film more rigid.

Wu characterized the interfacial materials isolated from the w/o emulsion and found the composition of the interface containing 32% of asphaltene and 20.9 % by weight of clay pallets with sizes within 1-3 μm.[19]

Using kaolinite particles with asphaltenes adsorbed to different extent, Yan et al.[20] found that the solids-stabilized oil/water emulsions have higher average droplets size when the hydrophobicity of the particles is increased. They suggested addition of fresh oil droplets to promote the coalescence of the already present oil droplets.

They discussed the mechanism of fresh oil activation based on the hydrophobicity of the solids and their resulting equilibrium position at the oil/water interface.

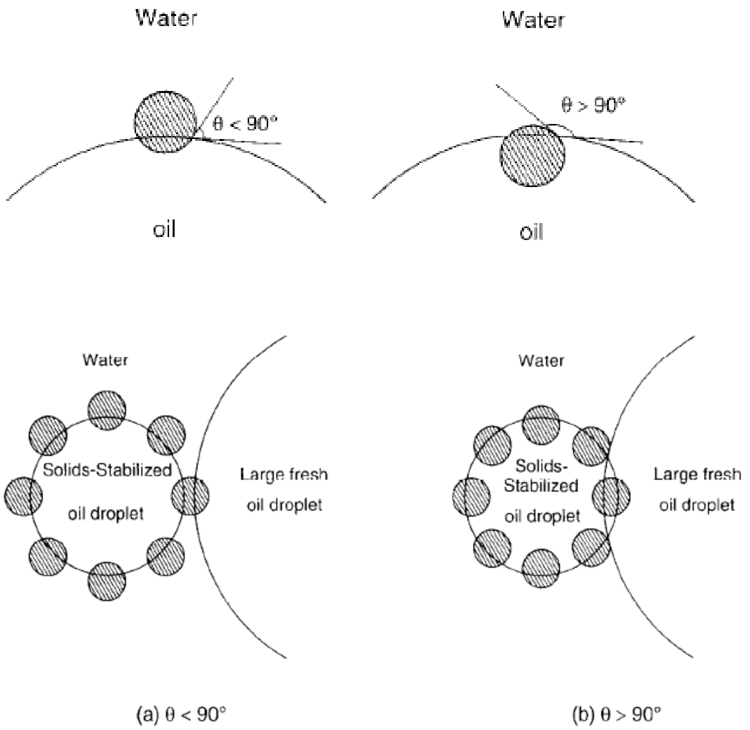

Figure 2.4 Position of solids at the oil/water interface for: (a) hydrophilic solids and (b) hydrophobic solids.[20]

As shown in Figure 2.4, for more hydrophilic solids, the equilibrium could be reached before the surfaces of oil droplets meet as only a small fraction of the solids volume is engulfed by the oil droplets to reach equilibrium. For a more hydrophobic solids however, a large volume of solid particles are engulfed that would result in oil coalescence. Though this is an example of o/w emulsions, the principle introduced here can be applied to w/o emulsions as well.

2.2.3 Resins

The resins are another component from bitumen that can be separated using chromatographic methods. The structure of resins is similar to that of asphaltenes but with smaller molecular weight, higher H/C ratios and less heteroatoms in their structure. As resins have hydrophobic and hydrophilic groups co-existing in the structure, they are also more surface active. While asphaltenes are widely acknowledged as emulsion stabilizer, resins, as for their affinity with asphaltenes, are considered as solublizers of asphaltenes.

Mclean and Kilpatrick studied the change of emulsion stability with the solvency of asphaltenes.[21] They proposed that hydrogen bonding between resins and asphaltenes via the polar functional groups tends to solvate asphaltene aggregates and lower their surface activity, and thus decreasing the emulsion stability.

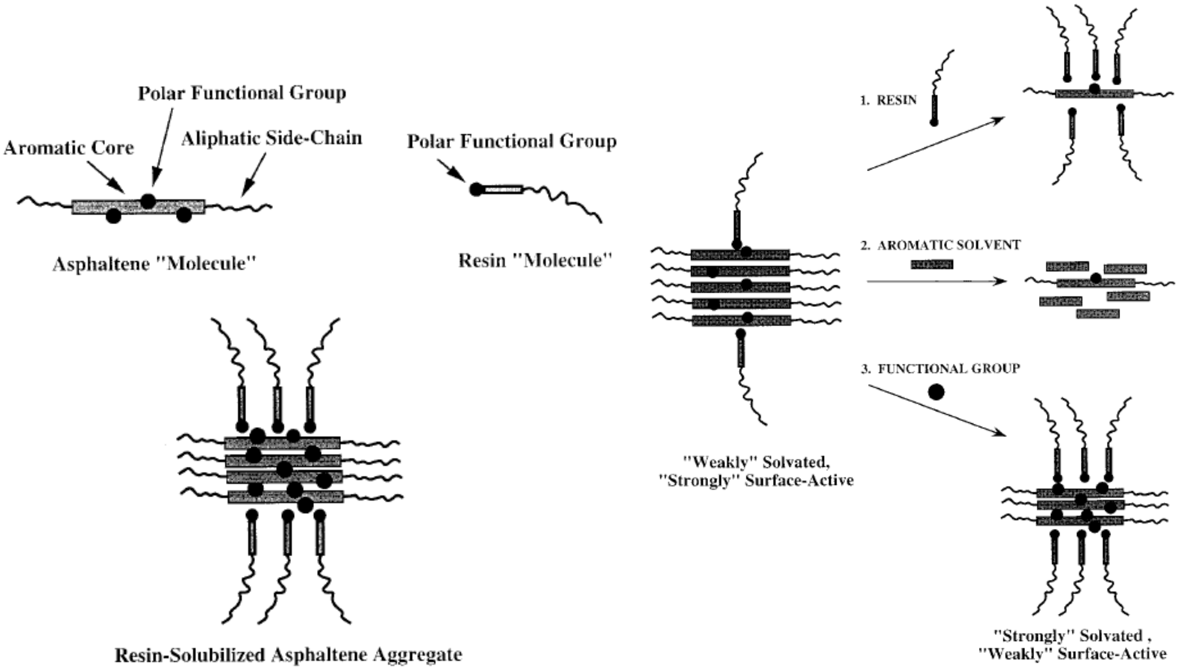

Figure 2.5 Mclean and Kilpatrick's model of aggregated asphaltene in crude oil. [21]

Their model of asphaltene aggregates in a crude oil is shown in Figure 2.5. With their planar structures, the asphaltene molecules would stack with each other via π-π stacking of polyaromatic rings and interactions between polar functional groups while being solvated on the edges by resins.

Yang et al. measured the stability of w/o emulsions containing both asphaltenes and resins using a critical electric field technique. They noticed that asphaltenes-only system would increase the emulsion stability monotonically with aging time while asphaltenes/resins binary system would exhibit a peak value with aging.[22] They suggested that both resins and asphaltenes would move onto the interface but resins tend to replace the adsorbed asphaltenes at the interface due to their higher surface activity and thus reduce the emulsion stability again.

2.2.4 Small Surfactants-Naphthenic Acids

Using the micropipette technique, Moran et al.[17] did series of coalescence tests, each using up to 50 pairs of emulsion droplets in maltene. They showed that the presence of naphthenic acid in maltene tends to "soften" the rigid surface and promote flocculation.

Czarnecki and Moran[23] considered competitive adsorption of asphaltenes and naphthenic acids. They believe that asphaltenes is responsible for the formation of the rigid w/o interface but the adsorption of asphaltenes is slow and irreversible. The smaller surfactants would first occupy the interface, followed by the competition from asphaltene molecules, which would eventually replace them due to their irreversible adsorption.

They used this mechanism to explain the phenomenon that the rigid skin is observed only at a low concentration of bitumen when there are no sufficient surfactant-like molecules to cover the interface.

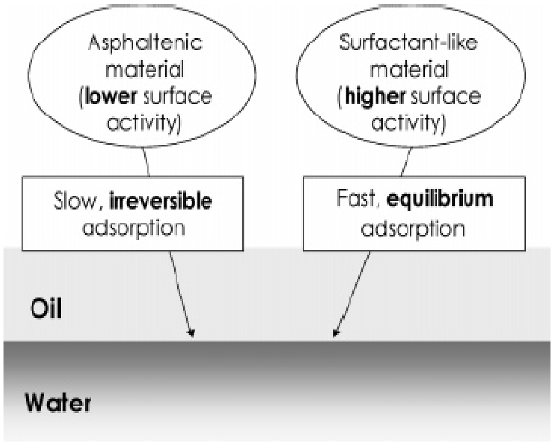

Figure 2.6 Competitive adsorption between asphaltenic material and surfactant like material.[23]

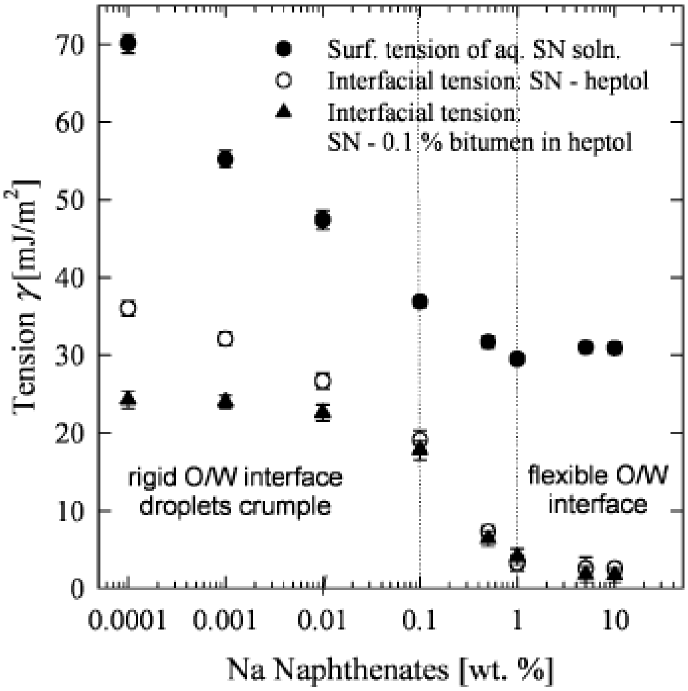

Figure 2.7 Na-naphthenates used as surfactants to block the adsorption of asphaltene onto the interface.[23]

By introducing a high concentration of Na-Naphthenates (above CEC concentration) as the surfactant, they successfully demonstrated that the adsorption of asphaltene onto the interface was blocked. As shown in Figure 2.7 the interfacial tensions are the same for the two systems, one of which has 0.1% bitumen and naphthenates and the other has only naphthenates in the system.

2.3 MODEL COMPOUNDS FOR ASPHALTENES AND NAPHTHENIC ACIDS

As was discussed above, the bitumen composition is very complex and varies with its origin. Many controversies were reported as the result of trying to generalize some common characteristics from studying a whole solubility class. Sjoblom et al. proposed the use of model asphaltene and naphthenic acid compounds as a new approach to study the emulsion problems. [24] With the synthesis of organic compounds of well-defined structures that would fall into the definition of asphaltene or naphthenic acids, they hope to use these synthesized compounds as a tool to understand the emulsion problems caused by indigenous surfactants.

Four kinds of model asphaltene compounds and two kinds of model naphthenic acids were synthesized by Sjoblom et al.[24] to mimic the indigenous asphaltene and naphthenic acids.

The names of these asphaltene compounds were determined by the type of amino acids on each compound as β-alanine (C5), phenylalanine (PA) and tryptophan (TP), and their aromatic perylene cores. The names of the model naphthenic acids were MTAPe10 and MTABP10, indicating that they are model TetraAcids with a perylene core or benzophenone core, respectivly.[24]

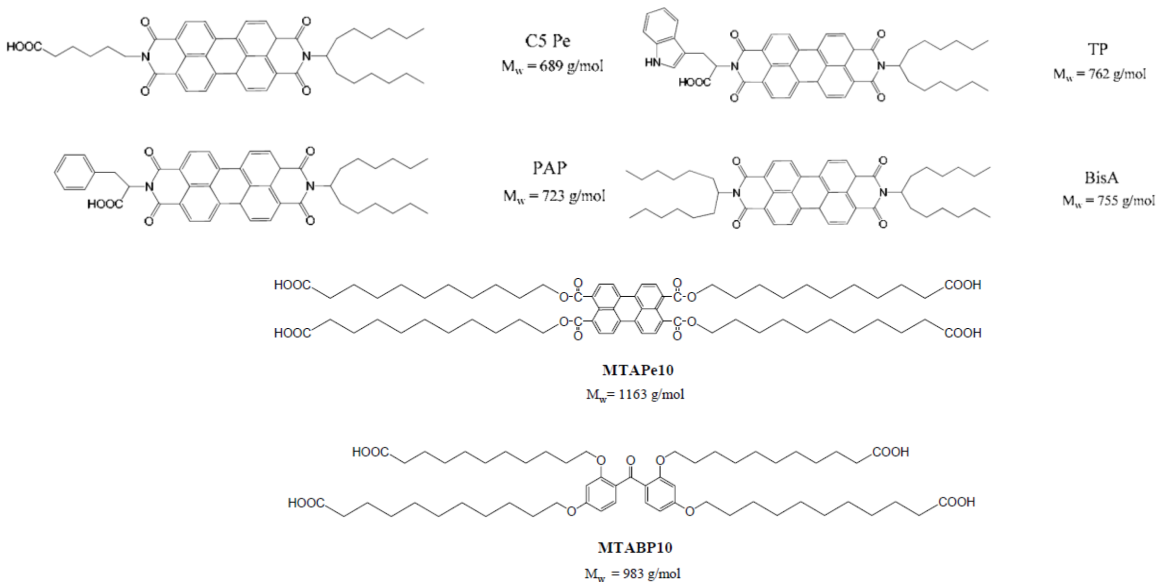

Figure 2.8 Structures and molecular weights of model compounds synthesized by Sjoblom et al. to mimic the indigenous bitumen components. C5Pe, TP, PAP, BisA are model asphaltene compounds, MTAPe10 and MTABP10 are naphthenic acids model compounds. [24]

In order to investigate the resemblance of the model compounds to the corresponding indigenous molecules in heavy oil systems, the interfacial activity of these compounds were characterized by means of interfacial tension measurement at the interface of toluene and water (pH 9).[24] It was found that all of these asphaltene model compounds are very interfacially active, with their surface activity increasing with decreasing aqueous pH. This trend indicates that the surface activity of these compounds is due to the acidic functional groups in the structure. BisA is the only compound that did not show any surface activity, that is probably due to its lack of acid functional groups, even though it has several C=O groups.

By measuring the interfacial tension of chloroform and water at pH 9, the model naphthenic acids compounds were also found to exhibit similar interfacial activities as indigenous naphthenic acids. The surface activities were found at ppm levels of these model compounds.[25]

The asphaltene model compounds were reported to form stable interfacial films between chloroform and water, which resemble the asphaltene film in Langmuir surface pressure-area isotherms.[25] The fluorescence investigation of these films indicated a close proximity of the aromatic cores in the films, suggesting a stacking mechanism via lateral force between polyaromatic rings. The surface activity was also found to be related to the acidic groups, and aggregates of these molecules would show depleted surface activities.[24]

Comparison between C5Pe and PAP in their ability to stabilize emulsions showed that C5Pe is more capable of stabilizing emulsions as it generates smaller emulsion droplets under the same conditions. C5Pe was also found to adsorb more readily to silica surfaces. It was found from the Langmuir interfacial trough investigation that C5Pe is more closely packed at the interface, which is considered to be responsible for the higher emulsion stability in this case.[26]

To sum up, the water in crude oil emulsion stabilization is a very complex phenomenon which involves the adsorption of different bitumen fractions on to the oil/water interface and their resulted interactions on the interface. Different species on the interface translate to different important interfacial parameters, such as interfacial tension, viscoelasticity, compressibility, rigidity, which are going to favor or work against emulsion stability.

REFERENCES

---

1 . Alvarez, G., Poteau, S., Argillier, J. F., Langevin, D., & Salager, J. L. (2008). Heavy oil− water interfacial properties and emulsion stability: Influence of dilution. *Energy & Fuels*, *23*(1), 294-299.

2 . Fingas, M., & Fieldhouse, B. (2009). Studies on crude oil and petroleum product emulsions: Water resolution and rheology. *Colloids and Surfaces A: Physicochemical and Engineering Aspects*, *333*(1), 67-81.

3 . Quintero, C. G., Noïk, C., Dalmazzone, C., & Grossiord, J. L. (2009). Formation kinetics and viscoelastic properties of water/crude oil interfacial films. *Oil & Gas Science and Technology-Revue de l'IFP*, *64*(5), 607-616.

4 . Zhang, L. Y., Lawrence, S., Xu, Z., & Masliyah, J. H. (2003). Studies of Athabasca asphaltene Langmuir films at air–water interface. *Journal of Colloid and Interface Science*, *264*(1), 128-140.

5. Zhang, L. Y., Xu, Z., & Masliyah, J. H. (2003). Langmuir and Langmuir-Blodgett films of mixed asphaltene and a demulsifier. *Langmuir*, *19*(23), 9730-9741.

6. Alvarez, G., Poteau, S., Argillier, J. F., Langevin, D., & Salager, J. L. (2008). Heavy oil− water interfacial properties and emulsion stability: Influence of dilution. *Energy & Fuels*, *23*(1), 294-299.

7 . Yeung, A., Dabros, T., Masliyah, J., & Czarnecki, J. (2000). Micropipette: a new technique in emulsion research. *Colloids and Surfaces A: Physicochemical and Engineering Aspects*, *174*(1), 169-181.

8 . Bartell, F. E., & Niederhauser, D. O. (1949). Fundamental Research on Occurrence and Recovery of Petroleum 1946-47. *American Petroleum Institute, New York*, 57-80.

9. Kimbler, O. K., Reed, R. L., & Silberberg, I. H. (1966). Physical characteristics of natural films formed at crude oil-water interfaces. *Society of Petroleum Engineers Journal*, *6*(02), 153-165.

10 . Wu, X. (2003). Investigating the stability mechanism of water-in-diluted bitumen emulsions through isolation and characterization of the stabilizing materials at the interface. *Energy & Fuels*, *17*(1), 179-190.

11. Taylor, S.D. (2002) Colloidal interactions in water in diluted bitumen emulsions, Thesis for PhD at University of Alberta

---

12 . Ortiz, D. P., Baydak, E. N., & Yarranton, H. W. (2010). Effect of surfactants on interfacial films and stability of water-in-oil emulsions stabilized by asphaltenes. *Journal of Colloid and Interface Science*, *351*(2), 542-555.

13 . Yarranton, H. W., Hussein, H., & Masliyah, J. H. (2000). Water-in-hydrocarbon emulsions stabilized by asphaltenes at low concentrations. *Journal of Colloid and Interface Science*, *228*(1), 52-63.

14 . Xu, Y., Dabros, T., Hamza, H., & Shefantook, W. (1999). Destabilization of water in bitumen emulsion by washing with water. *Petroleum Science and Technology*, *17*(9-10), 1051-1070.

15. Sedghi, M., & Goual, L. (2009). Role of resins on asphaltene stability. *Energy & Fuels*, *24*(4), 2275-2280.

16 . Hannisdal, A., Ese, M. H., Hemmingsen, P. V., & Sjöblom, J. (2006). Particle-stabilized emulsions: effect of heavy crude oil components pre-adsorbed onto stabilizing solids. *Colloids and Surfaces A: Physicochemical and Engineering Aspects*, *276*(1), 45-58.

17 . Gao, S., Moran, K., Xu, Z., & Masliyah, J. (2010). Role of naphthenic acids in stabilizing water-in-diluted model oil emulsions. *The Journal of Physical Chemistry B*, *114*(23), 7710-7718.

18 . Sztukowski, D. M., & Yarranton, H. W. (2004). Characterization and interfacial behavior of oil sands solids implicated in emulsion stability. *Journal of Dispersion Science and Technology*, *25*(3), 299-310.

19. Wu, X. A. (2008). Selective Creaming: A novel technique to isolate interfacial organics and mineral solids from water-in-oil emulsions. *Energy & Fuels*, *22*(4), 2346-2352.

20 . Yan, Y., & Masliyah, J. H. (1993). Solids-stabilized oil-in-water emulsions: scavenging of emulsion droplets by fresh oil addition. *Colloids and Surfaces A: Physicochemical and Engineering Aspects*, *75*, 123-132.

21. McLean, J. D., & Kilpatrick, P. K. (1997). Effects of asphaltene aggregation in model heptane–toluene mixtures on stability of water-in-oil emulsions. *Journal of Colloid and Interface Science*, *196*(1), 23-34.

22. Yang, X., Verruto, V. J., & Kilpatrick, P. K. (2007). Dynamic asphaltene-resin exchange at the oil/water interface: Time-dependent W/O emulsion stability for asphaltene/resin model oils. *Energy & Fuels*, *21*(3), 1343-1349.

23 . Czarnecki, J., & Moran, K. (2005). On the stabilization mechanism of water-in-oil emulsions in petroleum systems. *Energy & Fuels*, *19*(5), 2074-2079.

---

24 . Nordgård, E. L., Landsem, E., & Sjöblom, J. (2008). Langmuir films of asphaltene model compounds and their fluorescent properties. *Langmuir*, *24*(16), 8742-8751.

25 . Nordgård, E. L., Sørland, G., & Sjöblom, J. (2009). Behavior of asphaltene model compounds at W/O interfaces. *Langmuir*, *26*(4), 2352-2360.

26 . Nordgård, E. L., Magnusson, H., Hanneseth, A. M. D., & Sjöblom, J. (2009). Model compounds for C 80 isoprenoid tetraacids: Part II. Interfacial reactions, physicochemical properties and comparison with indigenous tetraacids. *Colloids and Surfaces A: Physicochemical and Engineering Aspects*, *340*(1), 99-108.

CHAPTER 3 THIN FILM DRAINAGE AND THIN LIQUID FILM PRESSURE BALANCE TECHNIQUE

3.1 THIN LIQUID FILM DRAINAGE

While a large amount of work has been performed on the interfacial properties of water in crude oil emulsions, only recently thin emulsion films were investigated in relation to the stability of W/O emulsions.[1,2] When two water emulsion droplets in diluted bitumen come close to each other, the colloidal interaction would force the oil between the two droplets to drain and as a result thin oil film forms. The curvature of the interface would change to a flat disk when the two interfaces are within several hundreds of nanometers. Due to the curvature change, a capillary pressure difference would arise between the film and neighboring Plateau border and further film thinning occurs. Film drainage would eventually lead to its rupture or formation of a stable film due to the stabilizing repulsive surface forces acting in the film (disjoining pressure). Thus, the stability of the thin films controls the coalescence of emulsions. In case of rupturing films, water droplets coalesce to form larger water droplets, which facilitate water removal from diluted bitumen. The described picture of film formation and droplet coalescence is illustrated in Figure 3.1.

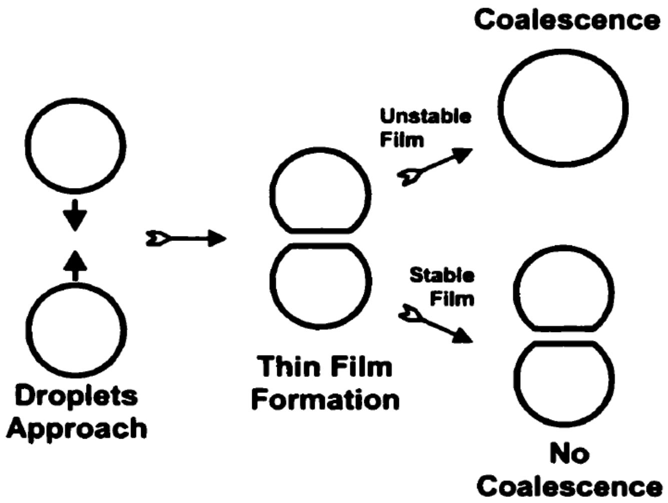

Figure 3.1 Thin film between two water emulsion droplets in oil.[3]

While the properties of the thin liquid films are strongly related to the properties of oil/water interfaces, other factors such as surface forces and hydrodynamics of film thinning are also very important for their stability. These specific film properties cannot be investigated in conventional interfacial experiments or in emulsion studies. However, they are conveniently studied by Thin Liquid Film Technique.[4]

3.2 THE THIN LIQUID FILM PRESSURE BALANCE TECHNIQUE (TLF-PBT)

The Thin Liquid Film-Pressure Balance Technique (TLF-PBT) has been extensively used to study the stability of foams and O/W emulsion systems.[5] Recently this technique was adapted to W/O emulsions.[3] The schematic view of this technique is shown in Figure 3.2.

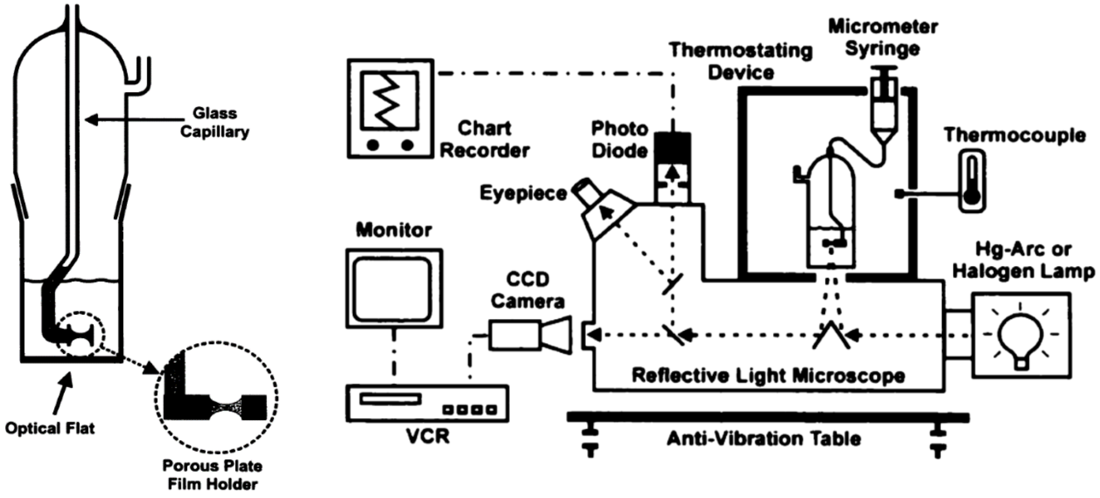

(a) (b)

Figure 3.2 Schematic view of TLF-PBT. [3]
(a) the measuring cell in TLF-PBT (b) the TLF-PBT apparatus setup

In TLF-PBT, thin liquid film is generated in the measuring cell as shown in Figure 3.2 (a). The cell consists of an enclosed chamber in which the pressure is adjustable. A porous plate film holder is soaked in oil and attached to a capillary, which serves as oil phase reservoir. During the experiment, the porous plate holder with a small hole drilled in, is soaked in oil and immersed into an aqueous phase. The oil film is generated at the center of the hole by withdrawing some liquid from the film into the reservoir. The films are observed in reflected light under microscope. Recently, a new version of the TLF-PBT was developed that allows for parallel study of optical and electrochemical properties of water-in-oil emulsion films.[6]

3.2.1 Film Thickness Measurement

From the intensity of monochromatic light reflected from the film, film thickness can be calculated using the equation developed by Scheludko and Platikanov:[7]

$$h = \left(\frac{\lambda}{2\pi n_f}\right)\arcsin\left\{\frac{\Delta}{1+[4N/(1-N)^2][1-\Delta]}\right\}^{1/2} \text{..Eq 3-1}$$

Where $\Delta = (\mathrm{I} - \mathrm{I}_{\mathrm{min}})/(\mathrm{I}_{\mathrm{max}} - \mathrm{I}_{\mathrm{min}})$, $\mathrm{N} = (\mathrm{n}_{\mathrm{f}} - \mathrm{n}_{\mathrm{s}})^2/(\mathrm{n}_{\mathrm{f}} + \mathrm{n}_{\mathrm{s}})^2$, h is the calculated film thickness, I is the intensity of the reflected light from the film, $\mathrm{I}_{\mathrm{max}}$ and $\mathrm{I}_{\mathrm{min}}$ correspond to the maximum and minimum in the light intensity, n_{f} and n_{s} correspond to the refractive indexes of the thin film liquid and the surrounding liquid, respectively, and λ is the wavelength of the monochromic light.

3.2.2 Disjoining Pressure Measurement

For a thin liquid film that had reached equilibrium, the capillary force in the thin liquid film shall be balanced by the disjoining pressure, which is the force between the two approaching surfaces. Thus, according to the force balance in Figure 3.3, the following equation is developed.

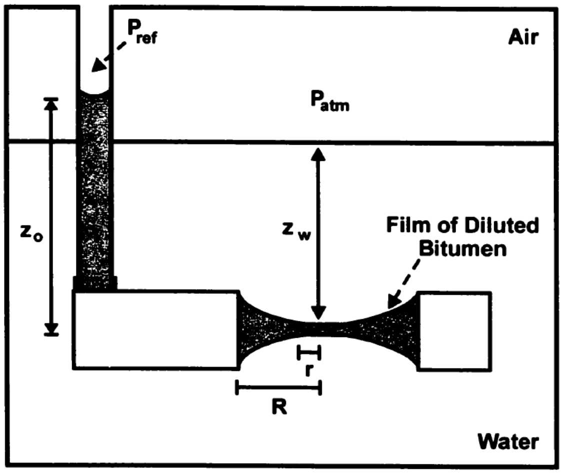

Figure 3.3 Schematic view of the cell and the holder.

$$\pi = P_c = P_{atm} + \rho_w g z_w - \rho_o g z_o - P_{ref} \qquad \text{Eq 3-2}$$

where π is the disjoining pressure, P_c is the capillary pressure, P_{atm} is the atmospheric pressure and P_{ref} is the pressure inside the cell, and ρ_w and ρ_o are the densities of the water and the oil, respectively, and z_w and z_o are the depth of film in water and the height of oil in the capillary, respectively. As $P_{ref} = P_{atm} + P_{applied}$, thus,

$$\pi = P_c = \rho_w g z_w - \rho_o g z_o - P_{applied} \qquad \text{Eq 3-3}$$

The disjoining pressure thus can be evaluated from the applied pressure. As for each applied pressure, a corresponding equilibrium film thickness could be measured if equilibrium is ever achieved. The isotherm of disjoining pressure vs. film thickness is then determined by varying the applied pressure while determining the corresponding thickness of the film.

3.3 REVIEW OF TLF-PBT STUDIES RELATED TO BITUMEN EXTRACTION

Here, a short review of the TLF work related to the bitumen recovery from oil sands is presented. Measurements of film lifetimes and thicknesses have shown that the film behaviour depends on the bitumen concentration and on the aromaticity of solvent used to dilute the bitumen.[2,8] Toluene diluted bitumen films are flexible for most of the cases. In a heptane/heptol diluted bitumen, however, the film behavior would be very different depending on whether it is above and below the so called critical bitumen concentration (where the precipitation happens).[8] Above the critical bitumen concentration, film behavior is similar to that of toluene-diluted bitumen films. Below the critical bitumen concentration however, significant variations in the film thickness is observed despite the prior removal of precipitates from the solution. At this condition, the formation of rigid oil/water interfaces is observed in film experiments. It is worth noting that the reported critical bitumen concentrations in film experiments8 agree with those found in emulsion studies.[9,10] A summary of the conditions at which the rigid interface is formed, and the dependence of the critical bitumen concentration on the aromaticity of the solvent is given in Table 3.1.[8]

Table 3.1 Summary of observed transition from fluid to rigid interfaces in film experiments as a function of solvent aromaticity. The thick line in the table represents the critical S/B as reported.[8]

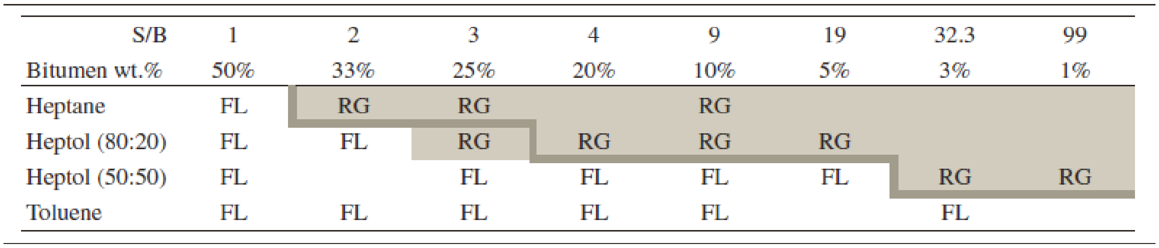

S/B	1	2	3	4	9	19	32.3	99
Bitumen wt.%	50%	33%	25%	20%	10%	5%	3%	1%
Heptane	FL	RG	RG		RG			
Heptol (80:20)	FL	FL	RG	RG	RG	RG		
Heptol (50:50)	FL		FL	FL	FL	FL	RG	RG
Toluene	FL	FL	FL	FL	FL		FL	

These earlier studies have not reported a direct correlation between rigidity of water-in-oil interface and stability of the films. By generating a thin film of heptol diluted bitumen in water, the film was found to be as stable as the film formed with toluene diluted bitumen, even though a rigid water-oil interface would form (Figure 3.4a) when the bitumen concentration is below its critical value. However, after aging and removal of all the precipitated asphaltenes using a centrifuge, a very stable thick homogeneous film is obtained (Figure 3.4b.)

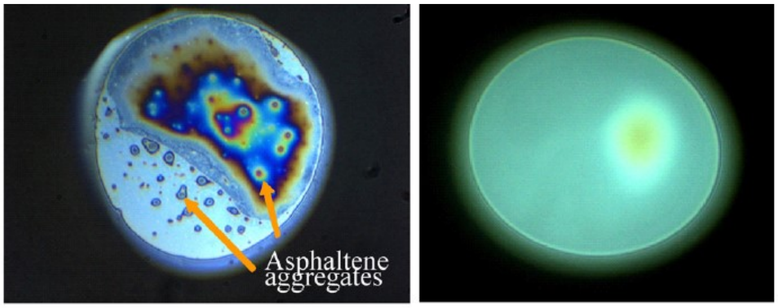

Figure 3.4 Film of 10 wt.% bitumen in heptol of 80:20 heptane to toluene volume ratio. (a) 2.5 h aged water/oil interface - skin formation and secondary precipitates; (b) after extended aging of one night and additional centrifugation of diluted bitumen prior to film experiment – very stable, thick, homogeneous film.[8]

Taylor et al.[11] measured disjoining pressure isotherms of toluene-diluted bitumen and asphaltene emulsion films. These authors found that at high bitumen and asphaltene concentrations films are significantly more stable and films rupture at higher external pressures. The similar disjoining pressure isotherms obtained for toluene diluted bitumen and asphaltene films indicate that the asphaltene fraction of bitumen is most likely responsible for film stability.

REFERENCE

---

1. Khristov, K., & Czarnecki, J. (2010). Emulsion films stabilized by natural and polymeric surfactants. *Current Opinion in Colloid & Interface Science*, *15*(5), 324-329.

2 . Khristov, K., Taylor, S. D., Czarnecki, J., & Masliyah, J. (2000). Thin liquid film technique—application to water–oil–water bitumen emulsion films. *Colloids and Surfaces A: Physicochemical and Engineering Aspects*, *174*(1), 183-196.

3. Taylor, S.D. (2002). Colloidal Interactions in Water in Diluted Bitumen Emulsions", Thesis for PhD at University of Alberta

4. Sheludko, A. (1967). Thin liquid films, *Advances in Colloid and Interface Science*, 1, 391-464

5 . Platikanov, D., Exerowa, D. (2005) Ch. 6. Thin liquid films, In: Fundamental of interface and colloid science, Ed. J. Lyklem, Academic Press, pp. 1-91

6. Panchev, N., Khristov, K., Czarnecki, J., Exerowa, D., Bhattacharjee, S., & Masliyah, J. (2008). A new method for water-in-oil emulsion film studies. *Colloids and Surfaces A: Physicochemical and Engineering Aspects*, *315*(1), 74-78.

7. Scheludko, A., & Platikanov, D. (1961). Utersuchung dünner Flüssinger Schichten auf Quecksiber. *Kolloid-Zeitschrift and Zeitschrift fur Polymere*, *175*(2), 150-158.

8 . Tchoukov, P., Czarnecki, J., & Dabros, T. (2010). Study of water-in-oil thin liquid films: Implications for the stability of petroleum emulsions. *Colloids and Surfaces A: Physicochemical and Engineering Aspects*, *372*(1), 15-21.

9. Long, Y., Dabros, T., & Hamza, H. (2007). Selective solvent deasphalting for heavy oil emulsion treatment. In *Asphaltenes, Heavy Oils, and Petroleomics* (pp. 511-547). Springer New York.

10 . Wu, X. (2003). Investigating the stability mechanism of water-in-diluted bitumen emulsions through isolation and characterization of the stabilizing materials at the interface. *Energy & Fuels*, *17*(1), 179-190.

11. Taylor, S. D., Czarnecki, J., & Masliyah, J. (2002). Disjoining pressure isotherms of water-in-bitumen emulsion films. *Journal of Colloid and Interface Science*, *252*(1), 149-160.

CHAPTER 4 ROLE OF DIFFERENT BITUMEN FRACTIONS IN DRAINAGE OF WATER-IN-CRUDE OIL THIN LIQUID EMULSION FILMS

4.1. INTRODUCTION

Formation of stable water-in-oil (W/O) emulsions is highly undesirable but inevitable in the petroleum industry. Emulsified water, in form of micron sized water droplets, carries dissolved salts, which cause severe corrosion problems for downstream refinery equipment and transporting pipelines.[1] The production of high quality crude oil or bitumen requires cost efficient methods for removal of emulsified water. Despite its critical importance to solving the problem, molecular mechanisms that govern the stability of W/O emulsions in petroleum industry remain unresolved.[2-4] Among the all components of crude oil and bitumen, asphaltenes are generally recognized to play a central role for stabilization of W/O emulsions.[5-7] Although a large number of studies support this view, there is no clear view on how asphaltenes stabilize W/O emulsions. Typical asphaltene molecules cannot be considered to be amphiphilic with well-defined hydrophilic and hydrophobic molecular architecture.[8] Affinity of asphaltenes toward the oil/water interface and their ability to reduce the interfacial tension are lower than that of resins and some other indigenous crude oil/bitumen fractions. Therefore, the asphaltenes cannot stabilize emulsions in the same way as conventional surfactants do, namely, by lowering the interfacial tension, slowing down the drainage of the oil film between droplets through the well-known Gibbs-Marangoni effect and forming an adsorption layer that gives rise to repulsive surface forces preventing droplets coalescence. However, it is well established that asphaltenes form a viscoelastic layer (usually referred to as “rigid” or “skin like”) at oil/water interface.[9,10] This rigid interfacial layer possesses a significant mechanical strength and is commonly considered responsible for stabilizing W/O emulsions. More aliphatic solvent and higher solvent-to-heavy crude oil ratios promote formation of rigid layers at the oil/water interface. While, such rigid layers might prevent the coalescence of water droplets, they also promote the flocculation/coagulation of water droplets that, in fact, facilitate water removal by centrifugation or gravitational settling.[11,12] It should be noted that the formation of rigid oil/water interface is not a prerequisite for emulsion stability, e.g., toluene diluted bitumen form very stable emulsions without any noticeable rigidity of the oil/water interface.[11,13] Most likely different mechanisms are responsible for emulsion stability, depending on the solvent aromaticity and solvent-to-bitumen ratio. Systematic studies on specific contributions of each crude oil/bitumen fraction to stability of W/O emulsion are critical for finding solutions to emulsion stability problems in industrial operations.

The asphaltenes are defined as a solubility class of molecules that are soluble in light aromatics such as toluene and insoluble in alkanes such as pentane or heptane.[14] This definition implies that a large variety of structures and molecular properties such as molecular weight, functional groups, polarity, interfacial activity, are possible within the asphaltene fraction, and only their solubility in aromatic and aliphatic solvents are similar. For example, the average molecular weight of asphaltenes was controversially reported to be in range from few hundreds up to tens of millions of Daltons. Only recently, were more consensual values of 400-1000 Da (average of about 750 Da) accepted.[14] Aggregation behavior of asphaltenes in crude oil is another subject of controversy. Even in good solvents such as toluene, asphaltenes are known to aggregate.[15] In early studies, it was proposed that asphaltenes form micelles which are peptized in the oil by resins.[16] However, as it was pointed out by Buckley et al.[17] and Friberg,[18] the analogy with surfactant micelles is misleading and should not be used for description of asphaltene aggregation. Dickie and Yen [19] and later Mullins et al.[20-22] proposed a hierarchical asphaltene aggregation model driven by π-π stacking of aromatic rings, including formation of nanoaggregates and clusters. Agrawala and Yarranton[23] suggested aggregation model analogous of "linear polymerization" where different functional groups in asphaltene molecule are considered to be active sites, which to link asphaltene molecules. Recently Gray et al.[24] proposed a "supramolecular assembly model", in which the cumulative effect of multiple interactions, including acid-base interactions, hydrogen bonding, metal coordination complexes, aromatic π-π stacking, etc., results in complex asphaltene structures and formation of porous structure of asphaltene aggregates.

To understand the problem of water-in-oil emulsions in oil industry, a variety of experimental techniques have been applied. Probing the emulsion as a whole, e.g., by using "bottle tests", can be very useful in finding appropriate conditions for industrial applications. However, more microscopic and modern approaches are required to probe the underlying molecular mechanisms of emulsion stability. Adsorption behaviour of asphaltenes at oil/water interface and colloidal interactions between water droplets are two important aspects, which have been studied extensively. Czarnecki and Moran [25,26] pointed out that emulsion stability is governed by the competitive adsorption of asphaltenes and low molecular weight indigenous surfactants at oil/water interface. Interfacial dilatation rheology experiments of Freer and Radke[27] and Langmuir trough work performed by Zhang et al.[28,29] showed that asphaltenes adsorb irreversibly at water/toluene interface. With time, asphaltenes at oil/water interface form a compact adsorption layer that cannot be washed with fresh toluene.[28] These interfacial materials do not migrate to water phase. Adsorption of low molecular weight surfactants prevent formation of rigid asphaltene interfacial layers.[25] Similar effect was observed using indigenous naphthenic acids extracted from bitumen [30] and with non-ionic surfactant [31] dissolved in the oil phase.

Direct measurements of micron-size water droplet-droplet interactions have been performed using micropipette[32] and microcollider [33] techniques. Using micropipette technique Gao et al.[34] evaluated stability against coalescence for water droplets in asphaltenes, maltenes and bitumen in heptol 80:20 (a mixture of heptane and toluene at volume ratio 80:20) solutions. They found that water droplets are stable against coalescence in asphaltenes and bitumen solutions above 0.01 wt% concentrations, but coalesce in maltenes solutions over a wide range of concentrations. Studies using atomic force microscopy (AFM) and surface force apparatus (SFA) provided information on the surface forces between asphaltene coated solid surfaces in organic solvents. Using AFM, for example, Wang et al.[35,36] measured forces between asphaltene coated silica in different organic solvents. These authors found a long-range repulsive force of steric nature between asphaltene surfaces in toluene, and van der Waals attraction in poor solvent (heptane). SFA study of Natarajan et al.[37] showed repulsion between two asphaltene coated mica surfaces at separations as far as ~ 40 nm and hard core repulsion at ~ 20 nm.

Whether two approaching water droplets will coalesce or flocculate depend on the properties of the thin oil layer that separates them. Thin liquid film technique (TLF)[38,39] provides a convenient way to directly probe the film properties and interactions between liquid interfaces. An advantage of TLF is the possibility to study both drainage kinetics of thin liquid film and surface forces responsible for film stability. The model system of thin oil film sandwiched between two water phases closely resembles the real situation of W/O emulsions. TLF has been widely used in studies of dispersion systems like foams and oil-in-water emulsions[40] but only recently this technique was adapted to study W/O emulsions. [41] Taylor et al. [42] determined disjoining pressure isotherms of water-in-toluene diluted bitumen films. They reported repulsive forces below 40 nm and bilayer thickness of about 9 nm at high compression. In our previous work,[43] we found that film drainage depends strongly on the type of solvent used (toluene or heptane). In the presence of aliphatic solvent and above a critical solvent-to- bitumen ratio, the film properties change abruptly: film thicknesses increased significantly; aggregates were formed in the film despite the fact that all solutions were centrifuged initially to remove precipitated asphaltenes; and film becomes extremely rigid. To explain these results, we proposed that asphaltenes form a multilayer structure network at the oil/water interface driven by their poor solubility in aliphatic solvents. However, in our previous studies [8,43] the exact role of asphaltenes was masked by the presence of other bitumen fractions.

In this chapter, we used TLF technique to characterize water-in-oil emulsion films obtained from asphaltenes-, bitumen-, and maltenes solutions in toluene. Film lifetimes were measured to evaluate stability of W/O emulsions against coalescence. Film drainage kinetics and equilibrium thicknesses were measured to understand the mechanisms of emulsion stabilization.

4.2. EXPERIMENTAL

4.2.1. Materials

4.2.1.1 Preparation of asphaltenes and maltenes

Asphaltenes and maltenes (deasphalted bitumen) were extracted from Athabasca coker feed bitumen (from Syncrude Canada Ltd.) using pentane. About 20 g bitumen was mixed with toluene (Optima, Fisher Scientific) at a mass ratio of 1:1 and equilibrated on a shaker (Eberbach model 6000) for about 30 min. Then n-pentane (>98%, EMD Chemical Inc.) was added to the mixture at a pentane to bitumen-in-toluene solution mass ratio of 40:1. The mixture was shaken for 30 min and left overnight for the asphaltenes to precipitate and settle. The supernatant was collected and fresh n-pentane was added again to the settled phase at a pentane to settled phase mass ratio of ~ 40:1. The mixture was shaken for 30 min and left to settle overnight before the second batch of supernatant was collected. The precipitated phase was separated using vacuum filtration apparatus with Buchner funnel and Whatman filter paper of grade 50 (2.75μm). The precipitates were washed several times with n-pentane. Each washing involved addition of n-pentane to the precipitated phase, equilibration for 10 min and then vacuum filtration. The filter paper was changed from time to time when the pass-through rate of the liquid was slow. This washing procedure was repeated until the dripping washing solvent became visually clear. After washing, the extracted asphaltenes were collected and dissolved in toluene at a toluene to precipitates mass ratio of 20:1 and centrifuged at 4000*g* for 20 min to remove any solids. The remaining asphaltene-in-toluene solutions were transferred to rotary evaporator to remove the solvent. The asphaltenes dried and were chipped out using liquid nitrogen and kept in a desiccator for 2 days to remove any condensed water. The supernatants collected during the whole process were combined and rotary evaporated to obtain the deasphalted bitumen, known in this study as maltenes.

4.2.1.2 Simulated industrial water

Simulated industrial water, which contains 0.012M $NaHCO_3$, 0.014M NaCl, 0.004M Na_2SO_4 dissolved in Milli-Q water with a resistivity 18.2 MΩ·cm at 25 °C was used in all experiments. The salts from Fisher Scientific were of A.C.S. grade. This water composition gives ionic strength and pH similar to Syncrude recycled plant water. The pH of the aqueous phase was measured to be ~ 8.5. Toluene is slightly soluble in water. We therefore saturated the aqueous phase with toluene in order to prevent possible change in the composition of thin oil film when it was placed in the aqueous phase. For comparison, we also conducted additional experiments with pure deionized water as an aqueous phase. No significant differences in the film behavior between these two different aqueous phases were observed.

4.2.2. Experimental methods

4.2.2.1 Thin liquid film method and setup

Water-in-oil emulsion films were generated in the Scheludko-Exerowa cell. [38,40] A porous glass holder with a 0.8 mm hole was soaked in oil phase and then immersed in the water-filled bottom part of the measuring cell. The films were formed in the center of the hole when the liquid was slowly withdrawn through the capillary until two biconcave meniscuses approached each other. At this point the withdrawal of liquid was stopped and the film size was adjusted to a desired radius of 100 μm by changing the pressure in the cell. The films drained under the pressure differences in the film and neighboring meniscus (due to the curvature) and disjoining pressure in the film, whenever present. The films were observed in reflected light with an inverted microscope (Carl Zeiss Axio Observer). High-resolution and high-sensitivity Leica DFC500 digital camera was used for recording film drainage process. For thickness measurements, HBO lamp was used as a light source, and a low-noise Hamamatsu Si photodiode S8745-01 as a light detector. Pressure was controlled by Hamilton Syringe Drive - PSD/2 and measured by a sensitive pressure transducers from Omega. A custom-build LabVIEW program was used to control the experiment and record the data. The cell was kept at constant temperature (± 0.1 °C). The porous glass plate was made hydrophobic by soaking it for 24 h in 20% dichlorodimethylsilane (> 99.5%, Fluka) solution in cyclohexene (reagent grade, Fisher Scientific).

4.2.2.2 Film thickness measurement

The thickness of thin liquid film was measured using monochromatic light obtained by an interference filter (IF) of 546 nm. The intensity (I) of the light reflected from a small film area (spot diameter about 15 μm) was recorded during film thinning. The film thickness was calculated using the formula proposed by Scheludko and Platikanov [44]:

$$h = \frac{\lambda}{2\pi n_f}\left(m\pi \pm \arcsin\sqrt{\frac{I/I_{\max}}{1+\left[4N/(1-N)^2\right]\left[1-I/I_{\max}\right]}}\right) \tag{1}$$

In eq 1, λ= 546 nm, I_{max} is the light intensity in the interference maximum, m is the order of interference, $N=(n_f-n_s)^2/(n_f+n_s)^2$, where n_f and n_s are refractive indexes of the film liquid and surrounding aqueous phase. The calculated film thickness is referred to as equivalent film thickness of the film and assumes uniform refractive index throughout the film. For very thin films (below 10 nm) a correction for the multilayer structure of the films should be considered with different refractive indexes for each layer. [40] In this work all of the measured films were above 10 nm thick and the correction was not necessary. The equivalent film thicknesses were referred to as the film thicknesses in the text.

4.2.2.3 Film drainage

For thin films stabilized with surfactants, Scheludko[38] proposed that film interfaces could be effectively immobilized due to Gibbs-Marangoni effect and therefore the rate of film thinning,

$V = -\frac{dh}{dt}$, can be described by Stephan-Reynolds equation (SRE) for the squeezing flow between two circular disks:

$$V_{\mathrm{Re}} = -\frac{\mathrm{d}h}{\mathrm{d}t} = \frac{2h^3 \Delta P}{3\mu R^2}, \ \Delta P = P_\gamma - \Pi(h) \tag{2}$$

where μ is the viscosity of film liquid, R is the film radius, and ΔP is the pressure difference driving film drainage. The pressure difference consists of capillary pressure, P_γ, due to shape of the meniscus, and so-called disjoining pressure $\Pi(h)$, that accounts for specific surface forces in thin films. [45] More sophisticated film drainage models that consider a slip at film boundaries, and non-homogenous film thickness during the drainage were discussed elsewhere. [46-48]

4.2.2.4 Other experimental techniques

Interfacial tension between toluene diluted asphaltenes, maltenes or bitumen solutions and simulated industrial water was measured using Krüss drop volume tensiometer combined with Harvard Apparatus 22 syringe pump. A Hamilton syringe of 1000 μl of volume and standard capillary of 0.254 mm inner diameter were used. Flow rate was adjusted to vary the age of oil/water interface. The interfacial tension was measured at room temperature (~ 23 °C). For each concentration and time at least five individual droplets were evaluated and for longer times, 1 h, three droplets were used. The viscosity of solutions was measured at 23.0± 0.1 °C using a Cambridge Applied Systems viscometer with a piston of 0.5-10 cP range. The refractive indexes of oil and aqueous phases required for thickness calculation were measured with Mettler Toledo Refracto 30GS.

4.2.3 Experimental Procedures

For each experiment fresh solutions were prepared from stock solutions of 100 g/L asphaltenes-, maltenes-, or bitumen- dissolved in toluene (Optima, Fisher Scientific). Asphaltene and bitumen solutions were centrifuged at 20,000 *g*, 18 °C for 30 min to remove any fine solid particles. All experiments were performed at (23 ± 0.1 °C). In all film experiments the porous plate was presoaked in the oil solutions for 10 min and then immersed in aqueous phase. After initial water-oil contact the system was left to equilibrate for about 30 - 40 min before any measurements were conducted. The time of initial water-oil contact was recorded to evaluate the ageing effects in film properties. Cells and glassware were cleaned with toluene and acetone in a sonication bath and then dried in a vacuum oven before use.

4.3 RESULTS AND DISCUSSION

4.3.1. Interfacial tension and viscosity

Interpretation of film drainage kinetics data requires information on interfacial tension and viscosity of the systems (see eq 2). Interfacial tension data of water and toluene diluted asphaltene and maltene solutions is shown in Figure 4.1. The results were obtained for one-hour ageing time of oil/water interface, which corresponds to the time scale of film experiments. The results in Figure 4.1 show that the maltenes could reduce the interfacial tension to lower values than asphaltenes at concentration higher than 1 g/L. It is clear that the asphaltenes are not the most interfacially active fraction of bitumen/crude oil and their specific contribution to emulsion stability is unlikely to be related to reduction of interfacial energy of the system.

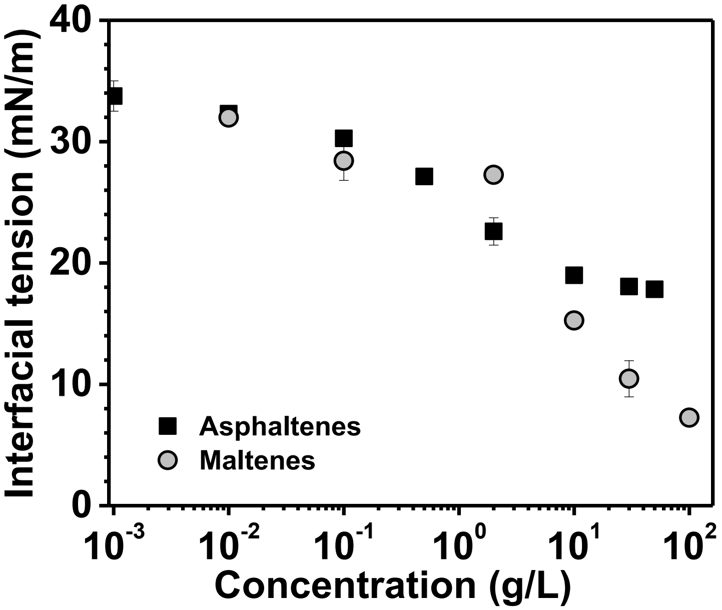

Figure 4.1 Interfacial tension of simulated industrial water - toluene diluted asphaltenes/maltenes solutions. The aging of oil/water interfaces is 1 h (± 5 min).

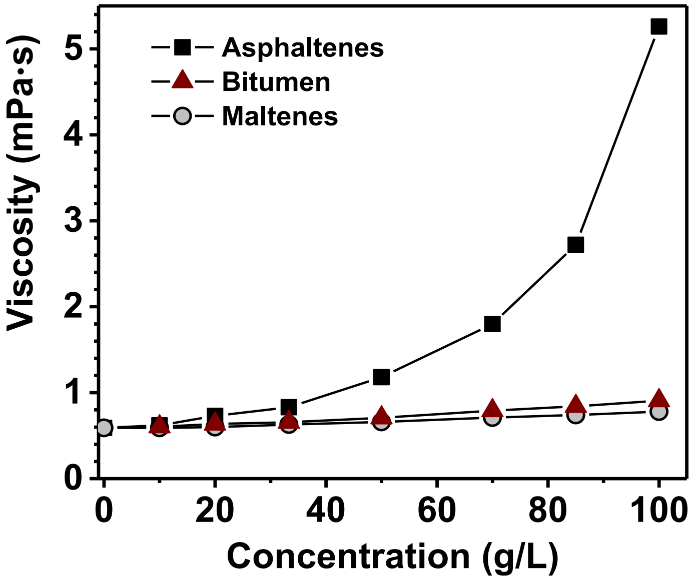

Figure 4.2 Viscosity of bitumen, asphaltenes and maltenes diluted in toluene at 23.0 °C.

The viscosity of asphaltenes, maltenes and bitumen in toluene solutions is shown in Figure 4.2. For a given concentration, asphaltenes in toluene solutions are of higher viscosity than maltenes and bitumen in toluene solutions. If we consider these asphaltene in toluene solutions as diluted colloidal dispersions, the relative viscosity of the dispersion μ_r (defined as a ratio of solution viscosity μ and pure solvent viscosity μ_0) in the first approximation is given by the Einstein equation $\mu_r = 1 + 2.5\,\phi$, where ϕ is the volume fraction of the dispersed phase. Einstein equation is valid for spherical and non-interacting particles. It assumes that the mass, the size and the number density of solute are not affecting the viscosity of the dispersion directly but through the effective volume fraction of dispersed phase. The effective volume includes the volume of the bound solvent. For non-spherical shapes with high axial ratio the effective volume could be much larger than true particle volume.[49] The results in Figure 4.2 show that for the same mass concentration the suspended asphaltenes have much higher effective volume than maltenes. The aggregation of asphaltenes in the solutions and formation of prolonged or porous aggregates as reported in literature [23,24] appears to be the cause for much high effective volume of asphaltenes in toluene solutions.

4.3.2. Film Lifetimes

The dewatering of petroleum emulsions is aided by coalescence of small water droplets into larger drops, which are easier to remove. In thin liquid film experiments stability against coalescence can be evaluated by measuring film lifetime. Film lifetime was measured from the moment of film formation until its rupture (coalescence event). Defined in such a way, film lifetime can be divided into film drainage time (rapid film thickness decrease) and surviving time (negligible film thinning). Films that do not rupture for a certain period of time (25 min) were considered stable against coalescence. The lifetime of films with 100 μm (±10 μm) film radius is shown in Figure 4.3a.

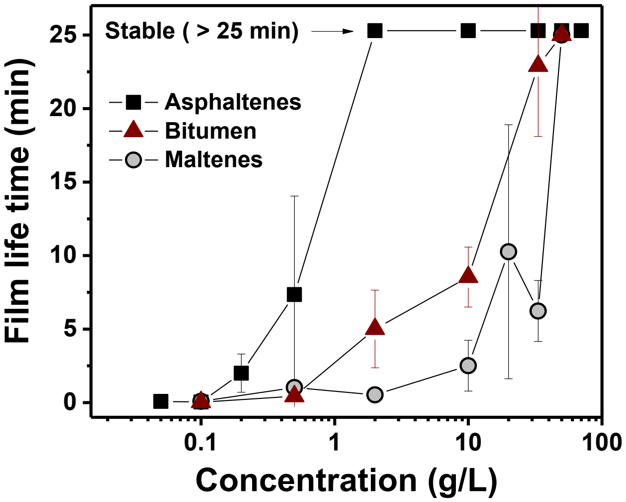

(a)

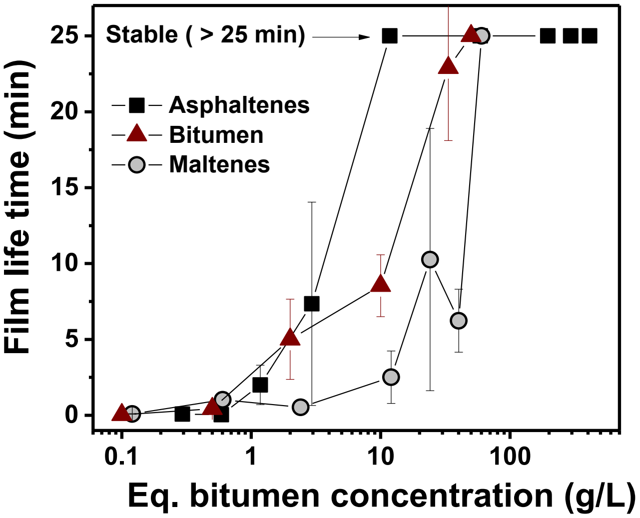

(b)

Figure 4.3 Lifetime of films obtained from asphaltenes, maltenes and bitumen diluted in toluene. The aqueous phase is simulated industrial water. Films that survived for more than 25 min are considered stable. (a) Lifetimes vs. concentration; (b) Lifetimes vs. equivalent bitumen concentration.

In the case of rupturing films, we measured the lifetime for at least of 8 films for each concentration and standard deviations are also shown in the figure as error bars. When the films were stable for more than 25 min, 3-5 films were measured. For concentrations below 0.1 g/L all films ruptured within seconds after their formation. For asphaltene films, film lifetimes increased gradually with the concentration from 0.1 g/L to 2 g/L, at which and above the films were stable up to 25 min. Much higher concentrations, about 50 g/L, were required to obtain stable films from maltenes and bitumen. Recently, Nenningsland et al. [50] reported "critical" asphaltene concentration (defined as transition from unstable to stable emulsions) of water-in-xylene diluted asphaltenes solutions. They used asphaltenes extracted from a crude oil and aqueous phase of pH 8. Xylene is a good solvent for asphaltenes with solubility properties similar to toluene. These authors reported "critical" asphaltene concentration in the range of 0.5 – 1.5 g/L, which is in good agreement with the results reported here for film lifetime. To better understand the role of asphaltenes in stabilizing thin liquid films, the lifetime results are presented in Figure 4.3b in terms of equivalent bitumen concentration, i.e. bitumen concentration that contains the same amount of asphaltenes or maltenes. The Athabasca bitumen used in this study contained 17 wt. % asphaltenes and 83 wt. % maltenes. It is clear that even in terms of equivalent bitumen concentration, the asphaltenes are better stabilizer of W/O emulsions against coalescence than bitumen. It appears that surface active components in maltenes compete with asphaltenes to make the film less stable, which was confirmed in micropipette experiments of emulsified water droplet coalescence by Gao et al. [34]

4.3.3. Evolution and drainage kinetics of films from asphaltene, maltene and bitumen in toluene solutions

Here, for first time we report the data on the drainage kinetics of films made of solutions of asphaltenes and maltenes and results are compared to the drainage of bitumen in toluene films.

4.3.3.1. Bitumen

A typical evolution of 10 g/L bitumen in toluene film is shown in Figure 4.4a. The initial dimple was seen to drain out into the meniscus in less than a minute. After that, toluene-diluted bitumen film continued to thin slowly, which was observed as indicated by the film becoming increasingly darker. The measured evolution of bitumen films thickness with time is shown in Figure 4.5. The thickness was measured slightly off center of the film to avoid the dimple. The experimental data are compared with the thinning kinetics described by SRE (eq 2). The capillary pressure is estimated using $P_\gamma = 2\gamma r/(r^2 - R^2)$, where γ is water-oil interfacial tension, r is the radius of the hole drilled in the porous plate, and R is film radius.[51] The disjoining pressure is neglected in these calculations, i.e. as $\Pi(h)=0$. Considering assumption of $\Pi(h)=0$ and experimental uncertainties, the observed agreement between the measured and SRE predicted film drainage kinetics is remarkable. It should be noted that film behavior did not change with ageing of the oil/water interface within the time frame of our experiment (four hours). These results agree with previous studies [42,43], which also found bitumen-in-toluene films to drain at fluid interfaces without any peculiarities and their thinning kinetics to be reasonably well described by SRE. These are in great contrast to the drainage of bitumen films dissolved in heptane or in heptol. [43,52]

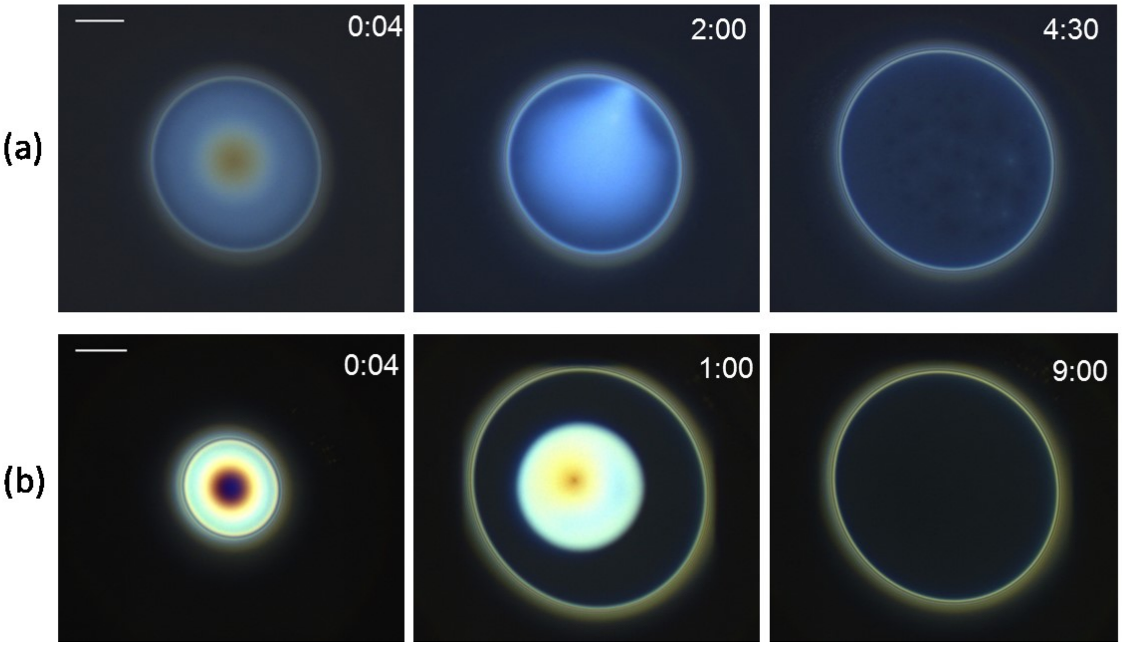

Figure 4.4 Film evolution of water-in-toluene diluted films aged for 1h. (a) 10 g/L bitumen; (b) 10 g/L maltenes. The scale bar is 50 µm and stamps show the time after film formation in minutes:seconds.

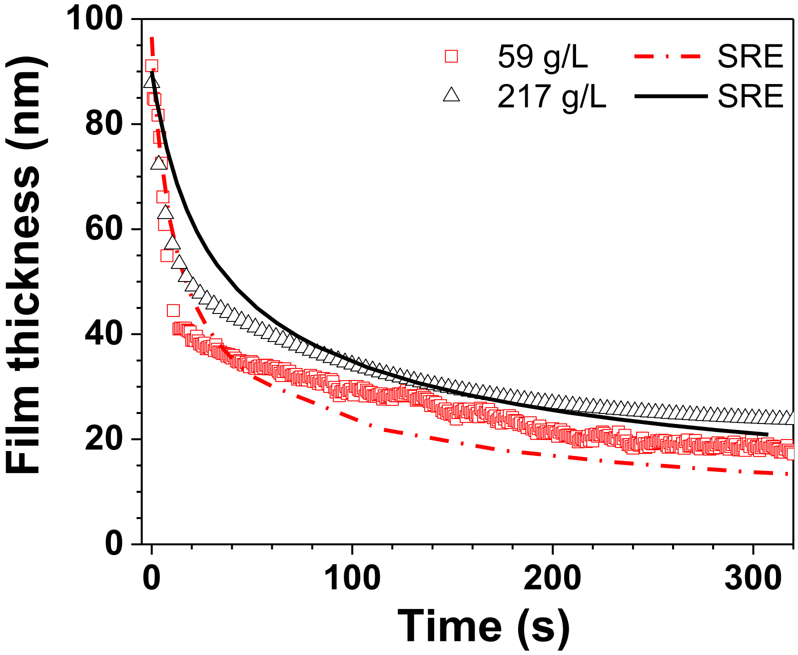

Figure 4.5 Drainage kinetics of water-in-toluene diluted bitumen films. Ageing time is one hour and the film radius is 100 ±10 µm.

4.3.3.2. Maltenes

A typical evolution of 10 g/L maltenes-in-toluene film is shown in Figure 4.4b. Film drainage was much faster than in the case of bitumen, especially in the area of barrier ring (thinner film area around the dimple). Not all of the liquid that was initially in the dimple succeed to drain out. Some liquid remained to be trapped (the white spots in the film). The trapped liquid continued to drain slowly through the barrier ring and disappeared where the entire film became black (last image in Figure 4.4b). The results for the evolution of film thickness in time are shown in Figure 4.6. The drainage kinetics curves were almost identical for all concentrations from 10 g/L to 50 g/L solutions. For lower concentrations of 10 g/L we observed similar film drainage behavior but the film ruptured quickly. The final film thicknesses before rupture were 10 – 11 nm. It is interesting to note that the film at higher maltene concentration reached a similar final film thickness, but remained stable, indicating limited development of film thickness for maltene films. It should be noted that film drainage and final film thicknesses were very reproducible and did not change with ageing of the oil/water interface.

In contrast to bitumen in toluene films, the maltene in toluene film in Figure 4.4b does not drain as plane parallel film but rather shows a transition from relatively thick grey film to black film (denoted with arrow in Figure 4.6) at very early stages of its evolution, before second image in Figure 4.4b. Thus, the observed drainage for maltenes is quite different from that of bitumen films and it is not described by SRE model. Possible explanation for this difference is that with asphaltenes removed from bitumen, the interfaces of maltene-in-toluene films become mobile and films drain faster (especially in the barrier ring). For complete understanding of this drainage behavior future work is required.

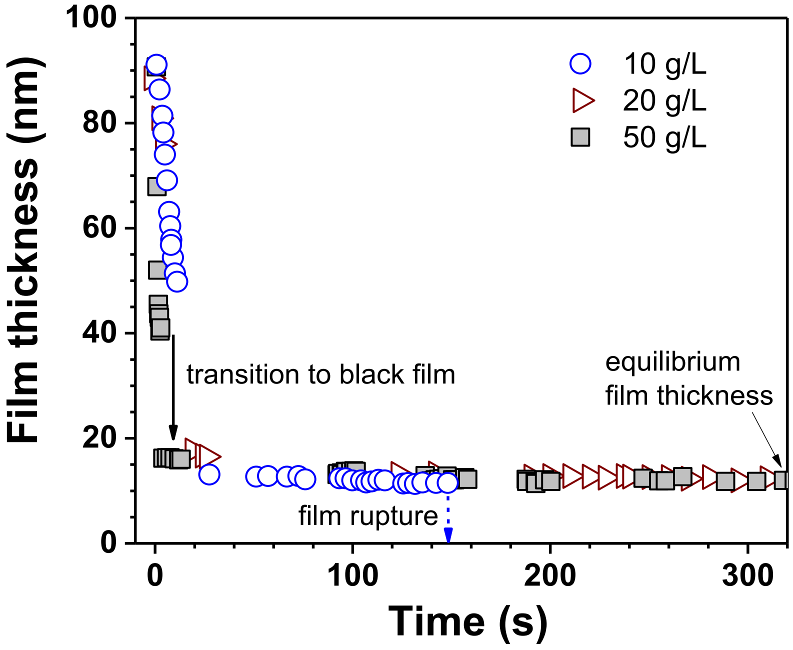

Figure 4.6 Drainage kinetics of water-in-toluene diluted maltenes films. Ageing time is one hour and the film radius is 100 ±10 µm.

4.3.3.3 Asphaltenes

Images in Figure 4.7 show the evolution of film obtained from 10 g/L asphaltene-in-toluene solution. The image sequences presented in Figure 4.7 (a) and (b) are taken in the same experiment at different ageing times. Film in Figure 4.7a is obtained soon after initial contact of oil/water interface (15 min). Films drain relatively slowly. While the background thickness decreases (become darker), small white spots become more visible in the film. These white spots represent thicker areas in the film and most likely they correspond to small aggregates that already exist in the oil film. The lateral size of the white spots in the second image in 7 (a) was about 5 µm. From the pixel intensity of film images in monochromatic light and using eq 1 one can evaluate that thicknesses of these white spots was about 75-80 nm.

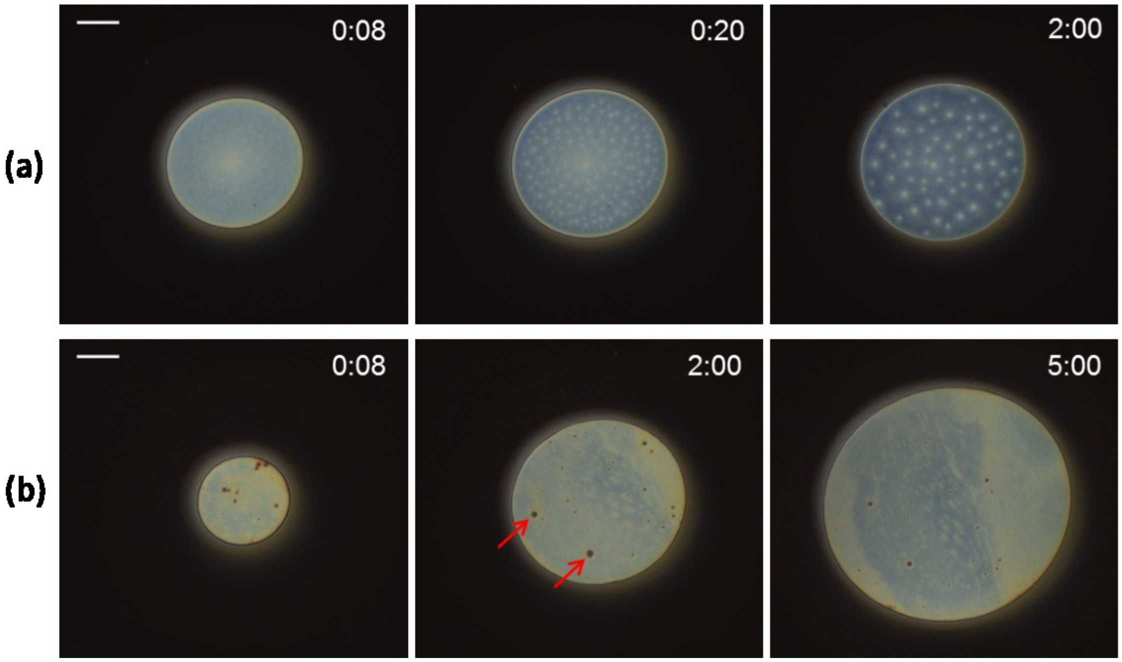

Figure 4.7 Film evolution for 10 g/L asphaltene diluted in toluene. (a) Ageing time 15 min;(b) Ageing time of 1 h. The scale bar is 50 µm and stamps show the time after film formation in minutes:seconds.

These white spots were observed to move slowly in the film, which indicated that they were not anchored to the interface. As film drained, smaller spots merged and formed larger ones, visible in last two images in Figure 7a. The larger spots had diameter about 7.5-12 µm.

After the film featured in Figure 4.7a was closed, the reservoir asphaltene in toluene solution was pumped slowly into the film to a thick oil layer of about 2 mm. The film interfaces were left to rest in contact with aqueous phase. During this ageing time additional material may adsorb to the interfaces or aggregation may continue in the bulk of the oil layer. After certain ageing time (1h in this case) the thin film was formed again and its evolution is shown in Figure 4.7b. These aged films were brighter, which indicates thicker films. The drainage was slower in comparison with case in Figure 4.7a. A few dark dots (see the arrows in Figure 4.7b) represent thicker film areas and most likely correspond to larger aggregates in the film. The diameter and thickness of these dark spots are in the range of 1 - 6 μm and 130 – 180 nm, respectively. These larger aggregates (dark spot) did not move in the film and they appeared to be anchored at the interface. These qualitative observations and size estimations provide a new insight into the aggregation process and increase of film thickness with ageing time. The features discussed above are specific for asphaltenes and were not observed for maltene or bitumen in toluene films.

The ageing effects and variation in film thickness for asphaltene films make measurement of film drainage kinetics more difficult. To avoid some of the complications we started the film thickness measurement before the severe ageing took place (about 40 min after initial oil/water contact). The results for selected concentrations are shown in Figure 4.8. For comparison, the film thinning calculated using SRE ($\Pi(h)=0$) is shown in the figure by dashed lines. The drainage of asphaltene films is much slower than the theoretical prediction of eq 2. Possible explanation for this and drastic discrepancy with theoretical prediction will be explored further in the discussion section.

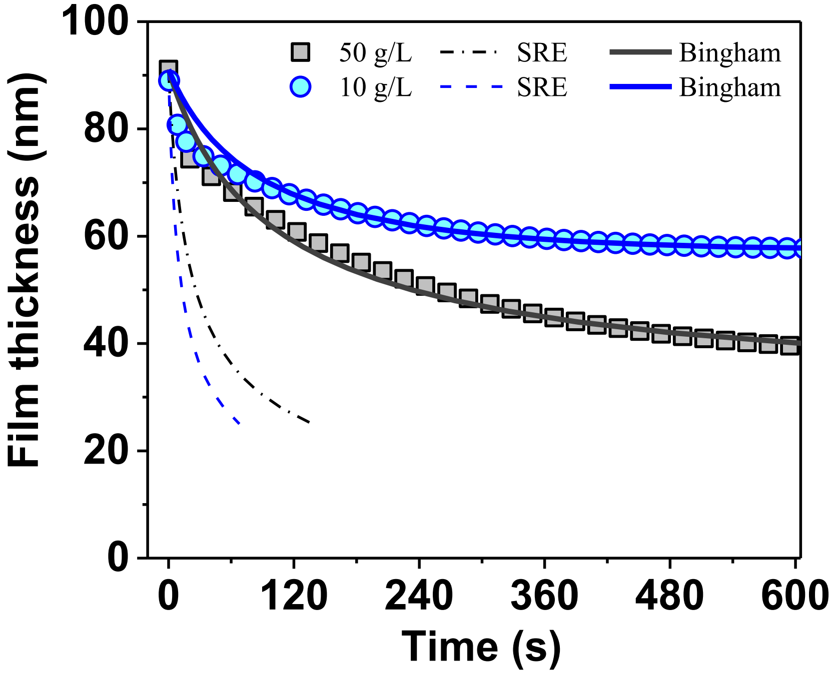

Figure 4.8 Drainage kinetics of water-in-toluene diluted asphaltenes.

4.3.4. Asphaltenes in poor solvent

As discussed above, toluene diluted asphaltene films showed ageing effects. Severe aging and formation of “rigid” interfaces were also reported for films from bitumen diluted in heptane or heptol above the critical solvent-to-bitumen ratio. [43,51] It is believed that the ageing effects and rigidity of interfaces are primarily due to the asphaltenes and their poor solubility in aliphatic solvent. Here, we wanted to probe the effect of solvent property on aging effects and film properties of asphaltene films without interference from other bitumen components. Heptane was added to asphaltenes dissolved in toluene to obtain solution of 10 g/L asphaltenes in 50:50 heptol. When heptane was added, a significant fraction of asphaltenes precipitated and was removed by centrifugation before the experiment. Thus the actual concentration of asphaltenes in 50:50 heptol is determined by its solubility and is lower than the initially prepared concentration of 10 g/L. The images of film evolution are shown in Figure 4.9. From the colored interference patterns one can deduce that the films are much thicker and more inhomogeneous compared to corresponding films of 10 g/L asphaltenes dissolved in toluene (Figure 4.7). Virtually there is little or no drainage in these films. Films aged for 2 h (Figure 4.9b) are thicker, and even more inhomogeneous than those aged for 30 min. Larger aggregates are formed in the film. In this case, the poorer character of the solvent is a much more important factor for the formation of thick and inhomogeneous films and more pronounced ageing in solution. This observation supports the notion these small scale features are solubility driven.

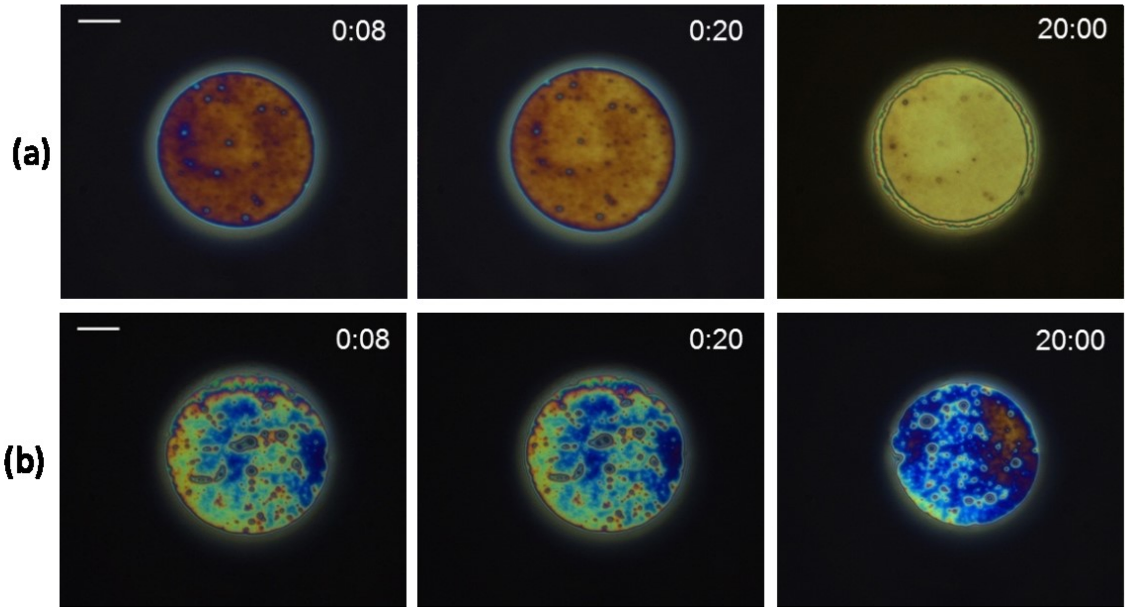

Figure 4.9 Evolution of water-in-oil emulsion film form 10 g/L asphaltenes in heptol 50:50. (a) Age of W/O interface 30 min; (b) Age of W/O interface 2 h. The scale bar is 50 µm and stamps show the time after film formation in minutes:seconds.

4.3.5. Discussion on the role of asphaltenes for stability of W/O emulsions

Our study showed that asphaltenes stabilize emulsion films at much lower concentration than maltenes, producing much thicker films and exhibiting much slower film drainage. More detailed analysis on film drainage kinetics and operative surface forces in the film can provide better understanding of the role of asphaltenes in W/O emulsions stabilization. As shown in Figure 4.8, SRE cannot describe drainage kinetics of asphaltene films while it provides reasonable descriptions of the drainage of bitumen in toluene films (see Figure 4.5). SRE is suitable for describing film drainage of bitumen in heptol solutions below critical S/B ratio[43]. Usual corrections of Stefan - Reynolds model by considering the effect of interfacial mobility at film boundaries [47] and thickness inhomogeneties [46,48] would result in accelerated film drainage kinetics, and therefore cannot explain experimental observations for asphaltenes in toluene films studied here. The theoretical models that are usually applied to describing drainage kinetics of thin liquid films stabilized with surfactants assume Newtonian behavior of the film liquid. However, as we pointed out in our previous work [43,52], the films of bitumen diluted in heptane or heptol above the critical S/B show particularities, which does not conform to Newtonian fluid based models. The observed film features in Figures 4.7 and 4.9 show continuing aggregation of asphaltenes in the films and at oil/water interfaces. Even in a good solvent, such as toluene, asphaltenes are known to aggregate. [20-22] In Figure 4.7a, white spots likely represent small aggregates in the film. From their grain morphology one can corroborate that these are not small dimples of trapped liquid. In fresh films (Figure 4.7a) these white spots move slowly in the films and rearrange in the film, forming relatively flat disk-like flocs (about 70-100 nm thick and about with 5-12 μm diameter). It is plausible to assume that these white spots are loose flocs of asphaltene nanoaggregates as described by Mullins et al. [22] With ageing, the size of the aggregates increases. Some of them become anchored to the interface as shown in Figure 4.7b. Another effect of ageing is that the background film thickness increases as shown in Figures 4.7 and 4.9. This result supports the notion that the asphaltene aggregation for the current system is a continues process, not limited to the formation of small asphaltene nano-aggregates, clusters, flocs and precipitates, as reported in bulk studies, but continue to the development of a 3D network in the confined geometry of thin film between two oil/water interfaces. The possible interactions responsible for formation of such extended network were recently discussed by Gray et al. [24] These authors proposed that asphaltenes form a complex network driven by various interactions, including aromatic π-π stacking, acid-base interactions, hydrogen bonding, metal coordination complexation, etc. Regardless of the exact bonding mechanisms, such self-organization of asphaltenes and formation of an extended network in the films would significantly modify the rheological properties and result in non-Newtonian behaviour of the film fluid. In our previous study [8,43] we have proposed the existence of yield stress in the film liquid as the cause of the observed non-draining dimples in films of bitumen diluted in heptane or heptol above a critical S/B ratio.

Here we will further explore the consequences for film drainage kinetics and emulsion stability if film liquid behaves as a Bingham plastic fluid with a yield stress. A solution of the film drainage for a Bingham plastic fluid was obtained by Hartland and Jeelani. [53] Their results will be used in the discussion here. For a Bingham plastic fluid with yield stress τ_B the relationship between shear stress τ and shear strain $-du/dy$ is given by: $\tau = \tau_B + \mu_B(-du/dy)$ for $\tau \geq \tau_B$; and $0 = \mu_B(-du/dy)$ for $\tau < \tau_B$, where for μ_B is plastic viscosity. For Bingham plastic fluid with yield stress τ_B there will be a minimum thickness, $h_{\min}$, below which the film cannot drain. The $h_{\min}$ is given by

$$h_{\min} = \pi n \tau_B R^3 / 3F , \tag{3}$$

where R is the film radius, F is the force acting on the film, and $n\,(=2)$ is the number of immobile film surfaces. If no external pressure is applied on the film and disjoining pressure is assumed to be negligible at relatively large film thicknesses (40-100 nm for asphaltene films), the driving force for the film drainage is then due to the capillary pressure difference between the film and the neighboring Plateau border, i.e., $P_\gamma = 2\gamma/r$, where γ is interfacial tension and $r\,(= 400\ \mu\text{m})$ the radius of the hole in porous plate. If one knows $h_{\min}$, which is the measured equilibrium film thickness, the minimum yield stress τ_B required to stop film drainage can be calculated using eq 3.

To describe the drainage kinetics of toluene diluted asphaltene films, instead of SRE, we applied an equation derived for planar films with immobile boundaries of Bingham plastic fluid [53]:

$$t = \frac{3\pi n^2 \mu_B R^4}{8 K_1 F h_{\min}^{\ 2}} \left(\ln\left(\frac{1 - h_{\min}/h_i}{1 - h_{\min}/h} \right) - \left(h_{\min}/h - h_{\min}/h_i \right) \right), \tag{4}$$

where t is the time, h_i is the initial film thickness, $K_1 = 3/2$ gives an asymptotic solution when film thickness h approaches the minimum film thickness $h_{\min}$. We used eq 4 to fit the experimental data for drainage of asphaltene films and the results are presented in Figure 4.8 by solid lines. The values for $h_{\min}$ and film radius R were experimentally measured and the driving force was calculated by $F = P_\gamma \pi R^2$. The only fitting parameter was the plastic viscosity μ_B. Using eq 4, we were able to describe the film drainage reasonably well. As shown in Table 4.1, values obtained for plastic viscosity are about an order of magnitude higher than viscosities of the corresponding solutions μ. This is not surprising given the increased asphaltene concentration in proximity of film interfaces and the aggregation of asphaltenes.

Table 4.1 Parameters used in the modeling of asphaltene films drainage.

Conc	P_γ	h_{min}	τ_B	μ_B	μ
g/L	Pa	nm	Pa	mPa·s	mPa·s
10	101	57.2	0.09	6.0	0.62
50	95	34.0	0.05	7.0	1.18

Aggregation of asphaltenes and build-up of a network on the length scale comparable to the film thickness efficiently stabilize the emulsion films. For a film to rupture, the thickness of the film is required to decrease to a critical film thickness, defined as the thickness where surface instabilities with some characteristic length can grow due to favorable decrease in total free energy of the film.[38] For thin films stabilized with surfactants, the film stability is determined by the competition between the local capillary pressure that dumps surface waves and attractive surface forces, $d\Pi/dh > 0$. As discussed above, for thin films that behave as a plastic fluid, the minimum thickness that can be reached is determined by the yield stress of film liquid. Thus, if the film thinning is stopped at higher thickness than the critical thickness due to the development of network with yield stress in the film, the film will then not rupture. Therefore the corresponding emulsion will be stable against coalescence. The critical film thickness for viscoelastic films could be additionally decreased due to additional stabilizing contribution arised from the elastic component that resist the growth of the film instabilities.[54,55]

It should be noted that none of the peculiarities described in the case of asphaltene films were observed for toluene diluted bitumen and deasphalted bitumen films. Films from maltenes in toluene are much thinner and do not age. In Figure 4.10 we present a comparison of film drainage kinetics of asphaltene, bitumen and maltene in toluene films. The concentrations of 10 g/L asphaltenes and 50 g/L maltenes correspond to about 59 g/L equivalent bitumen concentration. To make a link to previous studies, behavior of bitumen films strongly depends on the solvent aromaticity and dilution ratio, [43] and is governed by competitive adsorption of asphaltenes and indigenous surfactant-like components in bitumen. [25] In poor solvents such as heptane or heptol, the aggregation of asphaltene is enhanced. The aggregation dominates interfacial and film properties, forming a gel-like network that stabilizes the emulsion films against coalescence. In the case of bitumen dissolved in good solvent, however, the presence of maltenes limits asphaltene aggregation and buildup of viscoelastic layer at oil/water interface.

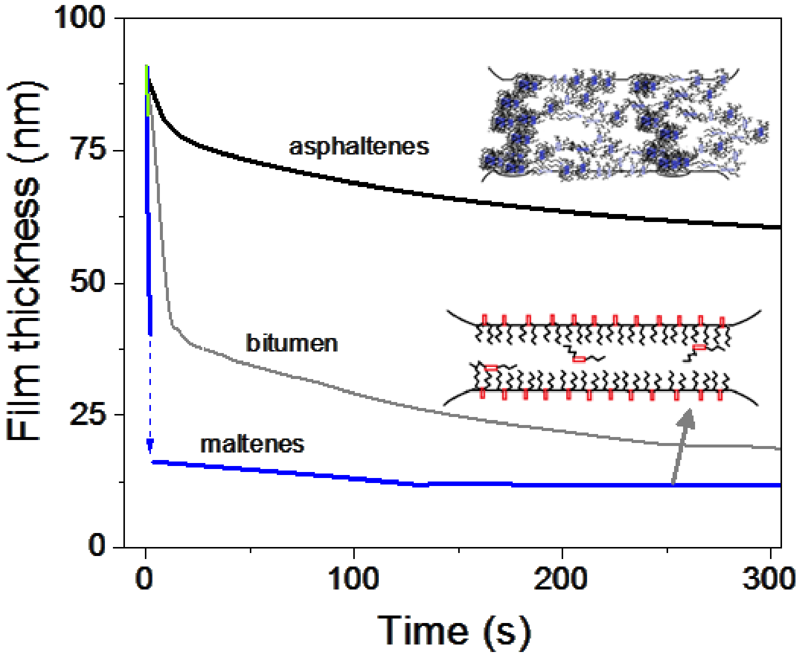

Figure 4.10 Schematic of drainage kinetics of thin films obtained from 10 g/L asphaltenes, 59 g/L bitumen and 50 g/L maltenes dissolved in toluene.

4.4 CONCLUSIONS

Film lifetime is a good measure of stability of water-in-oil films obtained from asphaltenes, maltenes and bitumen dissolved in toluene. Asphaltenes stabilize emulsion films at relatively low concentrations of 0.5 – 2 g/L, while for maltenes and bitumen much higher concentrations of 10 - 50 g/L are required. Equilibrium thicknesses of asphaltene films in the order of 40 - 90 nm are much higher than maltene films of 11 nm thick. Such a large difference in the film thicknesses points to different film structure, operative surface forces and mechanisms of film stabilization. The drainage kinetics of asphaltene films is much slower than that for maltenes and bitumen. The drainage of asphaltene films cannot be explained within the frame of surfactant based models that assume Newtonian behavior for film liquid. Asphaltene films show strong aging effects resulting in a significant increase in thickness and inhomogeneities of thick film profiles. Greater thickness of asphaltene films and significant ageing effect are a result of continuous aggregation of asphaltenes and formation of 3D network at the interface and in the film. The development of such gel like film modifies rheological properties of film fluid, so that the film drainage fits the Bingham plastic film drainage model with yield stress. We showed that the development of yield stress in the film (~ 10^{-2} Pa) can stop the drainage of the film before it reaches the critical thickness, where rupture can occur (coalescence event). For the film of this stabilizing mechanism, a different emulsion breaking strategy to break yield stress using different types of demulsifiers is required.

REFERENCES

1. Masliyah, J., Czarnecki, J., & Xu, Z. (2010). Handbook on Theory and Practice of Bitumen Recovery from Athabasca Oil Sands. *Vol. I. Theoretical basis*.

2. Kilpatrick, P. K., & Spiecker, P. M. (2001). Asphaltene emulsions. *Encyclopedic Handbook of Emulsion Technology*, *3*, 707-730.

3. Czarnecki, J. (2001) Water-in-Oil Emulsions in Recovery of Hydrocarbons from Oil Sands. In *Encyclopedic Handbook of Emulsion Technology;* CRC Press, 497-514.

4. Sjöblom, J., Hemmingsen, P. V., & Kallevik, H. (2007). The role of asphaltenes in stabilizing water-in-crude oil emulsions. In *Asphaltenes, Heavy Oils, and Petroleomics* (pp. 549-587). Springer New York.

5. Yan, Z., Elliott, J. A., & Masliyah, J. H. (1999). Roles of various bitumen components in the stability of water-in-diluted-bitumen emulsions. *Journal of Colloid and Interface Science*, *220*(2), 329-337.

6. Sjöblom, J., Aske, N., Auflem, I. H., Brandal, Ø., Havre, T. E., Sæther, Ø., ... & Kallevik, H. (2003). Our current understanding of water-in-crude oil emulsions.: Recent characterization techniques and high pressure performance. *Advances in Colloid and Interface Science*, *100*, 399-473.

7. Spiecker, P. M., Gawrys, K. L., & Kilpatrick, P. K. (2003). Aggregation and solubility behavior of asphaltenes and their subfractions. *Journal of colloid and interface science*, *267*(1), 178-193.

8. Czarnecki, J., Tchoukov, P., & Dabros, T. (2012). Possible role of asphaltenes in the stabilization of water-in-crude oil emulsions. *Energy & Fuels*, *26*(9), 5782-5786.

9. Dabros, T., Yeung, A., Masliyah, J., & Czarnecki, J. (1999). Emulsification through area contraction. *Journal of Colloid and Interface Science*, *210*(1), 222-224.

10. Spiecker, P. M., & Kilpatrick, P. K. (2004). Interfacial rheology of petroleum asphaltenes at the oil-water interface. *Langmuir*, *20*(10), 4022-4032.

11. Wu, X. (2003). Investigating the stability mechanism of water-in-diluted bitumen emulsions through isolation and characterization of the stabilizing materials at the interface. *Energy & Fuels*, *17*(1), 179-190.

12. Long, Y., Dabros, T., & Hamza, H. (2002). Stability and settling characteristics of solvent-diluted bitumen emulsions. *Fuel*, *81*(15), 1945-1952.

13. Xu, Y., Dabros, T., Hamza, H., & Shefantook, W. (1999). Destabilization of water in bitumen emulsion by washing with water. *Petroleum Science and Technology*, *17*(9-10), 1051-1070.

14. Mitchell, D. L., & Speight, J. G. (1973). The solubility of asphaltenes in hydrocarbon solvents. *Fuel*, *52*(2), 149-152.

15. Mullins, O. C. (2011). The asphaltenes. *Annual Review of Analytical Chemistry*, *4*, 393-418.

16. Pfeiffer, J. P., & Saal, R. N. J. (1940). Asphaltic bitumen as colloid system. *The Journal of Physical Chemistry*, *44*(2), 139-149.

17. Buckley, J.; Wang, J.; Creek, J. (2007) Solubility of the Least-Soluble Asphaltenes. In *Asphaltenes, Heavy Oils, and Petroleomics,* Mullins, O., Sheu, E., Hammami, A., Marshall, A., Eds.;Springer: New York, 401-437.

18. Friberg, S. Micellization. (2007) In *Asphaltenes, Heavy Oils, and Petroleomics*, Mullins, O., Sheu, E., Hammami, A., Marshall, A., Eds.; Springler: New York, 189-203.

19. Dickie, J. P., & Yen, T. F. (1967). Macrostructures of the asphaltic fractions by various instrumental methods. *Analytical Chemistry*, *39*(14), 1847-1852.

20. Buenrostro-Gonzalez, E., Groenzin, H., Lira-Galeana, C., & Mullins, O. C. (2001). The overriding chemical principles that define asphaltenes. *Energy & Fuels*, *15*(4), 972-978.

21. Mostowfi, F.; Indo, K.; Mullins, O. C.; McFarlane, R. (2009) Asphaltene nanoaggregates studied by centrifugation. *Energy & Fuels*, *23,* 1194-1200.

22. Mullins, O. C. (2010). The Modified Yen Model. *Energy & Fuels*, *24*(4), 2179-2207.

23. Agrawala, M., & Yarranton, H. W. (2001). An asphaltene association model analogous to linear polymerization. *Industrial & Engineering Chemistry Research*, *40*(21), 4664-4672.

24. Gray, M. R., Tykwinski, R. R., Stryker, J. M., & Tan, X. (2011). Supramolecular assembly model for aggregation of petroleum asphaltenes. *Energy & Fuels*, *25*(7), 3125-3134.

25. Czarnecki, J., & Moran, K. (2005). On the stabilization mechanism of water-in-oil emulsions in petroleum systems. *Energy & Fuels*, *19*(5), 2074-2079.

26. Moran, K., & Czarnecki, J. (2007). Competitive adsorption of sodium naphthenates and naturally occurring species at water-in-crude oil emulsion droplet surfaces. *Colloids and Surfaces A: Physicochemical and Engineering Aspects*, *292*(2), 87-98.

27. Freer, E. M., & Radke, C. J. (2004). Relaxation of asphaltenes at the toluene/water interface: Diffusion exchange and surface rearrangement. *Journal of Adhesion*, *80*(6), 481-496.

28. Zhang, L. Y., Breen, P., Xu, Z., & Masliyah, J. H. (2007). Asphaltene films at a toluene/water interface. *Energy & Fuels*, *21*(1), 274-285.

29. Zhang, L. Y., Lopetinsky, R., Xu, Z., & Masliyah, J. H. (2005). Asphaltene monolayers at a toluene/water interface. *Energy & Fuels*, *19*(4), 1330-1336.

30. Gao, S., Moran, K., Xu, Z., & Masliyah, J. (2010). Role of naphthenic acids in stabilizing water-in-diluted model oil emulsions. *The Journal of Physical Chemistry B*, *114*(23), 7710-7718.

31. Fan, Y., Simon, S., & Sjöblom, J. (2010). Interfacial shear rheology of asphaltenes at oil–water interface and its relation to emulsion stability: influence of concentration, solvent aromaticity and nonionic surfactant. *Colloids and Surfaces A: Physicochemical and Engineering Aspects*, *366*(1), 120-128.

32. Yeung, A., Dabros, T., Masliyah, J., & Czarnecki, J. (2000). Micropipette: a new technique in emulsion research. *Colloids and Surfaces A: Physicochemical and Engineering Aspects*, *174*(1), 169-181.

33. Wu, X., Laroche, I., Masliyah, J., Czarnecki, J., & Dabros, T. (2000). Applications of colloidal force measurements using a microcollider apparatus to oil sand studies. *Colloids and Surfaces A: Physicochemical and Engineering Aspects*, *174*(1), 133-146.

34. Gao, S., Moran, K., Xu, Z., & Masliyah, J. (2009). Role of bitumen components in stabilizing water-in-diluted oil emulsions. *Energy & Fuels*, *23*(5), 2606-2612.

35. Wang, S., Liu, J., Zhang, L., Xu, Z., & Masliyah, J. (2008). Colloidal interactions between asphaltene surfaces in toluene. *Energy & Fuels*, *23*(2), 862-869.

36. Wang, S.; Liu, J.; Zhang, L.; Masliyah, J.; Xu, Z. (2010) Interaction forces between asphaltene surfaces in organic solvents. *Langmuir***,** *26,* 183-190.

37. Natarajan, A., Xie, J., Wang, S., Liu, Q., Masliyah, J., Zeng, H., & Xu, Z. (2011). Understanding molecular interactions of asphaltenes in organic solvents using a surface force apparatus. *The Journal of Physical Chemistry C*, *115*(32), 16043-16051.

38. Sheludko, A. (1967). Thin liquid films. *Advances in Colloid and Interface Science*, *1*(4), 391-464.

39. Platikanov, D.; Exerowa, D. (2005) Thin liquid films. In *Fundamentals of Interface and Colloid Science Soft Colloids*; Volume 5; Lyklema, J., Ed.; Academic Press, 1-91.

40. Exerowa, D.; Kruglyakov, P. M. (1998) *Foam and Foam Films;* Elsevier: New York.

41. Khristov, K., Taylor, S. D., Czarnecki, J., & Masliyah, J. (2000). Thin liquid film technique—application to water–oil–water bitumen emulsion films. *Colloids and Surfaces A: Physicochemical and Engineering Aspects*, *174*(1), 183-196.

42. Taylor, S. D., Czarnecki, J., & Masliyah, J. (2002). Disjoining pressure isotherms of water-in-bitumen emulsion films. *Journal of Colloid and Interface Science*, *252*(1), 149-160.

43. Tchoukov, P., Czarnecki, J., & Dabros, T. (2010). Study of water-in-oil thin liquid films: Implications for the stability of petroleum emulsions. *Colloids and Surfaces A: Physicochemical and Engineering Aspects*, *372*(1), 15-21.

44. Scheludko, A.; Platikanov, D. (1961) Utersuchung dünner Flüssinger Schichten auf Quecksiber. *Kolloid Z.,175,* 150-158.

45. Israelachvili, J. N. (1992) *Intermolecular and Surface Forces;* Academic Press: London.

46. Manev, E., Tsekov, R., & Radoev, B. (1997). Effect of thickness non-homogeneity on the kinetic behaviour of microscopic foam film. *Journal of Dispersion Science and Technology*, *18*(6-7), 769-788..

47. Radoev, B. P., Dimitrov, D. S., & Ivanov, I. B. (1974). Hydrodynamics of thin liquid films effect of the surfactant on the rate of thinning. *Colloid and Polymer Science*, *252*(1), 50-55.

48. Ruckenstein, E., & Sharma, A. (1987). A new mechanism of film thinning: enhancement of Reynolds' velocity by surface waves. *Journal of Colloid and Interface Science*, *119*(1), 1-13.

49. Pal, R., & Vargas, F. (2014). On the interpretation of viscosity data of suspensions of asphaltene nano-aggregates. *The Canadian Journal of Chemical Engineering*, *92*(3), 573-577.

50. Nenningsland, A. L., Gao, B., Simon, S., & Sjöblom, J. (2011). Comparative study of stabilizing agents for water-in-oil emulsions. *Energy & Fuels*, *25*(12), 5746-5754.

51. Exerowa, D.; Ivanov, I.; Scheludko, A. (1964) In *Issledovaniya v oblasti poverkhnostnykh sil;* Nauka: Moscow, 158.

52. Czarnecki, J., Tchoukov, P., Dabros, T., & Xu, Z. (2013). Role of asphaltenes in stabilisation of water in crude oil emulsions. *The Canadian Journal of Chemical Engineering*, *91*(8), 1365-1371.

53. Hartland, S., & Jeelani, A. K. (1987). Drainage in thin planar non-newtonian fluid films. *The Canadian Journal of Chemical Engineering*, *65*(3), 382-390.

54. Sharma, A. (2003). Many paths to dewetting of thin films: anatomy and physiology of surface instability. *The European Physical Journal E*, *12*(3), 397-408.

55. Tambe, D. E., & Sharma, M. M. (1991). Hydrodynamics of thin liquid films bounded by viscoelastic interfaces. *Journal of Colloid and Interface Science*, *147*(1), 137-151.

CHAPTER 5 ASPHALTENE SUB-FRACTIONS RESPONSIBLE FOR STABILIZING WATER-IN-CRUDE OIL EMULSIONS - INTERFACIAL BEHAVIORS

5.1 INTRODUCTION

During production of crude oil or bitumen, stable water-in-oil emulsions are unavoidably formed. To effectively break such stable emulsions, fundamental understanding of the role of different oil (bitumen) fractions in emulsion stabilization is required. It is now generally accepted that among all the heavy oil components, including resins, naphthenic acids, fine solids etc., asphaltenes are the single most important emulsion stabilizing component.[1-9] Asphaltenes have been found to form aggregates in the bulk[10,11] and a rigid, "skin-like" layer[12] at the oil/water interface, providing mechanical strength that prevents coalescence of emulsified water droplets in the crude oil environment. It was suggested that the interfacial rigidity is due to the crosslinking of asphaltene aggregates.[3,13,14] Recently, Czarnecki et al.[15-17] argued that the general belief that the whole asphaltene fraction is responsible for emulsion stabilization, and the wide use of SARA terminology[18] in the emulsion stability context are in fact impeding the progress in understanding petroleum emulsions stability. These authors suggested that "only a small fraction of asphaltenes are in fact involved in the emulsion stabilization". Support for this notion can be found in a number of studies. Dabros and coauthors[19] performed a series of "washing" experiments to evaluate the amount of specific fractions of bitumen involved in stabilization of water-in-diluted bitumen emulsions. Bitumen washing experiments were performed by repeatedly emulsifying increased amounts of water in diluted bitumen and removing the emulsified water by centrifugation, while evaluating the stability of the subsequent emulsions. With this approach, these authors estimated that less than 2% of the total weight of bitumen is in fact responsible for emulsion stabilization. The typical asphaltene content in Athabasca bitumen used in their study was about 17 wt.%. Based on this fact, the authors concluded that only a small fraction of the total asphaltenes in bitumen was responsible for emulsion stabilization. Wu [20] developed an elegant method of collecting interfacial material (IM) accumulated at the oil/water interface in a heavy water (D_2O)-in-diluted bitumen emulsion. The interfacially active material extracted from diluted bitumen was characterized by Stanford et al. using electrospray ionization Fourier transform ion cyclotron resonance mass spectrometry (ESI FT-ICR MS).[21,22] These authors compared the relative abundance of several selected chemical classes containing oxygen and sulfur (OS classes) in the whole bitumen, IM, asphaltene and resin fractions. It was found that the IM collected from the water droplets emulsified in diluted bitumen at different solvent-to-diluted bitumen ratios was different from asphaltenes, resins, and their parent bitumen. Independent of the abundances of O_2 and O_4S species available in the parent oil, the O_2 and O_4S species were enriched in the IM fraction together with nitrogen-containing cationic species. These results indicate that the real contributor to water-in-oil (W/O) emulsion stability is most likely a specific asphaltene sub-fraction, and further sub-fractionation of asphaltenes in studying the stability of petroleum water-in-oil emulsions could be critically important to better understand the W/O emulsion stabilization mechanism. Most existing work on the fractionation of asphaltenes in relation to emulsion stability separates asphaltenes based on their solubility and polarity by precipitating different fractions of asphaltenes from solvents of different aromaticity and/or increasing dilution ratios.[13,23] Using such an approach, Spiecker et al.[23] found that the less soluble asphaltene fractions are stronger emulsion stabilizers. However, to understand the stabilization mechanism, it is more instructive to fractionate asphaltene molecules based on their interfacial activity and emulsion stabilization potential. To our knowledge, there is no previous work that extracts the most interfacially active fraction of asphaltenes from the whole asphaltenes by isolating the interfacial material from emulsified water droplets and characterizes their interfacial properties in the context of emulsion stability. As mentioned earlier, a similar approach has been applied to the whole bitumen and provided valuable information.[19] The characterization of such interfacially active sub-fraction of asphaltenes will provide better understanding of particular molecular structures and functional groups that are most important for emulsion stabilization.

Another parameter that needs better understanding but is often neglected is the property of thin liquid films between emulsion droplets. When two approaching water droplets are within a small distance, a flat intervening liquid film forms between them. This film consists of two oil/water interfaces and a thin oil core. Emulsions remain stable when the repulsive disjoining pressure between the two interfaces is sufficiently strong to counter-balance the capillary pressure from the deformation of the droplets. The coalescence between water droplets is a two-step process, consisting of film drainage (a) and film rupture (b). These two steps are conveniently studied using Thin Liquid Film (TLF) technique.[24,25]

TLF technique has been used extensively in studying the stability of foams and oil-in-water emulsions. [24] Recently this technique was adapted[26] and applied to water-in-crude oil emulsions. [17,26-30] Previous TLF work provided some important insights into the mechanism of emulsion stabilization. It was shown that for a water-in-diluted bitumen system, film properties changed abruptly at a critical solvent-to-bitumen (S/B) dilution ratio, which depended on the aromaticity of the solvent used. [28] Interestingly, the critical S/B ratio was often found to coincide with the onset of asphaltene precipitation. In addition, films stabilized by asphaltenes were different from those stabilized by bitumen and de-asphalted bitumen in a few aspects.[30] (1) Asphaltenes formed stable films at much lower concentration (0.5 - 2 g/L) than bitumen and de-asphalted bitumen films (10 - 50 g/L). (2) The drainage of asphaltene films was found to be significantly slower than the drainage of films obtained from maltenes (deasphalted bitumen) or from its parent-bitumen. (3) The films stabilized by asphaltenes were much thicker (40 - 90 nm) than the maltene films (~10 nm). (4) The ageing of film, an observation that the film became thicker and rigid with time, was a characteristic feature of asphaltenes-in-toluene films only and was not observed for maltene- or bitumen-in-toluene films. All these differences in film properties were believed to be related to the aggregation propensity of asphaltenes and their ability to form a “gel-like” network structure, resulting the formation of thicker and stable films.[17,28,30] It was proposed that a complex intermolecular interactions and bonds including acid-base interactions, hydrogen bonding, metal coordination complexes, pi-pi stacking, etc., were involved in the aggregation of asphaltenes.[31] To better understand the characteristics and chemical structures of asphaltene species that are responsible for emulsion stabilization, it is instructive to further fractionate the asphaltenes that accumulate at the oil-water interface and characterize the structural and interfacial properties of such sub-fraction.

In this chapter, we propose a new method to separate whole asphaltenes into two sub-fractions based on their potency of partition at the oil-water interface. The emulsion stabilization capacity and interfacial behavior of these asphaltene sub-fractions were characterized using TLF technique, bottle tests, and Langmuir trough experiments. The results obtained shed light on the role of asphaltene sub-fractions in emulsion stabilization mechanism.

5.2 MATERIALS AND EXPERIMENTAL METHODS

5.2.1 Extraction of Asphaltene Sub-fractions.

The protocol of interfacial material extraction is schematically shown in Figure 5.1. Asphaltenes were extracted from Athabasca coker feed bitumen (Syncrude Canada Ltd.) following the procedures described elsewhere.[30,32] Briefly, asphaltenes were precipitated from coker feed bitumen using excessive amount of n-pentane (40:1 by volume) and further washed extensively with pentane. These asphaltenes were then separated into two fractions using the method described below. 10 g/L asphaltene-in-toluene solution was prepared followed by the addition of 10% (v/v) of deionized water. The mixture was then homogenized at 30,000 rpm for 5 min using a homogenizer (Power Gen 1000, Fisher Scientific). The resultant emulsion was shaken on a mechanical shaker (E5900, Eberbach) for 24 hours to equilibrate the water/oil interface before centrifugation at 20,000 *g* to separate the stabilized emulsion drops from the continuous oil phase. No free water was resolved during the centrifugation and the water remained encapsulated as stable emulsion drops in the form of a cake after centrifuging. After removing the supernatant, the cake was carefully pipetted into a separate jar containing 80 mL fresh toluene to remove entrapped asphaltene-in toluene solutions or asphaltene species loosely bounded to the interface. The cake-toluene mixture was gently shaken by hand and the sample was left undisturbed to allow the re-dispersed droplets to settle. The washing procedure was repeated until the supernatant appeared colorless. Typically, 6 to 7 rounds of washing were required to ensure that only the interfacially active fraction of asphaltenes remained at the oil-water interface. During the washing, no visible bulk water was observed, indicating that the low-shear hand mixing was insufficient to drive drop-drop coalescence. The washed emulsion droplets were then transferred to a pre-weighed jar and placed in a vacuum oven at 60 °C to evaporate the water and remaining solvent. After evaporation, the resulting asphaltene sub-fraction was collected and named as interfacially-active asphaltenes (IAA). On the other hand, the concentration of asphaltenes remaining in the supernatant of the original emulsions was measured by spraying 5 ml of the supernatant onto a pre-weighed filter paper and measured the weight gain of the filter paper after evaporation of the solvent. The IAA samples and remaining asphaltene (RA) in toluene solutions (supernatant collected above the cake) were then re-dissolved into fresh toluene at different concentrations and used throughout the study.

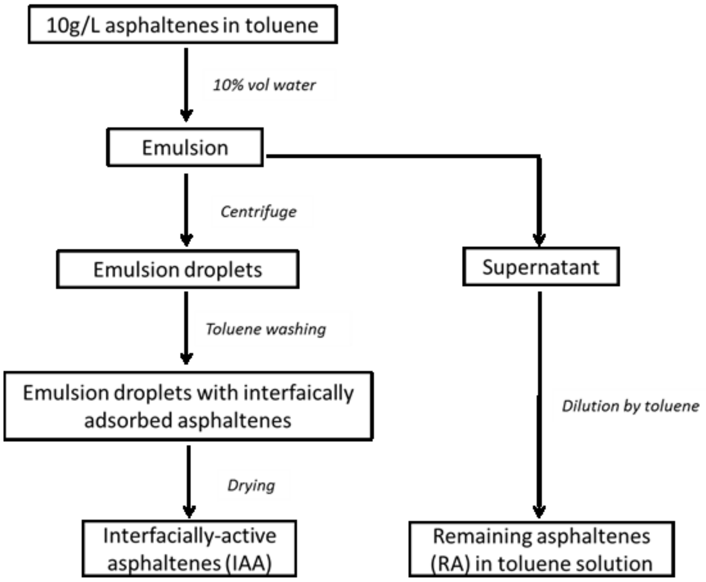

Figure 5.1 Procedures for isolation of interfacially active asphaltenes from whole asphaltenes.

The following terminology to describe different asphaltene fractions is used throughout the chapter: Whole asphaltenes (WA) refers to the asphaltenes extracted from bitumen using 40:1 n-pentane addition; IAA refers to the interfacially-active asphaltenes extracted by the separation of water droplets from water-in-oil emulsion; RA refers to the asphaltene fraction remaining in the supernatant after extraction of IAA. It needs to be noted that the terms of IAA and RA are defined by this specific procedure. It is possible that some species sharing the property of IAA remained with the RA fraction.

5.2.2 Bottle tests.

The effect of removing the IAA fraction from WA on the stability of W/O emulsions was studied by bottle tests. The W/O emulsion was made by dispersing 20 mL of DI water into 100 mL of 10 g/L asphaltene in toluene solution using a homogenizer (Power Gen 1000 Fisher Scientific) operating at 30,000 rpm for 5 min. The water content in the prepared emulsion was 18.7 wt.%. The stability of the emulsion was evaluated by measuring the change of water content of emulsion samples (approximately 200 μg) taken at 1/8 of the total sample height with settling time, using a Coulometric Karl Fisher titrator (Cou Lo 2000, GR Scientific, UK).

5.2.3 Interfacial Tension.

Interfacial tension measurements were conducted using a DVT-10 drop volume tensiometer (Krüss, Germany). The setup included a glass tube and a small bore tungsten carbide capillary tip (inner diameter 0.25 mm) attached to a gas-tight syringe. To measure the interfacial tension, the glass cell was filled with water while small oil droplets were expelled from the capillary tip at controlled flow rates using a micro-syringe pump (Harvard Apparatus, USA). Interfacial tension γ is calculated at the moment when the oil drop detached from the capillary tip using equation $\gamma = V(\rho_W - \rho_O)g/2\pi r$, where ρ_w is the density of DI water, ρ_o is the density of oil phase, V is the volume of the oil droplet and r is the radius of the capillary tip. During the measurement, the oil flow rate was adjusted such that the oil drop would detach from the tip at desired ageing time.

5.2.4 Interfacial Pressure – Area ($\pi - A$) isotherms.

Interfacial pressure – area isotherms were collected using a Langmuir mini-trough (KSV, Finland). The instrument consists of a 2-compartment (liquid-liquid) trough and two symmetrical barriers made of hydrophilic Delrin®. The water/oil interface is located at the intersection between the two compartments. Before each measurement, the trough and the barriers were washed multiple times with toluene and acetone until the trough was considered clean. The cleanness of the trough was determined by a surface pressure change of less than 0.2 mN/m upon a full compression of DI water-air interface. For each compression ($\pi - A$) isotherm, 120 mL of DI water was pipetted in the lower compartment of the trough, followed by placing a lighter oil phase composed of 100 mL toluene and 100 µL of 1.0 g/L asphaltene in toluene solution on top of the water layer. The interface was left to equilibrate for 30 min before the compression was initiated. The compression speed was controlled at 10 mm/min and the interface was compressed from the maximum area of 170 cm^2 to the minimum area of 12 cm^2. All compression isotherms were obtained under room temperature.

5.2.5 Thin Liquid Film Technique.

An oil film enclosed by water (mimicking a thin liquid oil film formed between two water droplets in W/O emulsion) was generated in a Scheludko-Exerowa cell[24,25] as shown in Figure 5.2. A porous glass holder with a 0.8 mm hole was first soaked in the oil solution for 10 min and then immersed in the water-filled measuring cell. An oil film was formed in the center of the hole as the oil solution in the hole was slowly withdrawn through the capillary using a gas tight syringe pump. Once the thin film was formed, the pressure in the measuring cell was adjusted by a micro-syringe to obtain the desired film radius of ~100 µm. The film remained undisturbed and allowed to drain under capillary pressure due to the curvature of the interface in neighboring meniscus. Using an Axio Observer inverted microscope (Carl Zeiss, Germany) the films were observed in reflected light. A high-resolution and high-sensitivity DFC500 digital camera (Leica, Germany) was used to take the film images. Film thickness was evaluated using interferometric technique.[24,25] A custom LabVIEW program was used to control the experiment and acquire the data. Details on the method and experimental setup can be found elsewhere.[24-26,28] The cell was kept at constant temperature (23 ± 0.1 °C). The porous glass plate was made hydrophobic by soaking for 24 hours in 20% dichlorodimethylsilane (> 99.5%, Fluka) in cyclohexene (reagent grade, Fisher Scientific) solution. Both fresh liquid films (generated immediately after immersing the porous plate in water), and aged liquid films (generated after aging the water/oil interface for 30 min) were studied.

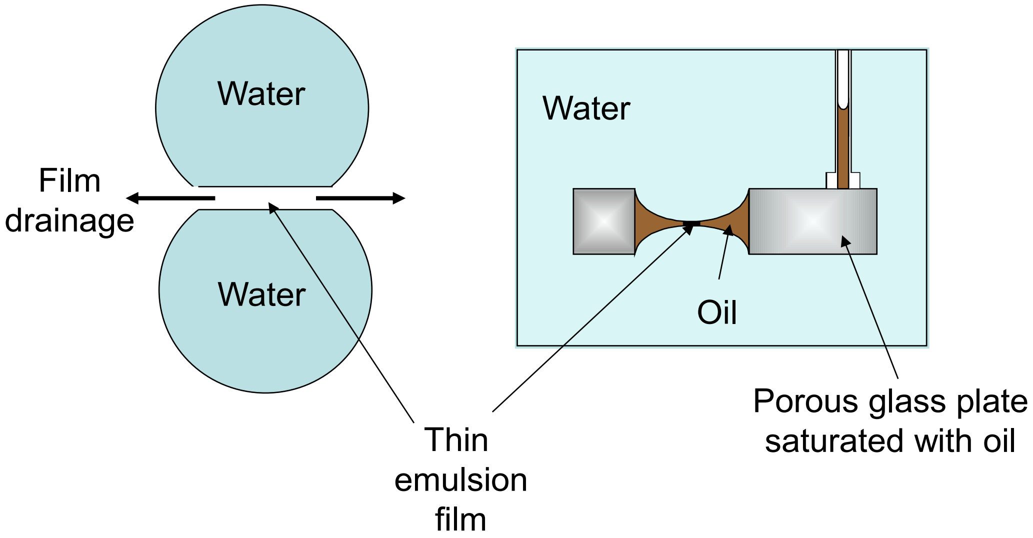

Figure 5.2 Schematics of the thin liquid film (TLF) technique.

5.3. RESULTS

5.3.1. Emulsion Stability

The effect of removing the IAA fraction from WA on the stability of W/O emulsions was studied by bottle tests. W/O emulsions were prepared from the original 10 g/L asphaltenes-in-toluene solution and 18.7 wt.% water as described in section 5.2. The water content was measured at different time intervals and results are shown in Figure 5.3 as percentage reductions in water content relative to the total amount of water initially present. After the measurement of water content of the top phase in the original emulsion for 4 hours, the emulsion was left to settle overnight. Clear separation between the cake of water droplets at the bottom of the tube and top oil phase was established. The supernatant with a negligible amount of water was collected. The asphaltene content remained in the supernatant was evaluated by spraying 5 mL of the supernatant onto a pre-weighed filter paper, followed by evaporation of the solvent in the fume hood at room temperature for 4 hours and weighing the weight gain of the filter paper. The amount of asphaltenes removed by oil/water interface was calculated from the difference between the asphaltene content of the supernatant and the initial asphaltene content in the solution. The rest of the supernatant was then subjected to another round of washing with water using the same procedures as described above to see the effect of subsequent removal of IAA fraction on the emulsion stability. Supernatant-I and supernatant-II refer to the supernatants collected after the first and second washing, respectively. The reduction of water content in these washed supernatants due to gravity setting was compared with that in the original solution in Figure 5.3. The microscopic images of water droplets in the samples collected from the cake at the bottom of the tubes for the cases of original asphaltene-in-toluene solution, Supernatant-I and Supernatant-II are shown in Figure 5.4. To gain more information on coalescence after removal of IAA fraction, the size distribution of water droplets in the bottom cake was determined.

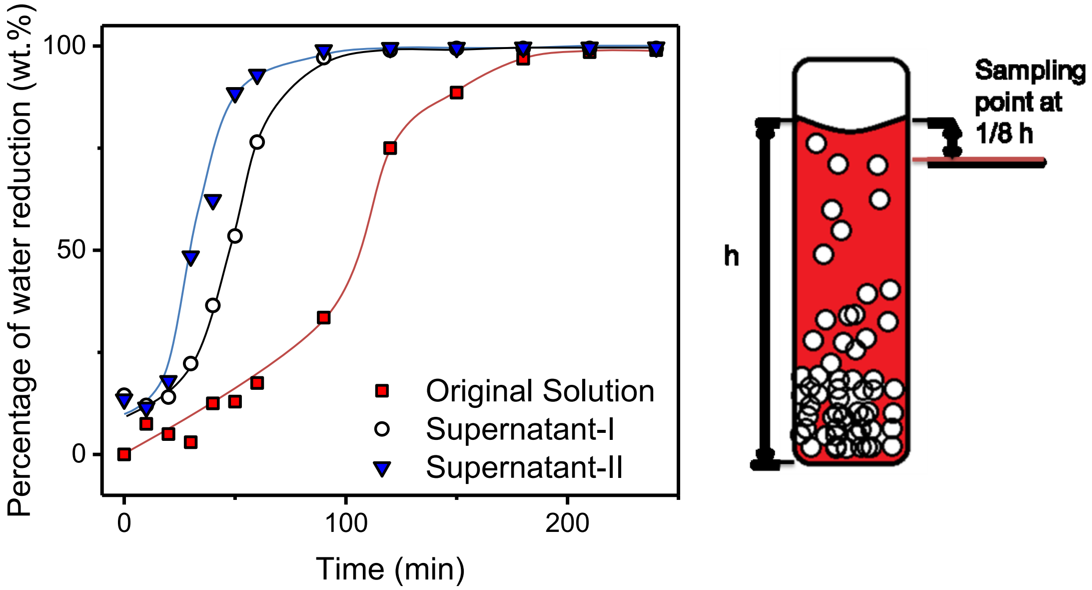

Figure 5.3 Reduction of water content as a function of settling time of emulsions made with original asphaltene-in-toluene solution (10 g/L in toluene), Supernatant-I and Supernatant-II. All emulsions were prepared to the same initial water content of 18.7 wt.% with the only difference being the consecutive water washing of the oil phase.

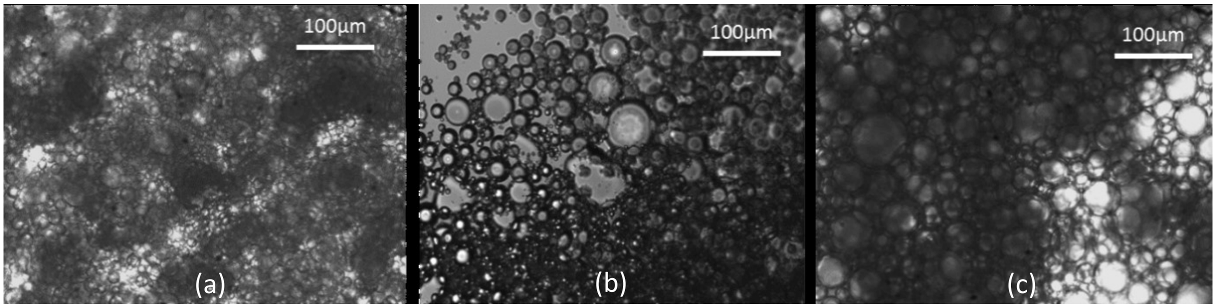

Figure 5.4 Microscopic images of the settled water droplets from: (a) asphaltene-in-toluene solution, (b) supernatant-I, and (c) supernatant-II.

The asphaltene concentration in supernatant-I and -II indicated that 1.8 wt. % of the total asphaltenes was removed during the first water wash. Additional amount of asphaltenes (~ 2 wt. %) was removed during the second wash. From the emulsion stability tests, it was shown that after removal of the first 1.8 wt.% asphaltenes, the stability of the emulsions prepared in supernatant-I decreased significantly. While 200 minutes were required to settle out more than 99% of water at 1/8th of the total sample height, the time to reach an equivalent condition was reduced to 120 min for the second emulsion (water emulsified in supernatant-I) and 90 min for the third emulsion (water emulsified in supernatant-II), indicating a faster sedimentation of emulsion droplets. While the viscosity of the continuous phase is not expected to change significantly, due to a small decrease in the asphaltene concentration (less than 4 wt.%),[30] the observed increase in emulsion settling rate most likely represents a significant increase in the mean size of the emulsified water droplets. On each image in Figure 5.4, 250 droplets were chosen randomly and their sizes were analyzed by image processing software (ImageJ at http://rsbweb.nih.gov/ij/). The droplet size distributions for these emulsions were shown in Figure 5.5. The microscopic image of the settled emulsion droplets from water-in-whole asphaltene in toluene solution, as shown in Figure 5.4 (a), reveals that the majority of droplets were in the size range of 1 μm – 20 μm with D_{50} to be 9.51 μm (± 0.96 μm) . The average droplet size in supernatant-I increased with D_{50} at 13.26 μm (± 1.31 μm). An increase in the average droplet size is possibly due to the decreased stability of the emulsified water droplets to coalescence after removal of < 2 wt.% of asphaltene. After the second water washing, the stability of the emulsion was observed to be further decreased, as indicated in Figure 5.5. Further increase in the D_{50} in settled phase from supernatant-II was observed. D_{50} size of droplets in the settled phase from supernatant-II was 23.10 μm (± 1.27 μm). The results of the above emulsion stability tests suggest that only a small fraction of asphaltenes is responsible for high stability of water-in-asphaltene solution emulsions.

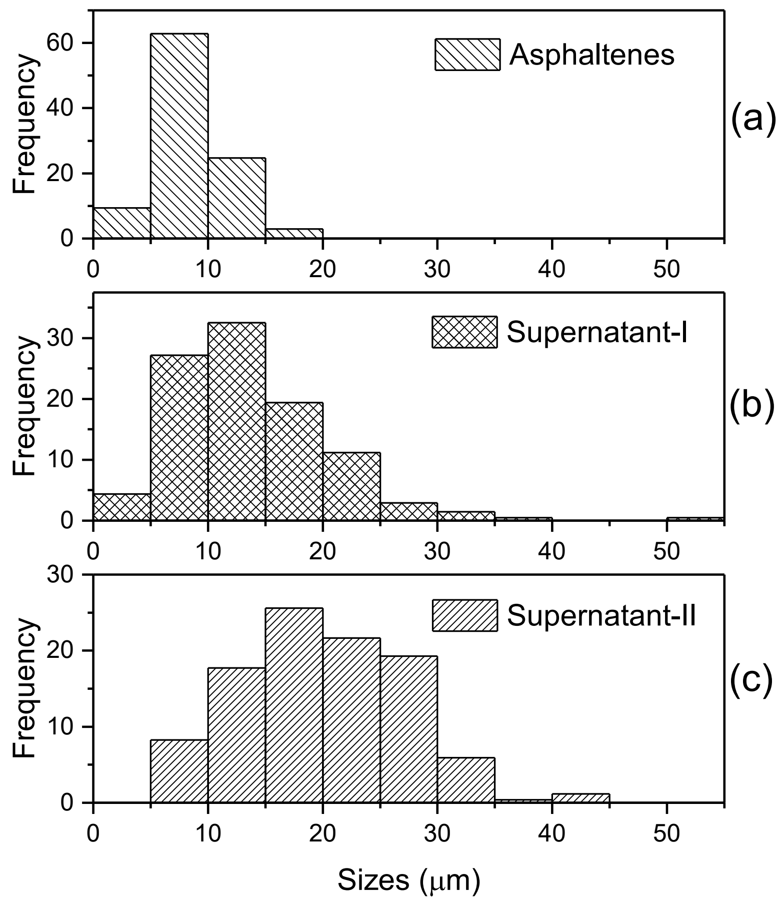

Figure 5.5 Size distribution of settled water droplets for emulsions of water in: (a) whole asphaltene-in-toluene solution; (b) supernatant-I; (c) supernatant-II.

5.3.2. Interfacial Properties

Interfacial tension. To understand the different stabilization behaviors of water in asphaltene-in toluene solutions prepared using the extracted IAA and RA asphaltenes, the interfacial tension between water and asphaltene-in toluene solution was determined using 0.1 g/L of asphaltene-in toluene solutions. The asphaltene-in-toluene solutions were sonicated for 5 min prior to their use. As shown in Figure 5.6, the interfacial tension decreases more significantly for solutions prepared using IAA than that using RA and WA. After equilibrated for 1 hour, the interfacial tensions for asphaltene-in-toluene solutions prepared using IAA and RA were 24.0 mJ/m^2 and 29.5 mJ/m^2, respectively. Both these observations suggest that the IAA is more surface active than RA. The interfacial tension between WA and water behaved very similarly to the interfacial tension obtained for RA/water system. This similarity is expected as only a small amount of asphaltene was extracted from WA.

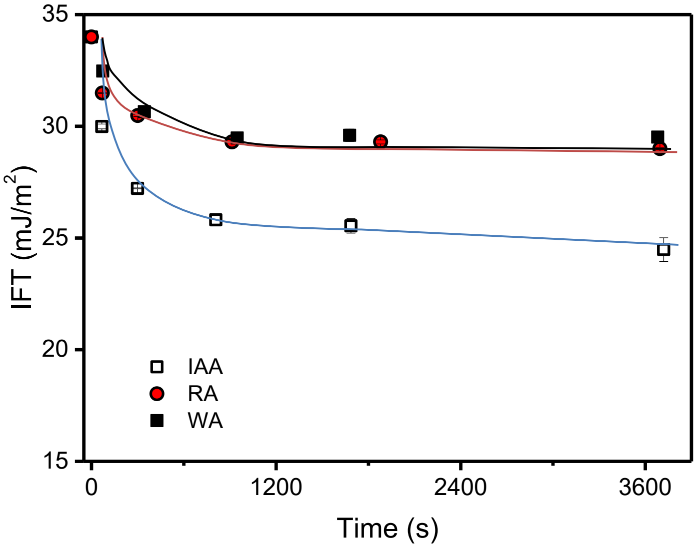

Figure 5.6 Interfacial tension of 0.1 g/L toluene diluted IAA, RA and WA solutions against DI water.

Interfacial (π−*A*) *isotherms.* Previous study [30] showed that asphaltenes form rigid interfacial layers. Here we aim to compare the interfacial compressibility of IAA, RA and WA. In these experiments the interfacial layer was formed following a diffusion protocol where 100 µL of 1 g/L asphaltene-in toluene solution was pre-dissolved into 100 mL of toluene prior to top phase addition. The interface was allowed to equilibrate for 30 min before interfacial layer was compressed. The results are shown in Figure 5.7. A baseline compression curve of DI water and pure toluene was recorded to confirm that, in the absence of asphaltenes, the interfacial pressure remains independent of the interfacial area. For the WA and RA, the interfacial pressures at large compressional areas were about 12.2 mJ/m^2, equal to the control experiment. Those pressures confirm that under such conditions (trough area: 170 cm^2 - 100 cm^2) the amount of asphaltene adsorbed on the water/oil interface is insufficient to affect the interfacial pressure. With further compression, interfacial pressure started to increase for both samples at almost equivalent interfacial area (~100 cm^2). Upon further compression, the interfacial pressure increased rapidly with decreasing the interfacial area, more so for WA than RA. The removal of the interfacially active asphaltenes (IAA) accounts for the less interfacial active nature of RA than whole asphaltenes. In contrast, the interfacial pressure of IAA-in-toluene solution in equilibrium with DI water at 14.9 mJ/m^2 is much higher comparing with the value of 12.2 mJ/m^2 for RA and WA-in-toluene solutions, confirming that IAA fraction is more interfacially active than RA and WA fractions. More importantly, immediate response of interfacial pressure to the compression of the interface was observed for IAA-in-toluene solutions, indicating that the population density of adsorbed species was so high that the gas phase was absent. Such data is in agreement with the results of interfacial tension measurement as shown in Figure 5.6.

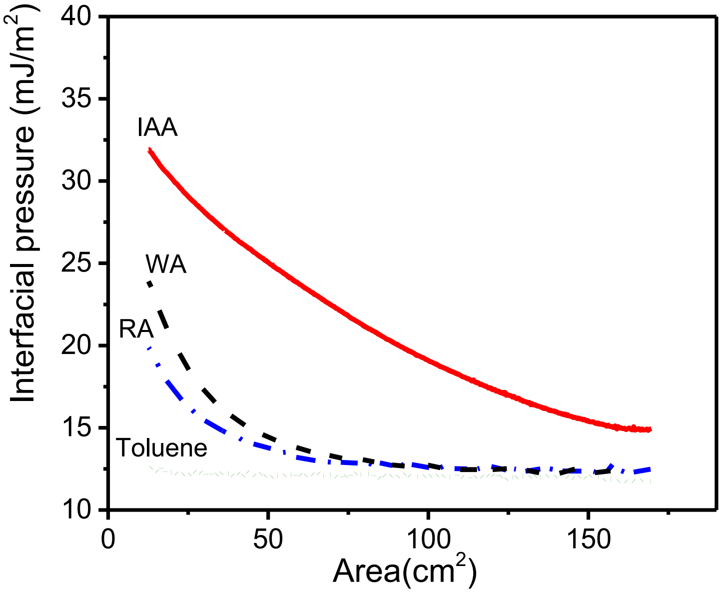

*Figure 5.7 Interfacial (**π − A**) isotherms of water/ IAA-, RA-, WA-in-toluene solutions. The top phase is 100 mL of toluene containing 100 µL of 1 g/L of studied asphaltene solutions.*

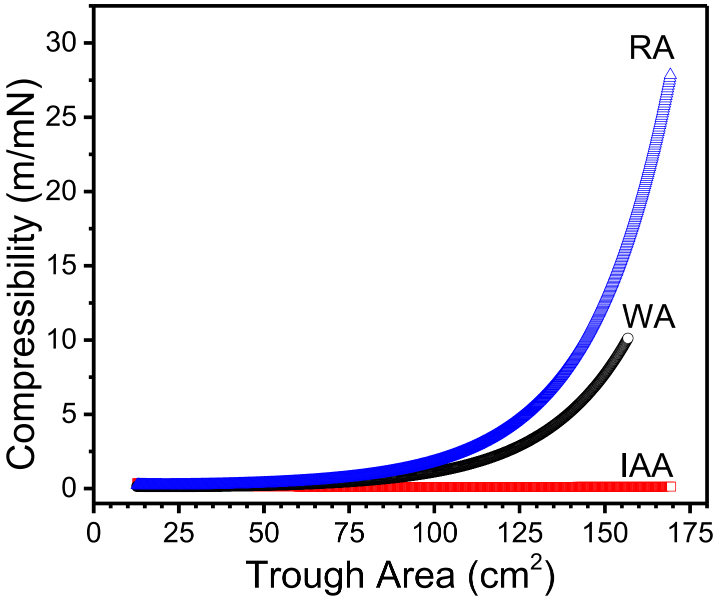

Figure 5.8 Compressibility of the interfaces containing IAA, RA and WA.

From the interfacial pressure – area isotherms it is possible to calculate the compressibility (C^s) of the interfacial layer by:

$$C^s = -\frac{1}{A}\left(\frac{d\pi}{dA}\right)^{-1}$$

where $d\pi/dA$ is the slope of the $(\pi - A)$ isotherm and A is the trough area. A large change in the interfacial pressure per unit reduction of interfacial area represents a less compressible, or more rigid interfacial layer. Figure 5.8 shows the change in interfacial layer compressibility for the two asphaltene fractions and whole asphaltene between a trough area of 170 cm^2 – 12 cm^2. For the WA and RA fractions, the films are soft at large interfacial areas, possibly due to relatively low interfacial concentration and less intermolecular association of asphaltenes adsorbed at the interface. As the interfacial area is further reduced, the compressibility of the interface decreases rapidly to a value below 0.5 m/mN at 50 cm^2, with the compressibility of interfacial films formed by WA being slightly less than that formed by RA. As anticipated for IAA, the compressibility of the interfacial film was below 0.5 m/mN even at large interfacial areas with little dependence on the interfacial area. Such response indicates that the interfacial layer formed by IAA is much more rigid than the films formed by the RA even though only a small fraction of asphaltenes was removed from the original asphaltenes (WA). The propensity of asphaltenes to form a rigid protective layer at a water/crude oil interface is considered to be the mechanism of stabilizing W/O emulsions. Our results show that only a relatively small fraction of asphaltenes is predominantly responsible for this characteristic property of asphaltenes.

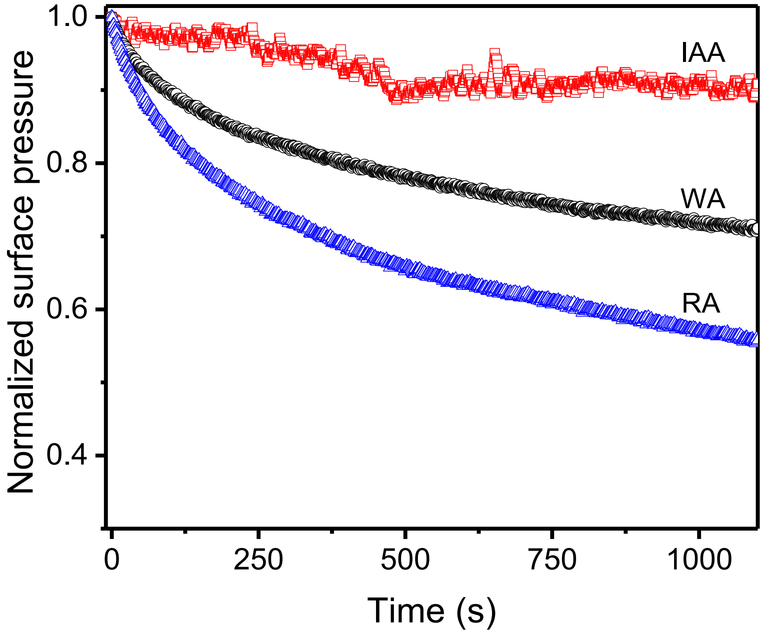

Figure 5.9 Relaxation isotherms of interfacial layers compressed to the same surface pressure of 20 mJ/m^2.

To further study the nature of asphaltene molecules or their aggregates at the oil-water interface that is responsible for the stability of W/O emulsions, the relaxation of the interfacial layers of three asphaltene fractions (WA, IAA and RA) was studied. The relaxation experiments were conducted by compressing the interface at 10 mm/min (per barrier) to a preset interfacial pressure of 20 mJ/m^2 (different compressional areas). Once the target pressure had been reached, the interfacial area was kept constant while the interfacial pressure was recorded for 20 min. Figure 5.9 shows the results of the relaxation response of the interfacial layers in time. The interfacial pressure was normalized by dividing the time dependent interfacial pressure due to the relaxation (base value at 170 cm^2 was subtracted) by the total increase in the surface pressure during the compression. The interfacial pressure drop for IAA interface during the relaxation is the smallest, followed by the interfaces formed by WA and then RA. After relaxing for 20 minutes, the surface pressure for IAA interface decreases by less than 10% while for the RA, this decrease is more than 40%. The decrease for the WA interface is intermediate at about 30%. The decrease in the surface pressure after compression is attributed to rearrangement or lateral self-association of adsorbed asphaltenes molecules/aggregates. The smaller reduction in interfacial pressure during relaxation of the films formed by IAA indicates less rearrangement of the adsorbed IAA at the interface, most likely as a result of strong self-association of IAA. The reduction in the interfacial pressure during relaxation could also result from the reduction in population of asphaltenes at the interface by their migration back into the bulk phase to reach the new equilibrium after the compression was stopped. The smaller reduction in the interfacial pressure of the film formed by IAA suggests that IAA fraction is predominantly irreversibly adsorbed at the water/oil interface. The decrease of the surface pressure for the RA fraction is much faster and continues at steady rate during our experiment. The contrast results show that while adsorption of IAA on the toluene/water interface is almost irreversible, the RA and WA fractions contain species, which might be reversibly adsorbed and can dissolve back into the bulk solution.

5.3.3. Thin Liquid Films

The properties of thin oil films that separate water droplets play a key role in the stability of an emulsion. In the previous chapter[30] we found that asphaltenes stabilize toluene diluted emulsion films at a much lower concentration (above 0.5 g/L) than bitumen and de-asphalted bitumen (above 10 g/L). In the current study, the film life time defined as the time from the moment of film formation to its rupture was measured to evaluate the capacity of IAA and RA fractions to stabilize water-in-oil emulsions. The results in Figure 5.10 show that the thin liquid films stabilized by IAA are of significantly longer lifetime as compared to films stabilized by RA and WA. While the films stabilized by RA ruptured in less than 20 s, thin films stabilized by IAA remained stable for more than 1200 s. These results are in line with the findings shown in Figure 5.3 from our emulsion stability tests.

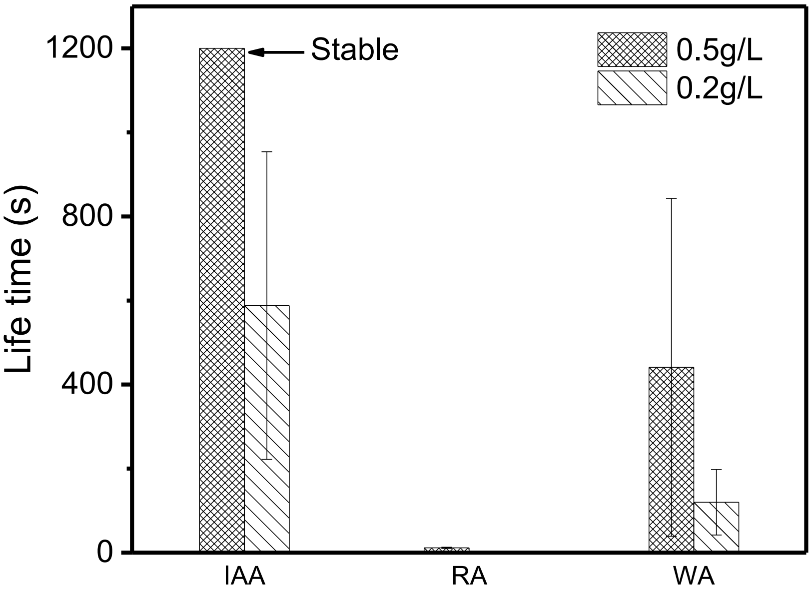

Figure 5.10 Film lifetime of water-in-oil emulsion films prepared from different asphaltene fractions dissolved in toluene.

As mentioned earlier in the last chapter,[30] we observed that the asphaltene fraction of bitumen is responsible for the ageing of films, producing thicker and heterogeneous films (40 - 90 nm). Deasphalted bitumen films did not show such ageing effects while producing thinner films of about 10 nm. Ageing, related to skin formation at the water/oil interface and increased film thickness, is an important physical property of the film for understanding emulsion stability. The results in Figure 5.11 and Figure 5.12 compare properties of thin films formed using IAA- and RA-in toluene solutions. For each case we have two sets of images showing thin film evolution. The first set (A) in each figure represents the fresh films, referring to the non-aged thin liquid films that were generated immediately after the porous glass cell was inserted into the water. The second set (B) in Figures 5.11 and 5.12 represents the aged films formed after the interfaces were aged for 30 min. For fresh films as shown in Figure 5.11A, the film was thick initially, with inclusions being observed in the film. These inclusions are likely due to the asphaltene aggregates formed at the interfaces. These inclusions caused uneven thickness of the film as indicated by the Newton rings in the film images. In less than a minute, the film drained and became much thinner, as indicated by the dark background in the film. The estimated film thickness in these dark regions is less than 40 nm. The life time of the film was more than 25 minutes. Interestingly, the inclusions observed at the beginning remained in the film, and their positions were not changed throughout the drainage process, indicating an immobile film interface.

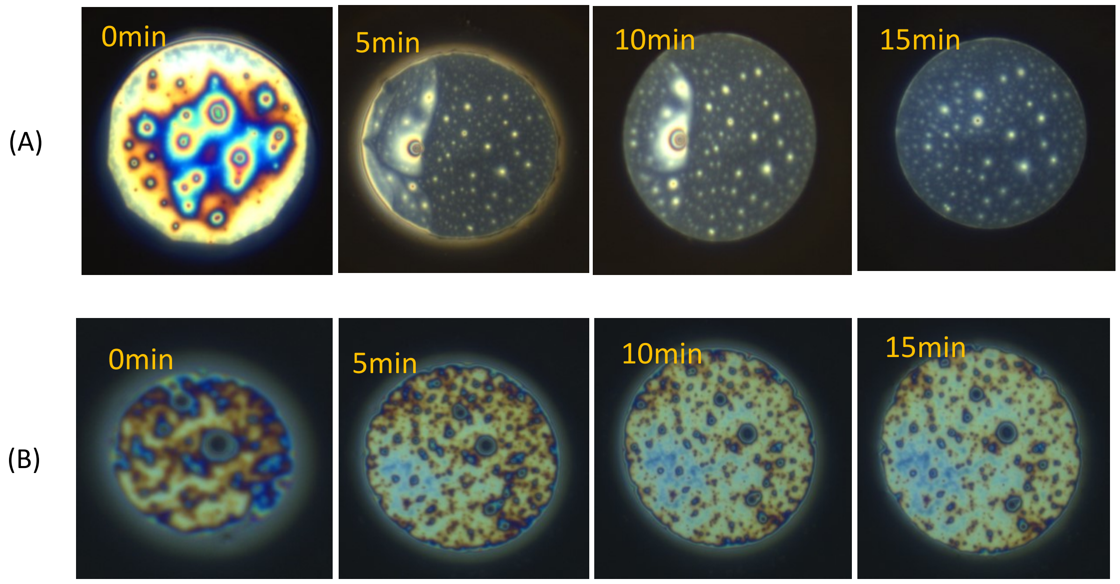

Figure 5.11 Images taken at 0 min, 5 min, 10 min and 15 min, respectively, for the fresh (A) and aged (B) thin liquid film formed by 0.5 g/L IAA in toluene solution.

After the interfaces were aged for 30 min, the feature of the thin film formed changed dramatically. As shown in Figure 5.11 (B), the initial film looked similar to the fresh thin liquid film, with many inclusions that caused uneven thickness of the film. However, the entire film appeared to be gel-like if it is not solid-like, as there was little change in the film thickness while the morphology of the film remained. Similar aging effect was observed in our previous experiments with aged asphaltene thin emulsion films[30], but the extent of ageing was much more severe in the present case of IAA fraction.

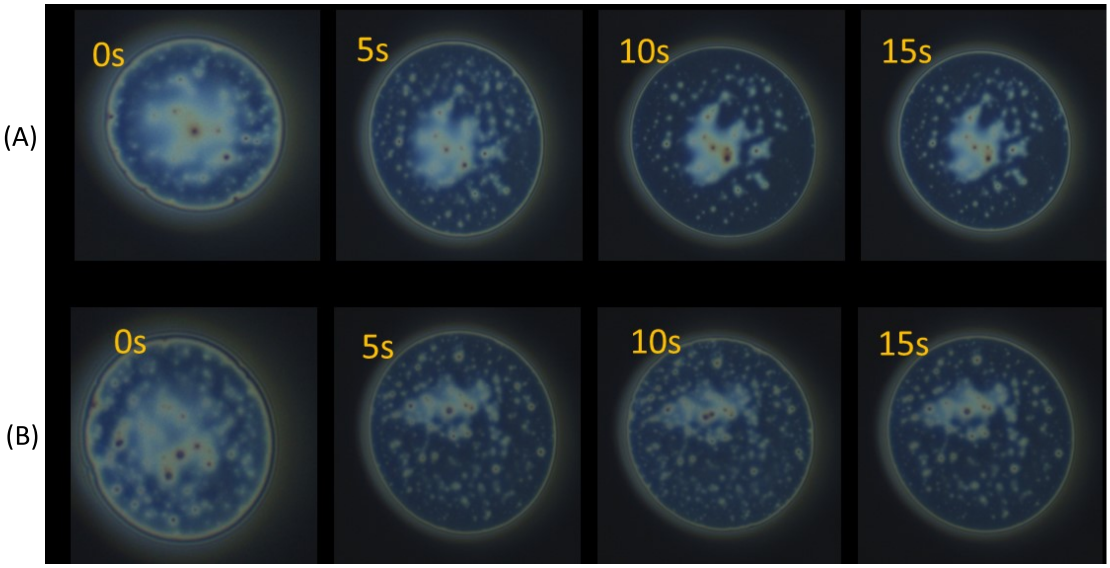

Figure 5.12 Images taken at 0 s, 5 s, 10 s and 15 s, respectively, for the fresh (A) and aged (B) thin liquid film formed by 0.5 g/L RA in toluene solutions

As shown in Figure 5.12, the severe ageing effects observed with film formed from IAA-in-toluene solutions were not observed in the film formed with RA-in-toluene solutions. The fresh and aged films formed by RA-in-toluene solution exhibited similar features. Films formed by RA-in-toluene solutions were relatively unstable, with the film ruptured within 30 s regardless of aging. Here, interfaces aged for 30 min were shown as an example, but longer ageing time did not change the features of the film. Film thickness in the background dark area was determined to be about 30 -

40 nm. The white spots observed indicate the formation of asphaltene aggregates in the film. In both cases, the films formed by RA did not show any signs of rigidity as those described for asphaltenes in toluene and bitumen in poor solvent films as discussed previously.[28,30]

5.4. DISCUSSION AND CONCLUSIONS

Defined as a solubility class, the asphaltenes consist of species with different chemical structures and properties. In a previous study, considering the asphaltenes as a whole was recognized to hinder the progress on understanding stabilization mechanisms of water-in-crude oil emulsions.[27] Research efforts were made to characterize emulsifications and interfacial properties of different asphaltenes sub-fractions.[36] Most of the methods used for asphaltenes sub-fractionation were based on their solubility in solvents of increasing aliphaticity. To our knowledge, there is no work on fractionation of asphaltenes based on their interfacial activity, which is in fact the property that is most directly related to emulsion stability. In this work, we developed a method that allows extraction of the most interfacially active fraction of asphaltenes. Previous study showed that in poor solvent (e.g., heptane or mixture of heptane and toluene) and above the critical solvent-to-bitumen ratio (or onset of asphaltene precipitation), rigid water/oil interface is formed. It was also reported that the asphaltenes are responsible for the formation of relatively thick emulsion films (> 40 nm) which exhibit very slow drainage dynamics.[30] In this study we isolated a small fraction (less than 2% of the total) of asphaltenes, referred to here as interfacially-active asphaltenes (IAA). This fraction of asphaltenes (IAA) is shown to be responsible for stabilizing emulsions of water in asphaltene-in toluene solutions. After removing this fraction, the stability of the emulsion decreased drastically. Interfacial tension isotherms confirmed that compared with RA, IAA has a much higher interfacial activity. Langmuir though pressure-area isotherm showed that IAA forms rigid layers and adsorbs irreversibly to water/toluene interface, while interfacial films formed with

WA and RA are softer and can partially desorb from the interface during the film relaxation after being compressed to a given interfacial pressure. The more severe aging was observed for the films formed with IAA than with WA. The aging of the film disappeared when the film was formed with RA, the remainer after removal of IAA from WA, indicating that the aging feature is strongly associated with the presence of IAA fraction. The results from current study collectively suggest that IAA fraction, which is only a small part of asphaltenes is actually responsible for the film stability. From this study, it is clear that we need to focus on the IAA fraction rather than asphaltenes as a whole, if we want to advance our understanding of molecular mechanism that stabilizes petroleum emulsions. More detailed knowledge on chemical structure of IAA, which is presented in the next chapter, can help in designing new generation of demulsifiers to solve the W/O emulsion problems in oil industry.

REFERENCES

1. Gao, S., Moran, K., Xu, Z., & Masliyah, J. (2010). Role of naphthenic acids in stabilizing water-in-diluted model oil emulsions. *The Journal of Physical Chemistry B*, *114*(23), 7710-7718.

2. McLean, J. D., & Kilpatrick, P. K. (1997). Effects of asphaltene aggregation in model heptane–toluene mixtures on stability of water-in-oil emulsions. *Journal of Colloid and Interface Science*, *196*(1), 23-34.

3. Ortiz, D. P., Baydak, E. N., & Yarranton, H. W. (2010). Effect of surfactants on interfacial films and stability of water-in-oil emulsions stabilized by asphaltenes. *Journal of Colloid and Interface Science*, *351*(2), 542-555.

4. Yang, X., Verruto, V. J., & Kilpatrick, P. K. (2007). Dynamic asphaltene-resin exchange at the oil/water interface: Time-dependent W/O emulsion stability for asphaltene/resin model oils. *Energy & Fuels*, *21*(3), 1343-1349.

5. Yarranton, H. W., Hussein, H., & Masliyah, J. H. (2000). Water-in-hydrocarbon emulsions stabilized by asphaltenes at low concentrations. *Journal of Colloid and Interface Science*, *228*(1), 52-63.

6. Zhang, L. Y., Xu, Z., & Masliyah, J. H. (2003). Langmuir and Langmuir-Blodgett films of mixed asphaltene and a demulsifier. *Langmuir*, *19*(23), 9730-9741.

7. Langevin, D., Poteau, S., Hénaut, I., & Argillier, J. F. (2004). Crude oil emulsion properties and their application to heavy oil transportation. *Oil & Gas Science and Technology*, *59*(5), 511-521.

8. Hirasaki, G. J., Miller, C. A., Raney, O. G., Poindexter, M. K., Nguyen, D. T., & Hera, J. (2010). Separation of Produced Emulsions from Surfactant Enhanced Oil Recovery Processes. *Energy & Fuels*, *25*(2), 555-561.

9. Kiran, S. K., Ng, S., & Acosta, E. J. (2011). Impact of Asphaltenes and Naphthenic Amphiphiles on the Phase Behavior of Solvent− Bitumen− Water Systems. *Energy & Fuels*, *25*(5), 2223-2231.

10. Goual, L., Sedghi, M., Zeng, H., Mostowfi, F., McFarlane, R., & Mullins, O. C. (2011). On the formation and properties of asphaltene nanoaggregates and clusters by DC-conductivity and centrifugation. *Fuel*, *90*(7), 2480-2490.

11. Hoepfner, M. P., Vilas Bôas Fávero, C., Haji-Akbari, N., & Fogler, H. S. (2013). The fractal aggregation of asphaltenes. *Langmuir*, *29*(28), 8799-8808.

12. Yeung, A., Dabros, T., Masliyah, J., & Czarnecki, J. (2000). Micropipette: a new technique in emulsion research. *Colloids and Surfaces A: Physicochemical and Engineering Aspects*,*174*(1), 169-181.

13. Spiecker, P. M., Gawrys, K. L., Trail, C. B., & Kilpatrick, P. K. (2003). Effects of petroleum resins on asphaltene aggregation and water-in-oil emulsion formation. *Colloids and Surfaces A: Physicochemical and Engineering Aspects*, *220*(1), 9-27.

14. Spiecker, P. M., & Kilpatrick, P. K. (2004). Interfacial rheology of petroleum asphaltenes at the oil-water interface. *Langmuir*, *20*(10), 4022-4032.

15. Czarnecki, J., & Moran, K. (2005). On the stabilization mechanism of water-in-oil emulsions in petroleum systems. *Energy & Fuels*, *19*(5), 2074-2079.

16. Czarnecki, J. (2008). Stabilization of Water in Crude Oil Emulsions. Part 2. *Energy & Fuels*, *23*(3), 1253-1257.

17. Czarnecki, J., Tchoukov, P., Dabros, T., & Xu, Z. (2013). Role of asphaltenes in stabilisation of water in crude oil emulsions. *The Canadian Journal of Chemical Engineering*, *91*(8), 1365-1371.

18. Kharrat, A. M., Zacharia, J., Cherian, V. J., & Anyatonwu, A. (2007). Issues with comparing SARA methodologies. *Energy & Fuels*, *21*(6), 3618-3621.

19. Xu, Y., Dabros, T., Hamza, H., & Shefantook, W. (1999). Destabilization of water in bitumen emulsion by washing with water. *Petroleum Science and Technology*, *17*(9-10), 1051-1070.

20. Wu, X. (2003). Investigating the stability mechanism of water-in-diluted bitumen emulsions through isolation and characterization of the stabilizing materials at the interface. *Energy & Fuels*, *17*(1), 179-190.

21. Stanford, L. A., Rodgers, R. P., Marshall, A. G., Czarnecki, J., Wu, X. A., & Taylor, S. (2007). Detailed elemental compositions of emulsion interfacial material versus parent oil for nine geographically distinct light, medium, and heavy crude oils, detected by negative-and positive-ion electrospray ionization Fourier transform ion cyclotron resonance mass spectrometry. *Energy & Fuels*, *21*(2), 973-981.

22. Stanford, L. A., Rodgers, R. P., Marshall, A. G., Czarnecki, J., & Wu, X. A. (2007). Compositional characterization of bitumen/water emulsion films by negative-and positive-ion electrospray ionization and field desorption/ionization Fourier transform ion cyclotron resonance mass spectrometry. *Energy & Fuels*, *21*(2), 963-972.

23. Spiecker, P. M., Gawrys, K. L., & Kilpatrick, P. K. (2003). Aggregation and solubility behavior of asphaltenes and their subfractions. *Journal of Colloid and Interface Science*, *267*(1), 178-193.

24. Platikanov, D.; Exerowa, D. (2005). Thin liquid films. In *Fundamentals of Interface and Colloid Science Soft Colloids*; Volume 5; Lyklema, J., Ed.; Academic Press: pp 1-91.

25. Sheludko, A. (1967). Thin liquid films. *Advances in Colloid and Interface Science*, *1*(4), 391-464.

26. Khristov, K., Taylor, S. D., Czarnecki, J., & Masliyah, J. (2000). Thin liquid film technique—application to water–oil–water bitumen emulsion films. *Colloids and Surfaces A: Physicochemical and Engineering Aspects*, *174*(1), 183-196.

27. Czarnecki, J., Tchoukov, P., & Dabros, T. (2012). Possible role of asphaltenes in the stabilization of water-in-crude oil emulsions. *Energy & Fuels*, *26*(9), 5782-5786.

28. Tchoukov, P., Czarnecki, J., & Dabros, T. (2010). Study of water-in-oil thin liquid films: Implications for the stability of petroleum emulsions. *Colloids and Surfaces A: Physicochemical and Engineering Aspects*, *372*(1), 15-21.

29. Taylor, S. D., Czarnecki, J., & Masliyah, J. (2002). Disjoining pressure isotherms of water-in-bitumen emulsion films. *Journal of Colloid and Interface Science*, *252*(1), 149-160.

30. Tchoukov, P., Yang, F., Xu, Z., Dabros, T., Czarnecki, J., & Sjöblom, J. (2014). Role of asphaltenes in stabilizing thin liquid emulsion films. *Langmuir*, *30*(11), 3024-3033.

31. Gray, M. R., Tykwinski, R. R., Stryker, J. M., & Tan, X. (2011). Supramolecular assembly model for aggregation of petroleum asphaltenes. *Energy & Fuels*, *25*(7), 3125-3134.

32. Ancheyta, J., Centeno, G., Trejo, F., Marroquin, G., Garcia, J. A., Tenorio, E., & Torres, A. (2002). Extraction and characterization of asphaltenes from different crude oils and solvents. *Energy & Fuels*, *16*(5), 1121-1127.

33. Zhang, L. Y., Breen, P., Xu, Z., & Masliyah, J. H. (2007). Asphaltene films at a toluene/water interface. *Energy & Fuels*, *21*(1), 274-285.

34. Zhang, L. Y., Lopetinsky, R., Xu, Z., & Masliyah, J. H. (2005). Asphaltene monolayers at a toluene/water interface. *Energy & Fuels*, *19*(4), 1330-1336.

35. Freer, E. M., & Radke, C. J. (2004). Relaxation of asphaltenes at the toluene/water interface: Diffusion exchange and surface rearrangement. *Journal of Adhesion*, *80*(6), 481-496.

36. Fossen, M., Kallevik, H., Knudsen, K. D., & Sjöblom, J. (2007). Asphaltenes precipitated by a two-step precipitation procedure. 1. Interfacial tension and solvent properties. *Energy & fuels*, *21*(2), 1030-1037.

CHAPTER 6 ASPHALTENE SUB-FRACTIONS RESPONSIBLE FOR STABILIZING WATER-IN-CRUDE OIL EMULSIONS - MOLECULAR REPRESENTATIONS AND MOLECULAR DYNAMIC SIMULATIONS

6.1 INTRODUCTION

During heavy oil processing, the presence of a small amount of residual water in the upstream bitumen product causes great concerns due to their severe potential in causing corrosion to the downstream pipelines and plant equipment. The residual water is well-documented to be present in the form of small droplets emulsified in the oil. Better understanding on mechanisms of stabilization of water-in-heavy oil emulsions is required to develop methods of enhancing droplets coalescence, subsequent water separation and hence obtaining a heavy oil product that meets the industrial standards. It is generally accepted that there are different types of interfacially active compounds present in the oil that can contribute to emulsion stability. These compounds include resins, natural surfactants and asphaltenes compounded with fine solids.[1-9] As a major stabilizer among these compounds, asphaltenes were found to form 'skin-like' layer at the oil/water interface. This interface prevents coalescence between water droplets by providing mechanical strength.[10-12] From the demulsification point of view, the design of high performance chemical demulsifiers would benefit from the understanding of the molecular structures of asphaltenes and their associations at the oil/water interface that are responsible for emulsion stabilization. As a solubility class, asphaltenes contain thousands of different molecular structures. Although the studies of asphaltene structure are abundant, the high variety of species included in asphaltenes and differences in oil chemistry due to its origin, extraction method and aggregation propensity have resulted in controversial conclusions regarding molecular structure and corresponding molecular aggregation mechanisms of asphaltenes. The definitive link between the molecular structure of asphaltenes and their interfacial and emulsion stabilization properties remains to be established.

Recently an increasingly extensive research effort has been devoted to resolving this challenging problem and significant progress has been made. For example, Mullin et al.[13,14] proposed a modification of the Yen's model,[15] which is also known as an 'island' model of asphaltenes that considers asphaltene molecules consisting of poly-aromatic cores (4-10 fused rings) surrounded by aliphatic chains. This model includes a hierarchical aggregation of asphaltene molecules, starting with nano-aggregation of ~6 asphaltene molecules which form a core from stacking of polycyclic aromatic hydrocarbon rings surrounded by alkane chains. The formation of nano-aggregates is believed to be driven by π-π attraction between poly-aromatic cores. The presence of aliphatic chains imposes a steric repulsion that limits the growth of nano-aggregates.

Another asphaltene molecular model proposed by Strausz et al. considers an "archipelago" structure that contains multiple but smaller aromatic cores (2-3 rings) interconnected by alkane chains.[16,17] More recent work of Agrawala and Yarranton, and Gray et al. proposed formation of more complex macro-molecular aggregates of asphaltene molecules through "linear polymerization"[18-19] or "supramolecular assembly" mechanism.[20] Gray et al.[20] suggested that various interactions such as acid-base interaction, π-π stacking, hydrogen bonding, hydrophobic pockets, metal coordination, etc. are all possibly at work for a multi-cooperative association of asphaltenes. Similar macromolecular asphaltene structure was deduced from our previous work on thin liquid films.[21,22] In Chapter 4, we found that such molecular association led to viscoelastic properties of oil/water interfaces that can provide structure to stabilize water-in-oil thin films and hence corresponding emulsions. Thin liquid film (TLF) studies showed an extension of the asphaltenes macrostructure networks up to 100 nm in the film between two water droplets, where the emulsions were stabilized by the drainage of the thin oil film being stopped and so prevented its rupture.[22,23]

Furthermore, in Chapter 5, we demonstrated that only a small fraction of asphaltenes (less than 2%) was found to provide the aforementioned viscoelastic properties of oil/water interfaces and hence structural stabilization of water-in-oil thin films.[23] In Chapter 5, we reported a new method to extract this asphaltene fraction named as interfacially active asphaltene (IAA). This method is based on isolation of emulsified water droplets from diluted asphaltene solution and recovering the interfacial materials accumulated at the oil/water interface. Compared with the remaining asphaltenes (RA), the extracted IAA showed a distinct interfacial behavior. In contrast to RA which accounts for more than 98% of the asphaltenes, IAA were more surface active and produced thicker and significantly more stable emulsion films with strong ageing effects. These findings indicate that the formation of extended supramolecular structure in the thin liquid films is likely not a common behavior for all asphaltene molecules but is due to unique molecular structure features of this specific fraction of asphaltenes.

Structure dictates functions. In this chapter, we aim to characterize the structural differences between this IAA fraction and RA, and to relate these structural differences to their distinct interfacial properties as reported previously.[23] The nuclear magnetic resonance (NMR) techniques have proven to be a useful tool for molecular characterization of petroleum fractions by providing information of carbon skeleton such as number of poly-aromatic rings, aromatic carbons, average length of aliphatic chains and aliphatic substitutions.[24] Fourier transform infrared (FTIR) spectroscopy is capable of identifying functional groups in asphaltene molecules.[25] By combining NMR and FTIR data with the results of elemental analysis, a quantitative representation of an average asphaltene molecular structure can be constructed. This approach was successfully implemented by Dettman et al. and provided useful information in characterizing petroleum samples.[26-29]

Construction of average structures for the remaining asphaltenes (RA) and IAA fractions allows us to perform molecular dynamic simulations. In a growing number of studies, MD has proven to provide important insights into aggregation and interfacial behavior of asphaltene molecules. Such studies have led to molecular level understanding of interfacial arrangements, interaction mechanisms, functional groups involved and phase partitioning of asphaltene molecules.[30-34] In this work, quantitative molecular representations of IAA and RA fractions, derived from the results of ^{1}H-NMR, ^{13}C-NMR, FTIR and elemental analyses are constructed. The aggregation and adsorption behavior at the oil/water interface of these representative asphaltene structures are studied by MD simulation. The results are discussed in relation to the previously established emulsion stabilization behavior of water-in-crude oil emulsions including their possible mechanisms.

6.2 MATERIALS AND EXPERIMENTAL METHODS

6.2.1 Materials and Fractionation Procedures

Toluene (Optima grade) was purchased from Fisher Scientific Canada. N-pentane (>98%) used to precipitate asphaltenes from bitumen was purchased from EMD Chemical Inc. Milli-Q water with resistivity of 18.2 mΩ/m was used throughout this study. Asphaltenes were extracted from Athabasca coker feed bitumen (Syncrude Canada Ltd.) following the procedures described elsewhere.[22,35] The procedure for extracting fractions of interfacially active asphaltenes was described in detail in Chapter 5 and only a brief description will be provided here. A 10 g/L whole asphaltene-in-toluene solution was prepared, followed by the addition of 10% (v/v) of deionized water. The mixture was homogenized at 60,000 rpm for 5 min using a homogenizer (Power Gen 1000, Fisher Scientific). The resultant emulsion was shaken for 24 hours to equilibrate, before centrifuging at 20,000 *g* to separate the stabilized emulsion drops from the continuous oil phase. The centrifugation was controlled in such an extent that no visible free water was resolved and the water that remained encapsulated in stable drops settled to form a cake. The water droplets cake was carefully separated and transferred into a separate jar for further washing in excess toluene (80 mL) to remove any asphaltenes loosely bounded to the interface or in toluene trapped among the droplets in the cake. The cake-toluene mixture was gently shaken by hand for several minutes and the sample was left undisturbed to allow the re-dispersed droplets to settle. The washing procedure was repeated until the supernatant appeared colorless. During the entire washing process, no visible bulk water was resolved. The washed emulsion droplets were then transferred to a jar and dried in a vacuum oven at 60 °C. The resulting asphaltene sub-fraction was named interfacially-active asphaltenes, (IAA).

6.2.2 Characterization Techniques

6.2.2.1 Elemental Analysis.

The carbon, hydrogen, nitrogen, and sulphur contents were measured using the ASTM D5291 method on an Elementar Variomicrocube Analyzer. Oxygen contents of the samples were measured using an Elementar Variomicrocube Analyzer and the method recommended by the manufacturer.

6.2.2.2 NMR (^{1}H and ^{13}C).

Nuclear magnetic resonance (NMR) analyses were performed at room temperature (19 ± 1ºC) on a Varian Unity Inova 600 NMR spectrometer, operating at 599.733 MHz for proton and 150.817 MHz for carbon. For carbon, 50 mg of asphaltenes were dissolved in 700 μL of deutero-chloroform. For proton measurement, 20 mg of asphaltenes was dissolved in 700 μL deutero-chloroform. Both proton and carbon spectra were run using a Varian 5 mm broadband ^{13}C{^{1}H} probe. The quantitative carbon spectra were acquired using an acquisition time of 1.0 s, a sweep width of 36003.6 Hz and a flip angle of 26.4° (3.4 μs). A relaxation delay of 5 s was used. Reverse-gated waltz proton decoupling was used to avoid nuclear Overhauser enhancements of the protonated carbon signals. The spectra were the results of 3200 scans. Line broadening of 10 Hz was used to improve the signal-to-noise ratio of the spectra. The spectra were referenced to deutero-chloroform at 77 ppm. The quantitative proton spectra were acquired using an acquisition time of 3 s, a sweep width of 20000 Hz, a pulse flip angle of 30.6º (3.3 μs) and a relaxation delay of 4 s. The spectra were the result of 128 scans. Line broadening of 0.30 Hz was used to improve the signal-to-noise ratio of the spectra. The spectra were referenced to deutero-chloroform at 7.24 ppm.

The CanmetENERGY carbon type analysis utilizes integral data from both ^{13}C and ^{1}H NMR spectra. The integral regions used and the calculations performed were based on the method published previously with enhancements.[36] The cluster size calculations of aromatic and cycloparaffinic rings are based on the method described in the previous work.[37] Integral values from proton and carbon spectra were used to calculate the mole % of the various carbon types. To check the fit of the data, the mole % carbon was converted to weight % carbon where the total was set to the values measured by the elemental analysis. The NMR data was then used to calculate the hydrogen content (wt.%). The difference between the elemental and NMR-derived hydrogen contents is usually within 1 wt.%.

6.2.2.3 FTIR Analysis.

Asphaltene samples were dissolved in methylene chloride (50 mg in 700 µl) and analyzed in a solution potassium bromide cell (0.1 mm path length). FTIR spectra were collected on a Bruker FTIR (model Tensor 27) spectrometer. Spectra of methylene chloride were obtained under similar conditions and were used as a reference to subtract the solvent signals from the spectrum.

The molecular representations were prepared manually using ChemDraw® purchased from PerkinElmer molecular drawing program. The fit of such representations was judged by comparing their structural data to the NMR results.

6.2.2.4 Electrospray-Mass Spectrometry (ES-MS) Analysis.

Electrospray ionization mass spectrometry (ES-MS) measurements were performed on a QTrap 4000 mass spectrometer (Applied Biosystems, Foster City, USA) equipped with a Turbo V™ ion source. Solution sample was introduced into mass spectrometer by a syringe pump (Harvard Apparatus) at 7 µL/min. The mass spectrometer was operated in positive ion mode with Q1 MS scan mode (m/z 100-2800 Da) and at a rate of 1000 Da s^{-1}. Mass spectrometer conditions were as follows: source temperature at 100 ºC, curtain gas (CUR) at 10 L/min, ion spray (IS) at -4500 V, nebulizer gas (GS1) at 10 L/min, interface heater is ON, declustering potential (DP) at -10 V, entrance potential (EP) at -13 V, and the cascade electron multiplier (CEM) at 2200 V. Data were collected and analyzed by Analyst 1.6 software (Applied Biosystems). Asphaltene samples were dissolved at 100 ppm concentration in solution comprising of 50 vol.% toluene, 50 vol.% methanol and 10 mM ammonium acetate, and used right away.

6.2.2.5 Molecular Dynamics (MD) Simulations.

In this study GROningen MOlecular Simulation (GROMOS) software package[38] and a united atom GROMOS96-53a6 force field were used.[39-41] Our previous MD work validated by numerous experimental techniques showed that GROMOS96-53a6 force field coupled with an accurate topology files can provide valuable dynamic and structural information regarding the initial molecular association and adsorption of asphaltene-like molecules in different organic solvents and at the oil/water interface.[30-32,42] The general MD simulation setup, methodologies, and topology files preparation have been reported in our previous works.[31,32] The hydrogen atoms in the polar sites and in the aromatic rings of the molecules were modeled explicitly. However, aliphatic methyl groups were treated as united atom sites, while all the double bonds in the aromatic rings and aliphatic chains were modeled with sp^2 hybridization of the carbon atom. Two simulation boxes were constructed initially with each box containing the studied molecular structures. The simulation cubic boxes were then solvated with separately parameterized toluene molecules followed by a steepest descent energy minimization to relax the unfavorable contacts among the molecules in the system. The simulation boxes were then extended in the z–direction by 5 nm and filled with SPC/E model water molecules. All the simulations were performed in an isothermal-isobaric (NPT) ensemble at 298 K and 1 bar pressure using Nosé-Hoover thermostat[44,45] and Parrinello-Rahman barostat.[46] The pressure and temperature coupling constants were set at $\tau_p = 3\,\text{ps}$ and $\tau_T = 0.3\,\text{ps}$, respectively for the entire simulation run. An isothermal compressibility of 9.08×10^{-5} bar^{-1} was used in the pressure coupling for the toluene molecules.[47] For both Coulomb and van der Waals interactions, a cutoff of 1.2 nm was used for the entire simulation. Each simulation was performed for 100 ns with a time step of 2 femtosecond (fs).

It should be noted that the size of IAA molecules was found to be about twice of the size of RA molecules as will be discussed later. To ensure similar concentration of solvent around the segments of asphaltene molecules in two systems, these two simulated systems are of different mass concentrations of asphaltene molecules. However, since the main theme of this chapter is to probe the structural differences between IAA fraction and RA and to relate these structural differences to their unique interfacial properties, such difference in simulation boxes is not anticipated to change the simulation results and hence overall conclusions.

6. 3 RESULTS

6.3.1 Investigation of Structural Properties of RA and IAA

The RA and IAA were characterized using Electrospray Mass Spectrometry, quantitative ^{13}C and ^{1}H NMR, FTIR and elemental analyses.

6.3.1.1 Electrospray Mass Spectrometry Analysis

ES-MS is a soft ionization technique that can transfer species in equilibrium from the solution into a gas phase by electro-spray ionization, producing charged intact molecular ions. Based on the mass to charge ratio (m/z) of the ions, the molecular weights of sample species were calculated. Shown in Figure 6.1 is the full ES-MS mass spectra obtained at 25ºC for solutions of RA (100 ppm) and IAA (100 ppm) in 50 vol.% toluene, 50 vol.% methanol and 10 mM ammonium acetate under positive ion mode. For RA samples, the average molecular weight is centered at about 700-750 g/mol, over a range between 400-2000 g/mol. However, for the IAA, the observed molecular weight distribution is peaked at 1000-1200 g/mol, with a distribution between 400-2000 g/mol. To further confirm that the higher molecular weight of IAA correspond to monomers, several peaks at higher m/z values (e.g., m/z=1100, 1200 and 1300) were isolated, on which the fragment test was run. All the three peaks were very stable and only started to fragment when high collision energy of 50 - 70 eV was applied. Since non-covalently bonded aggregates typically dissociate at low collision energy of 20 - 30 eV, these results indicate that the measured molecular weight corresponds mostly, if not entirely, to asphaltene monomers.

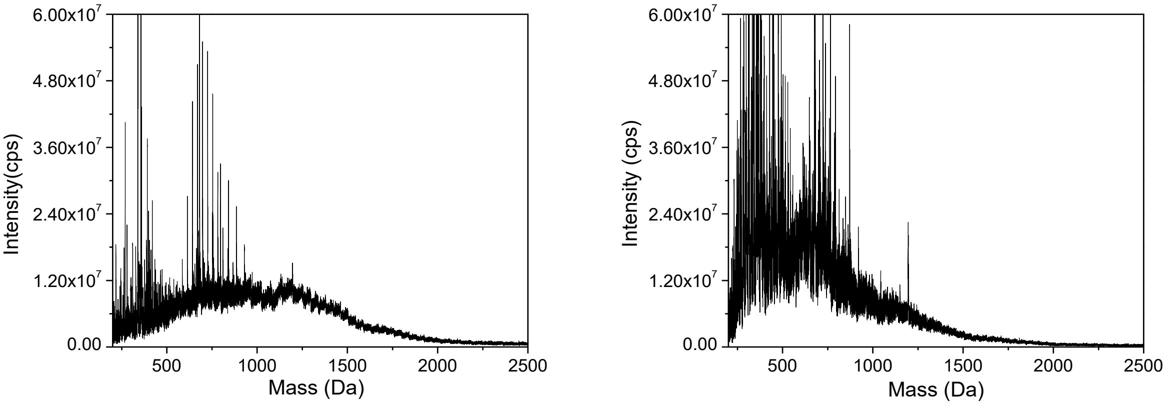

Figure 6.1 The molecular weight distribution of IAA (left) and RA (right) measured using ES-MS technique.

6.3.1.2 Elemental Analysis

The results from elemental analysis of IAA and RA samples are presented in Table 6.1. The main difference in the elemental composition of IAA and RA is the much higher oxygen content for IAA. The oxygen content of 1.68 wt% for RA sample is within the values from 1.5 wt% to 2.5 wt% reported in literature for Athabasca asphaltenes. However the oxygen content of 5.54 wt% for IAA fraction is more than three times higher than the oxygen content of RA. Possible oxygen-containing functional groups would include hydroxyl groups, carbonyl groups, and oxygenated sulphur species. Neither of the RA or IAA samples was found to contain silicon, indicating that the source of oxygen was not from clay solids contamination.

Table 6.1 Elemental content (wt.%) of RA and IAA

Elemental Content (wt%)	*RA*	*IAA*
Carbon	*80.52*	*76.00*
Hydrogen	*8.38*	*7.91*
Nitrogen	*1.12*	*1.13*
Sulfur	*8.29*	*9.42*
Oxygen	*1.68*	*5.54*
Total	*100*	*100*

6.3.1.3 FTIR Spectroscopy Analysis

FTIR spectra of IAA and RA are shown in Figure 6.2 and typical peak assignments are listed in Table 6.2. The regions from 3100-3640 cm^{-1} are featureless for both materials, indicating minimum content of hydroxyl containing species. Appearance of OH stretches would be due to carboxylic/hydroxyl groups in asphaltene molecules or presence of aluminosilicate (clays such as kaolinite and illite) co-precipitated with asphaltenes. In the latter case, the OH stretches are accompanied by peaks indicating Si-O and Al-OH stretches at 900-1100 cm^{-1}. The absence of peaks for OH groups suggests that our centrifugation process removed all the clay solids from the asphaltene samples. The distinctive difference between these two spectra is in the region representing sulfoxide groups at around 1020 cm^{-1}. Less significant but noticeable difference can also be seen in the region representing carbonyl groups at around 1700 cm^{-1}.

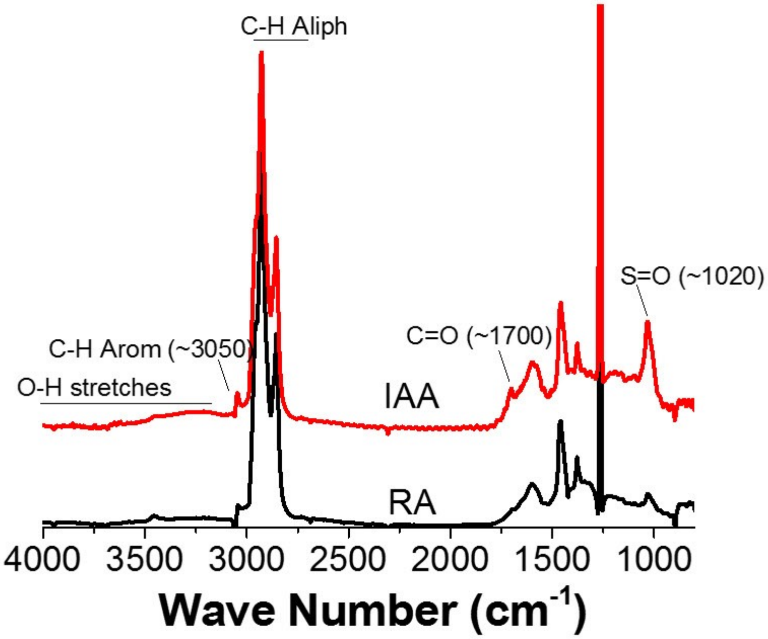

Figure 6.2 FTIR spectra of RA and IAA.

Table 6.2 FTIR peak assignment for typical asphaltene samples

v, cm-1	*Structural feature/functional groups*
3100-3640	O-H. N-H stretch
3000-3100	Aromatic C-H stretch
2780-3000	Aliphatic C-H stretch
1640-1800	Carbonyl C=O stretch
1620-1590	Aromatic C=C stretch
1370-1380	CH3 stretch
1020-1040	Sulfoxide S=O stretch
915-852	Aromatic CH out of plane deformation (1 adj. H)
760-730	Aromatic CH out of plane deformation (4 adj. H)

6.3.1.4 ^{1}H and ^{13}C Nuclear Magnetic Resonance Analyses

NMR spectroscopy is a powerful technique for quantifying both carbon and hydrogen types in petroleum samples. At CanmetENERGY, a processing method has been developed that uses information from both proton and carbon NMR spectra to quantify all of the carbon types present in the sample. Assignments are based on chemical shifts of model compounds and results from advanced NMR experiments, including distortionless enhanced polarization transfer [DEPT] and heteronuclear correlation [HETCOR]. Figures 6.3 and 6.4 illustrate the carbon types quantified. With quantifying "all" carbon species, additional calculations can be performed. For example, in Figure 6.5, the calculation of "average segment length of hydrocarbon chains" is illustrated. As well, the average cluster sizes for aromatic and cycloparaffinic rings can be calculated.

It should be noted that molecular characterizations by ES-MS, FTIR and NMR were also applied to parent whole asphaltenes (WA). No significant difference was observed between the results of RA and WA. Such results are anticipated as RA accounts for more than 98% of WA that these analytical techniques are not sufficiently sensitive to detect the differences contributed from subtle differences from IAA. Such results also explain why the study focusing on WA is hindering the progress of understanding molecular nature of asphaltenes aggregation and their stabilizing mechanism of water-in-oil petroleum emulsions.

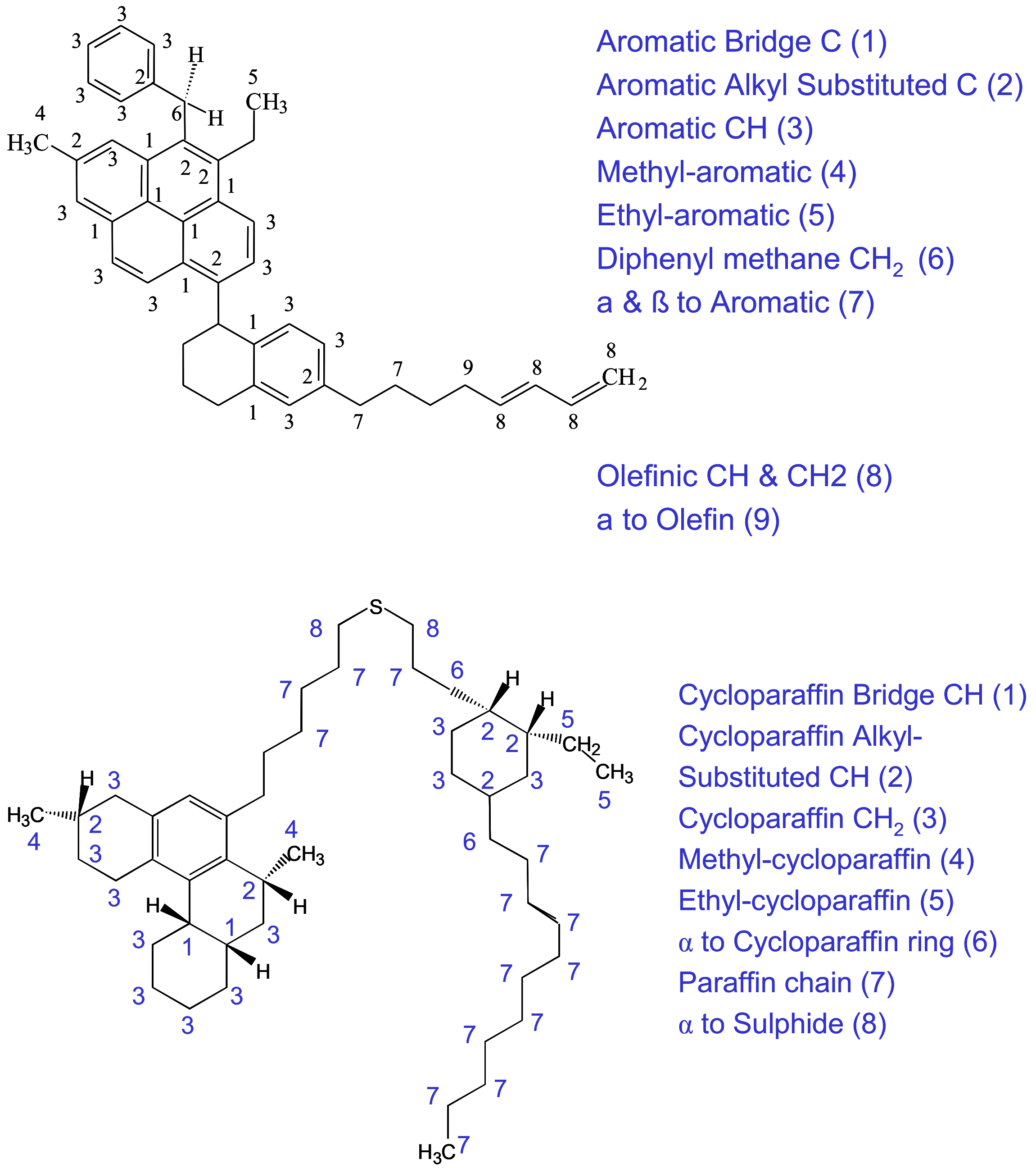

Figure 6.3 Molecular representations of aromatic, olefinic, cycloparaffinic, and paraffinic carbon types quantified using NMR data. The upper structure illustrates aromatic and olefinic species while the lower structure illustrates cycloparaffinic and paraffinic species.

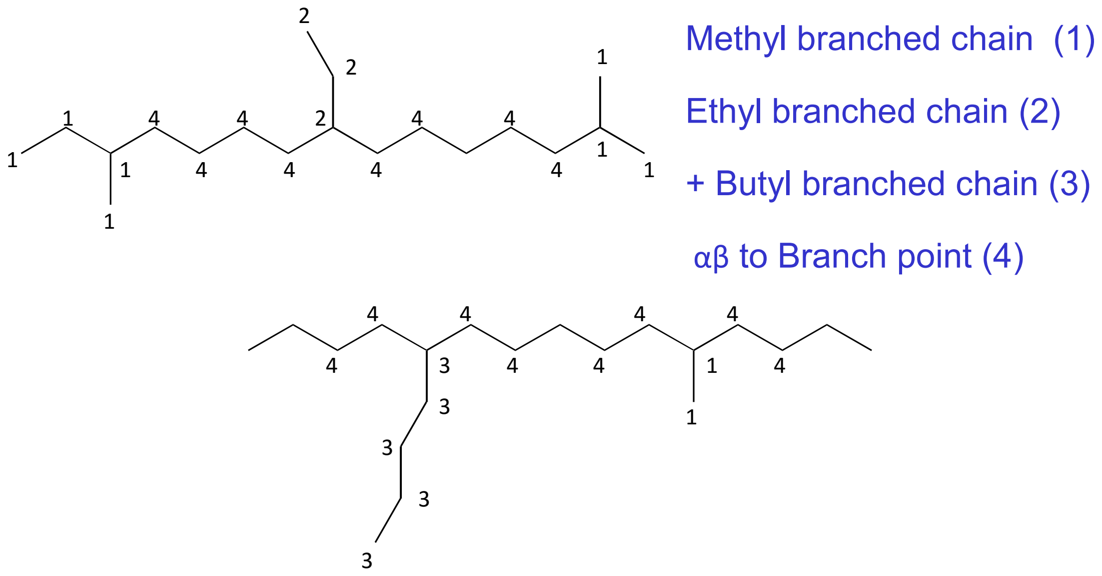

Figure 6.4 Molecular representations of branched paraffinic carbon types quantified using NMR data.

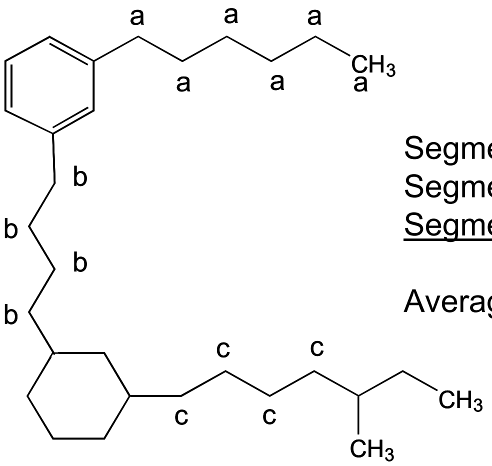

Segment “a” = 6 carbons
Segment “b” = 4 carbons
Segment “c” = 4 carbons

Average length = 14/3 = 4.7 carbon

Figure 6.5 Molecular structure that illustrates the calculation of the average “chain segment length”.

6.3.2 Molecular Representations for IAA and RA (ChemDraw)

As shown in Figure 6.6, we used a single large molecule to represent IAA (MW= 1457 Da) and two smaller molecules to represent RA (MW= 677 Da and 618 Da, respectively). Such molecular weight difference corresponds to the difference observed in the mass spectrometry analysis which suggested the IAA fraction to be dominated by larger molecules. It should be noted that NMR analysis itself is not sensitive to molecular weights. The use of ES-MS complements the NMR results by giving us a molecular weight basis to construct our molecular representations. For simulation simplicity, we used the minimum number of molecules that can achieve a reasonably good fit to our structural data to represent the asphaltene pool. As indicated by our molecular weight distribution results, minor percentage of RA was found having molecular weights higher than 1000 Da and a certain percentage of IAA was found having molecular weights less than 1000 Da.

The structural difference between the IAA and RA structures include their difference in molecular weights and the higher content of bridging chains in the IAA sample. Most of the increased oxygen content found in IAA sample is believed to be associated with sulfoxide groups as FTIR results suggested insignificant contents of hydroxyl and carbonyl groups. Compared to the RA asphaltenes, the IAA asphaltenes were found to have lower aromatic content, and higher cycloparaffinic and chain paraffinic contents. The carbon to sulfur atomic ratio is 26 for IAA and 22 for RA. About 75% of the sulfur atoms in RA and IAA were assigned as thiophenes, which is in agreement with literature.[43]

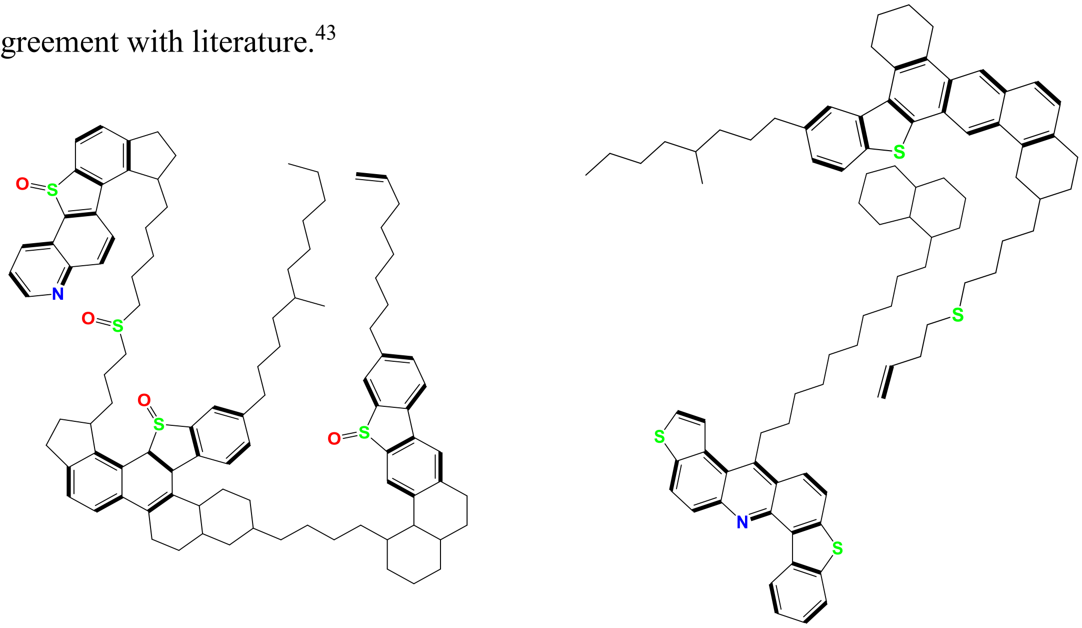

Figure 6.6 Molecular representations of IAA (left) and RA (right).

The comparison of the experimental NMR data and the fitted data for the proposed average structures of RA and IAA are given in Tables 6.3 and 6.4. The abbreviations used in the tables include C=O for carbonyl carbon; COOH for terminal carboxylic acid group; Ar, ArC and ArCa for aromatic, total aromatic carbon, and chain carbon that is α-to-aromatic ring, respectively; Cy, CyC and CyCa for cycloparaffinic, total cycloparaffinic carbon, and chain carbon that is α-to-cycloparaffinic ring, respectively; C for carbon; S, AlS and ArS for sulphur, aliphatic sulphur and aromatic sulphur, respectively; and N for nitrogen. It should be noted that the fitting of C/N ratio in Tables 6. 3 and 6.4 for RAs (86 vs 84) appears to be better than that (97 vs 79) for IAA. Such a big difference arises as a result that the C/N ratio was not used as a fitting criterion due to low content of N in asphaltene molecules. To perfectly fit the C/N ratios, the fit needs to use“units”of 84 and 79 carbons. The minimum number of carbons needed to fit the carbon type data was 86 and 97. So to fit the C/N ratio and maintain the chosen molecular weights, the numbers of molecules for each type of asphaltenes would need to be increased to include at least, for example, 168 and 158 carbons in the sets. Manual fitting of these larger numbers of carbon atoms becomes unwieldly. It should also be noted that the molecular representation shown for IAA is not exclusive. There could exist a number of isomers of slightly different molecular structures that fit the results of the elemental, NMR, FTIR and MS analyses. For the purpose of illustrating the role of distinct molecular structures of IAA and RA in determining their interfacial association, only the structure of IAA shown was simulated, although it would be of great interest to see how different isomers behavior at the oil-water interface, which is a subject of on-going research.

6.3.3 MD Simulations of the Molecular Representations of IAA and RA in Toluene Solutions and the Toluene-Water Interface

To establish a direct link between the microscopic and macroscopic behavior of the asphaltene fractions, molecular dynamics (MD) simulation was used to study molecular aggregation of IAA and RA subfractions in emulsion films. MD simulation is a powerful tool to explore the time-dependent behavior of the molecular associations and adsorption of the IAA and RA molecules at the oil/water interface over an enormous range of spatio-temporal domains.

Table 6.3 Comparison of the measured with NMR data-fitted molecular structures of the remaining asphaltenes (RA)

	Carbon Content (mole %)	
Carbon Type	Measured	NMR Fit
Aromatic	48.7	47.7
Cycloparaffinic	21.4	20.9
Branched Paraffinic	1.9	2.3
Chain Paraffinic (C1+)	26.7	26.7
Olefinic	1.2	2.3
C=O	0.0	0.0
Total	100.0	100.0
	Content (mole fraction) (±0.1)	
Chain End Type	Measured	NMR Fit
Aromatic	0.2	0.2
Olefinic	0.1	0.1
Cycloparaffinic	0.2	0.2
Branched Paraffinic	0.1	0.2
Paraffinic CH3	0.1	0.1
Sulphidic S	0.2	0.2
COOH	0.0	0.0
Total*	0.9	1.0
* Variance from 1.0 due to round-off error		
Parameter	Measured	NMR Fit
# Carbons		43
Molecular weight (g/mole)		648
Ar Cluster size (#carbons)	19	20.5
Cy Cluster size (#carbons)	7	7
ArC/CyC	2.3	2.3
ArCa/CyCa	1.1	1.0
Chain segment length	4.8	6.6
C/S	26	21.5
AlS/(AlS+ArS)	0.3	0.3
ArC/S	13	10.3
ArC/ArS	17	13.7
C/N	84	86.0
ArC/N	41	41.0

Table 6.4 Comparison of the measured with NMR data-fitted molecular structure of the extracted interfacially active asphaltenes (IAA)

	Carbon Content (mole %)	
Carbon Type	Measured	NMR Fit
Aromatic	43.5	44.3
Cycloparaffinic	23.1	22.7
Branched Paraffinic	2.7	2.1
Chain Paraffinic (C1+)	29.3	28.9
Olefinic	1.2	2.1
C=O	0.3	0.0
Total	100.0	100.0
	Content (mole fraction) (±0.1)	
Chain End Type	Measured	NMR Fit
Aromatic	0.2	0.2
Olefinic	0.1	0.1
Cycloparaffinic	0.4	0.3
Branched Paraffinic	0.0	0.2
Paraffinic CH3	0.1	0.1
Sulphidic S	0.2	0.2
COOH	0.0	0.0
Total*	1.0	1.1
* Variance from 1.0 due to round-off error		
Parameter	Measured	NMR Fit
# Carbons		97
Molecular weight (g/mole)		1425
Ar Cluster size (#carbons)	17	14.3
Cy Cluster size (#carbons)	8	6
ArC/CyC	1.9	2.0
ArCa/CyCa	0.4	0.5
Chain segment length	3.8	4.7
C/S	22	24.3
AlS/(AlS+ArS)	0.2	0.3
ArC/S	9	10.8
ArC/ArS	12	14.3
C/N	79	97.0
ArC/N	34	43.0

As discussed in section 6.3.2 and shown in Figure 6.6, the IAA is represented by a single molecule (MW= 1457 Da) while the RA is represented by two molecular structures (MW= 677 Da and 618 Da, respectively).

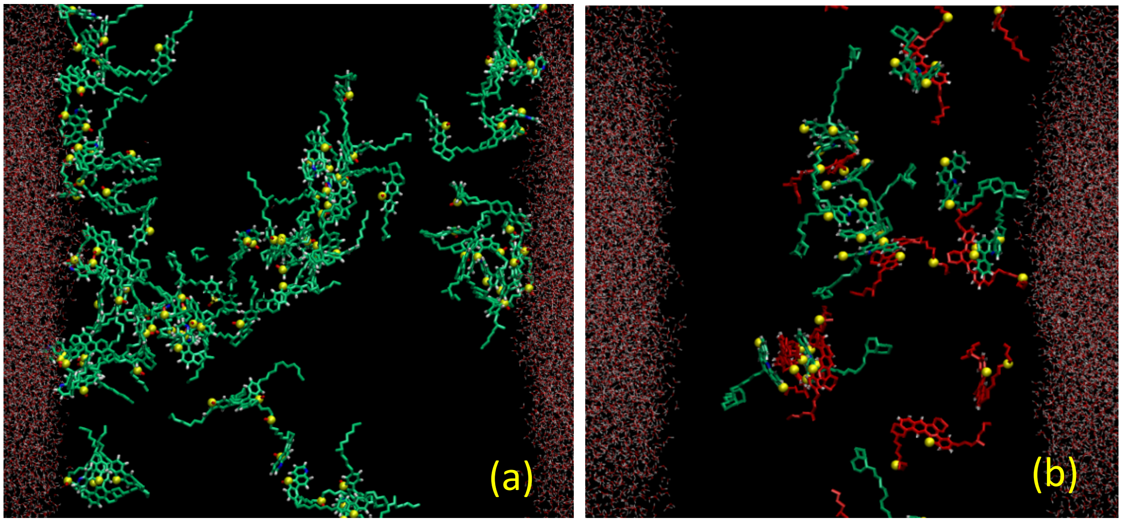

Figure 6.7 Molecular configurations of the two simulation system at the toluene/water interface (a) IAA, and (b) RA. The snapshots of the simulations were taken at the end of 100 ns simulation time. Toluene molecules were removed from the snapshots for clarity purpose. In all structures, sulfur, oxygen, nitrogen and hydrogen atoms are presented by yellow, red, blue and white color, respectively. Carbon atom is represented by green in IAA structure and green and red (for the purpose to differetate the two RA structures) in RA structure, respectively.

Figure 6.7 shows snapshots of simulation systems at the end of the simulation time (t = 100 ns). Qualitatively, IAA molecules showed a higher tendency to migrate to the toluene/water interface. Compared with RA, significantly more IAA molecules were found to be anchored at the toluene/water interface. This finding implies that IAA molecules exhibit a greater interfacial activity than RA molecules. These results are in good agreement with the results of interfacial tension measurement reported in our previous work.[23] During the simulation, all the asphaltene molecules remained within the boundary of the toluene phase, and did not partition into the water phase.

To quantitatively examine the nature of the interfacial activity of these molecules in the system, we computed the density profiles over the last 2 ns of the simulation and partition ratio of the molecules with time (see Figure 6.8 and 6.9). It should be noted that, although the average was performed over 2 ns simulation period, the simulations conducted over a longer period of 5 ns and 8 ns (shown in Appendix I) showed similar distributions, confirming that the average over 2 ns period is sufficient for accurate representation of the system state. To calculate the density distribution of the simulated system, we divided the entire simulation box into 50 slabs of equal thickness along the z-direction and calculated the density in each slab for all the asphaltene species.[32] The density was calculated by dividing the total mass of all atoms appeared in each slab by the volume of the slab. In all the simulations, z-direction is set perpendicular to the toluene/water interface. The toluene/water interfaces in the density profiles were located at the point where the toluene and water lines cross each other. Results from the density profiles show that IAA molecules tend to form higher peaks at the two interfaces, indicating that IAA has a stronger affinity to the toluene/water interface. In contrast, the density profile of RA showed a broad hump at the center of toluene phase, indicating that RA molecules prefer to concentrate more in the bulk solvent phase and do not exhibit affinity to the interface, as anticipated when considering the fact that most of surface active asphaltene molecules were already removed from RA as IAA by emulsion isolation. The simulation was also performed on single component RA-I and RA-II systems. The calculated density profiles for RA-I and RA-II were similar (shown in Appendix II), illustrating the importance of functional group in the molecules in determining molecular adsorption/association at the oil-water interface.

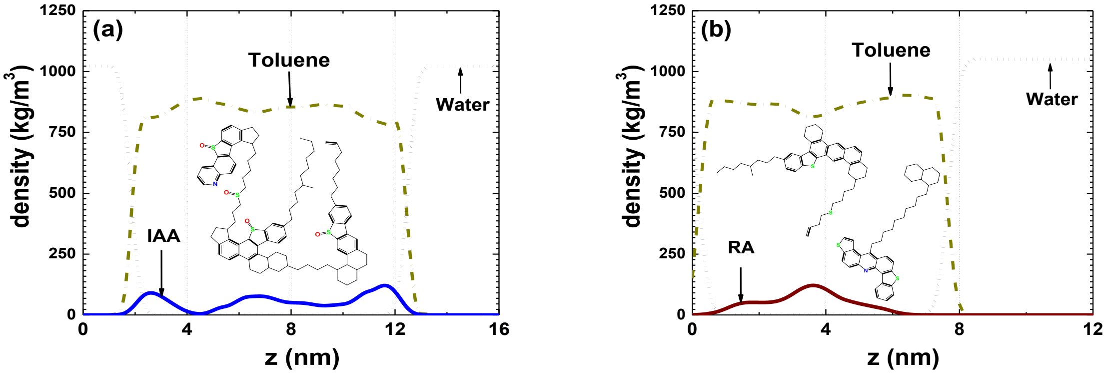

Figure 6.8 Density profiles of toluene/water system containing averaged IAA (a) and RA (b) structures over the last 2 ns of the simulation time.

The partition ratio, $P_{I/T} = N_I / N_T$, was plotted as a function of time to analyze the adsorption kinetics of these two asphaltene fractions towards the oil/water interface. N_I and N_T represent the number of interfacially-bound molecules and the total number of molecules in the system, respectively. To calculate the number of interfacially-bound RA and IAA molecules, we use a cutoff distance of 1 nm from the oil-water interface on both sides of the interface to the bulk oil phase. The interfacially bound molecules are defined as molecules that have at least one symmetrically defined atom fall within the cutoff distance from the interface. Then the total number of molecules bound to the interface was divided by the total number of simulated molecules to get the partition ratio.

As can be seen in Figure 6.9, IAA molecules have a much higher partitioning ratio than RA molecules, and such partitioning ratio increases with time, indicating that IAA molecules have a preference to reside on the interface. At the end of our simulation (100ns), around 50% of the IAA molecules were found within 1 nm distance from the interface, while RA molecules showed a partitioning ratio of around 12.5%. Considering a 10 nm thickness of the simulated toluene phase in contrast to a cutoff distance of 1 nm on each sides of the interface, an interfacial region represents 20% of the total oil phase. Therefore, a partition ratio of 12.5% indicates that RA molecules prefer to stay in the toluene phase.

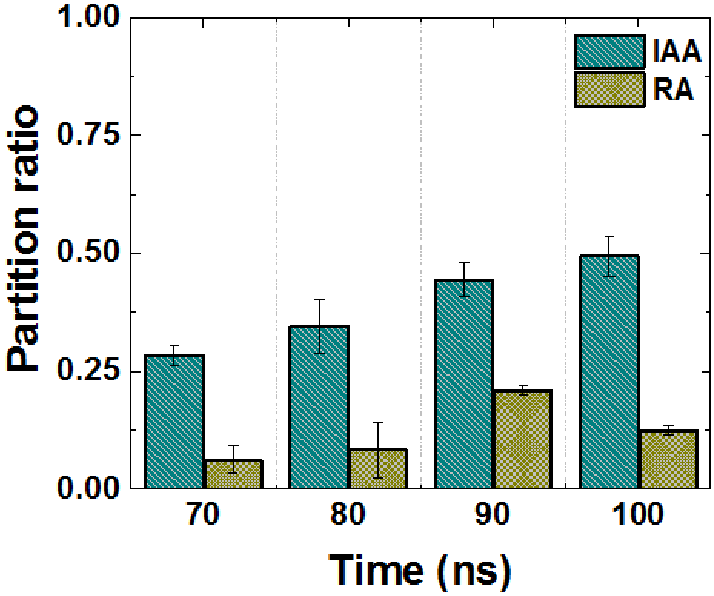

Figure 6.9 Partition ratio of IAA and RA molecules in toluene-water systems as a function of time. The averaging was performed over the last 2 ns of the simulation time (e.g., for a reference time of 70 ns the averaging was performed between 68-70 ns time interval)

From the snapshots in Figure 6.7 we can see that both RA and IAA asphaltene molecules showed a certain affinity to self-association in the solvent phase, but the degree of aggregation is much higher for IAA. Considering the variety and complex nature of the possible interactions between these molecules, we limited our investigation to π-π stacking and sulfur-sulfur associations that are considered to be the most relevant to our system. π-π stacking was selected for investigation as it is considered to be the major driving force for the formation of asphaltene nanoaggregates in a large number of recent studies.[13,14,30] Sulfur-sulfur interaction was selected because the oxygen content and sulfur in sulfoxide were the two major differences between IAA and RA in the elemental analysis and FTIR spectra. To examine such interactions, the radial distribution functions between poly-aromatic moieties and between sulfur –sulfur atoms were calculated as shown in Figure 6.10 a and b, respectively. The radial distribution function (RDF) or pair correlation function *g(r)* represents the probability to find a particle or atom in a shell d*r* at the distance *r* away from a given reference particle or atom. Thus, *g(r)* is defined as:

$$g(r) = N(r) / 4\pi r^2 \rho \, dr \qquad (1)$$

where $N(r)$ is the number of particles at a distance between r and $r + dr$ from a given reference atom, and ρ represents the number density which is taken as a ratio between the total number of atoms (N) to the volume of the computing box.

The results shown in Figure 6.10 a and b are the averaged **inter-**molecular interactions in the toluene phase over the last 2 ns of the simulation time (98 ns - 100 ns). The **intra-**molecular sulfur-sulfur interaction is removed from the total RDF results of the sulfur-sulfur association to reflect the role of sulfur-sulfur interaction in aggregation between asphaltene molecules. Similar methodology was also employed in removing the intramolecular π-π interactions from the total RDF results. The **intra-**molecular sulfur-sulfur and π-π interactions are shown in the Appendix III

Aggregation due to the π-π interaction for the IAA molecules is weaker as shown in Figure 6.10. This is probably due to the fact that IAA molecules possess much higher steric hindrance in comparison to the RA molecules, given their structural difference. In contrast, for the RA molecules, the π-π interaction is much stronger and is likely the main driving force for the aggregation of the molecules in the system. The radial distribution of poly-aromatic moieties in the RA molecule showed four higher peaks, indicating highly extended stacking of RA molecules. The first peak at around 0.45 nm in Figure 6.10b corresponds to the formation of strong poly-aromatic π-π stacking as reported in literature.[30-32] Since our radial distribution calculation was limited to the distance between the centers of poly-aromatic cores, the presence of three smaller peaks suggests the presence of off-set stacking. IAA molecules, on the other hand, show multiple and much higher peaks in their sulfur-sulfur RDF than RA molecules, suggesting a dominant role of sulfoxides in aggregation of IAA molecules, in contrast to a dominant role of π-π interactions in aggregation of RA molecules. The insets in Figure 6.10 show typical asphaltene aggregate clusters observed at the end of 100ns simulation time in our simulation. Clear difference between IAA and RA in their aggregation formation can be seen.

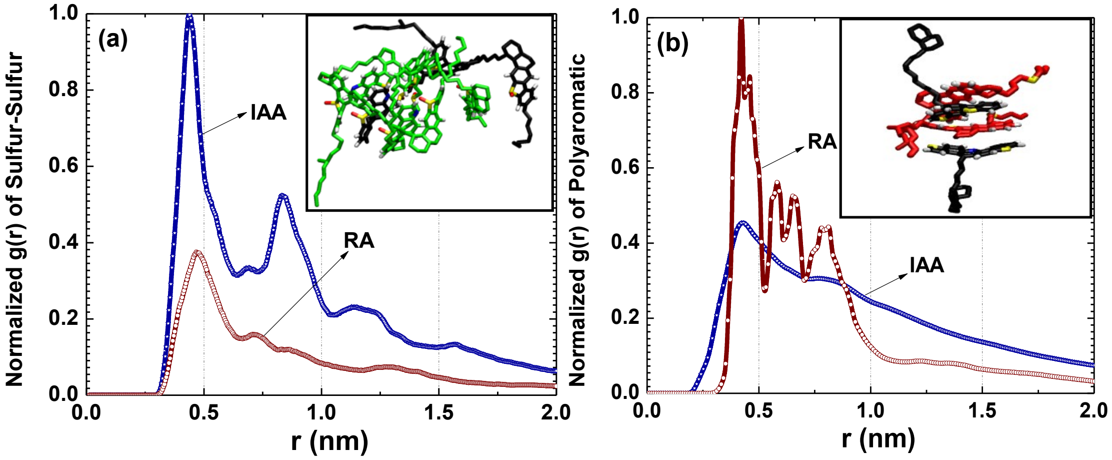

Figure 6.10 Normalized radial distribution functions, $g(r)/g(r)_{Max\,\mathrm{peak}}$ *of the sulfur-sulfur interaction (a) and poly-aromatic core (b) averaged over the last 2 ns of the simulation time (98 ns - 100 ns) at 298 K.*

6.4 DISCUSSION

The key role of asphaltenes in stabilizing water-in-oil emulsions has been well established for a long time.[1-12,21,22,26,27] However, the lack of molecular structures of asphaltenes that actually stabilize the emulsions hindered the progress in understanding the role of their aggregation and interfacial behavior in emulsion stabilization. Asphaltenes do not have well defined amphiphilic structure as in conventional surfactants [48,49] to explain their affinity to adsorb at the oil/water interface. Despite the recent progress in understanding asphaltene aggregation,[50] the role of different functionalities and interactions involved is still a subject of intense debate. The establishment of the importance of a specific fraction of asphaltenes for stabilizing water-in-oil emulsion stabilization and the extraction method proposed in our previous work to effectively isolate such a fraction [23] offers a promising starting point to further deepen our understanding of mechanisms of petroleum emulsion formation at molecular level.

The comprehensive chemical characterization of IAA fraction suggested that these species have higher average molecular weights and more polar functional groups comparing with the remaining asphaltenes. The molecular weight distribution of IAA and RA both cover a wide range, suggesting that both fractions contain diverse population of molecular structures. It is worth mentioning that the molecular representations of the asphaltene samples in Figure 6.6 correspond to structures that fit the major structural features derived from a suite of analytical techniques. It is popularly envisioned that π - π stacking interactions is the predominant model for asphaltene aggregation.[13,14] From the simulation data, these types of interactions were only significant for the RA asphaltenes. In contrast, π - π stacking interactions between IAA molecules were less favorable than that between RA molecules. The discussion below is focused on the influence of asphaltene structure and functional groups on two aspects related to emulsion stabilization, namely ***surface activity*** and ***film formation***.

6.4.1 Surface activity

The interfacial activity of asphaltenes is commonly related to the presence of heteroatoms which constitute polar functional groups. Indeed, compared with RA, the IAA fraction was more enriched in heteroatoms, most noticeably in oxygen. Oxygen atoms in bitumen or asphaltenes are often considered to indicate the presence of carbonyl or carboxylic acids, which are known to be surface active. However, the amount of carboxylic groups in the asphaltenes is supposed to be small, especially when compared with the deasphalted bitumen fractions. In our study, higher oxygen content in IAA was assigned to sulfoxides as revealed by FTIR analyses. MD simulation showed that IAA structure is more interfacially active than RA. Here, we attempt to relate the interfacial activity of IAA with its chemical structure by examining the interacting sites of IAA molecules with oil/water interface in MD simulation. Interestingly there is no clear indication of preferential orientation of the IAA molecule at the interface, which accounts for its non-amphiphilic structure. However, a combination of various weak associations is likely responsible for its interfacial activity as suggested by the sites of IAA molecules anchored at the oil/water interface. Possible associations would include S=O···H (water), Aromatic H···O (water), Aromatic π···H (water) and also acid-base interaction between pyridine moieties and water. On the other hand, MD simulation showed that RA molecules seldom attach to the interface although they share similar ring structures and pyridine moieties. To understand this major difference in the interfacial behavior of IAA and RA, it is helpful to examine the role of thiophene sulfoxides. More than 70% of the sulfoxides exist as thiophene sulfoxide in IAA structure, meaning their presence in the ring system is surrounded by unsaturated hydrogen atoms. The high polarity of sulfoxide groups in IAA molecules increases the interfacial activity of IAA molecules. The sulfoxide groups can form hydrogen bonds with water molecules at the interface. They also bring the neighboring hydrogen atoms to the interface with which weaker but multiple hydrogen bonds can be formed. Furthermore, as we will discuss below, the IAA molecules can self-associate with each other. Such self-association together with multiple interactions with water interface appear to explain the irreversible adsorption of IAA at the interface as experimentally observed.[23] RA molecules, on the other hand, might still be able to associate with the interface through the ring and pyridine system, but the strength of such association is weaker and less stable without sulfoxides. The self-association between RA molecules through π-π stacking is known to consume the active ring system that could otherwise associate with the water phase, further decreasing their surface activity.

6.4.2 Supramolecular self-assembly and network formation.

It was reported that the ability of asphaltenes to stabilize water-in-oil emulsions is related to the formation of an extended network in the oil film between water droplets[22] and a viscoelastic layer at the interface.[10,11] In the previous chapter,[23] we found a drastic difference in emulsion stabilization capacity of IAA and RA fractions. Characteristic properties previously attributed to the asphaltenes as a whole, such as formation of thick films, rigid interfaces and ageing, were found to be characteristic only for the IAA. The RA, with IAA removed, did not exhibit these peculiarities. Here, we attempt to relate these interfacial and film properties with the proposed structure of IAA fraction. The influence of sulfoxide groups on the asphaltene aggregation behavior has not been investigated and discussed in the literature. The only related work is on aging of road asphalts, where the ageing and oxidation were found to increase the amount of sulfoxides, which led to a higher viscosity of the asphalts.[51]

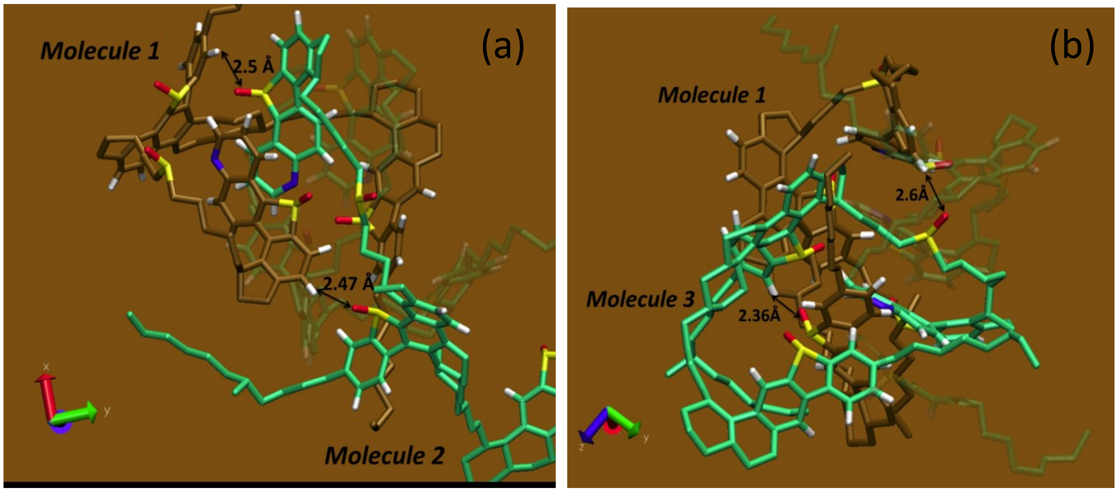

Figure 6.11. Possible hydrogen bonds formed between sulfoxide group and hydrogen atoms in an IAA cluster containing three molecules. (a) interaction between molecule 1 and molecule 2, (b) interaction between molecule 1 and molecule 3. In the structures, sulfur, oxygen, hydrogen, and nitrogen atoms are presented by yellow, red, white and blue, respectively; Carbon atoms are represented by green or brown.

The bonds between the sulfur and oxygen atoms give the sulfoxide group an electrostatic aspect with the oxygen atoms being negatively charged. Such a dipolar structure makes sulfoxide groups able to serve as strong hydrogen bond acceptors. Furthermore, the strong polarity of sulfoxide groups would promote intermolecular hydrogen bonding such as S=O···H-C-S=O by increasing the acidity on the adjacent hydrogen. Such bonding was believed to provide robust building blocks for supramolecular structures in crystal engineering.[52]

To further understand the role of sulfoxide groups for the observed association of IAA molecules, a cluster of IAA aggregates in the proximity of toluene-water interface was chosen and the relative positions of sulfoxide moieties to other atoms were examined to suggest possible interaction mechanisms, see Figure 6.11. One possible association is hydrogen bonding between the oxygen site of the sulfoxide moiety and the hydrogen near the sulfoxide moiety of another neighboring IAA molecule. Considering the promotion of acidity on the hydrogen due to the strong polarity of the near sulfoxide groups, such association is highly probable.[52] The distance between the oxygen site on sulfoxide moiety and the hydrogen was determined to be ~ 2.5 Å, suggesting possible formation of hydrogen bond between the sulfoxide and ring system. When such hydrogen bond is formed, the distance between the sulfoxide involved in the bond formation and another sulfoxide near to the hydrogen bond would fall into the range of 4.5-5 Å. Such a range corresponds well with the first peak in our radial distribution of intermolecular sulfur-sulfur pairs in IAA sample. The presence of the second peak at ~8.6 Å would suggest a passive association due to the structural distance between two sulfoxide groups in the same molecule. It is worth noticing that in the examined clusters, the association between each pair of molecules involved two sulfoxide groups, leaving the other two sulfoxide moieties either not-associated (active to accept hydrogen atoms) or associated with a third molecule. Examinations on other clusters suggested very similar association patterns. Such interactions might provide explanation for the 3D network formation and its extension upon aging. For example, in the cluster we had chosen in Figure 6.11, molecule 1 (brown color) served as a linker for molecules 2 and 3. For each of these molecules, there are another two 'un-used' sulfoxides that can interact with other clusters or individual molecules. The trajectories of our MD simulation suggest the association of the aliphatic chains with sulfoxide groups is less favorable

While the content of carbonyl and carboxylic groups was not significant in our IAA asphaltene sample, we cannot discount the possibility that the asphaltenes from a different source of origin could have a much higher content and involvement of C=O groups. It would be worth a great effort in the future to study asphaltenes from different sources to examine whether the enrichment of sulfoxide groups is a universal phenomenon for interfacial asphaltenes.

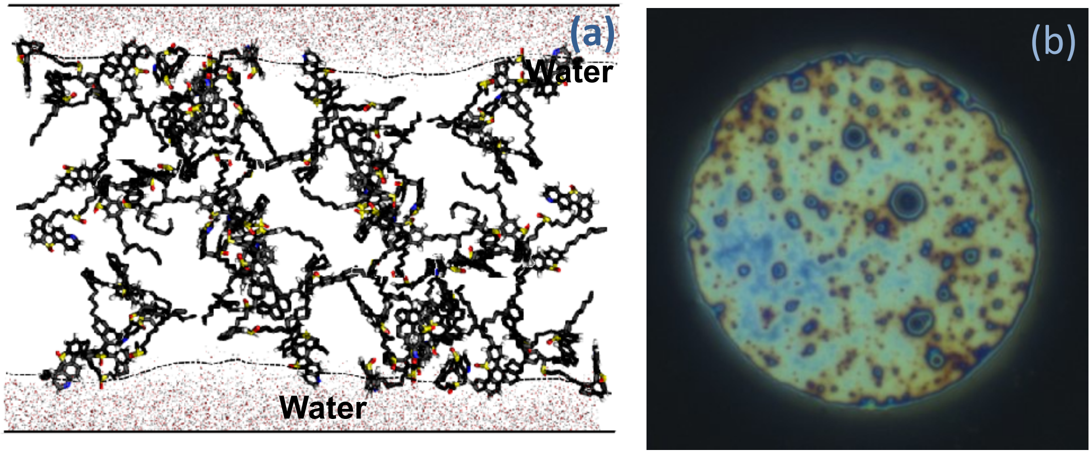

Figure 6.11 Possible schematic model of W/O emulsion stabilization by IAA (a) and thin liquid film formed by IAA (b) as reported previously.[23]

6.4.3 Mechanism of water-in-oil emulsion stabilization by asphaltenes.

Even though the IAA asphaltenes represent only a small fraction of the whole asphaltenes (< 2%), their molecular structure and chemical composition make them the main components that govern the interfacial and emulsion properties of water in heavy/crude oil emulsions. Similar to RA, the average IAA molecules are predominantly hydrophobic without well-defined amphiphilic structure. However, IAA molecules are much more surface active than RA and can self-associate to form a cross-linked network consisting of hydrocarbon backbones linked at multiple interaction sites. Figure 6.12 (a) shows a possible presentation of the initial network formed by IAA fraction. Such a network would serve as a framework on which aggregates would grow in size and density with increasing ageing time and asphaltene concentration. Such a structure would likely be porous and swell when filled with solvents. Similar swelling phenomenon was observed experimentally when asphaltene film on mica surface was put in contact with toluene.[53] The interaction between IAA and non-IAA molecules is also possible through hydrogen bonding between sulfoxides and the fused polyaromatic rings. Such interaction is likely to consume the interaction/binding sites available for network formation and hence slow down the aging effect, as this was also experimentally observed. The network with the pores being filled with solvent and other relevant molecules eventually behaves like a soft gel. The formation of such a gel phase is the reason that liquid inside the film has a non-Newtonian nature with yield stress as discussed in Chapter 4. This non-Newtonian nature of the film stops the film from draining out to reach the critical rupturing thickness, thus stabilizing the emulsion.

6. 5 CONCLUSION

Based on elemental analysis along with FTIR, MS and NMR characterization, it was found that compared to the remaining asphaltenes (RA), the interracially active fractions of asphaltenes (IAA) are generally larger molecules containing a higher amount of heteroatoms. The oxygen content of the IAA fraction was found to be approximately three times higher than that of the RA, with the oxygen being assigned to oxidation of sulphur to sulfoxides (S=O). Average molecular representations of IAA and RA were constructed based on structural information obtained.

Molecular representations of the IAA and RA were used in MD modeling to understand how the structural differences affect their aggregation in the organic bulk phase and the vicinity of the oil/water interface. The RA molecules were found to be less interfacially active. They self-associate in toluene via stacking of the fused polyaromatic rings, which is in line with the current understanding in the asphaltene literature. IAA structures were found to be much more interfacially active which promoted the formation of supramolecular structures. MD simulation results support the early experimental findings that IAA molecules adsorb irreversibly to the oil/water interface, forming a porous network that extends from the interface towards the oil phase. The profound differences in the interfacial and aggregation properties of IAA and RA were linked to the presence of sulfoxide groups that feature a high polarity and induce various molecular interactions. With only a small fraction of IAA (less than 2%) in the original asphaltenes, this study clearly illustrates the critical importance of probing the molecular structure and interfacial properties of IAA in order to advance our knowledge on molecular mechanisms of asphaltene-stabilized water-in-oil petroleum emulsions.

REFERENCES

1. Gao, S., Moran, K., Xu, Z., & Masliyah, J. (2010). Role of naphthenic acids in stabilizing water-in-diluted model oil emulsions. *The Journal of Physical Chemistry B*, *114*(23), 7710-7718.

2. McLean, J. D., & Kilpatrick, P. K. (1997). Effects of asphaltene aggregation in model heptane–toluene mixtures on stability of water-in-oil emulsions. *Journal of Colloid and Interface Science*, *196*(1), 23-34.

3. Ortiz, D. P., Baydak, E. N., & Yarranton, H. W. (2010). Effect of surfactants on interfacial films and stability of water-in-oil emulsions stabilized by asphaltenes. *Journal of Colloid and Interface Science*, *351*(2), 542-555.

4. Yang, X., Verruto, V. J., & Kilpatrick, P. K. (2007). Dynamic asphaltene-resin exchange at the oil/water interface: Time-dependent W/O emulsion stability for asphaltene/resin model oils. *Energy & Fuels*, *21*(3), 1343-1349.

5. Yarranton, H. W., Hussein, H., & Masliyah, J. H. (2000). Water-in-hydrocarbon emulsions stabilized by asphaltenes at low concentrations. *Journal of Colloid and Interface Science*, *228*(1), 52-63.

6. Zhang, L. Y., Xu, Z., & Masliyah, J. H. (2003). Langmuir and Langmuir-Blodgett films of mixed asphaltene and a demulsifier. *Langmuir*, *19*(23), 9730-9741.

7. Langevin, D., Poteau, S., Hénaut, I., & Argillier, J. F. (2004). Crude oil emulsion properties and their application to heavy oil transportation. *Oil & Gas Science and Technology*, *59*(5), 511-521.

8. Hirasaki, G. J., Miller, C. A., Raney, O. G., Poindexter, M. K., Nguyen, D. T., & Hera, J. (2010). Separation of Produced Emulsions from Surfactant Enhanced Oil Recovery Processes. *Energy & Fuels*, *25*(2), 555-561.

9. Kiran, S. K., Ng, S., & Acosta, E. J. (2011). Impact of Asphaltenes and Naphthenic Amphiphiles on the Phase Behavior of Solvent− Bitumen− Water Systems. *Energy & Fuels*, *25*(5), 2223-2231.

10. Yeung, A., Dabros, T., Masliyah, J., & Czarnecki, J. (2000). Micropipette: a new technique in emulsion research. *Colloids and Surfaces A: Physicochemical and Engineering Aspects*, *174*(1), 169-181.

11. Spiecker, P. M., Gawrys, K. L., Trail, C. B., & Kilpatrick, P. K. (2003). Effects of petroleum resins on asphaltene aggregation and water-in-oil emulsion formation. *Colloids and Surfaces A: Physicochemical and engineering aspects*, *220*(1), 9-27.

12. Spiecker, P. M., & Kilpatrick, P. K. (2004). Interfacial rheology of petroleum asphaltenes at the oil-water interface. *Langmuir*, *20*(10), 4022-4032.

13. Mullins, O. C. (2010). The Modified Yen Model. *Energy & Fuels*, *24*(4), 2179-2207.

14. Mullins, O. C., Sabbah, H., Eyssautier, J., Pomerantz, A. E., Barré, L., Andrews, A. B., ... & Zare, R. N. (2012). Advances in asphaltene science and the Yen–Mullins model. *Energy & Fuels*, *26*(7), 3986-4003.

15. Yen, T. F. (1974). Structure of petroleum asphaltene and its significance. *Energy Sources, Part A Recovery, Utilization, and Environmental Effects*, *1*(4), 447-463.

16. Strausz, O. P., Mojelsky, T. W., & Lown, E. M. (1992). The molecular structure of asphaltene: an unfolding story. *Fuel*, *71*(12), 1355-1363.

17. Strausz, O. P., Mojelsky, T. W., Faraji, F., Lown, E. M., & Peng, P. A. (1999). Additional structural details on Athabasca asphaltene and their ramifications. *Energy & Fuels*, *13*(2), 207-227.

18. Agrawala, M., & Yarranton, H. W. (2001). An asphaltene association model analogous to linear polymerization. *Industrial & Engineering Chemistry Research*, *40*(21), 4664-4672.

19. Yarranton, H. W. (2005). Asphaltene Self-Association. *Journal of Dispersion Science and Technology*, *26*(1), 5-8.

20. Gray Gray, M. R., Tykwinski, R. R., Stryker, J. M., & Tan, X. (2011). Supramolecular assembly model for aggregation of petroleum asphaltenes. *Energy & Fuels*, *25*(7), 3125-3134.

21. Tchoukov, P., Czarnecki, J., & Dabros, T. (2010). Study of water-in-oil thin liquid films: Implications for the stability of petroleum emulsions. *Colloids and Surfaces A: Physicochemical and Engineering Aspects*, *372*(1), 15-21.

22. Tchoukov, P., Yang, F., Xu, Z., Dabros, T., Czarnecki, J., & Sjöblom, J. (2014). Role of asphaltenes in stabilizing thin liquid emulsion films. *Langmuir*, *30*(11), 3024-3033.

23. Yang, F., Tchoukov, P., Pensini, E., Dabros, T., Czarnecki, J., Masliyah, J., & Xu, Z. (2014). Asphaltene subfractions responsible for stabilizing water-in-crude oil emulsions. Part 1: interfacial behaviors. *Energy & Fuels*, *28*(11), 6897-6904.

24. Ali, L. H., Al-Ghannam, K. A., & Al-Rawi, J. M. (1990). Chemical structure of asphaltenes in heavy crude oils investigated by NMR. *Fuel*, *69*(4), 519-521.

25. Coelho, R. R., Hovell, I., de Mello Monte, M. B., Middea, A., & de Souza, A. L. (2006). Characterisation of aliphatic chains in vacuum residues (VRs) of asphaltenes and resins using molecular modelling and FTIR techniques. *Fuel Processing Technology*, *87*(4), 325-333.

26. Dettman, H. D.; Li, N.; Luo, J. (2009) *Corrosion*, Paper No. 09336, 1-13

27. Mueller, C. J., Cannella, W. J., Bruno, T. J., Bunting, B., Dettman, H. D., Franz, J. A., ... & Wright, K. (2012). Methodology for formulating diesel surrogate fuels with accurate compositional, ignition-quality, and volatility characteristics. *Energy & Fuels*, *26*(6), 3284-3303.

28. Saxena, A., Diaz-Goano, C., & Dettman, H. (2012). Coking Behaviour During Visbreaking. *Journal of Canadian Petroleum Technology*, *51*(06), 457-463.

29. Hoff, A.; Dettman, H.D. Presented at the World Heavy Oil Congress in Aberdeen, Scotland, 2012, Paper No. WHOC 12-275.

30. Kuznicki, T., Masliyah, J. H., & Bhattacharjee, S. (2008). Molecular dynamics study of model molecules resembling asphaltene-like structures in aqueous organic solvent systems. *Energy & Fuels*, *22*(4), 2379-2389.

31. Teklebrhan, R. B., Ge, L., Bhattacharjee, S., Xu, Z., & Sjöblom, J. (2014). Initial Partition and Aggregation of Uncharged Polyaromatic Molecules at the Oil–Water Interface: A Molecular Dynamics Simulation Study. *The Journal of Physical Chemistry B*, *118*(4), 1040-1051.

32. Teklebrhan, R. B., Ge, L., Bhattacharjee, S., Xu, Z., & Sjöblom, J. (2012). Probing structure–nanoaggregation relations of polyaromatic surfactants: a molecular dynamics simulation and dynamic light scattering study. *The Journal of Physical Chemistry B*, *116*(20), 5907-5918.

33. Boek, E. S., Yakovlev, D. S., & Headen, T. F. (2009). Quantitative Molecular Representation of Asphaltenes and Molecular Dynamics Simulation of Their Aggregation†. *Energy & Fuels*, *23*(3), 1209-1219.

34. Headen, T. F., Boek, E. S., & Skipper, N. T. (2009). Evidence for Asphaltene Nanoaggregation in Toluene and Heptane from Molecular Dynamics Simulations†. *Energy & Fuels*, *23*(3), 1220-1229.

35. Ancheyta, J., Centeno, G., Trejo, F., Marroquin, G., Garcia, J. A., Tenorio, E., & Torres, A. (2002). Extraction and characterization of asphaltenes from different crude oils and solvents. *Energy & Fuels*, *16*(5), 1121-1127.

36. Japanwala, S., Chung, K. H., Dettman, H. D., & Gray, M. R. (2002). Quality of distillates from repeated recycle of residue. *Energy & Fuels*, *16*(2), 477-484.

37. Solum, M. S., Pugmire, R. J., & Grant, D. M. (1989). Carbon-13 solid-state NMR of Argonne-premium coals. *Energy & Fuels*, *3*(2), 187-193.

38. Van der Spoel, D.; van Buuren, A. R.; Apol, E.; Meulenhoff, P. J.; Tieleman, D. P.; Sijbers, A.; Feenstra, K. The GROMACS Manual (version 3.3); Groningen University, Groningen, The Netherlands, 2004.

39. Berendsen, H. J., van der Spoel, D., & van Drunen, R. (1995). GROMACS: A message-passing parallel molecular dynamics implementation. *Computer Physics Communications*, *91*(1), 43-56.

40. Lindahl, E., Hess, B., & Van Der Spoel, D. (2001). GROMACS 3.0: a package for molecular simulation and trajectory analysis. *Journal of Molecular Modeling*, *7*(8), 306-317.

41. Oostenbrink, C., Villa, A., Mark, A. E., & Van Gunsteren, W. F. (2004). A biomolecular force field based on the free enthalpy of hydration and solvation: The GROMOS force-field parameter sets 53A5 and 53A6. *Journal of Computational Chemistry*, *25*(13), 1656-1676.

42. Kuznicki, T., Masliyah, J. H., & Bhattacharjee, S. (2009). Aggregation and partitioning of model asphaltenes at toluene− water interfaces: Molecular dynamics simulations. *Energy & Fuels*, *23*(10), 5027-5035.

43. Mullins O. In: EY Sheu, OC Mullins. (1995). Eds. *Asphaltenes: Fundamentals and Applications*; Plenum Press: New York, 53-96.

44. Nosé, S. (1984). A molecular dynamics method for simulations in the canonical ensemble. *Molecular Physics*, *52*(2), 255-268.

45. Hoover, W. G. (1985). Canonical dynamics: equilibrium phase-space distributions. *Physical Review A*, *31*(3), 1695.

46. Parrinello, M., & Rahman, A. (1981). Polymorphic transitions in single crystals: A new molecular dynamics method. *Journal of Applied physics*, *52*(12), 7182-7190.

47. Knovel Critical Tables, 2nd ed.; Knovel: New York, NY, USA, 2008; Available online:http://www.knovel.com/web/portal/browse/display?_EXT_KNOVEL_DISPLAY_bookid=761&VerticalID=0 (accessed on 2 February 2015).

48. Czarnecki, J., Tchoukov, P., Dabros, T., & Xu, Z. (2013). Role of asphaltenes in stabilisation of water in crude oil emulsions. *The Canadian Journal of Chemical Engineering*, *91*(8), 1365-1371.

49. Czarnecki, J., Tchoukov, P., & Dabros, T. (2012). Possible role of asphaltenes in the stabilization of water-in-crude oil emulsions. *Energy & Fuels*, *26*(9), 5782-5786.

50. Yarranton, H. W., Ortiz, D. P., Barrera, D. M., Baydak, E. N., Barre, L., Frot, D., ... & Oake, J. (2013). On the size distribution of self-associated asphaltenes. *Energy & Fuels*, *27*(9), 5083-5106.

51. Petersen, J., & Harnsberger, P. (1998). Asphalt aging: dual oxidation mechanism and its interrelationships with asphalt composition and oxidative age hardening. *Transportation Research Record: Journal of the Transportation Research Board*, (1638), 47-55.

52. Brondel, N., Moynihan, E. J., Lehane, K. N., Eccles, K. S., Elcoate, C. J., Coles, S. J., ... & Maguire, A. R. (2010). Does intermolecular S= O··· H–C–S= O hydrogen bonding in sulfoxides and sulfones provide a robust supramolecular synthon in the solid state?. *Crystal Engineering Communication*, *12*(10), 2910-2927.

53. Natarajan, A., Xie, J., Wang, S., Liu, Q., Masliyah, J., Zeng, H., & Xu, Z. (2011). Understanding molecular interactions of asphaltenes in organic solvents using a surface force apparatus. *The Journal of Physical Chemistry C*, *115*(32), 16043-16051.

CHAPTER 7 DEMULSIFICATION MECHANISM OF ASPHALTENE-STABILIZED WATER-IN-OIL EMULSIONS BY A POLYMERIC EO-PO DEMULSIFIER

7.1 INTRODUCTION

The formation of stable water-in-oil (W/O) emulsions during bitumen extraction poses operational problems, such as rag layers[1] that create bottlenecks in gravity separation vessels. In addition, the high salt concentration in any retained water in the overflow oil promotes corrosion of downstream process equipment and catalyst poisoning.[2]Bitumen is a mixture of complex natural chemical components of largely unknown molecular structures, among which asphaltenes play a major role in stabilizing W/O emulsions.[3] Research conducted using the thin liquid film balance technique has shown that asphaltenes form aggregates that are capable of flocculating water droplets but hinder their coalescence by retarding the intervening liquid film drainage, producing steric repulsion and forming rigid skins at the oil-water interface.[4-6]

Polymeric demulsifiers are commonly used to address emulsion stability issues and separate water from oil. Separation of water from oil can occur by flocculation and/or coalescence of the water droplets, to form larger water droplets that readily separate from the oil. However, to achieve a free water layer under the separation zone, droplet coalescence should be the dominant destabilizing mechanism. While flocculation can promote coalescence by enhancing the contact between water droplets,[7] flocculated water droplets can also be stabilized by steric forces that resist thin liquid film drainage.[8] Although flocculants are often used to separate water from oil emulsions, the use of coalescers is preferable as it reduces oil losses to the phase-separated underflow aqueous phase.[9]

Coalescers destabilize emulsions by three major mechanisms: 1) they exhibit greater interfacial activity compared with the stabilizing species, and can thus penetrate stabilizing films at the oil-water interface[10, 11]; 2) they disrupt and soften (i.e. lower the viscoelastic moduli) the stabilizing interfacial film[10, 12, 13]; and 3) they suppress interfacial tension gradients which are responsible for emulsion stabilization by the Marangoni effect.[14] When demulsifier molecules penetrate the bitumen or asphaltene stabilized films, the structure and mechanical properties of the film can change. For example, ethyl-cellulose (EC) was shown to modify the interfacial film texture[12] and produce fractures within the film.[15] Those fractures have been identified to provide favorable zones for drop-drop coalescence.

However, drop-drop coalescence in a separation vessel is a dynamic process where droplets undergo shear and compressional deformations.[16] Those deformations and the mobility of stabilizing species are dependent on the drop-drop contact force and droplet interfacial rheology. As a result, studying shear and compressional rheology of oil-water interfacial films would shed light on the mechanism of emulsion stability and hence demulsification.[17-19] Different studies have shown that demulsifiers soften interfacial films under compression.[10, 12] However little research has considered the shear rheological properties of interfacial stabilizing films,[13] and only one study has correlated emulsion stability by surface active biopolymers to high shear and compressional elasticity of the interfacial film.[16] The relationship between the demulsifier performance and interfacial rheology has been recognized,[20-22] but never investigated systematically for an important class of EO-PO based polymer demulsifiers at toluene-water interfaces.

Extensive research has been conducted using a variety of chemical demulsifiers, including ethyl-cellulose,[10, 23] non-ionic surfactants,[24] and EO-PO demulsifiers[25-30] to assess the relationship between the structure, composition, molecular weight, and demulsifier performance. Studies conducted using a broad array of EO-PO demulsifiers showed that at a low dosage, demulsifiers of higher hydrophilicity are more effective than those of lower hydrophilicity.[26, 27, 29] The effect of the demulsifier concentration on demulsification performance has frequently been investigated. It was established that beyond an optimal dosage, the performance of a demulsifier can either plateau (type I behaviour) or degrade (type II behaviour, also known as overdose), resulting in an increase in the emulsion stability. Type I behaviour has been reported for EC[31] and for some EO-PO demulsifiers,[27, 32-34] while overdose was observed for octylphenyl-polyethoxylates and sodium bis(2-ethylhexyl)sulfosuccinate demulsifiers,[35] commercial demulsifiers,[36-38] polyoxyalkylates,[9] diethanolamines,[15] and some EO-PO demulsifiers.[27, 39] These demulsifiers act either as flocculants or coalescers.[41] Overdose for flocculating demulsifiers, such as polyoxyalkylates[9] and diethanolamines,[15] was attributed to the low density of formed flocs[9] as a result of electrosteric repulsion.[15] Studies conducted using a wide array of coalescer type EO-PO polymer demulsifiers demonstrated a correlation between the hydrophilicity of EO-PO demulsifiers and their demulsification efficiency, with hydrophilic demulsifiers showing overdose effects at high concentrations.[27] Such studies generated critical information on the effect of the demulsifier composition and structure on its performance. However, the mechanisms of overdose by coalescer type demulsifiers remains to be explored.

Studies relating emulsion stability to the mechanical properties and morphology of asphaltene interfacial films are very limited and have only been conducted at the air-water interface.[40, 41] Although not directly related to emulsion films, studies on air-water interfaces laid the foundation in the context of new approaches to investigate stabilization mechanisms. The current study represents the first of its kind to relate the dewatering efficiency and the overdose of an EO-PO demulsifier to the interfacial shear and the compressional rheological properties of the films, and to their morphological structure studied by Brewster Angle Microscopy (BAM). Macroscopic observations were supplemented by molecular level morphologies of interfacial films transferred on silicon wafers by Langmuir-Blodgett method and determined by Atomic Force Microscopy (AFM) and Scanning Electron Microscopy (SEM). Finally, X-ray Photoelectron Spectroscopy (XPS) was used to study the change in chemical composition of asphaltene films upon the addition of the demulsifier.

7.2 MATERIALS

7.2.1 EO-PO demulsifier

An EO-PO block-copolymer demulsifier was provided by Baker Hughes and used throughout this study. The demulsifier had a star-like structure of five arms, a molecular weight of ~12,000 g/mol and an EO content of 35% (number of EO% per mole). The EO groups in the structure conferred hydrophilic properties and the PO groups added hydrophobic properties to the demulsifier molecule. The amphiphilicity of the demulsifier enabled preferential sorption at the oil-water interface, exceeding the interfacial activity of the stabilizing species (Figure 7.1). The relative solubility number (RSN) of the demulsifier was determined to be 18 following a standard protocol.[42]

7.2.2 Solvents and water

HPLC grade toluene and pentane (Fisher Scientific, Canada) were used as received. The water used throughout this study was purified with a Millipore system and had a resistivity of 18.2 mΩ/m (Milli-Q water).

7.2.3 Asphaltenes precipitation

C5 asphaltenes were extracted from coker feed bitumen (Syncrude, Canada) with a standard protocol of using excess pentane.[43] Briefly, bitumen was dissolved in HPLC grade pentane at 1:40 bitumen to pentane volume ratio (one part bitumen and 40 parts pentane) for 24 hrs. The mixture was then filtered and washed with excess pentane until the eluent was clear. The precipitated asphaltenes were then dissolved in toluene and the toluene-insoluble solids that originate from the bitumen were removed by 30 min centrifugation at 20,000 RCF (Relative Centrifugal Force). The asphaltenes were obtained after the evaporation of toluene and storage in a desiccator. The same asphaltene batch was utilized in all the tests reported here.

7.3 EXPERIMENTAL METHODS

7.3.1 Interfacial tension

Interfacial tension measurements were conducted to assess the activity of individual components and the potential for the demulsifier to penetrate a preformed asphaltene film on the interface. Two types of interfacial tension were measured, namely the static and the dynamic interfacial tension. The equilibrium toluene-water interfacial tension was measured using the Du Noüy ring technique (Kruss K12, Germany). The measurement was repeated periodically until the interfacial tension change remained below 0.1 mN/m during a 30 min measurement period. The interfacial tension of water and asphaltenes in a toluene solution was measured for an asphaltene concentration range from ~1 ppm to ~10^5 ppm in toluene, while the demulsifier concentration in the toluene phase ranged between 0.06 ppm to 288.4 ppm.

To elucidate the adsorption kinetics of asphaltenes and demulsifier at the toluene-water interface and to probe their ability to compete for such interface, the dynamic toluene-water interfacial tension was measured for asphaltenes (0.25 g/L, 332 ppm) and demulsifier (0.3 ppm and 1.2 ppm) and then for a mixed system (equivalent concentrations) using the pendant drop technique (Theta Optical Tensiometer, Attension, Finland). For the mixed system, asphaltenes were first adsorbed to the interface for 30 min, after which the demulsifier was injected in the toluene phase while continuously measuring the interfacial tension. All the interfacial tension measurements were conducted at room temperature (23°C) and atmospheric pressure.

7.3.2 X-ray Photoelectron Spectroscopy

Chemical composition of the interfacial films was characterized using X-ray Photoelectron Spectroscopy (XPS). Films of asphaltenes (produced by spreading 100 µL of 1 g/L asphaltene in toluene solution, cf. section 7.3.6), pure demulsifier, and mixed systems (with demulsifier added at 2.3 ppm and 11.5 ppm, based on the mass of toluene phase) were transferred onto gold substrates using the method described in section 7.3.8. The XPS measurements were performed on a Kratos Ultra instrument at the Alberta Centre for Surface Engineering and Science (ACSES), University of Alberta. The base pressure in the sample analytical chamber was maintained lower than 1×10^{-8} torr. A monochromatized Al Kα x-ray source (hv=1486.6 ev) was used. The spectral resolution of the instrument was 0.55 eV for Ag_{3d} and 0.70 eV for Au_{4f} peaks. The spot size of analysis was set to 300 x 700 μm^2. Survey scans spanned a binding energy range from 1100 to 0 eV. The spectra were collected with an analyzer pass energy of 160 eV and a step of 0.4 eV. For high resolution spectra, the pass energy was set at 20 eV and the step at 0.1 eV, with dwell time of 200 ms. The number of scans for high resolution spectra was determined according to the spectrum intensities of the elements to be analyzed. An electron flood neutralizer was used to compensate sample charging. Instrument software Vision2 was used to calculate the composition with relative sensitivity factor (RSF) of Scofield and Shirley background from the high-resolution spectra.

7.3.3 Bottle tests

Bottle tests were conducted to assess the potential of the demulsifier to destabilize asphaltene-stabilized emulsions. Asphaltenes were dissolved in toluene at 0.25 g/L (~332.6 ppm), assisted by sonication to ensure complete dissolution. W/O emulsions were prepared with 60 vol.% asphaltene in toluene solution and 40 vol.% water, homogenized for 5 min at 30,000 rpm using a Powergen 100 homogenizer (Fisher Scientific). The average drop size of the resultant emulsion was 22 μm, as determined by optical microscopy images (Axiovert 200, Zeiss). 20ml of the prepared emulsions were transferred to settling tubes. Demulsifier was then added drop-wise to the desired concentration between 0.1 and 288.4 ppm (based on the mass of the toluene phase) and the emulsion was hand-shaken for 1 min to aid dispersion of the demulsifier throughout the emulsion. The settling tubes were then positioned vertically and the height of the continuous water phase resolved was measured periodically during 90 min, assessing the ability of the demulsifier to promote water droplet coalescence. A control test conducted in the absence of demulsifier addition confirmed that the emulsion was stabilized by 0.25 g/L asphaltene (equivalent to 332.6 ppm) in toluene solution. Bottle tests were also conducted with demulsifier only in the toluene phase with the same mixing time and water content used in the control tests conducted with asphaltenes only, to determine if the demulsifier had intrinsic stabilizing properties.

7.3.4 Micropipette experiments

Micropipette experiments were conducted to investigate the effect of demulsifier addition on the coalescence of asphaltene-stabilized water droplets. Three systems were analyzed: 1) asphaltene-stabilized emulsions without demulsifier addition; 2) asphaltene-stabilized emulsions with 2.3 ppm demulsifier addition (optimal dosage determined by bottle tests); and 3) asphaltene-stabilized emulsions with 28.8 ppm demulsifier addition (concentration at which overdose was observed). Emulsions were prepared using procedures identical to those described previously for bottle test experiments. The prepared emulsions were transferred into the glass sample cell of the micropipette apparatus. The cell was mounted onto an optical microscope (Axiovert 200, Zeiss). Using a micropipette mounted on a three dimensional micro manipulator, an emulsified water droplet was picked up and held at the tip of the micropipette by a low suction pressure applied to the micropipette. Another emulsified water droplet was picked up in a similar manner by a second micropipette in an axial alignment with the first micropipette, manipulated to enable a direct "head-on" contact between the two water droplets of approximately the same size. The applied force was maintained for 1 min. The probability of coalescence is defined as the ratio of the number of contacts in which coalescence was observed to the total number of contacts (30 for each system considered) measured. Further details regarding the micropipette technique can be found elsewhere[44, 45].

7.3.5 Shear rheology: Double Wall Ring geometry

An AR-G2 controlled stress rheometer (TA Instruments, USA) with a Double Wall Ring (DWR) geometry was used to measure the shear viscoelastic properties (G': elastic and G": viscous) of an asphaltene-stabilized interfacial film. The formation and subsequent breakdown of the interfacial film by demulsifier addition were monitored. The viscoelasticity of the interfacial film was determined from the harmonic oscillation in both stress and strain while keeping the interfacial area constant. Applying a sinusoidal strain deformation (γ) of fixed amplitude to the interfacial film produced a sinusoidal shear stress (σ) response separated by a phase angle, δ. The strain deformation applied and the stress responses are given by:

$$\gamma(t) = \gamma_0 \sin(\omega t) \tag{1}$$

$$\sigma(t) = \sigma_0 \sin(\omega t + \delta) \tag{2}$$

where ω is the angular frequency, while σ_0 and γ_0 are the maximum stress and strain, respectively. From the theory of the complex shear modulus, $|G^*| = \frac{\sigma_0}{\gamma_0}$, the elastic ($G'$) and viscous ($G''$) components of the interfacial film are given by Equations 1 and 2. To ensure that the technique measures the integral structural properties of the film, it is essential to conduct the measurement below a critical strain (γ_{CR}). This condition is defined as the linear viscoelastic region where the shear moduli, G' and G", are independent of the applied strain.

For the current study the angular frequency and strain were fixed at 0.5 Hz and 0.8%, respectively. All experiments were conducted at a temperature of 23°C, kept constant using a Peltier plate. Time sweep measurements over several hours allowed tracking the development in the viscoelastic properties of an interfacial asphaltene film. At the critical condition G' ≈ G", a 1000 ppm demulsifier stock solution was added drop-wise to obtain a final demulsifier concentration of 2.3 ppm and 34.6 ppm in toluene. The shear rheological response of the film was continually measured at 30 s intervals, until steady-state conditions were attained. Further details regarding this technique can be found elsewhere.[46]

7.3.6 Langmuir trough: pressure-area isotherms

The compressional behavior of interfacial films at the toluene-water interface was characterized by interfacial pressure−area (π-A) isotherm measurements using a Langmuir trough. To study competitive adsorption of asphaltenes and demulsifier, π-A isotherms were collected for: i) asphaltenes in toluene alone; ii) demulsifier in toluene alone; and iii) mixed system of asphaltene and demulsifier in toluene. The Langmuir trough experiments were conducted using a computer controlled KSV trough (Biolin Scientific, Finland) with a trough area of 170 cm^2. The interfacial pressure was measured using a paper Wilhelmy plate sensor (Biolin Scientific, product ID. KN 0005). In the presence of interfacial material, the interfacial pressure (π) represents the change in interfacial tension (IFT) relative to the interfacial tension at clean interface (IFT_0), and is given by:

$$\pi = IFT_0 - IFT \qquad (3)$$

Prior to each measurement, the trough was carefully cleaned with toluene, acetone, and Milli-Q® water. The lower part of the trough was filled with 120 mL of Milli-Q® water as the sub-phase. The trough was considered clean when the pressure sensor reading was < 0.2 mN/m with the water phase being compressed to an area of 12.5 cm2. The balance was zeroed at the clean air-water interface prior to forming films at the toluene-water interface. This procedure allowed for obtaining information regarding the interfacial tension in the presence of asphaltenes and demulsifier. After setting the interfacial pressure to zero, 100 μL of 1 g/L asphaltene in toluene solution was evenly spread at the air-water interface using a Hamilton gastight syringe, while the trough area was wide-open. After asphaltene addition the solvent was evaporated completely over 20 min to allow for the formation of a uniform asphaltene film at the air-water interface. Finally, 100 mL of toluene was added as the top-phase. After equilibrating the film for 30 min compression was initiated.

To elucidate the effect of the demulsifier on the physical properties of asphaltene interfacial films, a diffusion protocol was used by introducing the demulsifier to the toluene top-phase. After topping the interfacial asphaltene film with 100 mL of toluene, the demulsifier was added in the toluene top-phase at the desired concentration (0.2 – 288.4 ppm of the toluene top- phase). Demulsifiers were allowed to diffuse for 30 min before compression was innitiated. This diffusion time was selected to reflect the typical residence time of demulsification in real oil field applications. As a control test, the demulsifier solution was added to the toluene top-phase in the absence of asphaltene interfacial films.

In order to evaluate if the interfacially active species in the system (demulsifier and asphaltenes) were reversibly or irreversibly adsorbed to the interface, wash-off experiments were conducted. In wash-off experiments, asphaltene and demulsifier films were produced and compressed as described above. After the films were compressed to an area of 12.5 cm2, the toluene top-phase was exchanged with fresh toluene while keeping the barriers closed. The barriers were subsequently expanded at a speed of 5 mm/min, and the films equilibrated for 30 min (first wash-off). Following this equilibration time, the films were compressed again and the wash-off process was repeated (second wash-off).

A reference isotherm was collected at a clean toluene-water interface. The surface pressure measured at a clean toluene-water interface equals to 11 mN/m, with minimal changes (less than 0.7 mN/m) upon compressing the area from 170 cm^2 to 12.5 cm^2. All experiments were conducted at room temperature, and the interfacial films were compressed at 10 mm/min for each barrier, following a previously published protocol.[10]

7.3.7 Brewster Angle Microscopy

Brewster Angle Microscopy (BAM) was used to image the morphology of an interfacial film in situ, without the need to transfer the film to a solid substrate. An advantage with this technique is that the morphological changes of asphaltene films after demulsifier addition could be imaged without disturbing the films in order determine the film-breaking mechanism in real time. In this technique the interfacial film is illuminated by a laser at the Brewster angle (θ_B). At this angle s-polarized light (i.e. the light perpendicular to the incident plane) can be reflected to the detector solely from the interface, not by the bulk phases below or above it. As a result, the images collected reflect the characteristic features of the interface. The BAM (Model EP3, Accurion GmbH, Germany) used in this study was equipped with light guides and a CCD camera to image films at the toluene-water interface at a magnification of 5X. Images were collected using EP3View2.x software (Accurion). The trough used for these experiments had a fixed area of 28 cm^2, at which all images were captured.

To form an asphaltene interfacial film at the oil-water interface, 30 mL of the aqueous phase was first added to the trough, followed by spreading 50 μL of 1 mg/mL asphaltene in toluene solution at the air-water interface. After 20 min evaporation, 100 mL toluene top-phase was added gently along the sidewall of the trough to prevent any disturbances of the interface. Asphaltene interfacial films were first equilibrated for 45 min and imaged at an angle of incidence (AOI) of 42°, while the polarizer and analyzer were set to 10°. With the drop-wise addition of demulsifier at 0.2 to 288.4 ppm (based on the mass of toluene phase), the mechanism by which the asphaltene film was modified and the time frame in which such changes occurred were analysed by collecting interfacial images at desired time intervals. In order to elucidate a possible dependence between demulsifier concentration and film structure, images were also taken for pure demulsifier films.

Demulsifier films were produced with the drop-wise addition of demulsifier-in-toluene solutions and imaged using the same setup conditions as previously described.

7.3.8 Langmuir-Blodgett film deposition

Langmuir-Blodgett (LB) films were transferred from the oil-water interface onto either silicon (for AFM measurements) or gold wafers (for XPS measurements). The wafers were first cleaned in a 1:1 toluene and acetone mixture by sonication for 30 min and subsequently soaked in 1 N HCl solution for a further 15 min to remove any surface contaminants. Asphaltene, demulsifier and mixed films were prepared following the procedure outlined in section 7.3.6. Films were transferred onto the silicon or gold substrates by first compressing the interfacial area to 40 cm^2 at a speed of 10 mm/min per barrier, followed by pulling the wafer upwards at a speed of 5 mm/min, while maintaining a constant interfacial pressure through a computer controlled feedback system. The transfer ratio, which is defined as the ratio between the decrease in the area of the interfacial layer to the area of the film transferred over the substrate, was close to unity in all cases.

7.3.9 Atomic Force Microscopy Imaging

Atomic Force Microscopy (AFM) images of LB films deposited on silicon wafers were obtained using an Agilent 5500 AFM (Agilent Technologies, Inc., USA) operating in AC mode in air. The substrates were fixed using double-sided tape on a sample platform, which was magnetically held in place on the AFM sample stage. Silicon cantilevers (ACT-200, Applied NanoStructures Inc., USA) with a nominal resonance frequency of 200-450 kHz and nominal spring constants of 25-75 N/m were used for imaging at a scan rate of 1 Hz. AFM imaging was carried out at room temperature (~20 °C). The vendor-supplied SPM software was used to control the probe and to scan the sample. The roughness (Sq) was calculated from AFM images using Picoimage basic v.5.1 software (Agilent Technologies, Inc.) using the following equation:

$$Sq = \sqrt{\frac{1}{N}(Z - \bar{Z})^2} \tag{4}$$

where N is the number of points analyzed, Z is the height of each point and $\bar{Z}$ is the average height of the N points analyzed.

7.3.10 Scanning Electron Microscopy

Scanning Electron Microscopy (SEM) micrographs of LB films were obtained using a Hitachi S-2700 SEM equipped with a Princeton gamma tech IMX digital imaging system. The accelerating voltage used was 10 KV.

7.4 RESULTS AND DISCUSSION

7.4.1. Interfacial tension.

The equilibrium interfacial tension of a clean toluene-water interface was measured using the Du Nüoy ring technique to be 36.2 mN/m. The equilibrium toluene-water interfacial tension in the presence of asphaltenes and/or demulsifier is given in Figure 7.1a. The data reveal that at equivalent concentrations in toluene, the demulsifier molecules are more interfacially active than asphaltenes. This result indicates that the demulsifier has the potential to compete with the asphaltenes for the toluene-water interface, disrupting the asphaltene network.

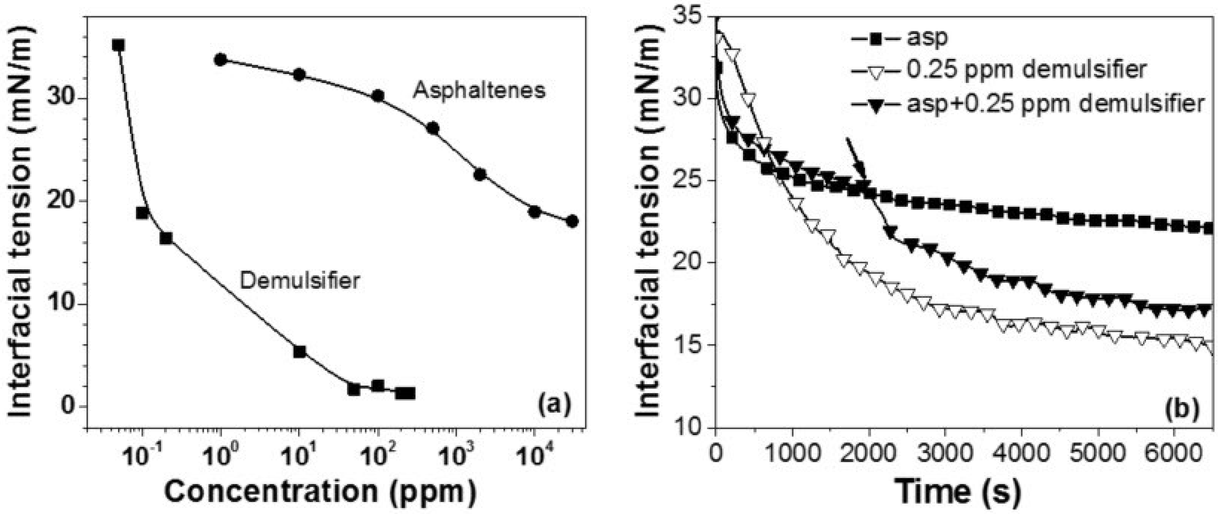

Figure 7.1 Equilibrium interfacial tension of asphaltenes and demulsifier at different concentrations of demulsifier in toluene (based on the toluene phase mass) (a); dynamic interfacial tension for asphaltenes, pure demulsifier and mixed system (b). The arrow indicates the time when demulsifier was injected in the cuvette (30 min).

To further probe the ability of the demulsifier to penetrate interfacial asphaltene films, the dynamic interfacial tension was measured before (asphaltene aging) and after demulsifier addition (Figure 7.1b). After 30 min asphaltene aging, 0.3 ppm demulsifier was added drop-wise to the toluene phase, causing a gradual decrease in the interfacial tension. The slope of the interfacial tension vs. time curve of the mixed system became very close to the slope of the interfacial tension curve measured for the pure demulsifier. Such characteristic behavior would confirm that the demulsifier molecules are effectively penetrating the asphaltene film network. The dynamic interfacial tension of the droplet after demulsifier addition was not the same as the interfacial tension value for the pure demulsifier (0.3 ppm) over one and a half hour observation period. This result indicates that both asphaltenes and demulsifier were adsorbed at the toluene-water interface one and a half hour after demulsifier was introduced in the system. Observations were not conducted for longer time periods, and complete penetration of demulsifier after longer time cannot be discounted.

Experiments were also conducted with 1.1 ppm demulsifier in the toluene phase (data not shown). In this case, the reduction in the interfacial tension and hence the penetration kinetics of demulsifier into the asphaltene film were found to be much faster as compared with the case of 0.3 ppm demulsifier. Dynamic interfacial tension measurement with higher demulsifier concentrations could not be conducted, as the low interfacial tension would promote droplet streaming from the needle tip. For this reason, the kinetics of demulsifier penetration into the asphaltene film network at demulsifier dosages greater than 1.1 ppm in toluene were probed using shear rheology.

While interfacial tension is a measure of the molecules ability to lower the interfacial energy of the system, it does not necessarily link directly to demulsification performance, with many studies showing a lack of agreement between demulsification performance and interfacial tension reduction by demulsifier addition.[27, 28, 47]

7.4.2 XPS.

To verify that the demulsifier could penetrate oil-water interfacial asphaltene films, asphaltene films transferred from oil-water interface by Langmuir-Blodgett (LB) method without and with demulsifier addition were analyzed by XPS. For comparison, the interfacial films of demulsifier alone were also analyzed by XPS.

Table 7.1. Oxygen to carbon (O/C) atomic ratio of different LB films, obtained by XPS analysis.

Sample	O/C atomic ratio
Asphaltenes*	0.042
Demulsifier (2.3 ppm in toluene)	0.363
Asphaltenes+2.3 ppm demulsifier in toluene	0.133
Asphaltenes+11.5 ppm demulsifier in toluene	0.157

The results showed an oxygen to carbon (O/C) atomic ratio of 0.042 for asphaltene films, in agreement with the results from previous studies.[48, 49] In contrast, a much higher O/C atomic ratio of 0.363 was obtained for the demulsifier films due to the presence of the EO and PO groups (Table 7.1). The O/C atomic ratio for the asphaltene LB interfacial films in the presence of the demulsifier fell between the values of the asphaltenes and demulsifier (Table 7.1), indicating penetration of the demulsifier into the asphaltene films. Since the measured O/C atomic ratio of the asphaltene film in the presence of the demulsifier is much lower than the value of the demulsifier film, it is reasonable to conclude that at the demulsifier concentrations tested, the demulsifiers could only partially displace the asphaltenes from the interface. Dynamic interfacial tension data, obtained by adding demulsifier at concentrations of 0.3 ppm and 1.1 ppm in toluene, also indicated that in the mixed systems of asphaltenes and demulsifier, both asphaltenes and demulsifier were adsorbed at the interface. At demulsifier dosages higher than 1.1 ppm in toluene, dynamic interfacial tension measurements could not be conducted because of very low interfacial tension that caused the droplet to stream out from the needle. At such dosages, the hypothesis of partial displacement is supported by the Langmuir trough compressional isotherms and the AFM images of films formed by pure demulsifier and film that formed by demulsifier diffusion into interfaces formed by asphaltenes. Significant differences in both isotherms and images were observed, suggesting adsorption of both demulsifier and asphaltenes at the toluene-water interface, as will be further discussed in sections 7.4.5 and 7.4.6.

7.4.3. Bottle tests and micro-pipette experiments.

While the interfacial tension and XPS results have confirmed the sorption of the demulsifier molecules at the asphaltene stabilized oil-water interface, such sorption does not necessarily translate to demulsifier performance. Bottle tests were conducted to assess the demulsification performance. Without demulsifier addition, emulsions remained stable for more than 1 day (data not shown). The results obtained with demulsifier addition are shown in Figure 7.2. The performance of the demulsifier reached its optimum at 2.3 ppm concentration in the toluene phase, with ~80% of the free water resolved after 15 min gravity separation. At 11.5 ppm demulsifier addition in toluene, the volume of free water resolved reached ~80% after approximately 80 min gravity separation. Furthermore, with 28.8 ppm demulsifier addition, only 30% free water was resolved even after 90 min gravity separation. Upon addition of demulsifier at 57.7 ppm or higher in the toluene phase, the emulsions were observed to be extremely stable with no free water resolved even after 24 hr gravity separation (data not shown). These results demonstrate that the demulsifier is only effective at low dosages.

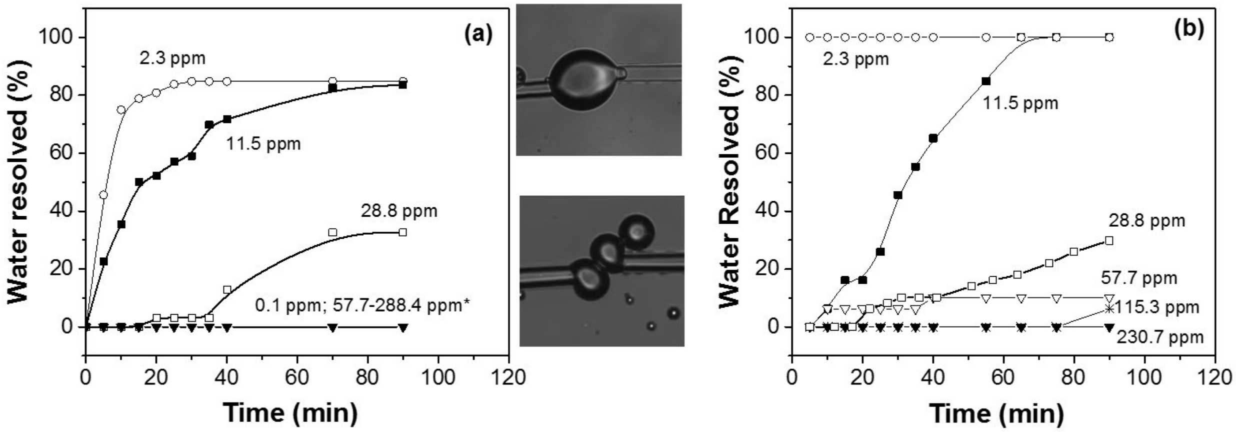

*Figure 7.2 Water resolved in bottle tests upon addition of demulsifier at different concentrations (based on the mass of toluene phase) to asphaltene stabilized emulsions (a) and in emulsions where only the demulsifier was present (b). Examples of coalescing and non-coalescing water droplets manipulated using micropipettes are shown as inset to Figure 7.2 (a). *It is noted that upon addition of demulsifier at 57.7 ppm or higher in the toluene phase, the emulsions were stable with no free water resolved even after 24 hr gravity separation.*

To determine if the demulsifier alone can stabilize the W/O emulsion, bottle tests were conducted with pure demulsifier. The results in Figure 7.2b show that emulsions were unstable when demulsifier was added at the optimal dosage of 2.3 ppm in toluene. At higher concentrations (≥ 11.5 ppm) however, the demulsifier displayed increasing stabilizing potential up to 230.7 ppm, at which the emulsion remained stable (no free water) over the 90 min test. The data confirms that the reduction in dewatering performance at higher demulsifier concentration (chemical overdose) results from the inherent stabilizing capacity of the demulsifier molecule.

To further study the role of demulsifier concentration on destabilizing and stabilizing droplets, the coalescence probability of asphaltene-stabilized emulsion water droplets was determined by micropipette technique with and without demulsifier addition in toluene. Typical images of coalescing and non-coalescing water droplets in the micropipette experiments are shown in Figure 7.2 as inset. The results showed a significant increase in the probability of coalescence from 0.09 to 0.85 upon addition of 2.3 ppm demulsifier in toluene, and then a significant decrease from 0.85 to 0.25 with a further increase in demulsifier addition from 2.3 ppm to 28.8 ppm. These results clearly illustrate the detrimental effect of demulsifier overdose. The micropipette results are in excellent agreement with the bottle test data shown in Figure 7.2, in which sample images of coalescing and non-coalescing droplets are also shown.

7.4.4. Shear rheology

With interfacial rheology known to affect the stability of emulsion droplets[17, 18], the shear rheological properties of asphaltene films at the water-oil interface before and after demulsifier addition were measured using the DWR geometry. The viscoelastic properties of the interface were measured as a function of aging time as the asphaltenes diffused to and adsorbed at the water-toluene interface. With gradual accumulation of asphaltenes at the toluene-water interface, the interface transitioned from a viscous to an elastic dominant microstructure. With particular focus on the effect of demulsifier addition, the first 6000 s of interfacial aging are not shown. Readers are referred to the following papers for the characteristic aging of an asphaltene film as measured by shear.[13 46]

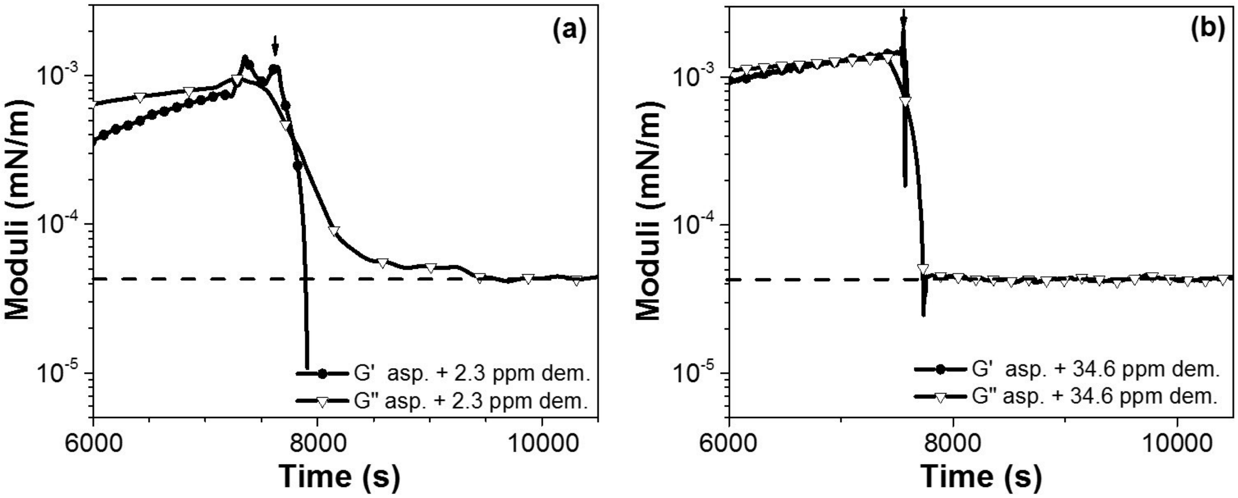

Figure 7.3 Shear elastic (G') and viscous (G") moduli obtained for asphaltene films prior and after addition of demulsifier at 2.3 ppm (a) and 34.6 ppm (b) in the toluene phase. The arrow indicates the time at which the demulsifier was added. Asphaltenes are abbreviated as "asp" in the legend. The dashed line represents the viscous modulus of a clean toluene-water interface or of the toluene-water interface when demulsifier was added at 57.6 ppm in toluene (G'= 0 N/m).

Once the condition G' = G" was met the demulsifier was added at 2.3 ppm (optimum dosage from the bottle tests) and 34.6 ppm (overdose). When the elastic contribution is substantial, asphaltenes are intimately linked and form a cohesive interfacial network. To assess demulsifier performance in penetrating and breaking the cohesive network of asphaltenes, the shear viscoelastic moduli were measured continuously.

Upon addition of 2.3 ppm demulsifier in toluene, both viscous and elastic shear moduli of the interfacial film decreased as shown in Fig. 7.3 (a). The elastic modulus decreased to an unmeasurable value within 10 min and the viscous modulus decreased to a value equivalent to that of "clean" toluene-water interface after approximately 30 min. At higher demulsifier concentration (34.6 ppm) a similar response for the viscoelastic moduli was measured albeit the kinetics of film disruption was accelerated as shown in Fig. 7.3 (b). Interestingly, from shear rheology one would be inclined to believe that a higher concentration of demulsifier would improve dewatering, with faster film disruption kinetics. However, the bottle test and micropipette data presented within this work suggested otherwise. The end condition of both systems studied were equivalent, with G’ = 0 N/m and G” = 4.5 x 10-5 N/m. With the G” contribution equivalent to that of a “clean” water-toluene interface, the response would suggest that the asphaltene interconnected network has been sufficiently disrupted (G’ = 0 N/m) and the remaining interfacial species offer no resistance to shear. To confirm the interfacial shear rheology of the demulsifier molecule, a study was conducted in the absence of asphaltenes. Adding 57.6 ppm demulsifier to a toluene top-phase, the G” and G’ (= 0 N/m) remain unchanged (cf. Figure 7.3). While the technique is useful to study the breakdown kinetics of an asphaltene-stabilized interface, the technique alone is limited when trying to understand the mechanism for overdose.

7.4.5. Pressure-area isotherms

While interfacial shear rheology can provide information on the kinetics of asphaltene-stabilized film disruption, the technique appears limited when predicting overall demulsification performance. Another property of the interface that can influence the emulsion stability is the compressional response of the interfacial film.[18] Specifically, low interfacial film rigidity under compression is reported to favor droplet coalescence.[50, 51] Interfacial pressure-area (π-A) isotherms were measured to probe the effect of demulsifier addition on the behaviour of asphaltene-stabilized interfacial films. For comparison, demulsifier π-A isotherms in the absence of asphaltenes were also measured. The π-A isotherms of asphaltenes, demulsifier and their mixture at the toluene-water interface are given in Figure 7.4a.

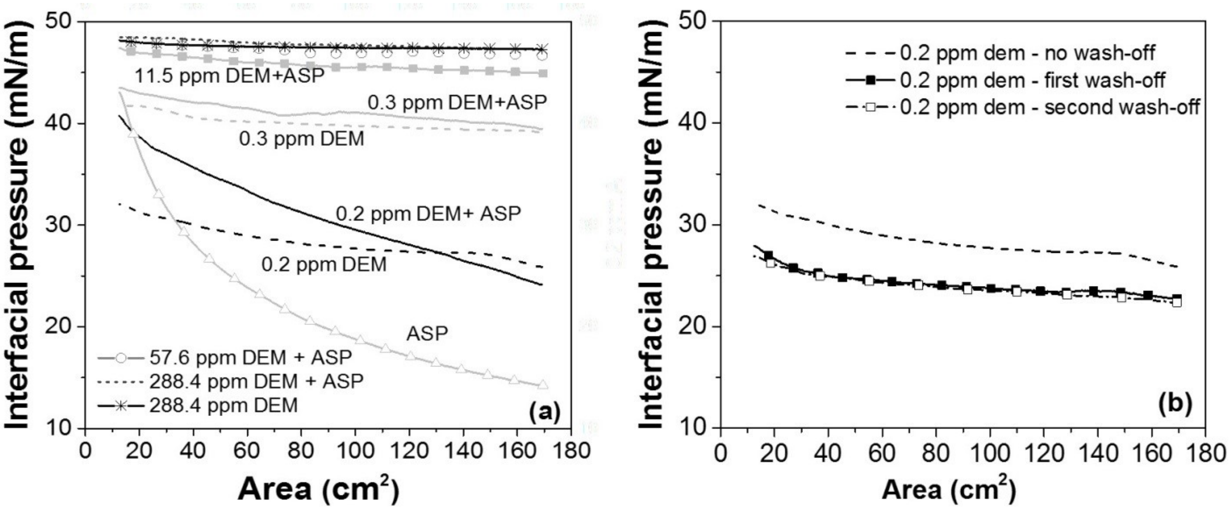

Figure 7.4 Comparison of π-A isotherms obtained for asphaltene, demulsifier and their mixture at the toluene-water interface (a), and isotherms measured for demulsifier at 0.2 ppm concentration in toluene before and after wash-off of the toluene top-phase (b). In the legend asphaltenes and demulsifier are abbreviated with "asp" and "dem" respectively. The demulsifier concentrations given in ppm are based on the mass of toluene.

The results in Figure 7.4a show that at the maximum trough area of 170 cm^2, demulsifier addition to the system caused a significant increase in the interfacial pressure, corresponding to a decrease in the interfacial tension (cf. Eq. 3). At low demulsifier concentration (0.2 ppm) the interfacial tension of the mixed system was intermediate between the values of the interfacial tension given by the two interfacially active species (asphaltenes and demulsifier), once again confirming partial substitution of the asphaltene film. At higher demulsifier concentrations the interfacial tension measured for the mixed system was close to that measured for pure demulsifier. These results once again indicate penetration and potentially more complete displacement of the asphaltenes film. Similar results were obtained in studies conducted with ethyl-cellulose.[31]

The results of wash-off experiments are shown in Figure 7.4b. Wash-off experiments conducted with pure demulsifier showed that the interfacial pressure measured when the barriers were fully expanded, decreased when the toluene top-phase was exchanged with fresh toluene following the first compression (first wash-off). The measured decrease in the pressure after wash-off shall correspond to an increase in the interfacial tension. Such an increase indicates that the molecules at the interface can desorbe[52-54]: the data thus shows that the demulsifier could partially desorb from the toluene-water interface after compression. When the toluene top-phase was exchanged for the second time (second wash-off), the interfacial pressure changes were negligible, suggesting that part of the demulsifier molecules were irreversibly adsorbed at the toluene-water interface. Unlike demulsifier, asphaltenes could not be washed off the interface (data not shown), consistent with previous studies.[55] Wash-off data at the toluene-water interface explain the characteristic features of the isotherms, as will be discussed below.

The increase in pressure upon compression was small for pure demulsifier films, at all demulsifier concentrations. The rationale for the limited increase in the pressure upon film compression can be two-fold: 1) The film formed by the molecules present at the oil-water interface is soft (i.e. the compressional viscoelastic moduli are low); 2) The molecules are reversibly adsorbed at the oil-water interface, and desorb when the interfacial film is compressed. Wash-off experiments suggest that both mechanisms were relevant, and that while some demulsifier molecules desorbed from the interface, others remained adsorbed onto it upon film compression, exhibiting soft film behaviour. It should be noted that in Langmuir trough experiments the compressional viscoelastic moduli were not measured. However, the compressional viscoelastic moduli are qualitatively related to the slope of the Langmuir trough isotherms, since the compressional viscoelastic moduli are proportional to the ratio between the change in pressure versus the change in the area of the interfacial film that is compressed ($\Delta\pi / \Delta A$).[56] When this ratio is high, the compressional isotherms measured with the Langmuir trough have a steep slope, indicating significant compressional viscoelastic moduli in comparison to films of small ratios which are typical of soft films (i.e. films having low compressional viscoelastic moduli and relatively “flat” compressional isotherms).

The isotherm measured for a mixed system of asphaltene and low demulsifier concentration (0.2 ppm) displayed a behaviour that was between that of pure asphaltenes and demulsifier. Specifically, the increase in the pressure upon compression was limited at large interfacial areas (low compression), and the slope of the π-A isotherm resembled that of the pure demulsifier isotherm. These results suggest that asphaltene molecules had been partially displaced from the toluene-water interface and demulsifier dominated the compressional behaviour of the system. However at smaller compressional areas the slope of the π-A isotherm increased, suggesting that asphaltenes molecules that had not been displaced by the demulsifier were tightly squeezed and resisted the compressional force. Therefore, with 0.2 ppm demulsifier added, at low compression the demulsifier molecules dominate the interfacial properties, but at high compression the interfacial properties are dominated by the asphaltenes. Interestingly this system would correspond to poor dewatering performance. At the optimum dewatering condition (demulsifier concentration = 2.3 ppm) the situation is somewhat different and the two π-A isotherms (asphaltene + demulsifier, and demulsifier only) were similar and displayed soft film characteristic as the interfacial area was reduced to 12.5 cm^2. It is often discussed that interfacial film rigidity (compressional and shear) is responsible for the enhanced stability of asphaltene stabilized emulsions.[4, 5, 46] Hence, film softening by demulsifier addition would promote favorable conditions for emulsion separation.[57] The data obtained with 2.3 ppm demulsifier would indicate that film softness under different levels of compression promotes dewatering. However, at demulsifier concentrations above the optimal, the two π-A isotherms measured for asphaltene + demulsifier and for demulsifier only were also similar, displaying soft film behaviour. These results show that the rheological data is somewhat limited when trying to explain the overdose phenomena. Therefore mechanisms other than rheology contribute to the stabilizing potential observed during overdose.

It is noted that in the Langmuir trough experiments demulsifier was added to the system after 30 minute asphaltene film aging. It is reported that the characteristics of asphaltene films are time dependent, and that the shear[58] and the compressional viscoelastic moduli[59] of asphaltene films increase in time (i.e. asphaltene films become more rigid) due to rearrangement and further association of the asphaltene molecules at the interface. It is therefore possible that different minimal demulsifier dosages are required to soften to the same extent the asphaltene films aged for different periods of time. However, the trends discussed above would not be altered: regardless of aging time, higher demulsifier dosages soften asphaltene films more effectively than lower demulsifier dosages under both shear and compression conditions, which will not change the general correlation between the coalescence of water droplets and the interfacial film rheology: film softening is beneficial and necessary for coalescence, but it may not be sufficient.

7.4.6. Morphology of the films at toluene-water interface.

Imaging of interfacial asphaltene films was conducted to visually observe the impact of demulsifier on asphaltene film morphology, and to better understand the ability of demulsifier to penetrate asphaltene films and alter their structure. BAM images of asphaltene films at the air-water interface revealed island-like structures (Fig. 7.5), in agreement with previously published data[60-62]. In previous studies the morphology of asphaltene films was probed in situ with BAM at the air-water interface[41, 60-62], while asphaltenes films at the toluene-water interface have also been imaged after being transferred onto solid substrates (LB films). [55, 57, 63] In the current study, after the toluene (good solvent) top phase was gently added, the cracks in the film were observed to “heal” (Fig. 7.5), to form a homogeneous film. When the toluene-water interface was imaged in situ using

BAM, the films interfacial features were not mobile, suggesting that the asphaltenes formed an interconnected, rigid-like film. This visual observation is in good agreement with the results from the shear rheology and π-A isotherm measurements discussed in the previous sections.

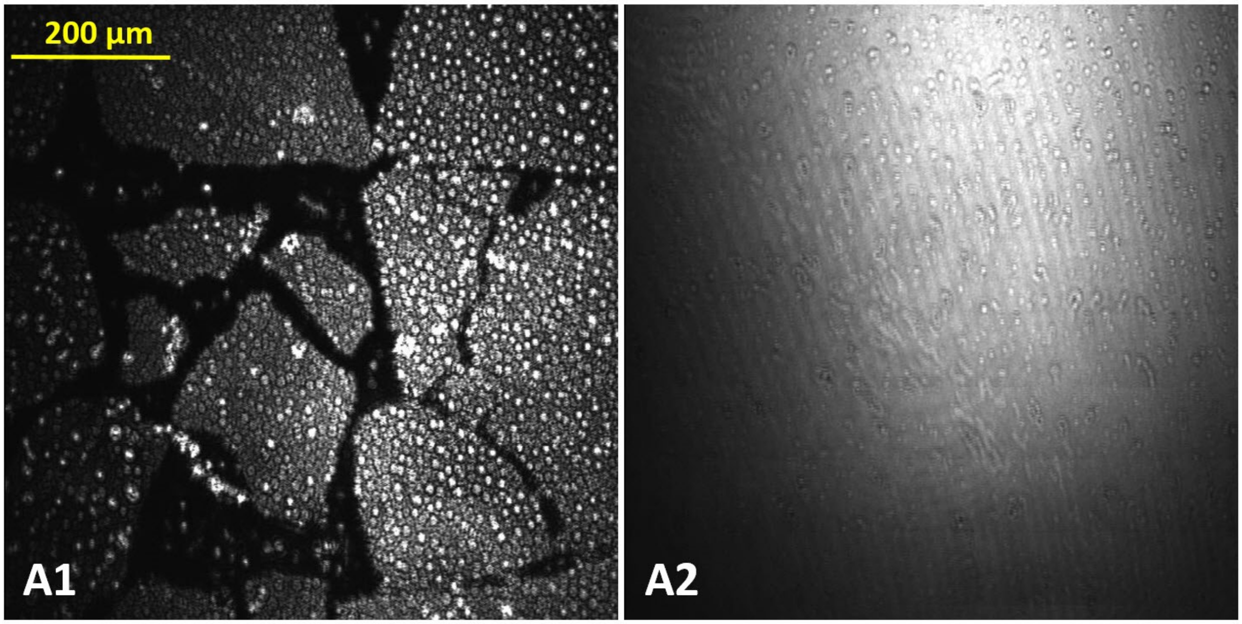

Figure 7.5 BAM images of asphaltenes without demulsifier at the air-water (A1) and toluene-water interface (A2).

In the demulsifier concentration range 0.2 ppm to 28.8 ppm the asphaltene film structure appeared unchanged when observed at the toluene-water interface at 5X magnification (Figure 7.6). Asphaltene film morphology at the lower demulsifier concentration was further studied using AFM, which enabled observation of the interfacial film at the nano-meter scale resolution (Figure 7.7). While BAM showed no measurable differences in the asphaltene film morphology, on visual inspection the film mobility was observed to increase after demulsifier addition. The observed mobility is in agreement with the drastic reduction in the film shear elasticity after 2.3 ppm demulsifier was added. In addition to the film mobility, the interface was observed to change position (lower z-axis position) and shape from an approximately flat to a convex film, due to the decrease in the interfacial tension. The change in the interfacial shape became more substantial at higher demulsifier concentrations. At concentrations greater than 28.8 ppm demulsifier in toluene, aggregates of several microns in diameter were observed to form at the toluene-water interface (Fig. 7.6). The morphology of asphaltene films changed further at higher demulsifier concentrations, acquiring a visible texture contrasting the smooth films observed at lower demulsifier concentration (Fig. 7.6). The observed changes in the film morphology and mobility at low demulsifier concentrations occurred within a few minutes following demulsifier addition, while the changes were instantaneous at higher demulsifier concentrations.

BAM images of pure demulsifier films at the toluene-water interface were also recorded. These images showed the formation of smooth films in the demulsifier concentration range 0.2 ppm to 28.8 ppm (Fig. 7.6), whereas at concentrations greater than 28.8 ppm aggregates were clearly visible at the toluene-water interface (Fig. 7.6). The population of the aggregates at the interface increased progressively when increasing the demulsifier concentration in toluene from 28.8 ppm to 288.4 ppm (Fig. 7.6), leading to the formation of densely packed networks having a 3-Dimensional appearance. SEM images of LB films deposited after diffusion of 288.4 ppm demulsifier in toluene confirmed the presence of large irregular structures at the toluene-water interface (Fig. 7.8).

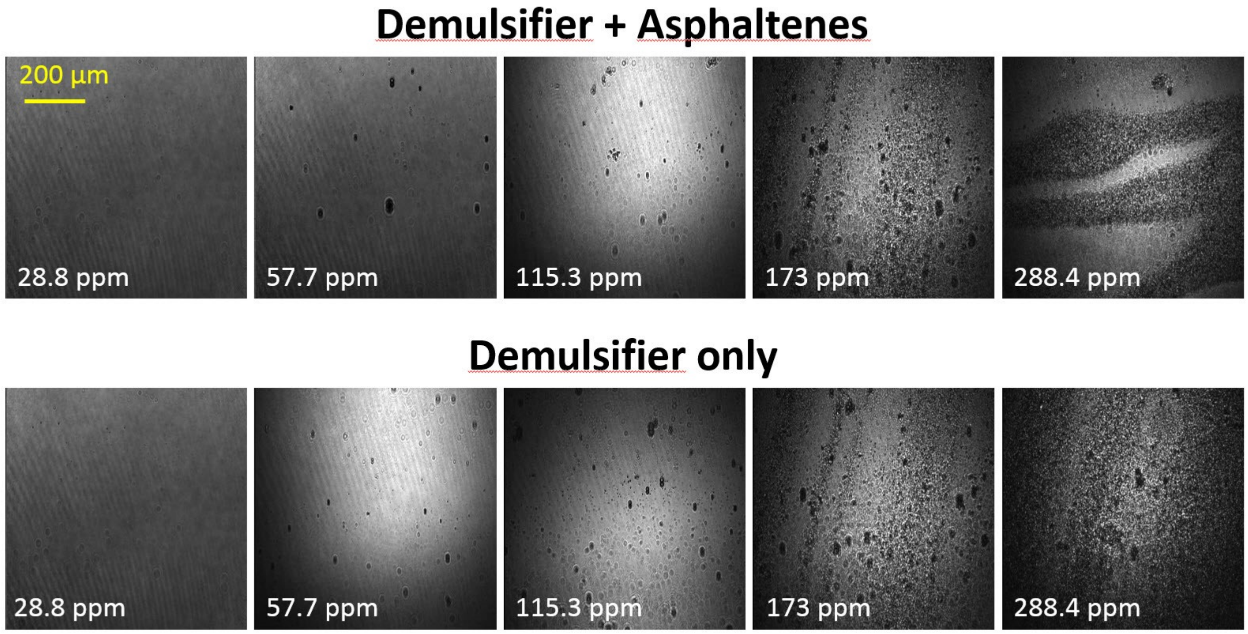

Figure 7.6 BAM images of asphaltenes after addition of the demulsifier (top row) and of pure demulsifier films (bottom row) at different concentrations in toluene. Demulsifier films formed with demulsifier concentrations in toluene below 28.8 ppm appeared smooth and similar to those formed with 28.8 ppm demulsifier concentrations in toluene. Such images are not shown here for brevity. The size of BAM images is 800 µm X 800 µm.

The presence of such structures suggests that steric forces can be responsible for the observed overdose effect and for the intrinsic stabilizing capacity of demulsifier at high concentrations in toluene. Such a hypothesis is in agreement with the results of previous studies that demonstrated the important role of steric repulsion in the interactions between polymer-coated surfaces,[64, 65] and in the stability of emulsions[66] and foams[67] in the presence of EO-PO co-polymers.

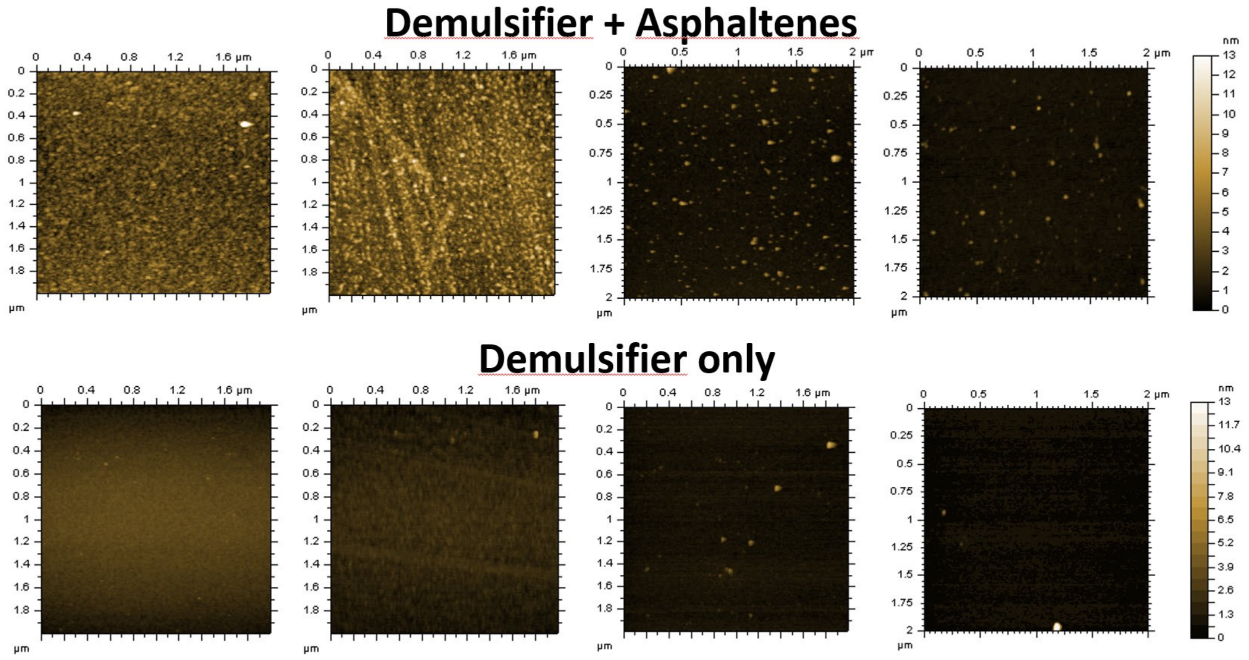

Figure 7.7 AFM images of asphaltene films after addition of demulsifier at different concentrations in toluene (top row) and of pure demulsifier toluene-water interfacial LB films at different concentrations in toluene (bottom row). The image of pure demulsifier at 10 ppm was similar to the one obtained at 28.8 ppm, and is not shown here for brevity. The color bar indicates the height scales (in reference to the lowest point of the sample): the brighter the color of the area, the higher the topology, with the brightest color representing 13 nm.

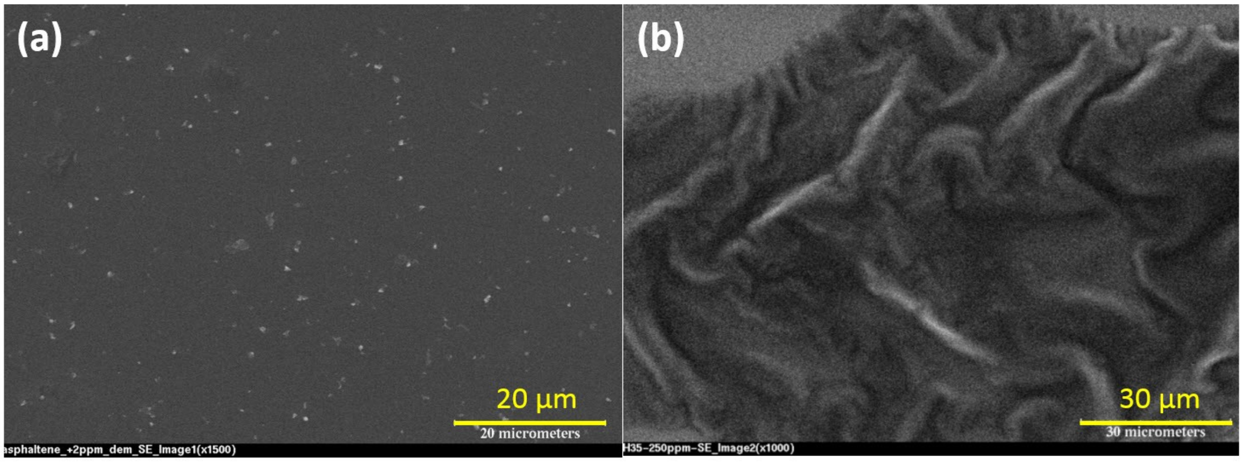

Figure 7.8 SEM images of asphaltene toluene-water interfacial LB films with 2 ppm (a), and SEM image of a pure demulsifier film produced by diffusing 250 ppm of demulsifier in toluene (b).

To increase understanding of the role of the demulsifier at lower concentrations, LB films of asphaltene + demulsifier, asphaltenes without demulsifier and pure demulsifier were deposited onto silica wafers for imaging analysis by AFM and SEM. AFM measurements allowed quantitative determination of nanometer resolution roughness of interfacial films (defined in Eq. (4)), with the values being given in Table 7.2. As shown in Fig. 7.7, asphaltene films were fairly homogenous, with small aggregates uniformly distributed on the surface. The surface had a roughness of approximately 1 nm. These results are in agreement with the results reported in previous studies.[55, 57] The addition of demulsifier at 0.2 ppm in toluene had a marginal effect on the morphology and roughness of asphaltene films as shown in Fig. 7.7. Increasing the demulsifier concentration to 2.3 ppm (i.e., at the optimal dosage determined in the bottle tests) or even higher significantly changed the morphology of the asphaltene film, as shown in Fig. 7.7 and Fig. 7.8. Specifically, addition of 2.3 ppm or 5.7 ppm demulsifier in toluene induced the formation of spherical aggregates, sparsely distributed on an otherwise smooth surface, but had a negligible effect on the roughness of asphaltene films as shown in Table 7.2. Such aggregates could be a result of the aggregation from asphaltenes that were displaced from the interface, which was preferentially occupied by the demulsifier. This hypothesis is in agreement with the results from the interfacial tension measurement and XPS analysis of the interfacial LB films that indicated partial asphaltene displacement. Similar findings were reported from previous studies on displacement of stabilizing asphaltene or bitumen films from the interface by different polymeric demulsifiers,[15, 23] including EC.[10, 45] Specifically, previous studies conducted using EC showed that EC preferential adsorption onto the oil-water interface caused bitumen or asphaltenes to segregate into micro-domains surrounded by EC.[10, 45]

Table 7.2 Roughness of LB films before and after demulsifier addition, determined by quantitative AFM imaging. All demulsifier concentrations expressed in ppm are based on the mass of toluene phase.

Type of film	Roughness (nm)
Asphaltene	1.1
Asphaltene + 0.2 ppm demulsifier	1.0
Asphaltene + 2.3 ppm demulsifier	1.1
Asphaltene + 5.8 ppm demulsifier	0.9
2.3 ppm, 11.5 ppm and 28.8 ppm demulsifier	0.4

LB interfacial films of demulsifiers diffused to the clean toluene-water interface (in the absence of asphaltenes) were imaged for comparison. The morphology of films obtained with pure demulsifier differed from those obtained when demulsifier was diffused into the interface where asphaltenes films were already formed. This result suggests that both the demulsifier and the asphaltenes were present at the interface. The roughness of demulsifier films without asphaltenes was small (0.4 nm) at a demulsifier in toluene concentration up to 28.8 ppm (Table 7.2, and Fig. 7.7), at which point an overdose was observed. These results show that roughness was not the cause for the overdose effects. It is important to note that the AFM images can only be analyzed to obtain the roughness, but not the absolute thickness of the transferred LB interfacial film. Therefore, the smoothness of pure demulsifier films at demulsifier concentrations up to 28.8 ppm does not contradict the hypothesis that steric repulsion caused by thickened demulsifier film may stabilize emulsions.

It should be noted that the asphaltene stabilized toluene-water interface certainly differs in many ways from “real” diluted bitumen-water interfaces. Nevertheless, using asphaltene in toluene as a model for diluted bitumen allowed us to probe the critical role of asphaltenes in stabilizing water in diluted bitumen emulsion and the role of demulsifiers in breaking such stable emulsions. As shown in this work, the importance of film rigidity and rheology, and the role played by additional factors such as steric forces were highlighted. The observations from our work shed lights on the stabilization and demulsification mechanisms of petroleum emulsions and corresponding over dose mechanisms that may be encountered in real systems.

7.5 CONCLUSIONS

The performance of an EO-PO demulsifier in the dewatering of asphaltene-stabilized water-in-oil emulsions was studied by bottle tests and micropipette coalescence tests. The properties of interfacial asphaltene films including surface tension, shear rheology, interfacial pressure-area isotherms, chemical composition, and nano and micro morphology, were probed using a suite of techniques.

Bottle tests and micropipette experiments showed the optimal performance of the demulsifier happened at a demulsifier concentration of 2.3 ppm in toluene. At higher concentrations, the performance degraded due to demulsifier overdosing. The observed optimal performance of the demulsifier was explained on the basis of asphaltene film softening (i.e. of the reduction of the viscoelastic moduli) under shear and compression, while the overdose was attributed to steric repulsion between water droplets.

Asphaltenes stabilize water-in-oil emulsions by forming rigid skins at the oil-water interface. The demulsifier used in this study was more surface active than asphaltenes, and thus competed effectively with asphaltenes for the interface. The demulsifiers penetrate into the asphaltene films and soften them under shear and compression. The softness of asphaltenes films was found to increase with increasing demulsifier addition up to 288.4 ppm in toluene. Faster kinetics of asphaltene film penetration was observed at higher demulsifier dosages. However, high demulsifier concentrations are likely to produce thick films, which would possibly increase steric repulsion between water droplets that prevents the droplets from coalescing.

This study shows that demulsification involves a complex interplay of competing mechanisms that are concentration-dependent. Such interplay must be taken into consideration in order to fully understand dewatering performance of the demulsifiers and to benefit the design of future demulsifiers.

REFERENCES

1. Kupai, M. M., Yang, F., Harbottle, D., Moran, K., Masliyah, J., & Xu, Z. (2013). Characterising rag−forming solids. *The Canadian Journal of Chemical Engineering*, *91*(8), 1395-1401.

2. McLean, J. D., & Kilpatrick, P. K. (1997). Effects of asphaltene solvency on stability of water-in-crude-oil emulsions. *Journal of Colloid and Interface Science*, *189*(2), 242-253.

3. Yan, Z., Elliott, J. A., & Masliyah, J. H. (1999). Roles of various bitumen components in the stability of water-in-diluted-bitumen emulsions. *Journal of Colloid and Interface Science*, *220*(2), 329-337.

4. Tchoukov, P., Czarnecki, J., & Dabros, T. (2010). Study of water-in-oil thin liquid films: Implications for the stability of petroleum emulsions. *Colloids and Surfaces A: Physicochemical and Engineering Aspects*, *372*(1), 15-21.

5. Czarnecki, J., Tchoukov, P., & Dabros, T. (2012). Possible role of asphaltenes in the stabilization of water-in-crude oil emulsions. *Energy & Fuels*, *26*(9), 5782-5786.

6. Tchoukov, P., Yang, F., Xu, Z., Dabros, T., Czarnecki, J., & Sjöblom, J. (2014). Role of asphaltenes in stabilizing thin liquid emulsion films. *Langmuir*, *30*(11), 3024-3033.

7. Feng, X., Mussone, P., Gao, S., Wang, S., Wu, S. Y., Masliyah, J. H., & Xu, Z. (2009). Mechanistic study on demulsification of water-in-diluted bitumen emulsions by ethylcellulose. *Langmuir*, *26*(5), 3050-3057.

8. Robins, M. M., Watson, A. D., & Wilde, P. J. (2002). Emulsions—creaming and rheology. *Current Opinion in Colloid & Interface Science*, *7*(5), 419-425.

9. Czarnecki, J., Moran, K., & Yang, X. (2007). On the “rag layer” and diluted bitumen froth dewatering. *The Canadian Journal of Chemical Engineering*, *85*(5), 748-755.

10. Hou, J., Feng, X., Masliyah, J., & Xu, Z. (2012). Understanding interfacial behavior of ethylcellulose at the water–diluted bitumen interface. *Energy & Fuels*, *26*(3), 1740-1745.

11. Fan, Y., Simon, S., & Sjöblom, J. (2009). Chemical destabilization of crude oil emulsions: effect of nonionic surfactants as emulsion inhibitors. *Energy & Fuels*, *23*(9), 4575-4583.

12. Ese, M. H., Sjöblom, J., Djuve, J., & Pugh, R. (2000). An atomic force microscopy study of asphaltenes on mica surfaces. Influence of added resins and demulsifiers. *Colloid and Polymer Science*, *278*(6), 532-538.

13. Fan, Y., Simon, S., & Sjöblom, J. (2010). Interfacial shear rheology of asphaltenes at oil–water interface and its relation to emulsion stability: influence of concentration, solvent aromaticity and nonionic surfactant. *Colloids and Surfaces A: Physicochemical and Engineering Aspects*, *366*(1), 120-128.

14. Kim, Y. H., & Wasan, D. T. (1996). Effect of demulsifier partitioning on the destabilization of water-in-oil emulsions. *Industrial & Engineering Chemistry Research*, *35*(4), 1141-1149.

15. Feng, X., Wang, S., Hou, J., Wang, L., Cepuch, C., Masliyah, J., & Xu, Z. (2011). Effect of hydroxyl content and molecular weight of biodegradable ethylcellulose on demulsification of water-in-diluted bitumen emulsions. *Industrial & Engineering Chemistry Research*, *50*(10), 6347-6354.

16. Erni, P., Windhab, E. J., Gunde, R., Graber, M., Pfister, B., Parker, A., & Fischer, P. (2007). Interfacial rheology of surface-active biopolymers: Acacia senegal gum versus hydrophobically modifed starch. *Biomacromolecules*, *8*(11), 3458-3466.

17. Dickinson, E. (2001). Milk protein interfacial layers and the relationship to emulsion stability and rheology. *Colloids and Surfaces B: Biointerfaces*, *20*(3), 197-210.

18. Erni, P. (2011). Deformation modes of complex fluid interfaces. *Soft Matter*, *7*(17), 7586-7600.

19. Angle, C. W., & Hua, Y. (2012). Dilational interfacial rheology for increasingly deasphalted bitumens and n-C5 asphaltenes in toluene/NaHCO3 solution. *Energy & Fuels*, *26*(10), 6228-6239.

20. Mohammed, R. A., Bailey, A. I., Luckham, P. F., & Taylor, S. E. (1994). The effect of demulsifiers on the interfacial rheology and emulsion stability of water-in-crude oil emulsions. *Colloids and Surfaces A: Physicochemical and Engineering Aspects*, *91*, 129-139.

21. Sun, H. Q., Zhang, L., Li, Z. Q., Zhang, L., Luo, L., & Zhao, S. (2011). Interfacial dilational rheology related to enhance oil recovery. *Soft Matter*, *7*(17), 7601-7611.

22. Ekott, E. J., & Akpabio, E. J. (2010). A review of water-in-crude oil emulsion stability, destabilization and interfacial rheology. *Journal of Engineering and Applied Sciences*, *5*(6), 447-452.

23. Feng, X., Wang, S., Hou, J., Wang, L., Cepuch, C., Masliyah, J., & Xu, Z. (2011). Effect of hydroxyl content and molecular weight of biodegradable ethylcellulose on demulsification of

water-in-diluted bitumen emulsions. *Industrial & Engineering Chemistry Research*, *50*(10), 6347-6354.

24. Wu, J., Xu, Y., Dabros, T., & Hamza, H. (2003). Effect of demulsifier properties on destabilization of water-in-oil emulsion. *Energy & Fuels*, *17*(6), 1554-1559.

25. Zaki, N. N., Abdel-Raouf, M. E., & Abdel-Azim, A. A. (1996). Propylene oxide-ethylene oxide block copolymers as demulsifiers for water-in-oil emulsions, II. Effects of temperature, salinity, pH-value, and solvents on the demulsification efficiency. *Monatshefte für Chemie/Chemical Monthly*, *127*(12), 1239-1245.

26. Wu, J., Xu, Y., Dabros, T., & Hamza, H. (2005). Effect of EO and PO positions in nonionic surfactants on surfactant properties and demulsification performance. *Colloids and Surfaces A: Physicochemical and Engineering Aspects*, *252*(1), 79-85.

27. Xu, Y., Wu, J., Dabros, T., Hamza, H., & Venter, J. (2005). Optimizing the polyethylene oxide and polypropylene oxide contents in diethylenetriamine-based surfactants for destabilization of a water-in-oil emulsion. *Energy & Fuels*, *19*(3), 916-921.

28. Ramalho, J. B.; Ramos, N.; Lucas, E.(2009).The influence of some interfacial properties of PEO-b-PPO copolymers on dewatering of water-in-oil asphaltene model emulsions. *Chem. Chem. Technol*, 3, 53-58.

29. Abdel‐Azim, A. A. A., Zaki, N. N., & Maysour, N. E. S. (1998). Polyoxyalkylenated amines for breaking water ‐ in ‐ oil emulsions: effect of structural variations on the demulsification efficiency. *Polymers for Advanced Technologies*, *9*(2), 159-166.

30. Angle, C. W., Dabros, T., & Hamza, H. A. (2007). Demulsifier effectiveness in treating heavy oil emulsion in the presence of fine sands in the production fluids. *Energy & Fuels*, *21*(2), 912-919.

31. Feng, X., Mussone, P., Gao, S., Wang, S., Wu, S. Y., Masliyah, J. H., & Xu, Z. (2009). Mechanistic study on demulsification of water-in-diluted bitumen emulsions by ethylcellulose. *Langmuir*, *26*(5), 3050-3057.

32. Kailey, I., Blackwell, C., & Behles, J. (2013). Collaborative interactions between EO-PO copolymers upon mixing. *Industrial & Engineering Chemistry Research*, *52*(50), 17913-17919.

33. Mohammed, R. A., Bailey, A. I., Luckham, P. F., & Taylor, S. E. (1994). Dewatering of crude oil emulsions 3. Emulsion resolution by chemical means. *Colloids and Surfaces A: Physicochemical and Engineering Aspects*, *83*(3), 261-271.

34. Zhang, Z., Xu, G., Wang, F., Dong, S., & Chen, Y. (2005). Demulsification by amphiphilic dendrimer copolymers. *Journal of Colloid and Interface Science*, *282*(1), 1-4..

35. Aveyard, R., Binks, B. P., Fletcher, P. D. I., & Lu, J. R. (1990). The resolution of water-in-crude oil emulsions by the addition of low molar mass demulsifiers. *Journal of Colloid and Interface Science*, *139*(1), 128-138.

36. Ramakers, R. R. M., Pöpel, H. J., & Koops, W. (1982). A new method for handling oil spill materials. *Oil and Petrochemical Pollution*, *1*(2), 129-137.

37. Stewart, A. C., El-Hamouz, A. M., & Davies, G. A. (1996). Effect of chemical additives on the stability of kerosene-water dispersions. *Journal of Dispersion Science and Technology*, *17*(6), 675-696.

38. Dimitrov, A. N., Yordanov, D. I., & Petkov, P. S. (2012). Study on the effect of demulsifers on crude oil and petroleum products. *International Journal of Environmental Research*, *6*(2), 435-442.

39. Mohammed, R. A., Bailey, A. I., Luckham, P. F., & Taylor, S. E. (1994). Dewatering of crude oil emulsions 3. Emulsion resolution by chemical means. *Colloids and Surfaces A: Physicochemical and Engineering Aspects*, *83*(3), 261-271.

40. Fan, Y., Simon, S., & Sjöblom, J. (2010). Influence of nonionic surfactants on the surface and interfacial film properties of asphaltenes investigated by Langmuir balance and Brewster angle microscopy. *Langmuir*, *26*(13), 10497-10505.

41. Hua, Y., & Angle, C. W. (2012). Brewster angle microscopy of Langmuir films of athabasca bitumens, n-C5 asphaltenes, and SAGD bitumen during pressure–area hysteresis. *Langmuir*, *29*(1), 244-263.

42. Kailey, I., & Feng, X. (2013). Influence of structural variations of demulsifiers on their performance. *Industrial & Engineering Chemistry Research*, *52*(2), 785-793.

43. Ancheyta, J., Centeno, G., Trejo, F., Marroquin, G., Garcia, J. A., Tenorio, E., & Torres, A. (2002). Extraction and characterization of asphaltenes from different crude oils and solvents. *Energy & Fuels*, *16*(5), 1121-1127.

44. Gao, S., Moran, K., Xu, Z., & Masliyah, J. (2009). Role of bitumen components in stabilizing water-in-diluted oil emulsions. *Energy & Fuels*, *23*(5), 2606-2612.

45. Feng, X., Mussone, P., Gao, S., Wang, S., Wu, S. Y., Masliyah, J. H., & Xu, Z. (2009). Mechanistic study on demulsification of water-in-diluted bitumen emulsions by ethylcellulose. *Langmuir*, *26*(5), 3050-3057.

46. Harbottle, D., Chen, Q., Moorthy, K., Wang, L., Xu, S., Liu, Q., ... & Xu, Z. (2014). Problematic stabilizing films in petroleum emulsions: Shear rheological response of viscoelastic asphaltene films and the effect on drop coalescence. *Langmuir*, *30*(23), 6730-6738.

47. Singh, B. P. (1994). Performance of demulsifiers: Prediction based on film pressure-area isotherms and solvent properties. *Energy Sources*, *16*(3), 377-385.

48. Speight, J. G.; Speros, E. M. (1981). On the molecular nature of petroleum asphaltenes. Chemistry of Asphaltenes,195, 1-15.

49. Andersen, S. I. (1994). Effect of precipitation temperature on the composition of n-heptane asphaltenes. *Fuel Science & Technology International*, *12*(1), 51-74.

50. Wang, Y., Zhang, L., Sun, T., Zhao, S., & Yu, J. (2004). A study of interfacial dilational properties of two different structure demulsifiers at oil–water interfaces. *Journal of Colloid and Interface Science*, *270*(1), 163-170.

51. Petkov, J. T., Gurkov, T. D., Campbell, B. E., & Borwankar, R. P. (2000). Dilatational and shear elasticity of gel-like protein layers on air/water interface. *Langmuir*, *16*(8), 3703-3711.

52. Ferri, J. K., Kotsmar, C., & Miller, R. (2010). From surfactant adsorption kinetics to asymmetric nanomembrane mechanics: Pendant drop experiments with subphase exchange. *Advances in Colloid and Interface Science*, *161*(1), 29-47.

53. Kotsmar, C., Grigoriev, D. O., Makievski, A. V., Ferri, J. K., Krägel, J., Miller, R., & Möhwald, H. (2008). Drop profile analysis tensiometry with drop bulk exchange to study the sequential and simultaneous adsorption of a mixed β-casein/C12DMPO system. *Colloid and Polymer Science*, *286*(8-9), 1071-1077.

54. Ferri, J. K., Gorevski, N., Kotsmar, C., Leser, M. E., & Miller, R. (2008). Desorption kinetics of surfactants at fluid interfaces by novel coaxial capillary pendant drop experiments. *Colloids and Surfaces A: Physicochemical and Engineering Aspects*, *319*(1), 13-20.

55. Zhang, L. Y., Lopetinsky, R., Xu, Z., & Masliyah, J. H. (2005). Asphaltene monolayers at a toluene/water interface. *Energy & Fuels*, *19*(4), 1330-1336.

56. Zhang, H., Xu, G., Wu, D., & Wang, S. (2008). Aggregation of cetyltrimethylammonium bromide with hydrolyzed polyacrylamide at the paraffin oil/water interface: interfacial rheological behavior study. *Colloids and Surfaces A: Physicochemical and Engineering Aspects*, *317*(1), 289-296.

57. Zhang, L. Y., Xu, Z., & Masliyah, J. H. (2003). Langmuir and Langmuir-Blodgett films of mixed asphaltene and a demulsifier. *Langmuir*, *19*(23), 9730-9741.

58. Spiecker, P. M., & Kilpatrick, P. K. (2004). Interfacial rheology of petroleum asphaltenes at the oil-water interface. *Langmuir*, *20*(10), 4022-4032.

59. Yang, X., Verruto, V. J., & Kilpatrick, P. K. (2007). Dynamic asphaltene-resin exchange at the oil/water interface: Time-dependent W/O emulsion stability for asphaltene/resin model oils. *Energy & Fuels*, *21*(3), 1343-1349.

60. Álvarez, L., Díaz, M. E., Montes, F. J., & Galán, M. A. (2010). Langmuir technique and Brewster angle microscope studies of the interfacial behavior of bitumen, asphaltenes and maltenes at the air–water interface. I. Effect of different spreading solution volumes. *Fuel*, *89*(3), 691-702.

61. Lobato, M. D., Pedrosa, J. M., Möbius, D., & Lago, S. (2009). Optical characterization of asphaltenes at the air− water interface. *Langmuir*, *25*(3), 1377-1384.

62. Cadena-Nava, R. D., Cosultchi, A., & Ruiz-Garcia, J. (2007). Asphaltene behavior at interfaces. *Energy & Fuels*, *21*(4), 2129-2137.

63. Zhang, L. Y., Xu, Z., & Masliyah, J. H. (2005). Characterization of adsorbed athabasca asphaltene films at solvent-water interfaces using a Langmuir interfacial trough. *Industrial & Engineering Chemistry Research*, *44*(5), 1160-1174.

64. Bosio, V., Dubreuil, F., Bogdanovic, G., & Fery, A. (2004). Interactions between silica surfaces coated by polyelectrolyte multilayers in aqueous environment: comparison between precursor and multilayer regime. *Colloids and Surfaces A: Physicochemical and Engineering Aspects*, *243*(1), 147-155.

65. Pensini, E., Yip, C. M., O'Carroll, D., & Sleep, B. E. (2013). Carboxymethyl cellulose binding to mineral substrates: Characterization by atomic force microscopy–based Force spectroscopy and quartz-crystal microbalance with dissipation monitoring. *Journal of Colloid and Interface Science*, *402*, 58-67.

66. Barnes, T. J., & Prestidge, C. A. (2000). PEO-PPO-PEO block copolymers at the emulsion droplet-water interface. *Langmuir*, *16*(9), 4116-4121.

67. Vieira, J. B., Li, Z. X., & Thomas, R. K. (2002). Adsorption of triblock copolymers of ethylene oxide and propylene oxide at the air/water interface: The surface excess. *The Journal of Physical Chemistry B*, *106*(21), 5400-5407.

CHAPTER 8 DEMULSIFICATION MECHANISMS OF WATER-IN-HEAVY OIL EMULSIONS STUDIED BY MODIFIED THIN LIQUID FILM TECHNIQUE

8.1 INTRODUCTION

During the production of crude oil from various sources, stable water-in-oil emulsions are formed.[1] The most efficient approach to remove the emulsified water is using chemical demulsifiers which are designed to enhance flocculation and/or coalescence of water droplets.[2] Demulsifiers modify the physicochemical properties of the oil-water interfaces to minimize interfacial conditions that favor stable emulsions. In the case of water in crude oil emulsions, such unfavorable interfacial conditions against emulsion destabilization (coalescence) are often described as rigid interfaces that present mechanical strength to hinder droplet coalescence.[3] Demulsification mechanisms are often found to be associated with interfacial softening which leads to weaker interfaces of lower elastic moduli.[4,5,6] This softening effect is often attributed to the ability of demulsifiers to replace the adsorbed asphaltenes which form interlinking aggregates at the interface, converting an elastic (rigid) interface to a viscous (soft) interface. In general due to their high interfacial activity, demulsifiers can stabilize emulsion themselves if over-dosed.[7,8,9] Demulsifiers, depending on their physicochemical properties, can stabilize emulsions by the same mechanisms as in the case of surfactants (lowered interfacial tension), polymers (steric repulsion) or solids (aggregates formation).[5,6,10,11]

In the commercial demulsification practice, polymeric surfactants are commonly used as demulsifiers due to their ability to penetrate into the oil-water interface, weakening the interface while extending their hydrocarbon chains into the oil phase to induce flocculation. Biodegradable ethylcellulose (EC) macromolecules are shown to exhibit a superior performance in removing emulsified water from the diluted bitumen system.[12] The efficient demulsification by EC polymers is believed to be related to their high interfacial activity and strong ability to break up stable interfacial layers.[5] Langmuir trough compression isotherm revealed that the EC addition to the diluted bitumen-water interface drastically decreased the compressibility of the interface, inducing a transition from a rigid to a soft interface.[5] Such an observation, however, is limited to explain the destabilization mechanism from the interfacial point of view.

Previous attempts to understand the emulsion stability based only on their interfacial properties were not effective and less predictive. Coalescence and flocculation properties of emulsified water droplets by chemical demulsifiers depend also on the surface forces in the intervening oil film, which in combination with the viscosity of the liquid determines intervening liquid film thinning dynamics. When two approaching water droplets are within a small distance, a flat thin liquid film forms between them. Emulsions remain stable when the repulsive disjoining pressure is sufficiently strong to counter-balance the capillary pressure difference across the curved liquid-liquid interfaces. The film drainage and stability can be conveniently studied using Thin Liquid Film (TLF) technique.[13,14,15,16]

In the Chapter 4, the film forming properties of asphaltenes (stabilization mechanism) were studied and compared with that of its parent bitumen and de-asphaltened bitumen using TLF technique.[2] In this study, thin films were obtained in Scheludko-Exerowa cell[16] at well controlled conditions (temperature and pressure). Distinctive differences were observed in film drainage kinetics and film life time among different bitumen components. Asphaltene films showed severe aging effect that the film became thicker and more heterogeneous in thickness with time. The asphaltene aggregation at the oil-water interface led to gradual formation of network to such an extent that the liquid in the film behaved as a non-Newtonian fluid with a yield stress, which was proposed as a possible mechanism for stabilization of water-in-petroleum emulsions.

Though proven to be highly useful in studying stabilization mechanism of water in oil emulsions, applying the existing TLF technique to studying demulsification process and mechanism is quite challenging. In dewatering operations, the demulsifiers and other chemical aids are added to the system after emulsion formation, where a stabilizing adsorption layer is already well developed at water-oil interface. As a result, the added demulsifiers have to disturb and displace the adsorbed material in order to reduce the mechanical strength and surface forces that stabilize the emulsion. The fundamental studies on premixed crude oil-demulsifiers systems are not representative of the case encountered in real industrial applications. To establish a condition that is similar to the real industrial demulsification process, the TLF technique needs to be modified by introducing a dosing system in order to change the composition of the studied film in situ and a mechanism for real time observation on the development/change of the film.

In this study, we propose a modified thin liquid film cell, which enables us to dose demulsifiers into the thin liquid film after the film interfaces are formed and developed. This modified TLF cell allows for direct basement on the effect of demulsifiers addition on thin film morphology and stability. Using this modified cell, the interfacial and film properties of pre-mixed system are shown to be not representative for demulsification process where the order of chemical addition is important.

8.2 MATERIALS AND EXPERIMENTAL SETUP

8.2.1 Materials

Demulsifier EC300 was provided by Baker Hughes and stored in desiccators. The molecular weight of EC300 is determined to be 182000 Da.[12] Asphaltenes were extracted from Athabasca coker feed bitumen (provided by Syncrude Canada Ltd.) using n-pentane (>98%, purchased from EMD Chemical Inc.), following the procedures described elsewhere.[14] Toluene (Optima grade, purchased from Fisher Scientific Canada) and heptane (HPLC grade, Fisher Scientific Canada) were used as received. Heptol (toluene-heptane mixture) prepared by mixing equal volumes of toluene and heptane was used as a solvent. Milli-Q water with resistivity 18.2 MΩ·cm at 25 °C was used as an aqueous phase.

8.2.2 Experimental techniques

8.2.2.1 Interfacial Tension Measurement.

The interfacial tension was measured using pendant drop shape analysis with an oneAttension Theta optical tensiometer (Biolin Scientific). Contained in a quartz cell was 5 mL of 2 g/L asphaltenes-in-heptol solution used as the oil phase. A water droplet of ~20 µL in volume was formed in the oil phase at the tip of a stainless steel needle using a syringe. The profile of the pendant drop was tracked using the vendor-provided imaging analysis software. The asphaltene-in-heptol solution-water interfacial tension was tracked for 15,000 s, followed by slow injection of 1ppm (final concentration in the oil phase) EC300-in-heptol solution into the oil phase by a micro-syringe. The interfacial tension after demulsifier injection was monitored for another 5,000 seconds.

8.2.2.2 Shear Rheology Measurement.

The shear elastic (G') and viscous (G") modulii of the asphaltene-in-heptol solution-water interface were measured using an AR-G2 rheometer with a Double Wall Ring geometry of 35 mm radius (TA instruments, USA). Contaminants on the ring were removed by soaking the ring using toluene and acetone followed by burning any residues using a butane flame gun before each experiment. After placing 19.2 ml of water into the sample holding channel in the Delrin trough, the cleaned double wall ring was carefully placed onto the surface of the water sub-phase, followed by the addition of 15 ml of asphaltene-in-heptol solution. Solvent evaporation was minimized using a Teflon cap to seal the trough. The temperature of the system during the experiment was controlled to be at 23.0 ºC using a Peltier plate. The viscoelasticity of the interfacial film was measured by applying a small oscillation of interfacial strain to the interface using the double wall ring. The angular frequency and strain during the time sweep in this study were set at 0.5 Hz and 0.8%, respectively.

The interface was allowed to build for half an hour and the developments of shear elastic moduli G' and shear viscous moduli G" were tracked. EC300-in-heptol solution at 1000ppm was then slowly dosed into the top oil phase to obtain a demulsifier concentration of 23 ppm. The change of the G' and G" modulus of the interface after the emulsifier additions was measured at a 30s interval for at least another 5,000 seconds.

8.2.2.3 Modified Thin Liquid Film Cell for Demulsifier Addition in Already Formed Films

As discussed in the introduction, understanding demulsification mechanisms requires an experimental method to observe the effect of demulsifier addition to thin films between the droplets that was already formed and aged. The Scheludko-Exerowa cell [17,18] is widely used to study the dynamics and stability of foams and emulsions. In this cell, a thin liquid film is formed in a hole drilled in a porous glass holder by withdrawing a liquid through a capillary. In the case of water-in-oil emulsion films, which are of interest in this work, the porous holder and the hole are soaked in the oil phase and immersed in the water-filled bottom part of the measuring cell. However, this set-up does not allow changing the composition and concentration of thin film liquid once the cell is loaded. As pointed out earlier, studying premixed asphaltene in solvent solution with added demulsifier is not representative of the real demulsification process in crude oil processing where interfacial films are formed prior to inducing the demulsifiers into the system. In order to mimic the real demulsification process, we proposed a new cell design that allows for dosing demulsifiers or other chemical additives of interest into the emulsion films already formed and aged. A schematic of the modified Scheludko-Exerowa cell is shown in Figure 8.1. In this design, an outlet was open to the side wall of the glass tube used to contain water phase for the TLF setup. A rubber membrane was installed to the end of the outlet to make it gas tight. A micro-syringe containing demulsifier solutions was used to punctuate the membrane and deposit solutions directly into the porous glass plate.

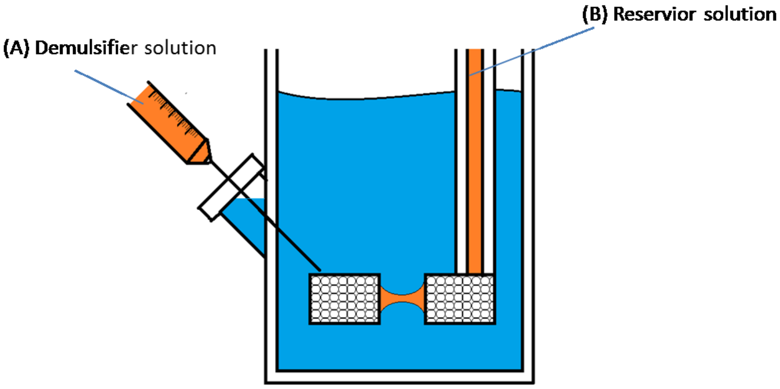

Figure 8.1 Schematic of the modified Scheludko-Exerowa cell for studying the effect of chemical addition (demulsifier) on thin emulsion films with already developed interfacial layers.

In our experiments, the cell was first loaded with original asphaltene-in-heptol solution and placed in water. A thick film (~2mm) was formed in the hole and the upper and lower organic solution-water interfaces were aged for a desired time. An oil film was formed in the center of the hole as the oil solution studied was slowly withdrawn through the capillary using a gas tight syringe pump. Once the thin film was formed, the pressure in the measurement cell was adjusted by a micro-syringe to obtain the desired film radius of ~100 μm. The film remained undisturbed and allowed to drain under capillary pressure due to the curvature of the interface in the neighboring meniscus. The morphology, thickness and lifetime of the thin liquid films were determined. The film then was made thick (~2mm) again by pushing oil from the capillary reservoir into the glass plate, followed by the dosing of demulsifier solution into the film accomplished by depositing small droplets of demulsifier solution onto the glass plate through the micro-syringe. Due to the hydrophobic property of the plate and the capillary pressure provided by the porous structure, droplets absorbed very quickly into the continuous oil phase contained in the glass plate. To reduce localized differences in the demulsifier concentration, each dose of demulsifier was separated into a few ~2 uL droplets and deposited at different locations on the plate. After demulsifier deposition, more oil in the glass capillary was pumped into the plate and then withdrawn back at least five times to distribute homogenously the demulsifiers throughout the entire oil phase inside the film and oil reservoir. The final concentration of demulsifiers in the thin liquid film (C_d) was calculated using:

$$C_d = (C_{d0} \times V_{d0})/(V_r + V_{d0}) \qquad (1)$$

where C_{d0} is the concentration of demulsifier in the mother solution that was dosed in, V_{d0} is the volume of demulsifier solution added and V_r is the total volume of the oil, which includes the volume of oil in the glass plate and also the capillary tube. The volumes of oil pumped in and out were kept relatively small so that the disturbance of the film interfaces was minimized. After demulsifier dosing, the interfaces were aged for a desired period of time before thin liquid films were generated again and film properties measured.

The modified cell was used in the thin film instrument already described in our previous work.[15,16] The films were observed in reflected light using Axio Observer inverted microscope (Carl Zeiss, Germany). A high-resolution and high-sensitivity DFC500 digital camera (Leica, Germany) were used to take the film images. A custom built LabVIEW program performed data acquisition and controlled the experiment. Details on the method and experimental setup can be found elsewhere.[19,20] During the experiment, the cell was kept at constant temperature of 23 °C. The porous glass plate was made hydrophobic by soaking in 20% dichlorodimethylsilane (> 99.5%, Fluka) in cyclohexene (reagent grade, Fisher Scientific) solution for 24 hours.

8.3 RESULTS AND DISCUSSION

8.3.1 Effect of emulsifier addition on already developed asphaltene interfacial layers

8.3.1.1 Interfacial tension.

Dynamic interfacial tension of asphaltene-in-heptol solution (oil)-water droplet interface was measured for a period of time to allow the buildup of asphaltene layers at the oil-water interface. A small amount of demulsifier was then added to the continuous oil phase. The objective of this experiment is to mimic the addition of demulsifiers to crude/heavy oil in practical emulsion dewatering operations, often with well-developed layers at the oil-water interface. The interfacial tension of asphaltene-in-heptol solution-water interface decreased from its initial value of ~38.4 mN/m to ~18.6 mN/m over an aging time of 15,000 seconds. As shown in Figure 8.2 the addition of 1 ppm EC300 demulsifier rapidly decreased the interfacial tension further to ~10 mN/m. The concentration of EC300 was controlled to be relatively low at 1 ppm to avoid extremely low interfacial tension as such interfacial tension could no longer be measured due to the streaming of water out from the needle tip. It should be noted that the addition of EC300 decreased the interfacial tension of asphaltene-in-heptol solution-water interfaces to the same level of 1 ppm EC300 alone in heptol solution-water interface. This finding indicates that EC300 is extremely interfacially active and capable of disrupting and displacing the asphaltene molecules even from aged interface. The process is rapid with similar kinetics to the adsorption of EC300 onto the heptol-water interface.

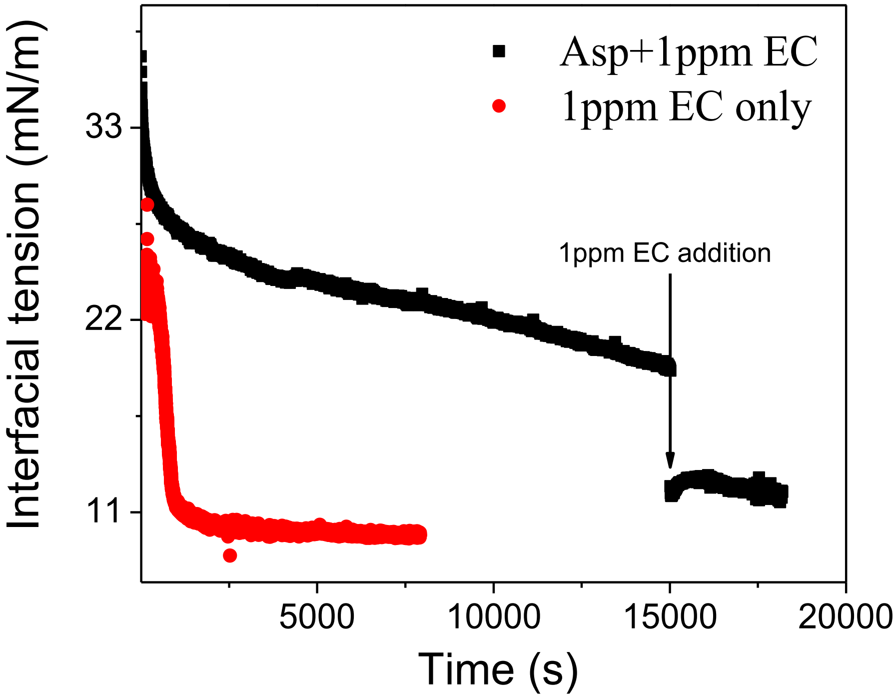

Figure 8.2 Interfacial tension of 2 g/L asphaltene in heptol solution-water interfaces with 1ppm EC300 doped into the oil phase after aging of the interface for 15000 seconds in comparison with 1ppm EC300 in heptol solution-water interfacial tension.

8.3.1.2 Shear viscoelastic properties of the water/oil interface.

Interfacial shear rheology measurement could provide valuable information not only on accumulation of materials at the interface but also on viscoelasitc properties of the interface. The interface in rheology experiments was prepared in the similar manner as in the interfacial tension measurements. Throughout the first 30 min we followed the evolution (aging) of asphaltene-in-heptol solution-water interface by measuring the elastic (G') and viscous (G") modulus. The results are shown in Figure 8.3. Both moduli increased with aging time, with G’ having a much higher value than G", which indicates the formation of an elastic-dominant interface. This finding is in good agreement with previous observations of asphaltenes forming a solid-like, elastically dominant oil-water interface.[21] It is worth noting that, at lower asphaltene concentration (0.4 g/L in heptol), it was found that there exists a transition time at which the interface developed itself from viscous dominated (G’<G’’) to elastic dominated (G’>G’’). The coalescence rate between water droplets was found to decrease drastically when such transition of viscoelasticity happened[22]. At the 30-minute mark, demulsifiers were dosed into the top oil phase at a concentration of 23 ppm in organic phase, which resulted in an immediate and steady decrease in both G' and G". Over the next 2,500 s, the viscous and elastic moduli decreased to the values close to zero, indicating complete disruption of the afore-mentioned rigid interface and making the interface entirely fluid-like as oil-water interface formed in the presence of demulsifiers alone.

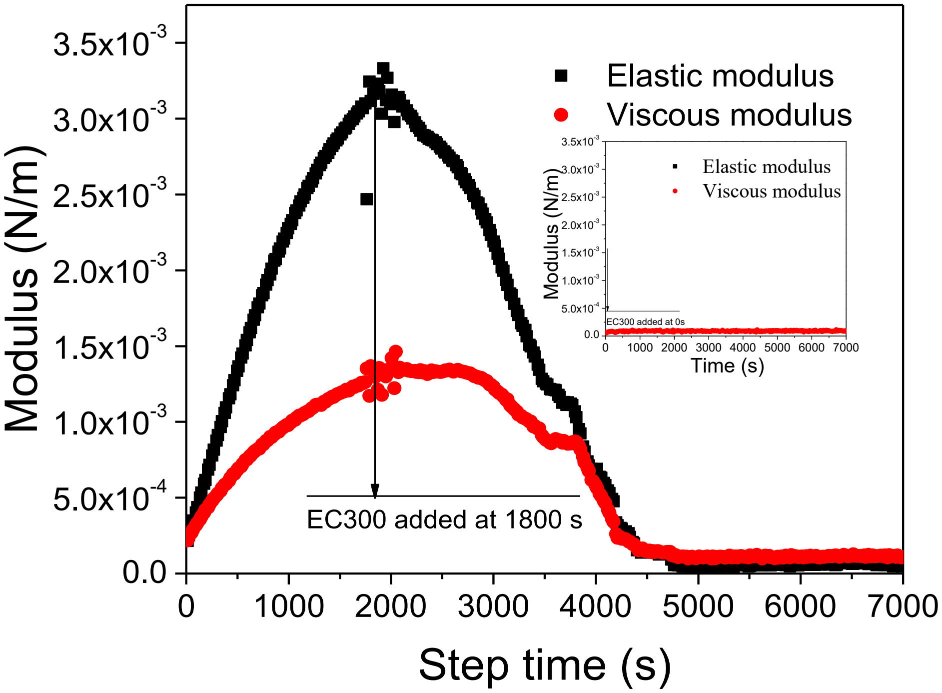

Figure 8.3 Change of elastic and viscous modulus of the oil-water interface formed by 2 g/L asphaltene in heptol solution and water when 23ppm of EC300 was doped at 1800s. Inset: Change of elastic and viscous modulus of the oil-water interface formed by 2 g/L asphaltene in heptol solution and water when 23ppm of EC300 was pre-mixed with asphaltene solution

To understand the interaction of EC 300 and asphaltene molecules and their competitive adsorption behavior, a second set of measurements (shown as inset in Figure 8.3) were conducted using asphaltene solutions of the same concentration but with 23 ppm of EC 300 demulsifier pre-blended into the solution. In contrast to the interface formed by pure asphaltene solution, the interface formed in the presence of 23 ppm of EC 300 demulsifier was found to be fluid-like with a negligible shear viscoelastic modulus. This finding confirms that in the presence of highly interfacially-active demulsifier molecules, the asphaltenes cannot effectively compete for the interface, and thus the formation of rigid interfaces is prevented.

8.3.2 Morphology and Life Times of Thin Liquid Films

The thin liquid film formed by 2 g/L asphaltene-in-heptol solution appeared to be thick and inhomogeneous after 30 minutes of aging. The inhomogeneity in the film thickness as indicated by observed Newton ring fringes is most likely related to the formation of asphaltene aggregates in the solutions. As shown in Figure 8.4A, very little drainage is observed in the thick film regions, indicating the formation of stable phases within the film. The films formed from 2 g/L asphaltene solutions were stable and did not rupture within 20 min time of each experiment. The results agree with previous those reported in earlier studies that emulsion water droplets in asphaltene-in-heptol solutions are stable against coalescence.[19]

After the film development (30 min), 23 ppm of EC 300 was dosed into the film following the procedure described in section 8.2.2.3. The addition of 23 ppm EC300 to the thin liquid film results in unstable films with significantly shorter lifetime of less than 20 s. The features of film changed dramatically from thick, inhomogeneous and rigid to thin, homogeneous and “fluid”, as shown in Figure 8.4B. Dark spots (these are areas in the film with thickness of less than 15 nm) were formed in the film and propagated quickly as soon as the film was generated. Within a few seconds, these thinner black spots occupied almost the entire film area except for a few brighter spots that indicate the formation of dimples by trapped film liquid.

By increasing the demulsifier dosage to 43 ppm, the thin liquid film became more stable, having a life time greater than 2 min, indicating an overdose of EC 300 happened at 43ppm for 2 g/L of asphaltene–in-heptol solution. The film contained similar features as the film formed in the presence of 23 ppm EC 300, a black film occupied the entire film area within seconds of film formation with a large dimple trapped in the film. However, the film formed as such became more stable due to the higher density of demulsifier molecules at the interface and their intrinsic emulsion stabilizing property. Further increasing the demulsifier dosage up to 63 ppm would lead to even more stable thin liquid films while the feature of the film remained the same, i.e., a uniform stable film in contrast to heterogeneous films formed from asphaltene solutions.

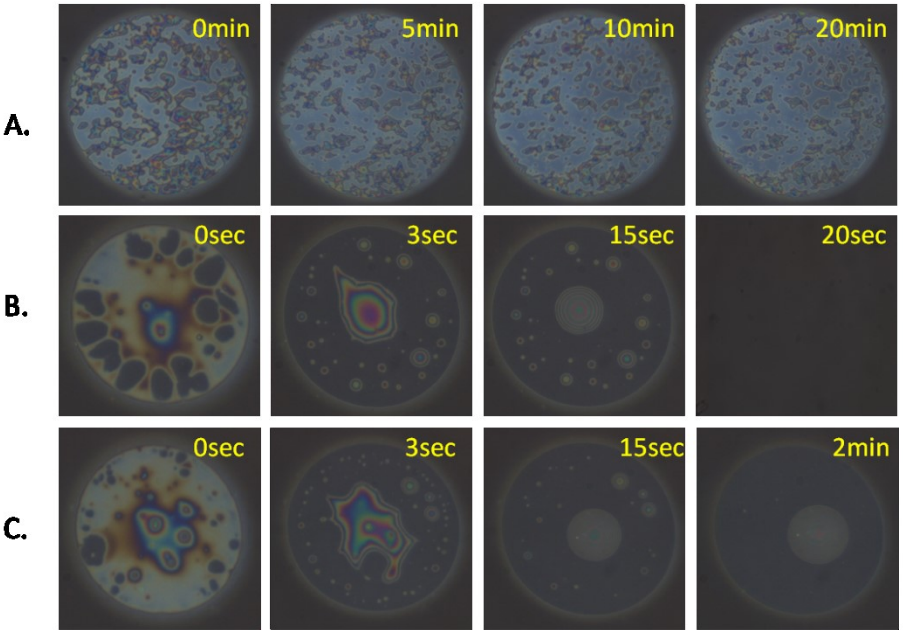

Figure 8.4 Evolution of thin liquid films formed by 2 g/L asphaltene in heptol and demuslifier EC 300. (A) Without demulsifier; (B) With 23 ppm of EC 300 doped; (C) With 43ppm of EC 300 doped.

As shown in Figure 8.5A, the thin liquid film formed from 10 g/L asphaltene-in-heptol solution was much thicker and more inhomogeneous in thickness than the film formed from 2 g/L solutions. The feature of the film remained the same after 15 min, indicating negligible drainage in the film. The formation of variable size aggregates was evident from the uneven thickness of the film shown by rich color variations. The domains in the film appeared irregular in shape, suggesting a rigid interface with a negligible liquid flow in the film. The film was found to be stable with a film life time longer than 20 minutes, an observation consistent with the stable emulsions under such conditions reported earlier.[13] The addition of 23 ppm of EC300 into such stable film caused cracking of the interfacial layer, resulting in two types of domains: a thinner region with a dimple inside and a thicker rigid region. Such an observation is in line with previous findings revealed by AFM imaging on Blodgett-deposited interface that the morphology of water-bitumen solution interface changed with EC demulsifier addition from a smooth and homogeneous interface to a bumpy and heterogeneous interface with micro-domains.[23] With the help of the new cell design, this is the first time that such phenomenon was observed in-situ. One important feature to notice was that the thicker regions became mobile at the interface, making it obvious that the thick area was not inside the film but at the interface of the aqueous side. The change of the domains from an immobile to mobile state at the interface suggests significant modification of the oil-water interface by demulsifiers to a state where asphaltene aggregates can no longer attach firmly to the interface. As a result, a new thin and flexible liquid film formed beneath the thick interface. A dimple was present in the film. The rapid drainage of the film in the dimple indicates a Newtonian nature of the liquid inside the thinner region. Despite extremely stable film formed by high concentration of asphaltenes-in-heptol solutions, the stability of the film is now governed by the nature of this thin area of the film, leading to a film life time of ~8 seconds. By further increasing the dosage of EC300 to 60 ppm, the thin liquid film was found to be stable again, with a similar feature as in the case of low asphaltene concentration (2 g/L) system. A close examination of the thinner area reveals that the thickness and morphology of these areas are very similar to that of the film stabilized by demulsifiers alone at the equivalent concentration as shown by the inset of Figure 8.6. However, a highly inhomogeneous film was observed, likely caused by the debris of asphaltene aggregates formed from the rupture of the original interface by demulsifiers.

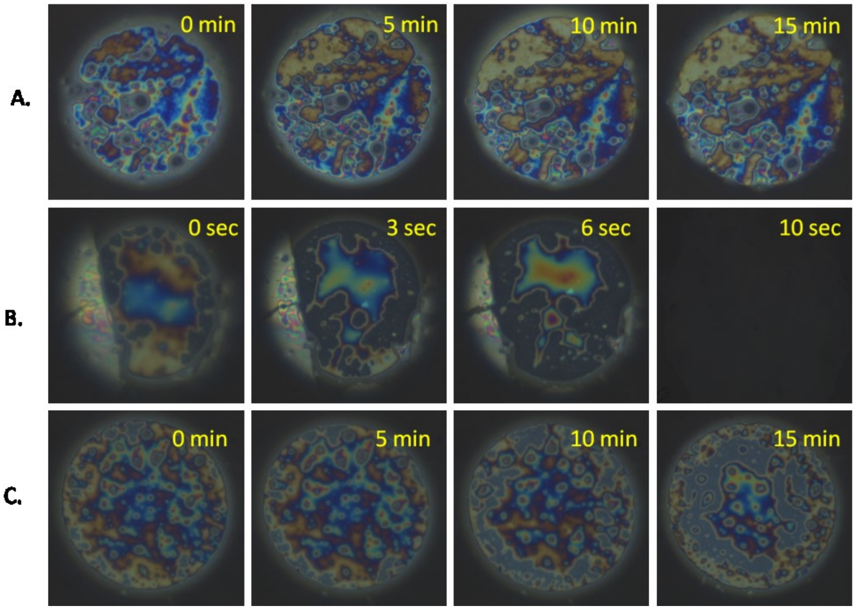

Figure 8.5 Evolution of thin liquid films formed by 10 g/L asphaltene in heptol. (A) Without demulsifier. (B) With 23ppm of EC 300 doped into film (C) With 60ppm of EC 300 doped into film.

Figure 8.6 shows the life time of the thin liquid films after adding different amount of demulsifier EC 300. The working dosage of EC 300 was found to be lower than 40 ppm, regardless of the concentration of asphaltenes in heptol solutions investigated. Any higher demulsifier concentration would cause over-dose, suggesting that demulsifier EC 300 can on its own stabilize the emulsion. To help confirm such effect of self-stabilization, 200 ppm of EC 300 in heptol solution was used instead of asphaltene solution with the TLF apparatus and a stable (up to 10 min) and homogenous film was observed (see the inset image of Figure 8.6).

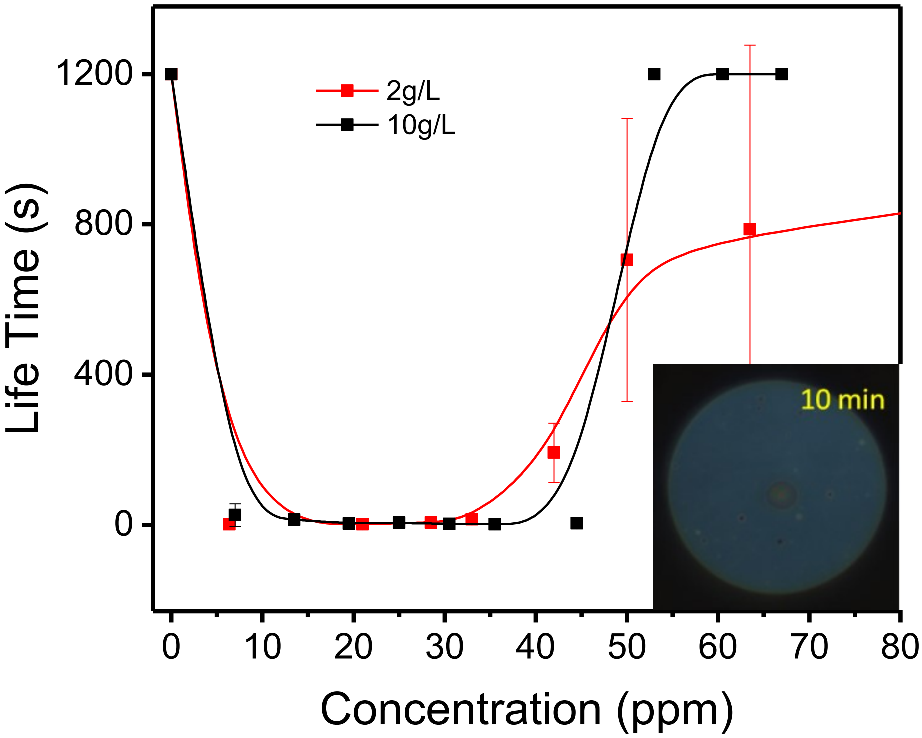

Figure 8.6 Thin liquid film life time of 2 g/L and 10 g/L asphlatene in heptol solution doped with EC300 at different concentrations. (Insert image shows the thin liquid film stabilized by 200 ppm EC300 in heptol)

8.4 CONCLUSIONS

With the newly designed TLF cell, the process of disrupting thin liquid film formed by asphaltene-in-heptol solution of different concentrations by demulsifier EC300 was studied. At lower asphaltene concentration (2 g/L), the asphaltene network formation was found to be destructed by demulsifiers with the thickness and draining behavior of film being changed significantly. At higher asphaltene concentration (10 g/L), the morphology of the film showed that EC300 demulsifiers penetrate into the interface of already-formed asphaltene films, making the asphaltene film to eventually peel off from the interface into small debris. Such competitive adsorption is confirmed by a rapid reduction in the measured interfacial tension of the asphaltene-in-heptol solution-water interface upon the addition of EC 300 into the oil phase to the interfacial tension value measured for EC 300-in-heptol solution-water interface of the same EC 300 concentration without asphaltenes. The analysis on viscoelastic property of the interface revealed the change of an elastic modulus dominated asphaltene film to a viscous modulus dominant interface within a half an hour after EC 300 addition, confirming the disruption of the asphaltene network already formed at the oil-water interface.

The modification of the thin film cell was demonstrated to provide an opportunity for studying the role of emulsifier molecular structure in breaking interfacial film interfaces already formed, which resembles the real demulsification process. The new cell can be used as a valuable tool to rapidly screen industry petroleum demulsifiers or formulations for complex emulsions of highly variable compositions and properties. It also allows for investigating the disruption of asphaltenes interfacial layers by chemical demulsifiers and their effects on film thickness, morphology and stability, providing a better understanding of demulsification mechanisms of petroleum emulsions.

REFERENCES

1. Masliyah, J., Zhou, Z., Xu, Z. (2004). Understanding water-based bitumen extraction from Athabasca oil sands, *The Canadian Journal of Chemical Engineering*, 82(4), 628-654

2. Kokal, S. L. (2005). Crude oil emulsions: A state-of-the-art review. *SPE Production & Facilities*, *20*(01), 5-13.

3. Yeung, A., Dabros, T., Masliyah, J., & Czarnecki, J. (2000). Micropipette: a new technique in emulsion research. *Colloids and Surfaces A: Physicochemical and Engineering Aspects*, *174*(1), 169-181.

4. Pensini, E., Harbottle, D., Yang, F., Tchoukov, P., Li, Z., Kailey, I., ... & Xu, Z. (2014). Demulsification Mechanism of Asphaltene-Stabilized Water-in-Oil Emulsions by a Polymeric Ethylene Oxide–Propylene Oxide Demulsifier. *Energy & Fuels*, *28*(11), 6760-6771.

5. Hou, J., Feng, X., Masliyah, J., & Xu, Z. (2012). Understanding interfacial behavior of ethylcellulose at the water–diluted bitumen interface. *Energy & Fuels*, *26*(3), 1740-1745.

6. Ese, M. H., Sjöblom, J., Djuve, J., & Pugh, R. (2000). An atomic force microscopy study of asphaltenes on mica surfaces. Influence of added resins and demulsifiers. *Colloid and Polymer Science*, *278*(6), 532-538.

7. Ramakers, R. R. M., Pöpel, H. J., & Koops, W. (1982). A new method for handling oil spill materials. *Oil and Petrochemical Pollution*, *1*(2), 129-137.

8. Stewart, A. C., EI-Hamouz, A. M., & Davies, G. A. (1996). Effect of chemical additives on the stability of kerosene-water dispersions. *Journal of Dispersion Science Andtechnology*, *17*(6), 675-696.

9. Dimitrov, A. N., Yordanov, D. I., & Petkov, P. S. (2012). Study on the effect of demulsifers on crude oil and petroleum products. *International Journal of Environmental Research*, *6*(2), 435-442.

10. Fan, Y., Simon, S., & Sjöblom, J. (2010). Interfacial shear rheology of asphaltenes at oil–water interface and its relation to emulsion stability: influence of concentration, solvent aromaticity and nonionic surfactant. *Colloids and Surfaces A: Physicochemical and Engineering Aspects*, *366*(1), 120-128.

11. Kim, Y. H., & Wasan, D. T. (1996). Effect of demulsifier partitioning on the destabilization of water-in-oil emulsions. *Industrial & Engineering Chemistry Research*, *35*(4), 1141-1149.

12. Feng, X., Xu, Z., & Masliyah, J. (2008). Biodegradable polymer for demulsification of water-in-bitumen emulsions. *Energy & Fuels*, *23*(1), 451-456.

13. Tchoukov, P., Yang, F., Xu, Z., Dabros, T., Czarnecki, J., & Sjöblom, J. (2014). Role of asphaltenes in stabilizing thin liquid emulsion films. *Langmuir*, *30*(11), 3024-3033.

14. Bi, J., Yang, F., Harbottle, D., Pensini, E., Tchoukov, P., Simon, S., ... & Xu, Z. (2015). Interfacial Layer Properties of a Polyaromatic Compound and its Role in Stabilizing Water-in-Oil Emulsions. *Langmuir*, *31*(38), 10382-10391.

15. Yang, F., Tchoukov, P., Pensini, E., Dabros, T., Czarnecki, J., Masliyah, J., & Xu, Z. (2014). Asphaltene subfractions responsible for stabilizing water-in-crude oil emulsions. Part 1: interfacial behaviors. *Energy & Fuels*, *28*(11), 6897-6904.

16. Yang, F., Tchoukov, P., Dettman, H., Teklebrhan, R. B., Liu, L., Dabros, T., Czarnecki, J., Masliyah, J. & Xu, Z. (2015). Asphaltene Subfractions Responsible for Stabilizing Water-in-Crude Oil Emulsions. Part 2: Molecular Representations and Molecular Dynamics Simulations. *Energy & Fuels*, 29 (8), 4783–4794

17. Platikanov, D., Exerowa, D. (2005) Thin liquid films. In Fundamentals of Interface and Colloid Science Soft Colloids (pp 1-91). Academic Press.

18. Sheludko, A. (1967). Thin liquid films. *Advances in Colloid and Interface Science*, *1*(4), 391-464.

19. Khristov, K., Taylor, S. D., Czarnecki, J., & Masliyah, J. (2000). Thin liquid film technique—application to water–oil–water bitumen emulsion films. *Colloids and Surfaces A: Physicochemical and Engineering Aspects*, *174*(1), 183-196.

20. Tchoukov, P., Czarnecki, J., & Dabros, T. (2010). Study of water-in-oil thin liquid films: Implications for the stability of petroleum emulsions. *Colloids and Surfaces A: Physicochemical and Engineering Aspects*, *372*(1), 15-21.

21. Fan, Y., Simon, S., & Sjöblom, J. (2010). Interfacial shear rheology of asphaltenes at oil–water interface and its relation to emulsion stability: influence of concentration, solvent aromaticity and nonionic surfactant. *Colloids and Surfaces A: Physicochemical and Engineering Aspects*, *366*(1), 120-128.

---

22. Harbottle, D., Chen, Q., Moorthy, K., Wang, L., Xu, S., Liu, Q., ... & Xu, Z. (2014). Problematic stabilizing films in petroleum emulsions: Shear rheological response of viscoelastic asphaltene films and the effect on drop coalescence. *Langmuir*, *30*(23), 6730-6738.

23. Feng, X., Wang, S., Hou, J., Wang, L., Cepuch, C., Masliyah, J., & Xu, Z. (2011). Effect of hydroxyl content and molecular weight of biodegradable ethylcellulose on demulsification of water-in-diluted bitumen emulsions. *Industrial & Engineering Chemistry Research*, *50*(10), 6347-6354.

CHAPTER 9 CONCLUSIONS AND RECOMMENDATIONS FOR FUTURE WORK

The overall conclusions with major contributions of the thesis and recommendation for future work are included as the following.

9.1 CONCLUSIONS AND MAJOR CONTRIBUTIONS

Stabilization of water in oil emulsion is a critical phenomenon to study in non-conventional petroleum production, as the dryness of the final bitumen product would influence the robustness of the subsequent refining process. A typical emulsion droplet coalescence process consists of two essential steps: first, the liquid film between two emulsion droplets drains under the capillary pressure until the thickness reaches a critical thickness, and second the film ruptures due to the localized instability to induce the coalescence of the droplets. This thesis studied the complex relationship between different bitumen components present in the system and their effect on emulsion/interfacial phenomena that are crucial to emulsion stabilization/destabilization. The major contributions and conclusions of the thesis are listed as below:

1. ***<u>The thesis probed the stabilization mechanisms of asphaltenes - the major stabilizer in bitumen:</u>***

It was found that asphaltenes stabilize thin liquid films at much lower concentrations, forming thicker films compared to their counterpart in bitumen (maltenes). The film formed by asphaltenes would age with time, leading to an increase in film thickness and inhomogeneity. Such inhomogeneity is likely caused by sub-micron size asphaltene aggregates. The drainage of such asphaltene films were found to be much slower than the drainage rate described by the Stephen-Reynolds-Young-Laplace equation applicable to typical Newtonian liquids between two interfaces. The drainage characteristics of asphaltenes in toluene thin liquid films sandwiched between two water droplets were found to be suitably described as a non-Newtonian Bingham plastic liquid with a yield stress. Such a yield stress is proposed as the major reason that drainage of the film stops at a finite thickness, which stabilizes the emulsion.

2. ***The thesis proposed that all the stabilizing feature of asphaltenes can be related to a small portion of asphaltenes and suggested that not all asphaltenes are good emulsion stabilizers.***

Using a washing procedure to remove a certain percentage of asphaltenes (2% in our case), it was found that the rest of asphaltenes are of a distinctively different interfacial properties as compared with the portion that was removed. The portion removed by the washing procedure (IAAs) was found to be much more interfacially active and the thin liquid films formed by their remaining counterpart (RAs) behave like maltene films with drastically decreased film stability and increased homogeneity in film morphology. The Langmuir compression test revealed that IAAs can form much more rigid interfaces in comparison with RAs and the adsorption of IAAs at the oil-water interface is much less reversible than RAs.

3. ***The thesis compared the differences in chemistry between IAAs and RAs and revealed the structural feature of IAAs that can explain their unique interfacial behaviors***

Elemental analysis revealed that IAAs contain more than three times of oxygen content as compared with its counterpart-RAs. Most of the oxygen atoms were found to be associated with sulfoxide groups as suggested by IR analysis. IAAs were also found to be the heavier portion of asphaltene pool with a significant percentage of them having molecular weight higher than 1000

Da. while the majority of RAs are lighter than 1000 Da. By integrating all the structural data obtained from a suite of complementary analytical techniques, the typical structures of IAAs and RAs were proposed. Molecular dynamics simulation revealed that the proposed IAA structure has a stronger tendency to self-associate through the hydrogen bonds involving sulfoxide groups, while the associations between RAs are mainly through stacking of aromatic cores. This finding implies that the widely accepted pi-pi stacking mechanism of asphaltene molecules might not be the major driving-force for emulsion stabilization, though such an interaction is common between asphaltene molecules.

4. ***The thesis probed the demulsification mechanism by an EO-PO demulsifier on water-in-asphaltene solution emulsions.***

The performance of EO-PO demulsifiers on the removal of emulsified water droplets from a diluted asphaltene-in-toluene solution was analyzed. The properties of interfacial asphaltene films were probed through a number of techniques, including surface tension measurement, shear rheology measurement, interfacial pressure-area isotherms, chemical composition analysis, and nano/micro morphology characterization. The demulsification efficiency was found to be related to the film softening by demulsifiers penetrating into the oil/water interface formed by asphaltenes. Such softening effect is resulted from the higher interfacial activity of demulsifiers and their intrinsic nature in forming interfaces of lower elastic moduli. The overdosing effect of the emulsifier was found to be attributed to the steric repulsion between the thicker films formed when higher dose of demulsifiers was used.

5. ***The thesis proposed a new Scheludko-Exerowa cell design to study demulsification using a Thin Liquid Film apparatus***

The modification of the thin film cell was demonstrated to provide an opportunity for studying the role of emulsifier molecular structure in breaking interfacial film interfaces already formed, which resembles the real demulsification process. The new cell can be used as a valuable tool to rapidly screen industry petroleum demulsifiers or formulations for complex emulsions of highly variable compositions and properties. It also allows for investigating the disruption of asphaltenes interfacial layers by chemical demulsifiers and their effects on film thickness, morphology and stability, providing a better understanding of demulsification mechanisms of petroleum emulsions.

9.2 FUTURE WORK

- In the oil sands froth treatment process, naphtha is commonly used to dilute the froth in order to reduce its viscosity. Different from toluene which is the major solvent used in the thesis, naphtha is a mixture containing both aromatic and paraffinic parts. It is essential to use a mixture of toluene and heptane to mimic the property of naphtha or to use naphtha itself in the future work. Also, from experiments using model asphaltene compounds (C5Pe), it was found that the aggregation propensity of molecules in the solvent was much higher when the solvents (toluene) is saturated with water. This leads to speculations that water might serve as bridging molecules between asphaltene molecules. It would be worthy investigation on how these different fractions of asphaltenes aggregate when different solvents and different water saturation levels are used. For example, dry toluene and water saturated toluene can be mixed in different ratios to study how the amount of water in the solvent affects aggregation of different asphaltene fractions.

- The content of IAAs in bitumen and the property of IAAs could be very different depending on the source of the oil sand ores or the extraction method. It will be worth future endeavor to investigate how these properties change with different ore sources. It will also be interesting to investigate how the content, interfacial property and chemistry fingerprints of IAAs could be controlled by aging the oil sand ore. It is supposed that the amount of IAAs shall be related to the oxidation history of the oil sand ores. Artificial oxidation methods such as oven oxidation or UV illumination on RAs can be used to investigate this relationship.

- Water chemistry such as ionic strength and pH is expected to influence the penetration of asphaltene molecules into the aqueous phase as well as their orientation on the interface. It is very likely that such penetration extent and orientation of molecules would influence the packing of molecules on the interface and eventually the strength of the interface. Besides, the first layer orientation and population density of asphaltenes on the interface is also expected to be related the growth of the asphaltene layer with time (aging). For example, a more vertical orientation is likely to promote pi-pi stacking between polyaromatic cores, but on the other hand, would expose the long chains into the oil phase, preventing the deposition of the second layer in order for the whole interfacial layer to grow in thickness. Thus it would be an interesting topic to study how the association pattern between molecules would change as a function of water chemistry and molecular structures (fractions of asphaltenes). The study of response of association pattern to different water chemistry using different fractions of asphaltenes with better defined structural features can help us develop a more detailed emulsification model for asphaltenes.
- In this thesis, the adsorption behavior on the interface and association tendency of RA and IAA have been proven to be very different. However, the interplay mechanism between RA and IAA on the interface remains to be established as bitumen is a mixture of the two.

RA has less active sites and would likely serve as “eliminator” to asphaltene aggregation while IAA would likely serve as “propagator” for their stronger association tendency afforded by more active sites per molecule. The interfacial behavior of the whole asphaltene pool is expected to be very different with varying ratios of RA and IAA. Model bitumen can be made by mixing RA and IAA at desired ratios or by treating the bitumen, for example, washing with solvents (removal of certain fractions) or oxidizing (formation of certain fractions). Understanding the interfacial behavior of asphaltenes containing known ratios of RA/IAA fractions would give us a fuller picture of emulsification phenomena by asphaltenes.

9.3 LIMITATION AND FUTURE MODIFICATION

The cell modification introduced in Chapter 8 added a dosing mechanism into TLF cell through which demulsifiers can be doped into the already built thin liquid film to study the demulsification performance of demulsifiers with different formulations. However, there is another limitation of the current design of TLF instrument. The TLF instrument can only recreate the thin liquid film phenomena between two water droplets in oil when they are slowly brought in contact with each other and stayed in their positions when the film drains. These phenonena do not always represent the circumstance when the system is in a kinetic state where droplets travelling at different speeds collide or shear with each other. Bearing such consideration in mind, it is our on-going effort to design a more versatile cell design that can study the film drainage behavior in a kinetic system.

BIBLIOGRAPHY

- Masliyah, J., Zhou, Z. J., Xu, Z., Czarnecki, J., & Hamza, H. (2004). Understanding water ‐ based bitumen extraction from Athabasca oil sands. *The Canadian Journal of Chemical Engineering*, *82*(4), 628-654.

- Masliyah.J. Fundamentals of oil sands extraction. <u>Course materials at University of Alberta</u>

- Sanford, E. C., & Seyer, F. A. (1979). Processibility of Athabasca tar sand using a Batch Extraction Unit-role of NaOH. *CIM bulletin*, *72*(803), 164-169.

- Romanova, U. G., Yarranton, H. W., Schramm, L. L., & Shelfantook, W. E. (2004). Investigation of oil sands froth treatment. *The Canadian Journal of Chemical Engineering*, *82*(4), 710-721.

- Long, Y., Dabros, T., & Hamza, H. (2002). Stability and settling characteristics of solvent-diluted bitumen emulsions. *Fuel*, *81*(15), 1945-1952.

- Alvarez, G., Poteau, S., Argillier, J. F., Langevin, D., & Salager, J. L. (2008). Heavy oil− water interfacial properties and emulsion stability: Influence of dilution. *Energy & Fuels*, *23*(1), 294-299.

- Fingas, M., & Fieldhouse, B. (2009). Studies on crude oil and petroleum product emulsions: Water resolution and rheology. *Colloids and Surfaces A: Physicochemical and Engineering Aspects*, *333*(1), 67-81.

- Quintero, C. G., Noïk, C., Dalmazzone, C., & Grossiord, J. L. (2009). Formation kinetics and viscoelastic properties of water/crude oil interfacial films. *Oil & Gas Science and Technology-Revue de l'IFP*, *64*(5), 607-616.

- Zhang, L. Y., Lawrence, S., Xu, Z., & Masliyah, J. H. (2003). Studies of Athabasca asphaltene Langmuir films at air–water interface. *Journal of Colloid and Interface Science*, *264*(1), 128-140.

- Zhang, L. Y., Xu, Z., & Masliyah, J. H. (2003). Langmuir and Langmuir-Blodgett films of mixed asphaltene and a demulsifier. *Langmuir*, *19*(23), 9730-9741.
- Alvarez, G., Poteau, S., Argillier, J. F., Langevin, D., & Salager, J. L. (2008). Heavy oil− water interfacial properties and emulsion stability: Influence of dilution. *Energy & Fuels*, *23*(1), 294-299.

- Yeung, A., Dabros, T., Masliyah, J., & Czarnecki, J. (2000). Micropipette: a new technique in emulsion research. *Colloids and Surfaces A: Physicochemical and Engineering Aspects*, *174*(1), 169-181.

- Bartell, F. E., & Niederhauser, D. O. (1949). Fundamental Research on Occurrence and Recovery of Petroleum 1946-47. *American Petroleum Institute, New York*, 57-80.

- Kimbler, O. K., Reed, R. L., & Silberberg, I. H. (1966). Physical characteristics of natural films formed at crude oil-water interfaces. *Society of Petroleum Engineers Journal*, *6*(02), 153-165.

- Wu, X. (2003). Investigating the stability mechanism of water-in-diluted bitumen emulsions through isolation and characterization of the stabilizing materials at the interface. *Energy & Fuels*, *17*(1), 179-190.

- Taylor, S.D. (2002) Colloidal Interactions in Water in Diluted Bitumen Emulsions, Thesis for PhD at University of Alberta

- Ortiz, D. P., Baydak, E. N., & Yarranton, H. W. (2010). Effect of surfactants on interfacial films and stability of water-in-oil emulsions stabilized by asphaltenes. *Journal of Colloid and Interface Science*, *351*(2), 542-555.

- Yarranton, H. W., Hussein, H., & Masliyah, J. H. (2000). Water-in-hydrocarbon emulsions stabilized by asphaltenes at low concentrations. *Journal of Colloid and Interface Science*, *228*(1), 52-63.

- Xu, Y., Dabros, T., Hamza, H., & Shefantook, W. (1999). Destabilization of water in bitumen emulsion by washing with water. *Petroleum Science and Technology*, *17*(9-10), 1051-1070.

- Sedghi, M., & Goual, L. (2009). Role of Resins on Asphaltene Stability. *Energy & Fuels*, *24*(4), 2275-2280.

- Hannisdal, A., Ese, M. H., Hemmingsen, P. V., & Sjöblom, J. (2006). Particle-stabilized emulsions: effect of heavy crude oil components pre-adsorbed onto stabilizing solids. *Colloids and Surfaces A: Physicochemical and Engineering Aspects*, *276*(1), 45-58.

- Gao, S., Moran, K., Xu, Z., & Masliyah, J. (2010). Role of naphthenic acids in stabilizing water-in-diluted model oil emulsions. *The Journal of Physical Chemistry B*, *114*(23), 7710-7718.

- Sztukowski, D. M., & Yarranton, H. W. (2004). Characterization and interfacial behavior of oil sands solids implicated in emulsion stability. *Journal of Dispersion Science and Technology*, *25*(3), 299-310.

- Wu, X. A. (2008). Selective Creaming: A novel technique to isolate interfacial organics and mineral solids from water-in-oil emulsions. *Energy & Fuels*, *22*(4), 2346-2352.

- Yan, Y., & Masliyah, J. H. (1993). Solids-stabilized oil-in-water emulsions: scavenging of emulsion droplets by fresh oil addition. *Colloids and Surfaces A: Physicochemical and Engineering Aspects*, *75*, 123-132.

- McLean, J. D., & Kilpatrick, P. K. (1997). Effects of asphaltene aggregation in model heptane–toluene mixtures on stability of water-in-oil emulsions. *Journal of Colloid and Interface Science*, *196*(1), 23-34.

- Yang, X., Verruto, V. J., & Kilpatrick, P. K. (2007). Dynamic asphaltene-resin exchange at the oil/water interface: Time-dependent W/O emulsion stability for asphaltene/resin model oils. *Energy & Fuels*, *21*(3), 1343-1349.

- Czarnecki, J., & Moran, K. (2005). On the stabilization mechanism of water-in-oil emulsions in petroleum systems. *Energy & Fuels*, *19*(5), 2074-2079.

- Nordgård, E. L., Landsem, E., & Sjöblom, J. (2008). Langmuir films of asphaltene model compounds and their fluorescent properties. *Langmuir*, *24*(16), 8742-8751.

- Nordgård, E. L., Sørland, G., & Sjöblom, J. (2009). Behavior of asphaltene model compounds at W/O interfaces. *Langmuir*, *26*(4), 2352-2360.

- Nordgård, E. L., Magnusson, H., Hanneseth, A. M. D., & Sjöblom, J. (2009). Model compounds for C 80 isoprenoid tetraacids: Part II. Interfacial reactions, physicochemical properties and comparison with indigenous tetraacids. *Colloids and Surfaces A: Physicochemical and Engineering Aspects*, *340*(1), 99-108.

- Khristov, K., & Czarnecki, J. (2010). Emulsion films stabilized by natural and polymeric surfactants. *Current Opinion in Colloid & Interface Science*, *15*(5), 324-329.

- Khristov, K., Taylor, S. D., Czarnecki, J., & Masliyah, J. (2000). Thin liquid film technique—application to water–oil–water bitumen emulsion films. *Colloids and Surfaces A: Physicochemical and Engineering Aspects*, *174*(1), 183-196.

- Taylor, S.D. (2002). Colloidal Interactions in Water in Diluted Bitumen Emulsions", Thesis for PhD at University of Alberta

- Sheludko, A. (1967). Thin liquid films, *Advances in Colloid and Interface Science*, 1, 391-464

- Platikanov, D., Exerowa, D. (2005) Ch. 6. Thin liquid films, In: Fundamental of Interface and Colloid Science, Ed. J. Lyklem, Academic Press, pp. 1-91

- Panchev, N., Khristov, K., Czarnecki, J., Exerowa, D., Bhattacharjee, S., & Masliyah, J. (2008). A new method for water-in-oil emulsion film studies. *Colloids and Surfaces A: Physicochemical and Engineering Aspects*, *315*(1), 74-78.

- Scheludko, A., & Platikanov, D. (1961). Utersuchung dünner Flüssinger Schichten auf Quecksiber. *Kolloid-Zeitschrift and Zeitschrift fur Polymere*, *175*(2), 150-158.

- Tchoukov, P., Czarnecki, J., & Dabros, T. (2010). Study of water-in-oil thin liquid films: Implications for the stability of petroleum emulsions. *Colloids and Surfaces A: Physicochemical and Engineering Aspects*, *372*(1), 15-21.

- Long, Y., Dabros, T., & Hamza, H. (2007). Selective solvent deasphalting for heavy oil emulsion treatment. In *Asphaltenes, Heavy Oils, and Petroleomics* (pp. 511-547). Springer New York.

- Wu, X. (2003). Investigating the stability mechanism of water-in-diluted bitumen emulsions through isolation and characterization of the stabilizing materials at the interface. *Energy & Fuels*, *17*(1), 179-190.

- Taylor, S. D., Czarnecki, J., & Masliyah, J. (2002). Disjoining pressure isotherms of water-in-bitumen emulsion films. *Journal of Colloid and Interface Science*, *252*(1), 149-160.

- Masliyah, J., Czarnecki, J., & Xu, Z. (2010). Handbook on Theory and Practice of Bitumen Recovery from Athabasca Oil Sands. *Vol. I. Theoretical basis*.

- Kilpatrick, P. K., & Spiecker, P. M. (2001). Asphaltene emulsions. *Encyclopedic Handbook of Emulsion Technology*, *3*, 707-730.
- Czarnecki, J. (2001) Water-in-Oil Emulsions in Recovery of Hydrocarbons from Oil Sands. In *Encyclopedic Handbook of Emulsion Technology;* CRC Press, 497-514.

- Sjöblom, J., Hemmingsen, P. V., & Kallevik, H. (2007). The role of asphaltenes in stabilizing water-in-crude oil emulsions. In *Asphaltenes, Heavy Oils, and Petroleomics* (pp. 549-587). Springer New York.

- Yan, Z., Elliott, J. A., & Masliyah, J. H. (1999). Roles of various bitumen components in the stability of water-in-diluted-bitumen emulsions. *Journal of Colloid and Interface Science*, *220*(2), 329-337.

- Sjöblom, J., Aske, N., Auflem, I. H., Brandal, Ø., Havre, T. E., Sæther, Ø., ... & Kallevik, H. (2003). Our current understanding of water-in-crude oil emulsions.: Recent characterization techniques and high pressure performance. *Advances in Colloid and Interface Science*, *100*, 399-473.

- Spiecker, P. M., Gawrys, K. L., & Kilpatrick, P. K. (2003). Aggregation and solubility behavior of asphaltenes and their subfractions. *Journal of colloid and interface science*, *267*(1), 178-193.

- Czarnecki, J., Tchoukov, P., & Dabros, T. (2012). Possible role of asphaltenes in the stabilization of water-in-crude oil emulsions. *Energy & Fuels*, *26*(9), 5782-5786.

- Dabros, T., Yeung, A., Masliyah, J., & Czarnecki, J. (1999). Emulsification through area contraction. *Journal of Colloid and Interface Science*, *210*(1), 222-224.

- Spiecker, P. M., & Kilpatrick, P. K. (2004). Interfacial rheology of petroleum asphaltenes at the oil-water interface. *Langmuir*, *20*(10), 4022-4032.

- Wu, X. (2003). Investigating the stability mechanism of water-in-diluted bitumen emulsions through isolation and characterization of the stabilizing materials at the interface. *Energy & Fuels*, *17*(1), 179-190.

- Long, Y., Dabros, T., & Hamza, H. (2002). Stability and settling characteristics of solvent-diluted bitumen emulsions. *Fuel*, *81*(15), 1945-1952.

- Xu, Y., Dabros, T., Hamza, H., & Shefantook, W. (1999). Destabilization of water in bitumen emulsion by washing with water. *Petroleum Science and Technology*, *17*(9-10), 1051-1070.
- Mitchell, D. L., & Speight, J. G. (1973). The solubility of asphaltenes in hydrocarbon solvents. *Fuel*, *52*(2), 149-152.

- Mullins, O. C. (2011). The asphaltenes. *Annual Review of Analytical Chemistry*, *4*, 393-418.

- Pfeiffer, J. P., & Saal, R. N. J. (1940). Asphaltic bitumen as colloid system. *The Journal of Physical Chemistry*, *44*(2), 139-149.

- Buckley, J.; Wang, J.; Creek, J. (2007) Solubility of the Least-Soluble Asphaltenes. In *Asphaltenes, Heavy Oils, and Petroleomics,* Mullins, O., Sheu, E., Hammami, A., Marshall, A., Eds.;Springer: New York, 401-437.

- Friberg, S. Micellization. (2007) In *Asphaltenes, Heavy Oils, and Petroleomics*, Mullins, O., Sheu, E., Hammami, A., Marshall, A., Eds.; Springler: New York, 189-203.

- Dickie, J. P., & Yen, T. F. (1967). Macrostructures of the asphaltic fractions by various instrumental methods. *Analytical Chemistry*, *39*(14), 1847-1852.

- Buenrostro-Gonzalez, E., Groenzin, H., Lira-Galeana, C., & Mullins, O. C. (2001). The overriding chemical principles that define asphaltenes. *Energy & Fuels*, *15*(4), 972-978.

- Mostowfi, F.; Indo, K.; Mullins, O. C.; McFarlane, R. (2009) Asphaltene nanoaggregates studied by centrifugation. *Energy & Fuels*, *23,* 1194-1200.

- Mullins, O. C. (2010). The Modified Yen Model. *Energy & Fuels*, *24*(4), 2179-2207.

- Agrawala, M., & Yarranton, H. W. (2001). An asphaltene association model analogous to linear polymerization. *Industrial & Engineering Chemistry Research*, *40*(21), 4664-4672.

- Gray, M. R., Tykwinski, R. R., Stryker, J. M., & Tan, X. (2011). Supramolecular assembly model for aggregation of petroleum asphaltenes. *Energy & Fuels*, *25*(7), 3125-3134.

- Czarnecki, J., & Moran, K. (2005). On the stabilization mechanism of water-in-oil emulsions in petroleum systems. *Energy & Fuels*, *19*(5), 2074-2079.

- Moran, K., & Czarnecki, J. (2007). Competitive adsorption of sodium naphthenates and naturally occurring species at water-in-crude oil emulsion droplet surfaces. *Colloids and Surfaces A: Physicochemical and Engineering Aspects*, *292*(2), 87-98.
- Freer, E. M., & Radke, C. J. (2004). Relaxation of asphaltenes at the toluene/water interface: Diffusion exchange and surface rearrangement. *Journal of Adhesion*, *80*(6), 481-496.

- Zhang, L. Y., Breen, P., Xu, Z., & Masliyah, J. H. (2007). Asphaltene films at a toluene/water interface. *Energy & Fuels*, *21*(1), 274-285.

- Zhang, L. Y., Lopetinsky, R., Xu, Z., & Masliyah, J. H. (2005). Asphaltene monolayers at a toluene/water interface. *Energy & Fuels*, *19*(4), 1330-1336.

- Gao, S., Moran, K., Xu, Z., & Masliyah, J. (2010). Role of naphthenic acids in stabilizing water-in-diluted model oil emulsions. *The Journal of Physical Chemistry B*, *114*(23), 7710-7718.

- Fan, Y., Simon, S., & Sjöblom, J. (2010). Interfacial shear rheology of asphaltenes at oil–water interface and its relation to emulsion stability: influence of concentration, solvent aromaticity and nonionic surfactant. *Colloids and Surfaces A: Physicochemical and Engineering Aspects*, *366*(1), 120-128.

- Yeung, A., Dabros, T., Masliyah, J., & Czarnecki, J. (2000). Micropipette: a new technique in emulsion research. *Colloids and Surfaces A: Physicochemical and Engineering Aspects*, *174*(1), 169-181.

- Wu, X., Laroche, I., Masliyah, J., Czarnecki, J., & Dabros, T. (2000). Applications of colloidal force measurements using a microcollider apparatus to oil sand studies. *Colloids and Surfaces A: Physicochemical and Engineering Aspects*, *174*(1), 133-146.

- Gao, S., Moran, K., Xu, Z., & Masliyah, J. (2009). Role of bitumen components in stabilizing water-in-diluted oil emulsions. *Energy & Fuels*, *23*(5), 2606-2612.

- Wang, S., Liu, J., Zhang, L., Xu, Z., & Masliyah, J. (2008). Colloidal interactions between asphaltene surfaces in toluene. *Energy & Fuels*, *23*(2), 862-869.

- Wang, S.; Liu, J.; Zhang, L.; Masliyah, J.; Xu, Z. Interaction forces between asphaltene surfaces in organic solvents. *Langmuir* **2010,** *26,* 183-190.

- Natarajan, A., Xie, J., Wang, S., Liu, Q., Masliyah, J., Zeng, H., & Xu, Z. (2011). Understanding molecular interactions of asphaltenes in organic solvents using a surface force apparatus. *The Journal of Physical Chemistry C*, *115*(32), 16043-16051.

- Sheludko, A. (1967). Thin liquid films. *Advances in Colloid and Interface Science*, *1*(4), 391-464.

- Platikanov, D.; Exerowa, D. (2005) Thin liquid films. In *Fundamentals of Interface and Colloid ScienceSoft Colloids*; Volume 5; Lyklema, J., Ed.; Academic Press, 1-91.

- Exerowa, D.; Kruglyakov, P. M. (1998) *Foam and Foam Films;* Elsevier: New York.
- Khristov, K., Taylor, S. D., Czarnecki, J., & Masliyah, J. (2000). Thin liquid film technique—application to water–oil–water bitumen emulsion films. *Colloids and Surfaces A: Physicochemical and Engineering Aspects*, *174*(1), 183-196.
- Taylor, S. D., Czarnecki, J., & Masliyah, J. (2002). Disjoining pressure isotherms of water-in-bitumen emulsion films. *Journal of Colloid and Interface Science*, *252*(1), 149-160.
- Tchoukov, P., Czarnecki, J., & Dabros, T. (2010). Study of water-in-oil thin liquid films: Implications for the stability of petroleum emulsions. *Colloids and Surfaces A: Physicochemical and Engineering Aspects*, *372*(1), 15-21.
- Scheludko, A.; Platikanov, D. (1961) Utersuchung dünner Flüssinger Schichten auf Quecksiber. *Kolloid Z.,175,* 150-158.
- Israelachvili, J. N. (1992) *Intermolecular and Surface Forces;* Academic Press: London.
- Manev, E., Tsekov, R., & Radoev, B. (1997). Effect of thickness non-homogeneity on the kinetic behaviour of microscopic foam film. *Journal of Dispersion Science and Technology*, *18*(6-7), 769-788.
- Radoev, B. P., Dimitrov, D. S., & Ivanov, I. B. (1974). Hydrodynamics of thin liquid films effect of the surfactant on the rate of thinning. *Colloid and Polymer Science*, *252*(1), 50-55.
- Ruckenstein, E., & Sharma, A. (1987). A new mechanism of film thinning: enhancement of Reynolds' velocity by surface waves. *Journal of Colloid and Interface Science*, *119*(1), 1-13.
- Pal, R., & Vargas, F. (2014). On the interpretation of viscosity data of suspensions of asphaltene nano-aggregates. *The Canadian Journal of Chemical Engineering*, *92*(3), 573-577.
- Nenningsland, A. L., Gao, B., Simon, S., & Sjöblom, J. (2011). Comparative study of stabilizing agents for water-in-oil emulsions. *Energy & Fuels*, *25*(12), 5746-5754.
- Exerowa, D.; Ivanov, I.; Scheludko, A. (1964) In *Issledovaniya v oblasti poverkhnostnykh sil;* Nauka: Moscow, 158.

- Czarnecki, J., Tchoukov, P., Dabros, T., & Xu, Z. (2013). Role of asphaltenes in stabilisation of water in crude oil emulsions. *The Canadian Journal of Chemical Engineering*, *91*(8), 1365-1371.

- Hartland, S., & Jeelani, A. K. (1987). Drainage in thin planar non-newtonian fluid films. *The Canadian Journal of Chemical Engineering*, *65*(3), 382-390.

- Sharma, A. (2003). Many paths to dewetting of thin films: anatomy and physiology of surface instability. *The European Physical Journal E*, *12*(3), 397-408.

- Tambe, D. E., & Sharma, M. M. (1991). Hydrodynamics of thin liquid films bounded by viscoelastic interfaces. *Journal of Colloid and Interface Science*, *147*(1), 137-151.

- Gao, S., Moran, K., Xu, Z., & Masliyah, J. (2010). Role of naphthenic acids in stabilizing water-in-diluted model oil emulsions. *The Journal of Physical Chemistry B*, *114*(23), 7710-7718.

- McLean, J. D., & Kilpatrick, P. K. (1997). Effects of asphaltene aggregation in model heptane–toluene mixtures on stability of water-in-oil emulsions. *Journal of Colloid and Interface Science*, *196*(1), 23-34.

- Ortiz, D. P., Baydak, E. N., & Yarranton, H. W. (2010). Effect of surfactants on interfacial films and stability of water-in-oil emulsions stabilized by asphaltenes. *Journal of Colloid and Interface Science*, *351*(2), 542-555.

- Yang, X., Verruto, V. J., & Kilpatrick, P. K. (2007). Dynamic asphaltene-resin exchange at the oil/water interface: Time-dependent W/O emulsion stability for asphaltene/resin model oils. *Energy & Fuels*, *21*(3), 1343-1349.

- Yarranton, H. W., Hussein, H., & Masliyah, J. H. (2000). Water-in-hydrocarbon emulsions stabilized by asphaltenes at low concentrations. *Journal of Colloid and Interface Science*, *228*(1), 52-63.

- Zhang, L. Y., Xu, Z., & Masliyah, J. H. (2003). Langmuir and Langmuir-Blodgett films of mixed asphaltene and a demulsifier. *Langmuir*, *19*(23), 9730-9741.
- Langevin, D., Poteau, S., Hénaut, I., & Argillier, J. F. (2004). Crude oil emulsion properties and their application to heavy oil transportation. *Oil & Gas Science and Technology*, *59*(5), 511-521.

- Hirasaki, G. J., Miller, C. A., Raney, O. G., Poindexter, M. K., Nguyen, D. T., & Hera, J. (2010). Separation of Produced Emulsions from Surfactant Enhanced Oil Recovery Processes. *Energy & Fuels*, *25*(2), 555-561.

- Kiran, S. K., Ng, S., & Acosta, E. J. (2011). Impact of Asphaltenes and Naphthenic Amphiphiles on the Phase Behavior of Solvent− Bitumen− Water Systems. *Energy & Fuels*, *25*(5), 2223-2231.

- Goual, L., Sedghi, M., Zeng, H., Mostowfi, F., McFarlane, R., & Mullins, O. C. (2011). On the formation and properties of asphaltene nanoaggregates and clusters by DC-conductivity and centrifugation. *Fuel*, *90*(7), 2480-2490.

- Hoepfner, M. P., Vilas Bôas Fávero, C., Haji-Akbari, N., & Fogler, H. S. (2013). The fractal aggregation of asphaltenes. *Langmuir*, *29*(28), 8799-8808.

- Yeung, A., Dabros, T., Masliyah, J., & Czarnecki, J. (2000). Micropipette: a new technique in emulsion research. *Colloids and Surfaces A: Physicochemical and Engineering Aspects*,*174*(1), 169-181.

- Spiecker, P. M., Gawrys, K. L., Trail, C. B., & Kilpatrick, P. K. (2003). Effects of petroleum resins on asphaltene aggregation and water-in-oil emulsion formation. *Colloids and Surfaces A: Physicochemical and Engineering Aspects*, *220*(1), 9-27.

- Spiecker, P. M., & Kilpatrick, P. K. (2004). Interfacial rheology of petroleum asphaltenes at the oil-water interface. *Langmuir*, *20*(10), 4022-4032.

- Czarnecki, J., & Moran, K. (2005). On the stabilization mechanism of water-in-oil emulsions in petroleum systems. *Energy & Fuels*, *19*(5), 2074-2079.

- Czarnecki, J. (2008). Stabilization of Water in Crude Oil Emulsions. Part 2. *Energy & Fuels*, *23*(3), 1253-1257.

- Czarnecki, J., Tchoukov, P., Dabros, T., & Xu, Z. (2013). Role of asphaltenes in stabilisation of water in crude oil emulsions. *The Canadian Journal of Chemical Engineering*, *91*(8), 1365-1371.

- Kharrat, A. M., Zacharia, J., Cherian, V. J., & Anyatonwu, A. (2007). Issues with comparing SARA methodologies. *Energy & Fuels*, *21*(6), 3618-3621.

- Xu, Y., Dabros, T., Hamza, H., & Shefantook, W. (1999). Destabilization of water in bitumen emulsion by washing with water. *Petroleum Science and Technology*, *17*(9-10), 1051-1070.

- Wu, X. (2003). Investigating the stability mechanism of water-in-diluted bitumen emulsions through isolation and characterization of the stabilizing materials at the interface. *Energy & Fuels*, *17*(1), 179-190.

- Stanford, L. A., Rodgers, R. P., Marshall, A. G., Czarnecki, J., Wu, X. A., & Taylor, S. (2007). Detailed elemental compositions of emulsion interfacial material versus parent oil for nine geographically distinct light, medium, and heavy crude oils, detected by negative-and positive-ion electrospray ionization Fourier transform ion cyclotron resonance mass spectrometry. *Energy & Fuels*, *21*(2), 973-981.

- Stanford, L. A., Rodgers, R. P., Marshall, A. G., Czarnecki, J., & Wu, X. A. (2007). Compositional characterization of bitumen/water emulsion films by negative-and positive-ion electrospray ionization and field desorption/ionization Fourier transform ion cyclotron resonance mass spectrometry. *Energy & Fuels*, *21*(2), 963-972.

- Spiecker, P. M., Gawrys, K. L., & Kilpatrick, P. K. (2003). Aggregation and solubility behavior of asphaltenes and their subfractions. *Journal of Colloid and Interface Science*, *267*(1), 178-193.

- Platikanov, D.; Exerowa, D. (2005). Thin liquid films. In *Fundamentals of Interface and Colloid Science Soft Colloids*; Volume 5; Lyklema, J., Ed.; Academic Press: pp 1-91.

- Sheludko, A. (1967). Thin liquid films. *Advances in Colloid and Interface Science*, *1*(4), 391-464.

- Khristov, K., Taylor, S. D., Czarnecki, J., & Masliyah, J. (2000). Thin liquid film technique—application to water–oil–water bitumen emulsion films. *Colloids and Surfaces A: Physicochemical and Engineering Aspects*, *174*(1), 183-196.

- Czarnecki, J., Tchoukov, P., & Dabros, T. (2012). Possible role of asphaltenes in the stabilization of water-in-crude oil emulsions. *Energy & Fuels*, *26*(9), 5782-5786.

- Tchoukov, P., Czarnecki, J., & Dabros, T. (2010). Study of water-in-oil thin liquid films: Implications for the stability of petroleum emulsions. *Colloids and Surfaces A: Physicochemical and Engineering Aspects*, *372*(1), 15-21.

- Taylor, S. D., Czarnecki, J., & Masliyah, J. (2002). Disjoining pressure isotherms of water-in-bitumen emulsion films. *Journal of Colloid and Interface Science*, *252*(1), 149-160.

- Tchoukov, P., Yang, F., Xu, Z., Dabros, T., Czarnecki, J., & Sjöblom, J. (2014). Role of asphaltenes in stabilizing thin liquid emulsion films. *Langmuir*, *30*(11), 3024-3033.

- Gray, M. R., Tykwinski, R. R., Stryker, J. M., & Tan, X. (2011). Supramolecular assembly model for aggregation of petroleum asphaltenes. *Energy & Fuels*, *25*(7), 3125-3134.

- Ancheyta, J., Centeno, G., Trejo, F., Marroquin, G., Garcia, J. A., Tenorio, E., & Torres, A. (2002). Extraction and characterization of asphaltenes from different crude oils and solvents. *Energy & Fuels*, *16*(5), 1121-1127.

- Zhang, L. Y., Breen, P., Xu, Z., & Masliyah, J. H. (2007). Asphaltene films at a toluene/water interface. *Energy & Fuels*, *21*(1), 274-285.

- Zhang, L. Y., Lopetinsky, R., Xu, Z., & Masliyah, J. H. (2005). Asphaltene monolayers at a toluene/water interface. *Energy & Fuels*, *19*(4), 1330-1336.

- Freer, E. M., & Radke, C. J. (2004). Relaxation of asphaltenes at the toluene/water interface: Diffusion exchange and surface rearrangement. *Journal of Adhesion*, *80*(6), 481-496.

- Fossen, M., Kallevik, H., Knudsen, K. D., & Sjöblom, J. (2007). Asphaltenes precipitated by a two-step precipitation procedure. 1. Interfacial tension and solvent properties. *Energy & fuels*, *21*(2), 1030-1037.

- Gao, S., Moran, K., Xu, Z., & Masliyah, J. (2010). Role of naphthenic acids in stabilizing water-in-diluted model oil emulsions. *The Journal of Physical Chemistry B*, *114*(23), 7710-7718.

- McLean, J. D., & Kilpatrick, P. K. (1997). Effects of asphaltene aggregation in model heptane–toluene mixtures on stability of water-in-oil emulsions. *Journal of Colloid and Interface Science*, *196*(1), 23-34.
- Ortiz, D. P., Baydak, E. N., & Yarranton, H. W. (2010). Effect of surfactants on interfacial films and stability of water-in-oil emulsions stabilized by asphaltenes. *Journal of Colloid and Interface Science*, *351*(2), 542-555.

- Yang, X., Verruto, V. J., & Kilpatrick, P. K. (2007). Dynamic asphaltene-resin exchange at the oil/water interface: Time-dependent W/O emulsion stability for asphaltene/resin model oils. *Energy & Fuels*, *21*(3), 1343-1349.

- Yarranton, H. W., Hussein, H., & Masliyah, J. H. (2000). Water-in-hydrocarbon emulsions stabilized by asphaltenes at low concentrations. *Journal of Colloid and Interface Science*, *228*(1), 52-63.

- Zhang, L. Y., Xu, Z., & Masliyah, J. H. (2003). Langmuir and Langmuir-Blodgett films of mixed asphaltene and a demulsifier. *Langmuir*, *19*(23), 9730-9741.

- Langevin, D., Poteau, S., Hénaut, I., & Argillier, J. F. (2004). Crude oil emulsion properties and their application to heavy oil transportation. *Oil & Gas Science and Technology*, *59*(5), 511-521.

- Hirasaki, G. J., Miller, C. A., Raney, O. G., Poindexter, M. K., Nguyen, D. T., & Hera, J. (2010). Separation of Produced Emulsions from Surfactant Enhanced Oil Recovery Processes. *Energy & Fuels*, *25*(2), 555-561.

- Kiran, S. K., Ng, S., & Acosta, E. J. (2011). Impact of Asphaltenes and Naphthenic Amphiphiles on the Phase Behavior of Solvent− Bitumen− Water Systems. *Energy & Fuels*, *25*(5), 2223-2231.

- Yeung, A., Dabros, T., Masliyah, J., & Czarnecki, J. (2000). Micropipette: a new technique in emulsion research. *Colloids and Surfaces A: Physicochemical and Engineering Aspects*, *174*(1), 169-181.

- Spiecker, P. M., Gawrys, K. L., Trail, C. B., & Kilpatrick, P. K. (2003). Effects of petroleum resins on asphaltene aggregation and water-in-oil emulsion formation. *Colloids and Surfaces A: Physicochemical and engineering aspects*, *220*(1), 9-27.

- Spiecker, P. M., & Kilpatrick, P. K. (2004). Interfacial rheology of petroleum asphaltenes at the oil-water interface. *Langmuir*, *20*(10), 4022-4032.

- Mullins, O. C. (2010). The Modified Yen Model. *Energy & Fuels*, *24*(4), 2179-2207.
- Mullins, O. C., Sabbah, H., Eyssautier, J., Pomerantz, A. E., Barré, L., Andrews, A. B., ... & Zare, R. N. (2012). Advances in asphaltene science and the Yen–Mullins model. *Energy & Fuels*, *26*(7), 3986-4003.

- Yen, T. F. (1974). Structure of petroleum asphaltene and its significance. *Energy Sources, Part A Recovery, Utilization, and Environmental Effects*, *1*(4), 447-463.

- Strausz, O. P., Mojelsky, T. W., & Lown, E. M. (1992). The molecular structure of asphaltene: an unfolding story. *Fuel*, *71*(12), 1355-1363.

- Strausz, O. P., Mojelsky, T. W., Faraji, F., Lown, E. M., & Peng, P. A. (1999). Additional structural details on Athabasca asphaltene and their ramifications. *Energy & Fuels*, *13*(2), 207-227.

- Agrawala, M., & Yarranton, H. W. (2001). An asphaltene association model analogous to linear polymerization. *Industrial & Engineering Chemistry Research*, *40*(21), 4664-4672.

- Yarranton, H. W. (2005). Asphaltene Self-Association. *Journal of Dispersion Science and Technology*, *26*(1), 5-8.

- Gray Gray, M. R., Tykwinski, R. R., Stryker, J. M., & Tan, X. (2011). Supramolecular assembly model for aggregation of petroleum asphaltenes. *Energy & Fuels*, *25*(7), 3125-3134.

- Tchoukov, P., Czarnecki, J., & Dabros, T. (2010). Study of water-in-oil thin liquid films: Implications for the stability of petroleum emulsions. *Colloids and Surfaces A: Physicochemical and Engineering Aspects*, *372*(1), 15-21.

- Tchoukov, P., Yang, F., Xu, Z., Dabros, T., Czarnecki, J., & Sjöblom, J. (2014). Role of asphaltenes in stabilizing thin liquid emulsion films. *Langmuir*, *30*(11), 3024-3033.

- Yang, F., Tchoukov, P., Pensini, E., Dabros, T., Czarnecki, J., Masliyah, J., & Xu, Z. (2014). Asphaltene subfractions responsible for stabilizing water-in-crude oil emulsions. Part 1: interfacial behaviors. *Energy & Fuels*, *28*(11), 6897-6904.

- Ali, L. H., Al-Ghannam, K. A., & Al-Rawi, J. M. (1990). Chemical structure of asphaltenes in heavy crude oils investigated by NMR. *Fuel*, *69*(4), 519-521.

- Coelho, R. R., Hovell, I., de Mello Monte, M. B., Middea, A., & de Souza, A. L. (2006). Characterisation of aliphatic chains in vacuum residues (VRs) of asphaltenes and resins using molecular modelling and FTIR techniques. *Fuel Processing Technology*, *87*(4), 325-333.

- Dettman, H. D.; Li, N.; Luo, J. (2009) *Corrosion*, Paper No. 09336, 1-13

- Mueller, C. J., Cannella, W. J., Bruno, T. J., Bunting, B., Dettman, H. D., Franz, J. A., ... & Wright, K. (2012). Methodology for formulating diesel surrogate fuels with accurate compositional, ignition-quality, and volatility characteristics. *Energy & Fuels*, *26*(6), 3284-3303.

- Saxena, A., Diaz-Goano, C., & Dettman, H. (2012). Coking Behaviour During Visbreaking. *Journal of Canadian Petroleum Technology*, *51*(06), 457-463.

- Hoff, A.; Dettman, H.D. Presented at the World Heavy Oil Congress in Aberdeen, Scotland, 2012, Paper No. WHOC 12-275.

- Kuznicki, T., Masliyah, J. H., & Bhattacharjee, S. (2008). Molecular dynamics study of model molecules resembling asphaltene-like structures in aqueous organic solvent systems. *Energy & Fuels*, *22*(4), 2379-2389.

- Teklebrhan, R. B., Ge, L., Bhattacharjee, S., Xu, Z., & Sjöblom, J. (2014). Initial Partition and Aggregation of Uncharged Polyaromatic Molecules at the Oil–Water Interface: A Molecular Dynamics Simulation Study. *The Journal of Physical Chemistry B*, *118*(4), 1040-1051.

- Teklebrhan, R. B., Ge, L., Bhattacharjee, S., Xu, Z., & Sjöblom, J. (2012). Probing structure–nanoaggregation relations of polyaromatic surfactants: a molecular dynamics simulation and dynamic light scattering study. *The Journal of Physical Chemistry B*, *116*(20), 5907-5918.

- Boek, E. S., Yakovlev, D. S., & Headen, T. F. (2009). Quantitative Molecular Representation of Asphaltenes and Molecular Dynamics Simulation of Their Aggregation†. *Energy & Fuels*, *23*(3), 1209-1219.

- Headen, T. F., Boek, E. S., & Skipper, N. T. (2009). Evidence for Asphaltene Nanoaggregation in Toluene and Heptane from Molecular Dynamics Simulations†. *Energy & Fuels*, *23*(3), 1220-1229.

- Ancheyta, J., Centeno, G., Trejo, F., Marroquin, G., Garcia, J. A., Tenorio, E., & Torres, A. (2002). Extraction and characterization of asphaltenes from different crude oils and solvents. *Energy & Fuels*, *16*(5), 1121-1127.
- Japanwala, S., Chung, K. H., Dettman, H. D., & Gray, M. R. (2002). Quality of distillates from repeated recycle of residue. *Energy & Fuels*, *16*(2), 477-484.

- Solum, M. S., Pugmire, R. J., & Grant, D. M. (1989). Carbon-13 solid-state NMR of Argonne-premium coals. *Energy & Fuels*, *3*(2), 187-193.

- Van der Spoel, D.; van Buuren, A. R.; Apol, E.; Meulenhoff, P. J.; Tieleman, D. P.; Sijbers, A.; Feenstra, K. The GROMACS Manual (version 3.3); Groningen University, Groningen, The Netherlands, 2004.

- Berendsen, H. J., van der Spoel, D., & van Drunen, R. (1995). GROMACS: A message-passing parallel molecular dynamics implementation. *Computer Physics Communications*, *91*(1), 43-56.

- Lindahl, E., Hess, B., & Van Der Spoel, D. (2001). GROMACS 3.0: a package for molecular simulation and trajectory analysis. *Journal of Molecular Modeling*, *7*(8), 306-317.

- Oostenbrink, C., Villa, A., Mark, A. E., & Van Gunsteren, W. F. (2004). A biomolecular force field based on the free enthalpy of hydration and solvation: The GROMOS force-field parameter sets 53A5 and 53A6. *Journal of Computational Chemistry*, *25*(13), 1656-1676.

- Kuznicki, T., Masliyah, J. H., & Bhattacharjee, S. (2009). Aggregation and partitioning of model asphaltenes at toluene− water interfaces: Molecular dynamics simulations. *Energy & Fuels*, *23*(10), 5027-5035.

- Mullins O. In: EY Sheu, OC Mullins. (1995). Eds. *Asphaltenes: Fundamentals and Applications*; Plenum Press: New York, 53-96.

- Nosé, S. (1984). A molecular dynamics method for simulations in the canonical ensemble. *Molecular Physics*, *52*(2), 255-268.

- Hoover, W. G. (1985). Canonical dynamics: equilibrium phase-space distributions. *Physical Review A*, *31*(3), 1695.

- Parrinello, M., & Rahman, A. (1981). Polymorphic transitions in single crystals: A new molecular dynamics method. *Journal of Applied physics*, *52*(12), 7182-7190.

- Knovel Critical Tables, 2nd ed.; Knovel: New York, NY, USA, 2008; Available online:http://www.knovel.com/web/portal/browse/display?_EXT_KNOVEL_DISPLAY_bookid=761&VerticalID=0 (accessed on 2 February 2015).

- Czarnecki, J., Tchoukov, P., Dabros, T., & Xu, Z. (2013). Role of asphaltenes in stabilisation of water in crude oil emulsions. *The Canadian Journal of Chemical Engineering*, *91*(8), 1365-1371.

- Czarnecki, J., Tchoukov, P., & Dabros, T. (2012). Possible role of asphaltenes in the stabilization of water-in-crude oil emulsions. *Energy & Fuels*, *26*(9), 5782-5786.

- Yarranton, H. W., Ortiz, D. P., Barrera, D. M., Baydak, E. N., Barre, L., Frot, D., ... & Oake, J. (2013). On the size distribution of self-associated asphaltenes. *Energy & Fuels*, *27*(9), 5083-5106.

- Petersen, J., & Harnsberger, P. (1998). Asphalt aging: dual oxidation mechanism and its interrelationships with asphalt composition and oxidative age hardening. *Transportation Research Record: Journal of the Transportation Research Board*, (1638), 47-55.

- Brondel, N., Moynihan, E. J., Lehane, K. N., Eccles, K. S., Elcoate, C. J., Coles, S. J., ... & Maguire, A. R. (2010). Does intermolecular S= O··· H–C–S= O hydrogen bonding in sulfoxides and sulfones provide a robust supramolecular synthon in the solid state?. *Crystal Engineering Communication*, *12*(10), 2910-2927.

- Natarajan, A., Xie, J., Wang, S., Liu, Q., Masliyah, J., Zeng, H., & Xu, Z. (2011). Understanding molecular interactions of asphaltenes in organic solvents using a surface force apparatus. *The Journal of Physical Chemistry C*, *115*(32), 16043-16051.

- Kupai, M. M., Yang, F., Harbottle, D., Moran, K., Masliyah, J., & Xu, Z. (2013). Characterising rag‐forming solids. *The Canadian Journal of Chemical Engineering*, *91*(8), 1395-1401.

- McLean, J. D., & Kilpatrick, P. K. (1997). Effects of asphaltene solvency on stability of water-in-crude-oil emulsions. *Journal of Colloid and Interface Science*, *189*(2), 242-253.

- Yan, Z., Elliott, J. A., & Masliyah, J. H. (1999). Roles of various bitumen components in the stability of water-in-diluted-bitumen emulsions. *Journal of Colloid and Interface Science*, *220*(2), 329-337.

- Tchoukov, P., Czarnecki, J., & Dabros, T. (2010). Study of water-in-oil thin liquid films: Implications for the stability of petroleum emulsions. *Colloids and Surfaces A: Physicochemical and Engineering Aspects*, *372*(1), 15-21.

- Czarnecki, J., Tchoukov, P., & Dabros, T. (2012). Possible role of asphaltenes in the stabilization of water-in-crude oil emulsions. *Energy & Fuels*, *26*(9), 5782-5786.

- Tchoukov, P., Yang, F., Xu, Z., Dabros, T., Czarnecki, J., & Sjöblom, J. (2014). Role of asphaltenes in stabilizing thin liquid emulsion films. *Langmuir*, *30*(11), 3024-3033.

- Feng, X., Mussone, P., Gao, S., Wang, S., Wu, S. Y., Masliyah, J. H., & Xu, Z. (2009). Mechanistic study on demulsification of water-in-diluted bitumen emulsions by ethylcellulose. *Langmuir*, *26*(5), 3050-3057.

- Robins, M. M., Watson, A. D., & Wilde, P. J. (2002). Emulsions—creaming and rheology. *Current Opinion in Colloid & Interface Science*, *7*(5), 419-425.

- Czarnecki, J., Moran, K., & Yang, X. (2007). On the "rag layer" and diluted bitumen froth dewatering. *The Canadian Journal of Chemical Engineering*, *85*(5), 748-755.

- Hou, J., Feng, X., Masliyah, J., & Xu, Z. (2012). Understanding interfacial behavior of ethylcellulose at the water–diluted bitumen interface. *Energy & Fuels*, *26*(3), 1740-1745.

- Fan, Y., Simon, S., & Sjöblom, J. (2009). Chemical destabilization of crude oil emulsions: effect of nonionic surfactants as emulsion inhibitors. *Energy & Fuels*, *23*(9), 4575-4583.

- Ese, M. H., Sjöblom, J., Djuve, J., & Pugh, R. (2000). An atomic force microscopy study of asphaltenes on mica surfaces. Influence of added resins and demulsifiers. *Colloid and Polymer Science*, *278*(6), 532-538.

- Fan, Y., Simon, S., & Sjöblom, J. (2010). Interfacial shear rheology of asphaltenes at oil–water interface and its relation to emulsion stability: influence of concentration, solvent aromaticity and nonionic surfactant. *Colloids and Surfaces A: Physicochemical and Engineering Aspects*, *366*(1), 120-128.

- Kim, Y. H., & Wasan, D. T. (1996). Effect of demulsifier partitioning on the destabilization of water-in-oil emulsions. *Industrial & Engineering Chemistry Research*, *35*(4), 1141-1149.

- Feng, X., Wang, S., Hou, J., Wang, L., Cepuch, C., Masliyah, J., & Xu, Z. (2011). Effect of hydroxyl content and molecular weight of biodegradable ethylcellulose on demulsification of water-in-diluted bitumen emulsions. *Industrial & Engineering Chemistry Research*, *50*(10), 6347-6354.

- Erni, P., Windhab, E. J., Gunde, R., Graber, M., Pfister, B., Parker, A., & Fischer, P. (2007). Interfacial rheology of surface-active biopolymers: Acacia senegal gum versus hydrophobically modifed starch. *Biomacromolecules*, *8*(11), 3458-3466.

- Dickinson, E. (2001). Milk protein interfacial layers and the relationship to emulsion stability and rheology. *Colloids and Surfaces B: Biointerfaces*, *20*(3), 197-210.

- Erni, P. (2011). Deformation modes of complex fluid interfaces. *Soft Matter*, *7*(17), 7586-7600.

- Angle, C. W., & Hua, Y. (2012). Dilational interfacial rheology for increasingly deasphalted bitumens and n-C5 asphaltenes in toluene/NaHCO3 solution. *Energy & Fuels*, *26*(10), 6228-6239.

- Mohammed, R. A., Bailey, A. I., Luckham, P. F., & Taylor, S. E. (1994). The effect of demulsifiers on the interfacial rheology and emulsion stability of water-in-crude oil emulsions. *Colloids and Surfaces A: Physicochemical and Engineering Aspects*, *91*, 129-139.

- Sun, H. Q., Zhang, L., Li, Z. Q., Zhang, L., Luo, L., & Zhao, S. (2011). Interfacial dilational rheology related to enhance oil recovery. *Soft Matter*, *7*(17), 7601-7611.

- Ekott, E. J., & Akpabio, E. J. (2010). A review of water-in-crude oil emulsion stability, destabilization and interfacial rheology. *Journal of Engineering and Applied Sciences*, *5*(6), 447-452.

- Feng, X., Wang, S., Hou, J., Wang, L., Cepuch, C., Masliyah, J., & Xu, Z. (2011). Effect of hydroxyl content and molecular weight of biodegradable ethylcellulose on demulsification of water-in-diluted bitumen emulsions. *Industrial & Engineering Chemistry Research*, *50*(10), 6347-6354.

- Wu, J., Xu, Y., Dabros, T., & Hamza, H. (2003). Effect of demulsifier properties on destabilization of water-in-oil emulsion. *Energy & Fuels*, *17*(6), 1554-1559.

- Zaki, N. N., Abdel-Raouf, M. E., & Abdel-Azim, A. A. (1996). Propylene oxide-ethylene oxide block copolymers as demulsifiers for water-in-oil emulsions, II. Effects of temperature, salinity, pH-value, and solvents on the demulsification efficiency. *Monatshefte für Chemie/Chemical Monthly*, *127*(12), 1239-1245.

- Wu, J., Xu, Y., Dabros, T., & Hamza, H. (2005). Effect of EO and PO positions in nonionic surfactants on surfactant properties and demulsification performance. *Colloids and Surfaces A: Physicochemical and Engineering Aspects*, *252*(1), 79-85.

- Xu, Y., Wu, J., Dabros, T., Hamza, H., & Venter, J. (2005). Optimizing the polyethylene oxide and polypropylene oxide contents in diethylenetriamine-based surfactants for destabilization of a water-in-oil emulsion. *Energy & Fuels*, *19*(3), 916-921.

- Ramalho, J. B.; Ramos, N.; Lucas, E.(2009).The influence of some interfacial properties of PEO-b-PPO copolymers on dewatering of water-in-oil asphaltene model emulsions. *Chem. Chem. Technol*, 3, 53-58.

- Abdel‐Azim, A. A. A., Zaki, N. N., & Maysour, N. E. S. (1998). Polyoxyalkylenated amines for breaking water ‐ in ‐ oil emulsions: effect of structural variations on the demulsification efficiency. *Polymers for Advanced Technologies*, *9*(2), 159-166.

- Angle, C. W., Dabros, T., & Hamza, H. A. (2007). Demulsifier effectiveness in treating heavy oil emulsion in the presence of fine sands in the production fluids. *Energy & Fuels*, *21*(2), 912-919.

- Feng, X., Mussone, P., Gao, S., Wang, S., Wu, S. Y., Masliyah, J. H., & Xu, Z. (2009). Mechanistic study on demulsification of water-in-diluted bitumen emulsions by ethylcellulose. *Langmuir*, *26*(5), 3050-3057.

- Kailey, I., Blackwell, C., & Behles, J. (2013). Collaborative interactions between EO-PO copolymers upon mixing. *Industrial & Engineering Chemistry Research*, *52*(50), 17913-17919.

- Mohammed, R. A., Bailey, A. I., Luckham, P. F., & Taylor, S. E. (1994). Dewatering of crude oil emulsions 3. Emulsion resolution by chemical means. *Colloids and Surfaces A: Physicochemical and Engineering Aspects*, *83*(3), 261-271.

- Zhang, Z., Xu, G., Wang, F., Dong, S., & Chen, Y. (2005). Demulsification by amphiphilic dendrimer copolymers. *Journal of Colloid and Interface Science*, *282*(1), 1-4.

- Aveyard, R., Binks, B. P., Fletcher, P. D. I., & Lu, J. R. (1990). The resolution of water-in-crude oil emulsions by the addition of low molar mass demulsifiers. *Journal of Colloid and Interface Science*, *139*(1), 128-138.
- Ramakers, R. R. M., Pöpel, H. J., & Koops, W. (1982). A new method for handling oil spill materials. *Oil and Petrochemical Pollution*, *1*(2), 129-137.

- Stewart, A. C., EI-Hamouz, A. M., & Davies, G. A. (1996). Effect of chemical additives on the stability of kerosene-water dispersions. *Journal of Dispersion Science and Technology*, *17*(6), 675-696.

- Dimitrov, A. N., Yordanov, D. I., & Petkov, P. S. (2012). Study on the effect of demulsifers on crude oil and petroleum products. *International Journal of Environmental Research*, *6*(2), 435-442.

- Mohammed, R. A., Bailey, A. I., Luckham, P. F., & Taylor, S. E. (1994). Dewatering of crude oil emulsions 3. Emulsion resolution by chemical means. *Colloids and Surfaces A: Physicochemical and Engineering Aspects*, *83*(3), 261-271.

- Fan, Y., Simon, S., & Sjöblom, J. (2010). Influence of nonionic surfactants on the surface and interfacial film properties of asphaltenes investigated by Langmuir balance and Brewster angle microscopy. *Langmuir*, *26*(13), 10497-10505.
- Hua, Y., & Angle, C. W. (2012). Brewster angle microscopy of Langmuir films of athabasca bitumens, n-C5 asphaltenes, and SAGD bitumen during pressure–area hysteresis. *Langmuir*, *29*(1), 244-263.
- Kailey, I., & Feng, X. (2013). Influence of structural variations of demulsifiers on their performance. *Industrial & Engineering Chemistry Research*, *52*(2), 785-793.
- Ancheyta, J., Centeno, G., Trejo, F., Marroquin, G., Garcia, J. A., Tenorio, E., & Torres, A. (2002). Extraction and characterization of asphaltenes from different crude oils and solvents. *Energy & Fuels*, *16*(5), 1121-1127.
- Gao, S., Moran, K., Xu, Z., & Masliyah, J. (2009). Role of bitumen components in stabilizing water-in-diluted oil emulsions. *Energy & Fuels*, *23*(5), 2606-2612.
- Feng, X., Mussone, P., Gao, S., Wang, S., Wu, S. Y., Masliyah, J. H., & Xu, Z. (2009). Mechanistic study on demulsification of water-in-diluted bitumen emulsions by ethylcellulose. *Langmuir*, *26*(5), 3050-3057.
- Harbottle, D., Chen, Q., Moorthy, K., Wang, L., Xu, S., Liu, Q., ... & Xu, Z. (2014). Problematic stabilizing films in petroleum emulsions: Shear rheological response of viscoelastic asphaltene films and the effect on drop coalescence. *Langmuir*, *30*(23), 6730-6738.
- Singh, B. P. (1994). Performance of demulsifiers: Prediction based on film pressure-area isotherms and solvent properties. *Energy Sources*, *16*(3), 377-385.
- Speight, J. G.; Speros, E. M. (1981). On the molecular nature of petroleum asphaltenes. Chemistry of Asphaltenes,195, 1-15.
- Andersen, S. I. (1994). Effect of precipitation temperature on the composition of n-heptane asphaltenes. *Fuel Science & Technology International*, *12*(1), 51-74.
- Wang, Y., Zhang, L., Sun, T., Zhao, S., & Yu, J. (2004). A study of interfacial dilational properties of two different structure demulsifiers at oil–water interfaces. *Journal of Colloid and Interface Science*, *270*(1), 163-170.

- Petkov, J. T., Gurkov, T. D., Campbell, B. E., & Borwankar, R. P. (2000). Dilatational and shear elasticity of gel-like protein layers on air/water interface. *Langmuir*, *16*(8), 3703-3711.

- Ferri, J. K., Kotsmar, C., & Miller, R. (2010). From surfactant adsorption kinetics to asymmetric nanomembrane mechanics: Pendant drop experiments with subphase exchange. *Advances in Colloid and Interface Science*, *161*(1), 29-47.

- Kotsmar, C., Grigoriev, D. O., Makievski, A. V., Ferri, J. K., Krägel, J., Miller, R., & Möhwald, H. (2008). Drop profile analysis tensiometry with drop bulk exchange to study the sequential and simultaneous adsorption of a mixed β-casein/C12DMPO system. *Colloid and Polymer Science*, *286*(8-9), 1071-1077.

- Ferri, J. K., Gorevski, N., Kotsmar, C., Leser, M. E., & Miller, R. (2008). Desorption kinetics of surfactants at fluid interfaces by novel coaxial capillary pendant drop experiments. *Colloids and Surfaces A: Physicochemical and Engineering Aspects*, *319*(1), 13-20.

- Zhang, L. Y., Lopetinsky, R., Xu, Z., & Masliyah, J. H. (2005). Asphaltene monolayers at a toluene/water interface. *Energy & Fuels*, *19*(4), 1330-1336.

- Zhang, H., Xu, G., Wu, D., & Wang, S. (2008). Aggregation of cetyltrimethylammonium bromide with hydrolyzed polyacrylamide at the paraffin oil/water interface: interfacial rheological behavior study. *Colloids and Surfaces A: Physicochemical and Engineering Aspects*, *317*(1), 289-296.

- Zhang, L. Y., Xu, Z., & Masliyah, J. H. (2003). Langmuir and Langmuir-Blodgett films of mixed asphaltene and a demulsifier. *Langmuir*, *19*(23), 9730-9741.
- Spiecker, P. M., & Kilpatrick, P. K. (2004). Interfacial rheology of petroleum asphaltenes at the oil-water interface. *Langmuir*, *20*(10), 4022-4032.

- Yang, X., Verruto, V. J., & Kilpatrick, P. K. (2007). Dynamic asphaltene-resin exchange at the oil/water interface: Time-dependent W/O emulsion stability for asphaltene/resin model oils. *Energy & Fuels*, *21*(3), 1343-1349.

- Álvarez, L., Díaz, M. E., Montes, F. J., & Galán, M. A. (2010). Langmuir technique and Brewster angle microscope studies of the interfacial behavior of bitumen, asphaltenes and maltenes at the air–water interface. I. Effect of different spreading solution volumes. *Fuel*, *89*(3), 691-702.

- Lobato, M. D., Pedrosa, J. M., Möbius, D., & Lago, S. (2009). Optical characterization of asphaltenes at the air− water interface. *Langmuir*, *25*(3), 1377-1384.

- Cadena-Nava, R. D., Cosultchi, A., & Ruiz-Garcia, J. (2007). Asphaltene behavior at interfaces. *Energy & Fuels*, *21*(4), 2129-2137.

- Zhang, L. Y., Xu, Z., & Masliyah, J. H. (2005). Characterization of adsorbed athabasca asphaltene films at solvent-water interfaces using a Langmuir interfacial trough. *Industrial & Engineering Chemistry Research*, *44*(5), 1160-1174.

- Bosio, V., Dubreuil, F., Bogdanovic, G., & Fery, A. (2004). Interactions between silica surfaces coated by polyelectrolyte multilayers in aqueous environment: comparison between precursor and multilayer regime. *Colloids and Surfaces A: Physicochemical and Engineering Aspects*, *243*(1), 147-155.

- Pensini, E., Yip, C. M., O'Carroll, D., & Sleep, B. E. (2013). Carboxymethyl cellulose binding to mineral substrates: Characterization by atomic force microscopy–based Force spectroscopy and quartz-crystal microbalance with dissipation monitoring. *Journal of Colloid and Interface Science*, *402*, 58-67.

- Barnes, T. J., & Prestidge, C. A. (2000). PEO-PPO-PEO block copolymers at the emulsion droplet-water interface. *Langmuir*, *16*(9), 4116-4121.

- Vieira, J. B., Li, Z. X., & Thomas, R. K. (2002). Adsorption of triblock copolymers of ethylene oxide and propylene oxide at the air/water interface: The surface excess. *The Journal of Physical Chemistry B*, *106*(21), 5400-5407.

- Masliyah, J., Zhou, Z., Xu, Z. (2004). Understanding water-based bitumen extraction from Athabasca oil sands, *The Canadian Journal of Chemical Engineering*, 82(4), 628-654

- Kokal, S. L. (2005). Crude oil emulsions: A state-of-the-art review. *SPE Production & Facilities*, *20*(01), 5-13.

- Yeung, A., Dabros, T., Masliyah, J., & Czarnecki, J. (2000). Micropipette: a new technique in emulsion research. *Colloids and Surfaces A: Physicochemical and Engineering Aspects*, *174*(1), 169-181.

- Pensini, E., Harbottle, D., Yang, F., Tchoukov, P., Li, Z., Kailey, I., ... & Xu, Z. (2014). Demulsification Mechanism of Asphaltene-Stabilized Water-in-Oil Emulsions by a Polymeric Ethylene Oxide–Propylene Oxide Demulsifier. *Energy & Fuels*, *28*(11), 6760-6771.

- Hou, J., Feng, X., Masliyah, J., & Xu, Z. (2012). Understanding interfacial behavior of ethylcellulose at the water–diluted bitumen interface. *Energy & Fuels*, *26*(3), 1740-1745.

- Ese, M. H., Sjöblom, J., Djuve, J., & Pugh, R. (2000). An atomic force microscopy study of asphaltenes on mica surfaces. Influence of added resins and demulsifiers. *Colloid and Polymer Science*, *278*(6), 532-538.

- Ramakers, R. R. M., Pöpel, H. J., & Koops, W. (1982). A new method for handling oil spill materials. *Oil and Petrochemical Pollution*, *1*(2), 129-137.

- Stewart, A. C., EI-Hamouz, A. M., & Davies, G. A. (1996). Effect of chemical additives on the stability of kerosene-water dispersions. *Journal of Dispersion Science Andtechnology*, *17*(6), 675-696.

- Dimitrov, A. N., Yordanov, D. I., & Petkov, P. S. (2012). Study on the effect of demulsifers on crude oil and petroleum products. *International Journal of Environmental Research*, *6*(2), 435-442.

- Fan, Y., Simon, S., & Sjöblom, J. (2010). Interfacial shear rheology of asphaltenes at oil–water interface and its relation to emulsion stability: influence of concentration, solvent aromaticity and nonionic surfactant. *Colloids and Surfaces A: Physicochemical and Engineering Aspects*, *366*(1), 120-128.

- Kim, Y. H., & Wasan, D. T. (1996). Effect of demulsifier partitioning on the destabilization of water-in-oil emulsions. *Industrial & Engineering Chemistry Research*, *35*(4), 1141-1149.

- Feng, X., Xu, Z., & Masliyah, J. (2008). Biodegradable polymer for demulsification of water-in-bitumen emulsions. *Energy & Fuels*, *23*(1), 451-456.

- Tchoukov, P., Yang, F., Xu, Z., Dabros, T., Czarnecki, J., & Sjöblom, J. (2014). Role of asphaltenes in stabilizing thin liquid emulsion films. *Langmuir*, *30*(11), 3024-3033.

- Bi, J., Yang, F., Harbottle, D., Pensini, E., Tchoukov, P., Simon, S., ... & Xu, Z. (2015). Interfacial Layer Properties of a Polyaromatic Compound and its Role in Stabilizing Water-in-Oil Emulsions. *Langmuir*, *31*(38), 10382-10391.

- Yang, F., Tchoukov, P., Pensini, E., Dabros, T., Czarnecki, J., Masliyah, J., & Xu, Z. (2014). Asphaltene subfractions responsible for stabilizing water-in-crude oil emulsions. Part 1: interfacial behaviors. *Energy & Fuels*, *28*(11), 6897-6904.

- Yang, F., Tchoukov, P., Dettman, H., Teklebrhan, R. B., Liu, L., Dabros, T., Czarnecki, J., Masliyah, J. & Xu, Z. (2015). Asphaltene Subfractions Responsible for Stabilizing Water-in-Crude Oil Emulsions. Part 2: Molecular Representations and Molecular Dynamics Simulations. *Energy & Fuels***,** 29 (8), 4783–4794

- Platikanov, D., Exerowa, D. (2005) Thin liquid films. In *Fundamentals of Interface and Colloid Science Soft Colloids* (pp 1-91). Academic Press.

- Sheludko, A. (1967). Thin liquid films. *Advances in Colloid and Interface Science*, *1*(4), 391-464.

- Khristov, K., Taylor, S. D., Czarnecki, J., & Masliyah, J. (2000). Thin liquid film technique—application to water–oil–water bitumen emulsion films. *Colloids and Surfaces A: Physicochemical and Engineering Aspects*, *174*(1), 183-196.

- Tchoukov, P., Czarnecki, J., & Dabros, T. (2010). Study of water-in-oil thin liquid films: Implications for the stability of petroleum emulsions. *Colloids and Surfaces A: Physicochemical and Engineering Aspects*, *372*(1), 15-21.

- Fan, Y., Simon, S., & Sjöblom, J. (2010). Interfacial shear rheology of asphaltenes at oil–water interface and its relation to emulsion stability: influence of concentration, solvent aromaticity and nonionic surfactant. *Colloids and Surfaces A: Physicochemical and Engineering Aspects*, *366*(1), 120-128.

- Harbottle, D., Chen, Q., Moorthy, K., Wang, L., Xu, S., Liu, Q., ... & Xu, Z. (2014). Problematic stabilizing films in petroleum emulsions: Shear rheological response of viscoelastic asphaltene films and the effect on drop coalescence. *Langmuir*, *30*(23), 6730-6738.

- Feng, X., Wang, S., Hou, J., Wang, L., Cepuch, C., Masliyah, J., & Xu, Z. (2011). Effect of hydroxyl content and molecular weight of biodegradable ethylcellulose on demulsification of water-in-diluted bitumen emulsions. *Industrial & Engineering Chemistry Research*, *50*(10), 6347-6354.

Appendix I

Density profiles of toluene-water system containing averaged RA-I over different simulation time

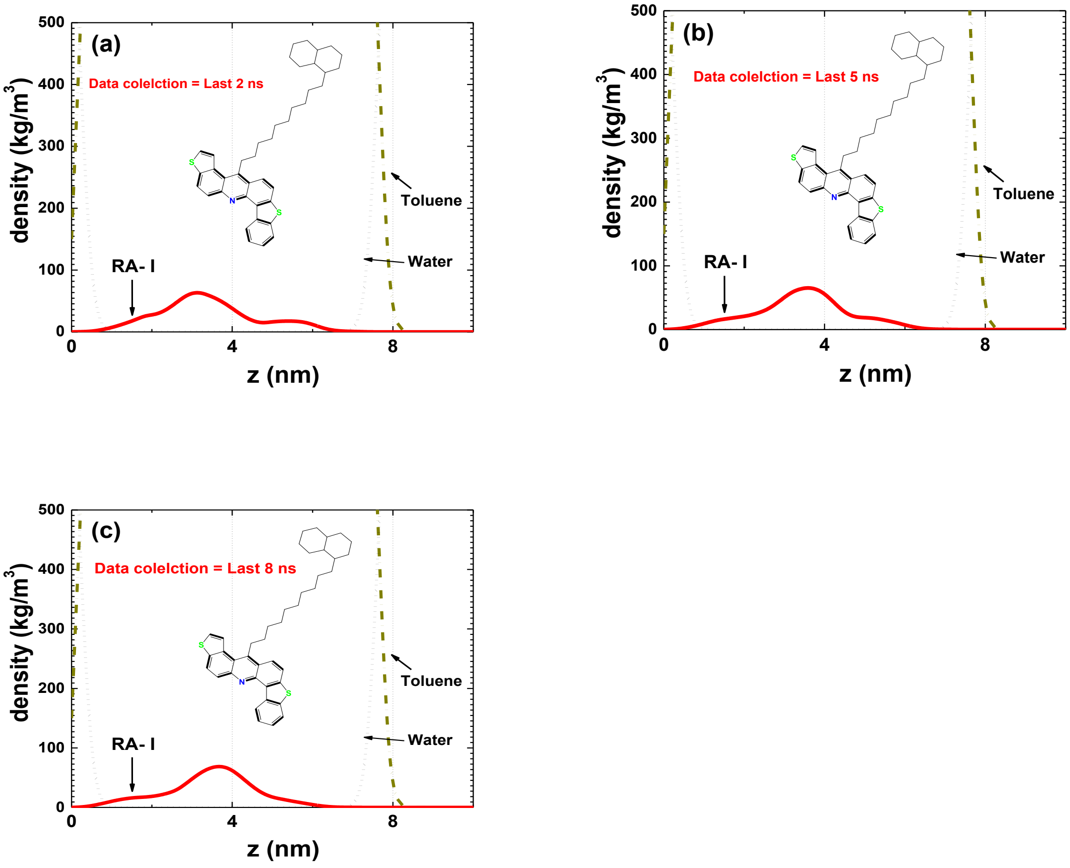

Figure A1. Density profiles of toluene-water system containing averaged RA-I structures over the last 2 ns (a), 5 ns (b), and 8 ns (c) of the simulation time.

Appendix II

Comparison of density profiles of toluene-water system containing averaged RA-I and RA-II over the last 2ns of the simulation time

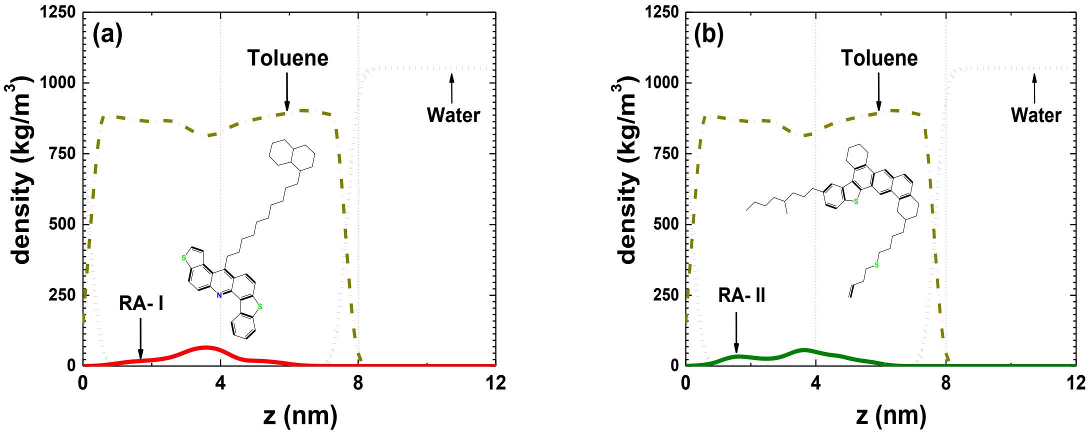

Figure A2. Density profiles of toluene-water system containing RA-I and RA-II structures over the last 2 ns of the simulation time.

Appendix III

Intramolecular sulfur-sulfur and polyaromatic core-polyaromatic core interaction for IAA and RA

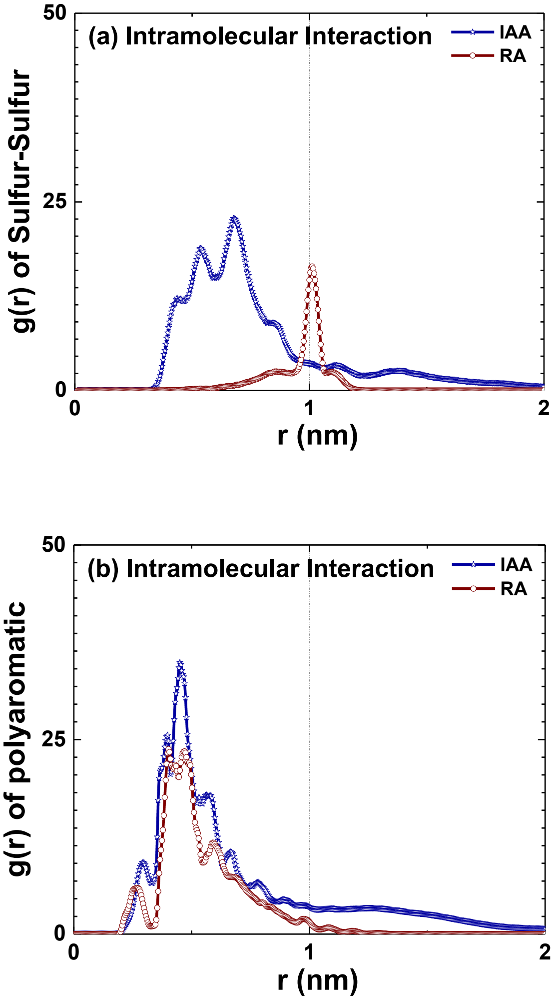

Figure A3. Distribution functions of the intramolecular sulfur-sulfur interaction (upper) and poly-aromatic core (bottom) averaged over the last 2 ns of the simulation time (98 ns - 100 ns) at 298 K.